ASYMMETRIC INDUCTION IN SOLID STATE PHOTOCHEMISTRY

By

Anna Dóra Guðmundsdóttir

B.Sc. Chemistry University of Iceland, 1985

M.Sc. Chemistry University of British Columbia, 1988

A THESIS SUBMITTED IN PARTIAL FULFILLMENT OF

THE REQUIREMENTS FOR THE DEGREE OF

DOCTOR OF PHILOSOPHY

in

THE FACULTY OF GRADUATE STUDIES

CHEMISTRY

We accept this thesis as conforming

to the required standard

In presenting this thesis in partial fulfilment of the requirements for an advanced degree at the University of British Columbia, I agree that the Library shall make it freely available for reference and study. I further agree that permission for extensive copying of this thesis for scholarly purposes may be granted by the head of my department or by his or her representatives. It is understood that copying or publication of this thesis for financial gain shall not be allowed without my written permission.

(Signature)

Department of _Chemistry_

The University of British Columbia
Vancouver, Canada

Date _27 april '93_

ABSTRACT

The enantioselectivity of the di-π-methane photorearrangement in chiral crystals was studied. Three achiral dibenzobarrelene carboxylic acid derivatives and one achiral amino dibenzobarrelene derivative were synthesized for this work. These compounds were induced to crystallize as chiral crystals by forming salts with chiral counterions. Photolysis of the chiral crystals resulted in asymmetric induction in the products.

The regioselectivity of the photorearrangements of the starting materials prior to salt formation was studied in solution as well as in the solid state. In addition, the photochemistry of the methyl and ethyl esters of the carboxylic acids was also investigated. The photochemistry of some of these dibenzobarrelene derivatives was found to be medium-dependent. Possible structure-reactivity correlations for these compounds, based on X-ray crystallographic data, are discussed.

The chiral salts of the dibenzobarrelene derivatives were photolyzed in solution and in the solid state. The extent of asymmetric induction in the crystalline phase was studied by measuring the enantiomeric excess of the photoproducts. No optical activity was observed for the solution photoproducts, presumably because the salts had dissociated. The enantioselectivity of the di-π-methane photorearrangement in the solid state varied from poor to good, depending on the chiral salt in each instance. The chiral counterion ensures chiral crystals, but the crystal lattice alone is accountable for asymmetric induction, and different salts crystallized in different crystal packing arrangements leading to varying degrees of asymmetric induction.

The absolute steric course of the di-π-methane rearrangement in the solid state was studied. Chiral salts for which the photorearrangements were both regio- and enantioselective were selected for this study. The reaction pathway was mapped by

comparing the absolute configuration of the starting material and the photoproduct. After the reaction pathways had been determined, the crystal structures of the starting materials were analyzed in order to identify the crystal forces that control the enantioselectivity of the di-π-methane rearrangement. A general explanation of the factors that control the asymmetric induction of the di-π-methane rearrangement in dibenzobarrelene derivatives was proposed. It was concluded that forming chiral salts of achiral molecules is a convenient and an effective way to study reactions in chiral crystals.

Finally, solid state photochromism was discovered for some of the bridgehead-substituted dibenzobarrelene derivatives. Possible intermediates responsible for the photochromic phenomena are suggested.

TABLE OF CONTENTS

vi

LIST OF TABLES

LIST OF FIGURES

ACKNOWLEDGMENT

DEDICATION

For Óskar, Guðmundur and Svanhildur

Fyrir handan fjöllin sjö
búa dverganir sjö
bíða þín Mjallhvít
með sjö gráðuga munna
sjöfaldar kvartanir
ný gólf tilað skúra.

Er ekki betra
að láta skera úr sér hjartað
en að gráta sig lifandi
bíðandi
eftir einhverjum kóngssyni
sem hefur líf þitt
í hendi sér uppfrá því
í glerkistu
sofandi
svefni vanans.

Þórdís Richardsdóttir: Ævintýramórall.

CHAPTER 1 INTRODUCTION

The design of reactions that yield optically active products from achiral starting materials is one of the core topics in organic chemistry. Numerous asymmetric reactions have been reported.[1] The strategy most of these reactions have in common utilizes the dissymmetric influence of a resolved chiral agent on the reaction pathway to accomplish asymmetric induction, which results in diastereomeric transition states. The dissymmetric influences arise from the chiral characteristics of the resolved reagent, catalyst, solvent or host molecule in most instances. Asymmetric reactions have also been carried out in the absence of any external chiral material. Such reactions are referred to as absolute asymmetric syntheses[2] and are obvious candidates for an explanation of the origin of the first chiral organic material in nature.[3]

Asymmetric induction in fluid phase photochemistry has not been widely studied, even though the hypothesis that circularly polarized light may have led to the generation of optical activity on earth dates back to the 19th century.[4] Direct irradiation with circularly polarized light has been shown to lead to optically active products, but only in extremely low optical yields. The most common method of generating dissymmetric influences in the photochemistry of fluid solutions is the use of chiral reagents. Methodologies such as chiral solvents, sensitizers and complexes have also been studied. Nevertheless these methods are limited owing to low optical yields.

In recent years topochemically controlled reactions in organic crystals have become of interest for asymmetric synthesis.[5] The literature lists examples of phototransformations in the solid state that occur with good optical yields. Most of these reactions make use of resolved chiral substituents that are chemically bonded to the reagents. In solution photochemistry, the chiral center alone is responsible for all

asymmetric induction, but for reactions in the solid state, it is not only the chiral center that resides in a chiral environment; the entire molecule is influenced by the chiral surrounding of the crystal.[5] Moreover, examples of absolute asymmetric transformations in the solid state have been reported that lead to high optical yields in the photoproducts.[5] In these instances, achiral molecules that form chiral crystals have been transformed into chiral products using the chiral environment of the crystals as the sole source of chirality in the photoreaction.

1.1 Photochemistry in the Solid State

Photoreactions in the solid state are capable of giving products that are very different from those observed in fluid phase owing to the fact that the crystal lattice influences the reactivity. Two important factors govern reactions in the solid state: the conformation and the packing arrangement of the reacting molecules. Compared to isotropic phases, in which a flexible organic molecule may adopt many conformations owing to the fast equilibrium between them, in crystals the molecule will rarely adopt more than one conformation, and it is most common that organic molecules crystallize in or near their minimum energy conformation.[6] The limitation on motion in crystals will consequently affect reactions that are sensitive to the conformation of the reactant and this can lead to increased selectivity. The packing of the reactant into a crystal is important, since the anisotropic environment of the crystal lattice can affect the course of a reaction.

Despite an interesting history that dates back to the early 20th century,[7] organic solid state photochemistry did not become a subject of systematic study until the 1960s when X-ray crystallography became readily available. With the aid of X-ray

2

crystallography, it is possible to analyze in detail the molecular conformation as well as the packing arrangement in the crystals, leading to a greater ability to interpret structure-reactivity relationships.

Considerable progress has been made in this field and many solid state reactions have been reported in recent years. In response, a number of review articles and books have been published.[8] A serious limitation of solid state chemistry is the inability to predict the packing arrangement of molecules in a crystal lattice, thus the study of solid state photochemistry tends to be of the "discover-and-explain" variety. This can be observed to be a normal procedure in laying out the foundations for a new field and undoubtedly, with a better understanding of crystal packing and topochemistry, solid state reactions will eventually be rationally planned and exploited.

1.2 The Topochemical Principle

The first principle of solid state chemical reactivity was proposed by Kohlshutter[9] in 1918 and was termed the topochemical postulate. According to Kohlshutter a topochemical reaction in the solid state recognizes the restriction of the rigid three-dimensional environment in the crystal and therefore all reactions take place with minimum atomic and molecular movement.

Many years later, Schmidt and his co-workers[10] carried out pioneering studies on the photodimerization of *trans*-cinnamic acid derivatives in the crystalline phase which allowed them to refine the topochemical postulate and establish it on a valid experimental basis. In their investigation they discovered that *trans*-cinnamic acid (1) crystallized in three polymorphic forms, α, β, γ, and each form showed characteristic photochemical behavior (Figure 1-1).
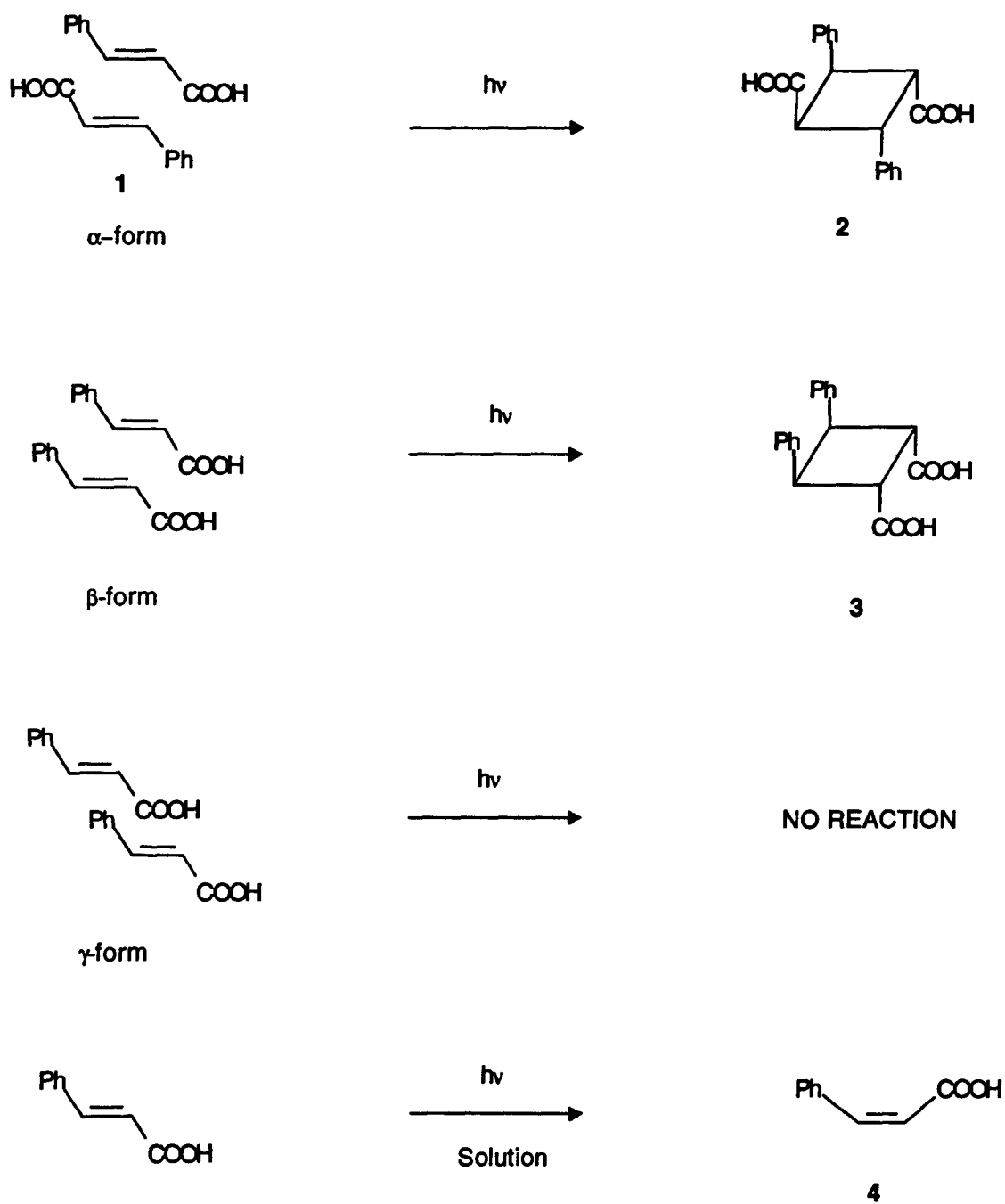
Figure 1-1   Photodimerization of *trans*-Cinnamic Acid (1) in the Crystalline State and in Solution

The centrosymmetric intermolecular arrangement in the α-type crystals led to centrosymmetric α-truxilic acid 2, whereas the parallel translation arrangement in the β-form gave the mirror-symmetric β-truxilic acid 3. Finally the γ-form was found to be unreactive because of the poorly overlapped arrangement of the two double bonds. In solution, however, *trans*-cinnamic acid 1 underwent only *trans-cis* photoisomerization and no dimerization was observed.

On the basis of crystallographic and photochemical studies of *trans*-cinnamic acid (1) and other derivatives, Schmidt suggested that the packing of the molecules in the crystal lattice, which determines the distance and orientation of the reactive centers with respect to one other, is the dominant factor in controlling solid state reactions.[11] This topochemical postulate has been viewed as the basic foundation of organic solid state photochemistry, even though some exceptions exist.[5b, 8i]

Allowed

Disallowed
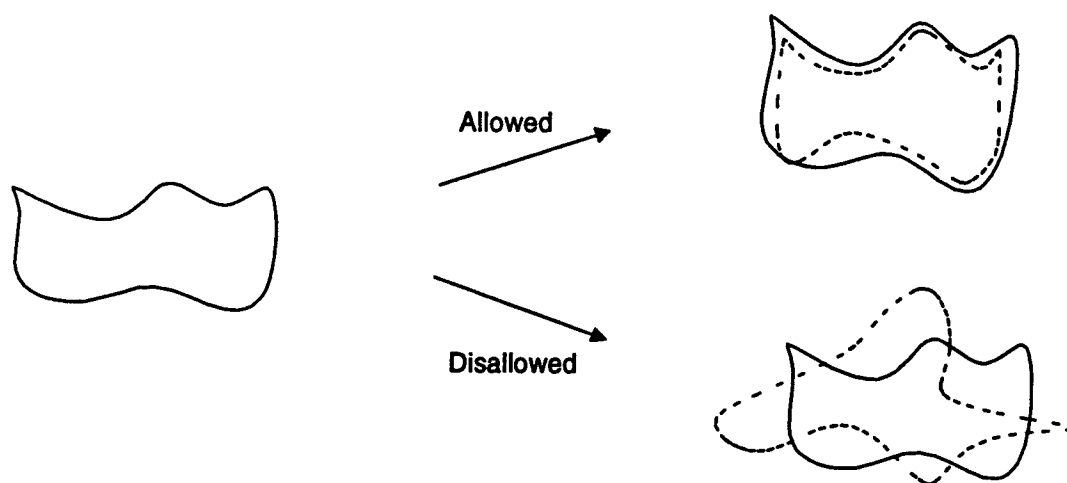
Figure 1-2   Pictorial Representation of the "Reaction Cavity" Concept. Reaction Cavity before Reaction (solid line) and at the Transition State (broken line)

An extension of the topochemical postulate which was introduced by Cohen is referred to as the reaction cavity.[12] It considers a reacting molecule in a crystal as a substance lying in a cavity formed by the presence of its adjacent molecules and the shape of the cavity is set by the packing of the crystals (Figure 1-2). Atomic and molecular movements necessary for a reaction cause pressure on the cavity wall which may become disordered, but any distortion in the shape of the cavity would be restricted by the closely packed environment. Cohen redefined the topochemical postulate to mean that those reactions which proceed under lattice control do so with minimal distortion of the surface of the reaction cavity. In cases where more than one reaction pathway is possible, the pathway leading to least disruption of the cavity would be favored.

Ramamurthy et al.[13] have further extended the concept of the reaction cavity and applied it to reactions in organized media other than crystals. This allowed them to rationalize reactivity in media such as organic inclusion hosts, silica and zeolite surfaces, micelles and liquid crystals.

The close fit of the reaction complex in the surrounding crystal results in product molecules which are a substitutional solute in the parent crystal. As the reaction proceeds, the product concentration increases until the solubility limit is exceeded and the reaction stops or the product crystallizes out in its own structure. In exceptional cases, where there is a structural similarity between the reactant and the product, the reaction preserves its crystallinity during the entire conversion of the starting material to the product. Such reactions are called topotactic or single crystal-to-single crystal transformations.[14] Very few examples of topotactic reactions are known. One that has been intensively studied, by Jones et al.,[15] is the photodimerization of pentanone 5 (Figure 1-3). It was observed that the packing arrangement of the starting material and the product are such that the reaction requires very little atomic motion. Most interestingly, the reaction was monitored directly during the dimerization by X-ray crystallography.
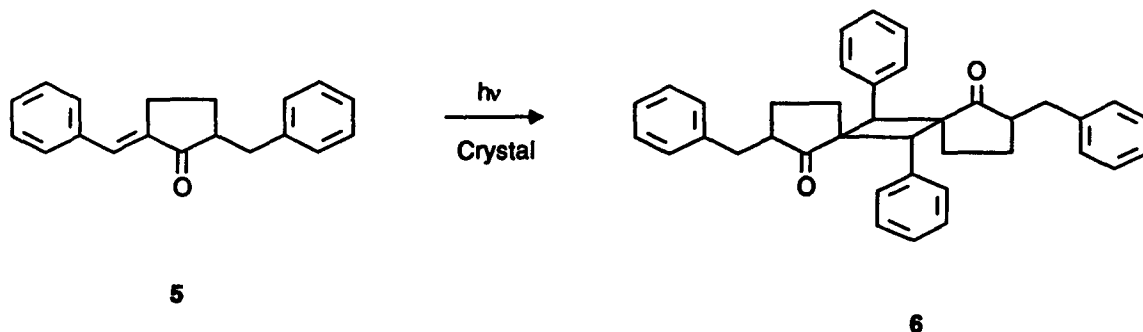
Figure 1-3   Photodimerization of Pentanone 5

Scheffer, Trotter and co-workers[8d,h,j,m] have systematically investigated unimolecular reactions in the solid state. They have identified a specific intermolecular effect, steric compression, that hypothetically modifies the solid state reactivity in a way similar to the reaction cavity concept.[16] They studied the photochemistry of cyclohexenone 7 and found that in solution, irradiation afforded quantitative yields of cage product 8, whereas irradiation of crystals of 7 gave compound 9 as the only product (Figure 1-4). The different reactivities in solution versus the solid state was explained in the following way: in solution relatively fast intramolecular [2+2] dimerization forms product 8 via the high energy conformation 7B. Since cyclohexenone 7 is locked in the minimum energy conformation 7A in the crystal, formation of product 8 is prevented and only the hydrogen abstraction-initiated product 9 is formed. This was unexpected because close analogues of compound 7 transfer a hydrogen to C(3), presumably to form the more stable radical center at C(2).[17] Biradical closure then leads to products similar to 10. X-ray crystallography revealed that there is close contact between the methyl group at C(3) and the methyl group of a neighboring molecule located below it in the lattice.
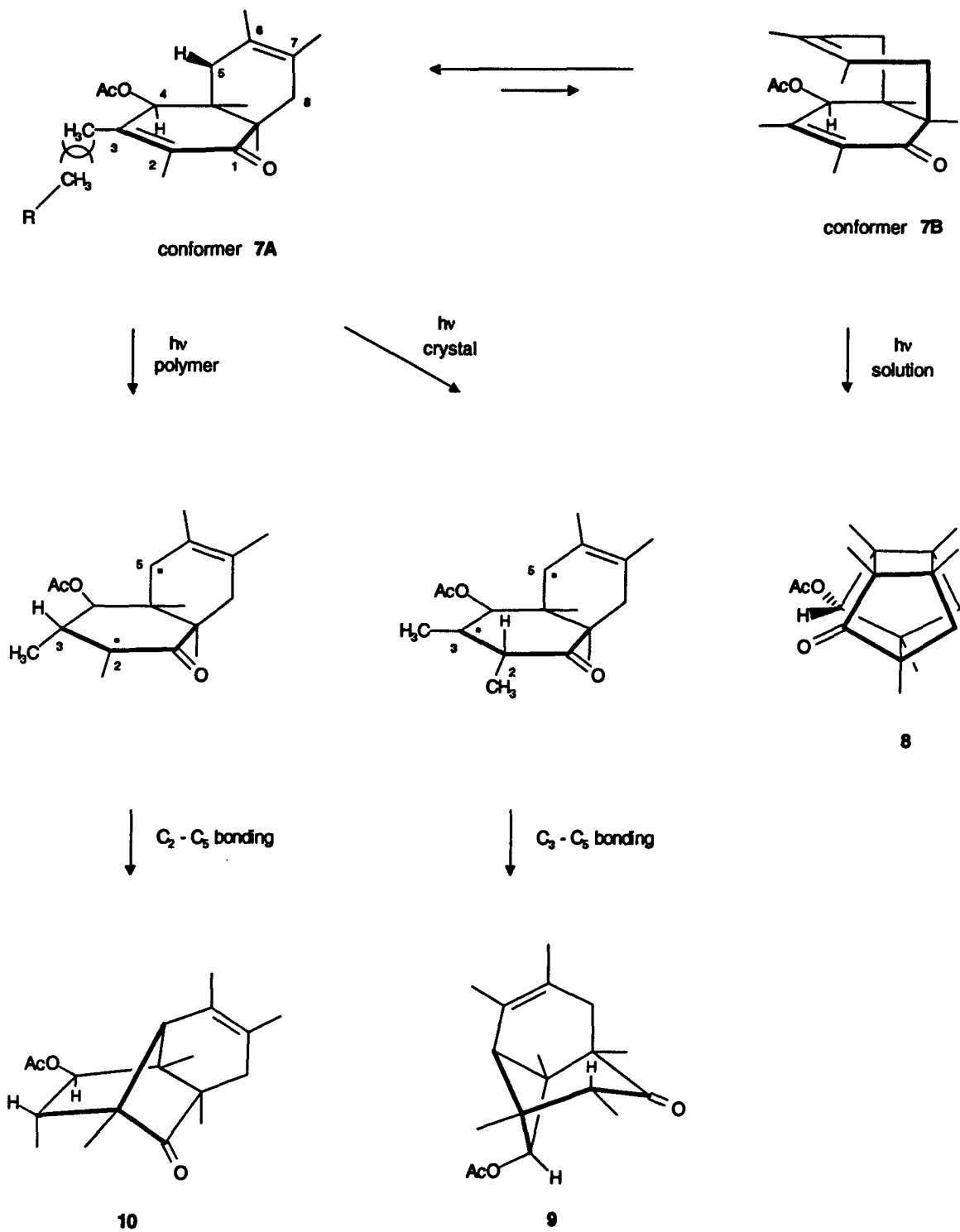
Figure 1-4   Medium Dependent Photochemistry of Cyclohexenone **7**

Consequently the authors suggested that this contact raises the activation energy of the normally favored hydrogen transfer to C(3) through steric hindrance caused by the downward motion of the methyl group which accompanies pyramidalization at this center. There is no such contact involving the methyl group attached to C(2), which explains formation of the observed product 9.

Further support for this hypothesis came from photolysis of enone 7 in polymer films.[18] It was expected that polymer matrices would provide a medium midway between solution and the solid state that lacks the specific close contact to the C(3) methyl group and also slows the conformational isomerization to 7B. Therefore, if steric compression was responsible for the unusual reactivity of enone 7 in the solid state, then in polymer films it should react normally to give compound 10 upon photolysis. Such was indeed what was observed experimentally.

Gavezzotti suggested that free volume or space in crystals determines reactivity in the solid state.[19] He explained that in the initial stage of a reaction the free volume or the available non-occupied space around the reactive centers controls the selectivity of the reaction because of the presence of relatively stationary neighbors. The free volume concept is by no means a departure from Cohen's reaction cavity concept, but can be viewed as an extension of it. The advantage of the Gavezzotti free volume concept is that it is better defined and can be quantitatively calculated. Furthermore it has been used successfully to explain solid state reactivity.[19,20]

The effects of a crystalline medium on a photoreaction can be divided into two categories. A primary effect controls the conformation of the reagent. In solution reactions can proceed from high energy conformations while in crystals reactions are generally limited to one low energy conformation. A secondary effect arises when the crystal lattice restricts the motions required for a given reaction through an intermolecular steric effect which depends on the crystal packing arrangement. Most of the postulates discussed above fall into this latter category.

1.3 Photoreactions in Organic Salt Crystals

Solid state photochemistry has focused mainly on reactions in molecular crystals while photoreactions of crystalline organic salts have not received much attention. The major difference between molecular crystals and crystals made from salts of the type $RCOO^-M^+$ and $RNH_3^+X^-$ is the force holding the crystal lattice together. Molecular crystals are held together by relatively weak dipole-dipole forces, van der Waals forces and in some cases by comparatively strong hydrogen bonds as well. As chemical changes in the solid state usually lead to softening and melting of the sample as the reaction proceeds, solid state reactions are stopped before any melting of the crystal is observed in order to obtain topochemical control. The lattice in salt crystals is held together by strong Coulombic attractive forces which are ionic in nature. This usually results in crystals with high melting points, increasing the chances of observing single crystal-to-single crystal reactions or at least allowing the solid state reactions to be carried out to higher conversions without loss of topochemical selectivity. Jones and co-workers[21] observed a topotactic photoreaction in organic salt crystals when they studied the [4+4] photodimerizations of various acridizinium salts (Figure 1-5). Interestingly the majority of these reactions were found to be of the single crystal-to-single crystal variety. X-ray structure analysis of the starting materials and dimers showed that dimerization requires considerable movement of the molecules in the crystal lattice. The authors suggested that concomitant movement of the anion minimizes the potential energy of the formed dimer crystals which allows topotactic reaction to be observed.
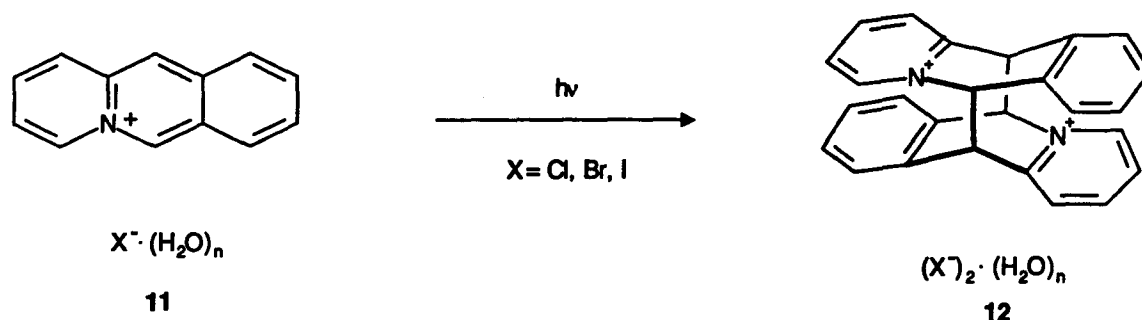
Figure 1-5   Photodimerization of Acridizinium Salt 11

The mutual solubility of most pairs of organic molecules is limited in the solid state,[8a] but the two component nature of organic salt crystals allows introduction of a chemically useful second constituent into the molecular crystal lattice. The normally passive counterion can thus be chosen to act as a sensitizer, quencher or optically active template for asymmetric synthesis. These properties of salts have not been widely exploited and one of the few example comes from Yap,[22] who utilized 3'-amino acetophenone as a solid state photosensitizer in an ammonium carboxylate type salt.

1.4 Asymmetric Photoreactions in the Solid State

A brief discussion of crystal chirality is necessary for a better understanding of solid state asymmetric synthesis. Molecules that are not superimposable on their mirror images are chiral and the molecular chirality derives from the dissymmetric, three-dimensional arrangement of the component atoms.[23] There are 230 possible ways to pack molecules into a crystal lattice and each corresponds to a different so-called space group.[24] Space groups can be chiral or achiral depending on the presence or absence of

symmetry elements that convert one enantiomorph into the other. Of the 230 possible space groups 65 are chiral. Crystal chirality arises from the dissymmetric spatial arrangement of molecules in the crystal lattice. Consequently, all resolved chiral molecules must crystallize in chiral space groups. Racemic compounds will either crystallize in racemic crystals that contain equal amounts of each enantiomer, or they will spontaneously resolve into chiral crystals of each enantiomer. It is far from common that racemic compounds resolve spontaneously upon crystallization,[3b] however, this phenomenon allowed Pasteur[25] in 1848 to perform the first optical resolution utilizing racemic sodium ammonium tartrate. Achiral molecules can also resolve spontaneously to yield chiral crystals. One of the most well studied examples of an achiral molecule which resolves into chiral crystals comes from Pincock et al.[26] They studied crystallizations of 1,1'-binaphthyl (13, Figure 1-6). Rapid equilibrium between the two enantiomeric conformations in the molten phase makes 1,1'-binaphthyl maintain its overall symmetry. Heating crystals of racemic 1,1'-binaphthyl leads to a metastable liquid, which crystallizes to form high melting crystals. When the melt crystallizes, random nucleation leads to the growth of chiral crystals containing mainly one of the enantiomeric conformations. The authors demonstrated that heating the low melting crystals without melting them led to formation of the high melting optically active crystals, that is the resolution occurs in the solid state as well.

S-(+)-13   R-(-)-13
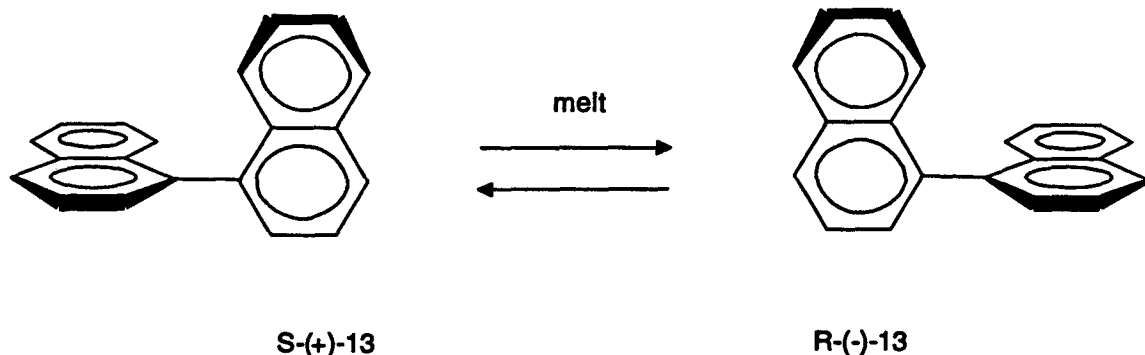
Figure 1-6   Enantiomeric Conformations of 1,1'-Binaphthyl

When chiral crystals are utilized to perform asymmetric synthesis, it is necessary to transform the chirality of the crystal into the molecular chirality of the product through a stereospecific solid state reaction. Only a few asymmetric syntheses in the crystalline phase have been reported in the literature due to the strict requirements for such reactions.[5] Absolute asymmetric reactions in the solid state are usually the result of accidental discoveries of an achiral compound which crystallizes in a chiral space group and undergoes a solid state reaction to give optically active products. Asymmetric syntheses can be studied systematically in the solid state using optically pure reagents to produce chiral crystals. An advantage of performing asymmetric transformations of chiral substances in the solid state over solutions is that the chiral center not only ensures chiral crystals but also exerts a second asymmetric influence in the chiral lattice of the crystal. In other words, it is not only the chiral center that resides in a chiral environment; the entire molecule is influenced by the chiral surrounding of the crystals.

It is possible to design an asymmetric reaction because structure-reactivity correlations make it possible to understand product formation and selectivity in the solid state. Planning an asymmetric reaction in the crystalline phase requires the molecules to pack into a crystal lattice in a manner which produces the necessary topochemical

13

characteristics to lead to the desired product. Crystal packing is hard to predict since the intermolecular forces that control the packing arrangement in crystals are not well understood. Attempts to steer molecules into certain pre-determined arrangements during crystallization (termed "crystal engineering") have been made.[11b, 27] Crystal engineering utilizes empirical packing generalizations, but this approach is not very advanced and consequently, obtaining specific crystal structures remains mainly heuristic.

The possibility of utilizing the chirality of crystals to achieve absolute asymmetric induction was first considered almost a century ago,[5b] but a better understanding of and experience with topochemically allowed reactions in the crystalline phase were needed before any success was achieved. The first example of an asymmetric photoreaction that made use of chiral crystals came from Schmidt and his co-workers,[28] who extended their study on [2+2] photodimerization in the crystalline phase and performed asymmetric photodimerizations as well. Their objective was to form crystals that contained a homogeneous distribution of two vinyl compounds. When this type of crystal is irradiated, it is possible to form homodimers as well as non-symmetrical heterodimers; crystals that are chiral may have the potential to exert enough face discrimination in the reaction so that an enantiomeric excess may be observed in the resulting heterodimers.

Schmidt and his co-workers[29] tested this concept on diarylbutadienes 14 and 15 (Figure 1-7). These compounds crystallize in the chiral space group $P2_12_12_1$, but yield achiral head to head dimers 16 and 17 when irradiated. However when a dilute (15%) solid solution of 15 in 14 was prepared and the longer wavelength-absorbing thiophene compound 15 selectively photolyzed, heterodimers 18 was obtained in 70% enantiomeric excess.
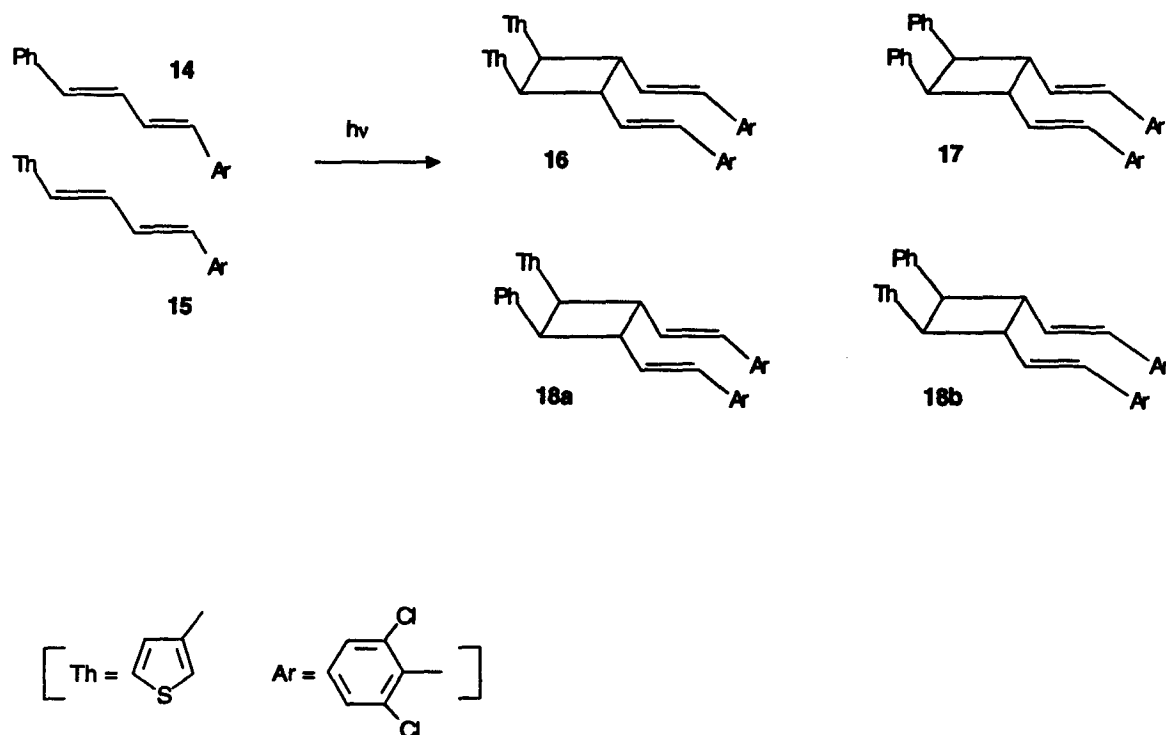
Figure 1-7   Absolute Asymmetric [2+2] Photodimerization of Compounds **14** and **15**

Analysis of the crystal structures[30] of the mixed crystals led Schmidt and co-workers to conclude that the ground state orientations of the reagents did not explain the enantiomeric selectivity. They suggested that compound **15** must deform in the excited state to favor formation of one of the enantiomers over the other. This hypothesis was further supported with theoretical calculations.[31]

Schmidt and his co-workers[28] recognized another approach for asymmetric [2+2] photodimerization which utilizes the packing arrangement of benzene-1,4-diacrylate derivatives. Hasegawa[32] had studied this type of compound earlier and discovered that it tends to crystallize in stacks in such a way that the two non-identical double bonds overlap.
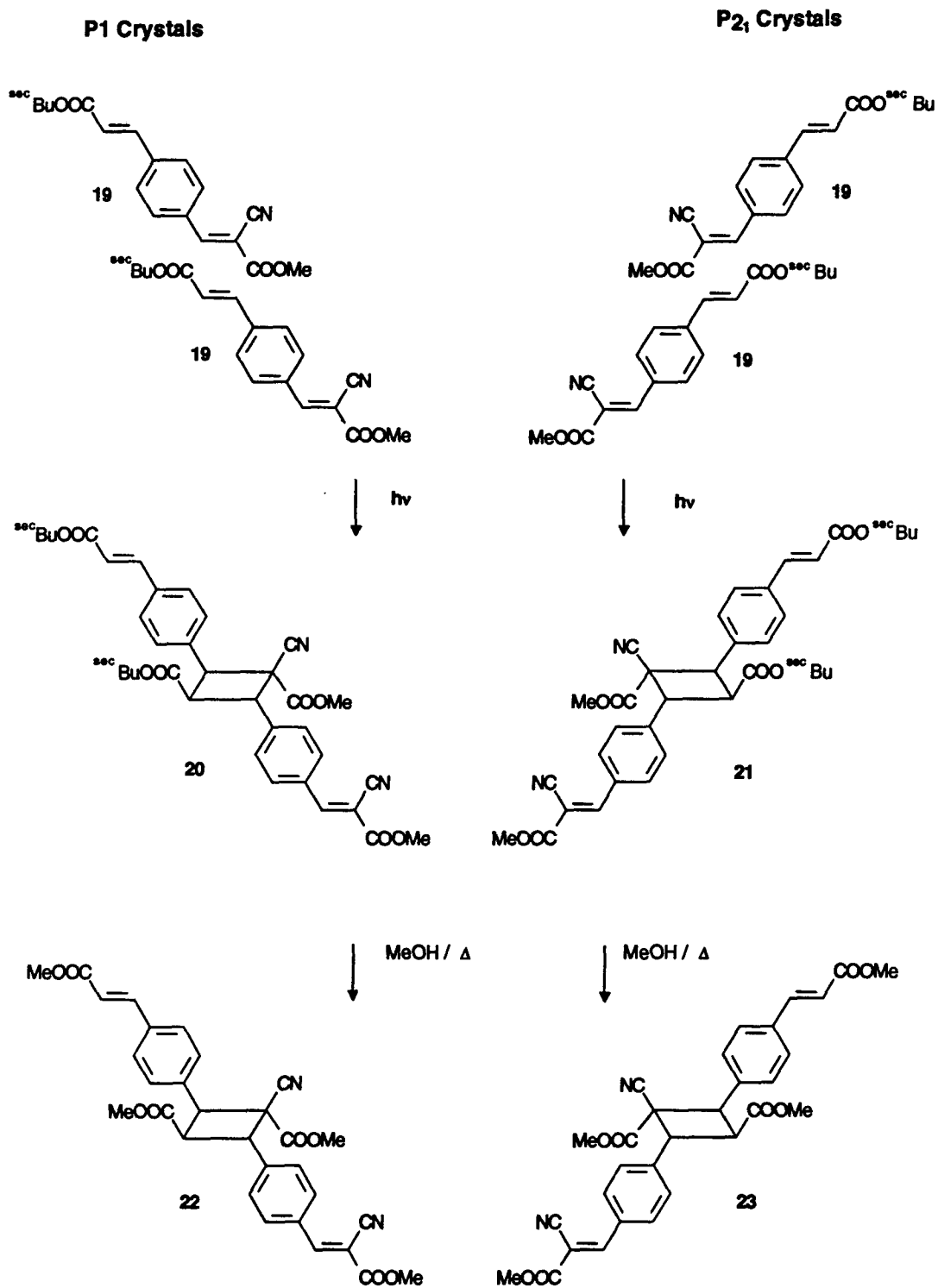
Figure 1-8   Asymmetric [2+2] Photodimerization of Compound **19**

Such an arrangement in the solid state leads to the generation of non-centric chiral photodimers. By inserting a chiral handle into this kind of molecule it is possible that the asymmetric induction of a solid state reaction in the chiral crystals yields enantiomeric excess in the photoproducts. Lahav and Addadi[33] tested this concept on benzene-1,4-diacrylate, **19**, which contains a resolved *sec*-butyl group to induce formation of chiral crystals (Figure 1-8). Compound **19** crystallized in two dimorphic modifications, P1 and P2₁. When crystals of the P1 form were photolyzed, quantitative diastereomeric yields of dimer **20** were obtained. In contrast, irradiation of the $P2_1$ form gave quantitative diastereomeric yields of dimer **21**. Transesterification of dimers **20** and **21** with methanol gave optically pure enantiomers **22** and **23** respectively. The authors argued that formation of both enantiomers of the same product in quantitative optical yields using only one handedness of chiral handle shows that the chiral crystal environment alone is responsible for the asymmetric induction. The chiral handle only serves to ensure the formation of chiral crystals.

Hasegawa[34] discovered an absolute asymmetric transformation in the solid state when he studied the [2+2] dimerization of compound **24** (Figure 1-9). Dimer **25** was formed in 100% enantiomeric excess when **24** was irradiated in the solid state. The photochemical behavior of compound **24**, as well as the asymmetric induction, could be readily interpreted by X-ray structure analysis. Molecule **24** crystallizes in the chiral space group $P2_12_12_1$ in a cisoid form. It is apparent from the X-ray structure that dimers of the same chirality are formed by reaction of either pairs of double bonds.

17
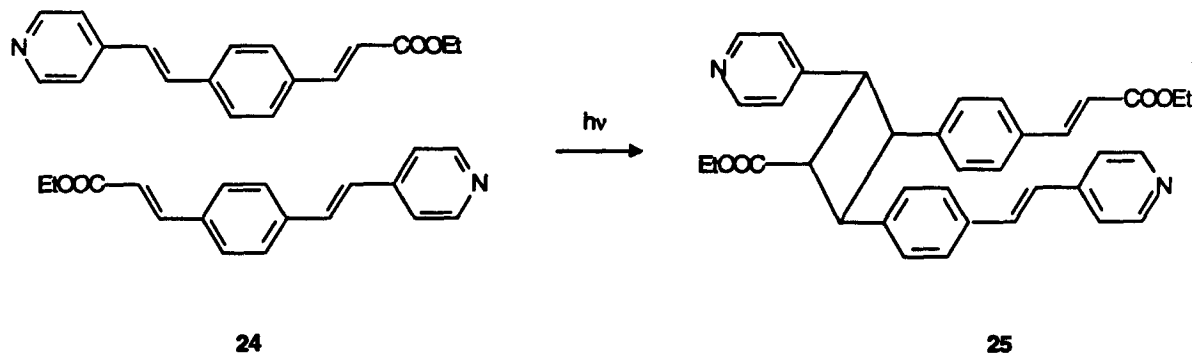
Figure 1-9   Absolute Asymmetric Photodimerization of Compound **24** in Chiral

Crystals

Asymmetric [2+2] photodimerizations have been studied systematically in the solid state and efforts have been made to design chiral crystals that have certain intramolecular as well as intermolecular features to gain selective reactions. This has resulted in a number of [2+2] photodimerizations in the solid state which afford products in good optical yields. Asymmetric unimolecular photoreactions have also been investigated but not as intensively. Two examples of absolute asymmetric Norrish type II reactions in chiral crystals have been reported. Scheffer, Trotter and co-workers[35] discovered that the adamantyl ketone **26** crystallizes in the chiral space group $P2_12_12_1$ (Figure 1-10). Solid state photolysis yielded cyclobutanol **27** in 80% enantiomeric excess via the Norrish type II reaction. The other example of an absolute asymmetric Norrish type II reaction in the solid state comes from Toda et al.[36] They found that compound **28**, which crystallizes in space group $P2_12_12_1$, yields β-lactam **29** in high optical yields when irradiated (Figure 1-10).
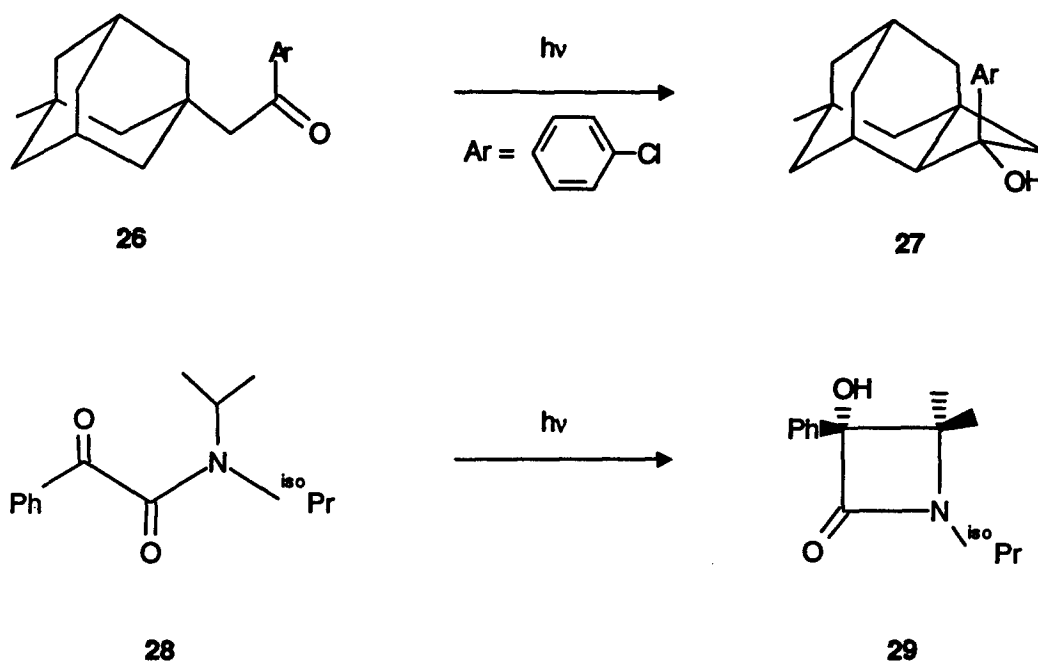
Figure 1-10   Absolute Asymmetric Norrish Type II Reactions in Chiral Crystals

An excellent example of how reaction pathways can be probed in chiral crystals comes from McBride and Feng.[37] The achiral compound **30a** crystallizes in chiral crystals and photolysis in the solid state yields a pair of 10-bromodecyl radicals (Figure 1-11). These radicals abstract an α-hydrogen to form secondary and primary pairs of radicals. ESR studies suggest that only one equatorial hydrogen is abstracted to form the α-pair. Further ESR studies of compound **30b** with deuterium in the α-positions demonstrated that when the α-hydrogens are replaced with deuterium, the two primary radicals abstract the δ-hydrogen to generate a pair of secondary radicals. This result was interpreted as being due to an isotope effect that changes the preferred site of abstraction from α to δ. The optically active form of the di-deuterated **30c** was synthesized in order to differentiate between the reactivity of the two α hydrogens in **30a** (Figure 1-11). The peroxide (**30c**) crystallizes in the chiral space group $P4_32_12$ or the enantiomorphous space

group $P4_12_12$, with almost equal probability since crystallization does not differentiate between deuterium and protium.
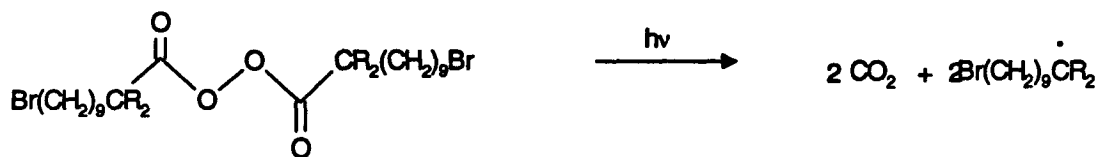
30: (a) R = H; (b) R = D
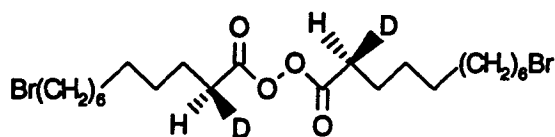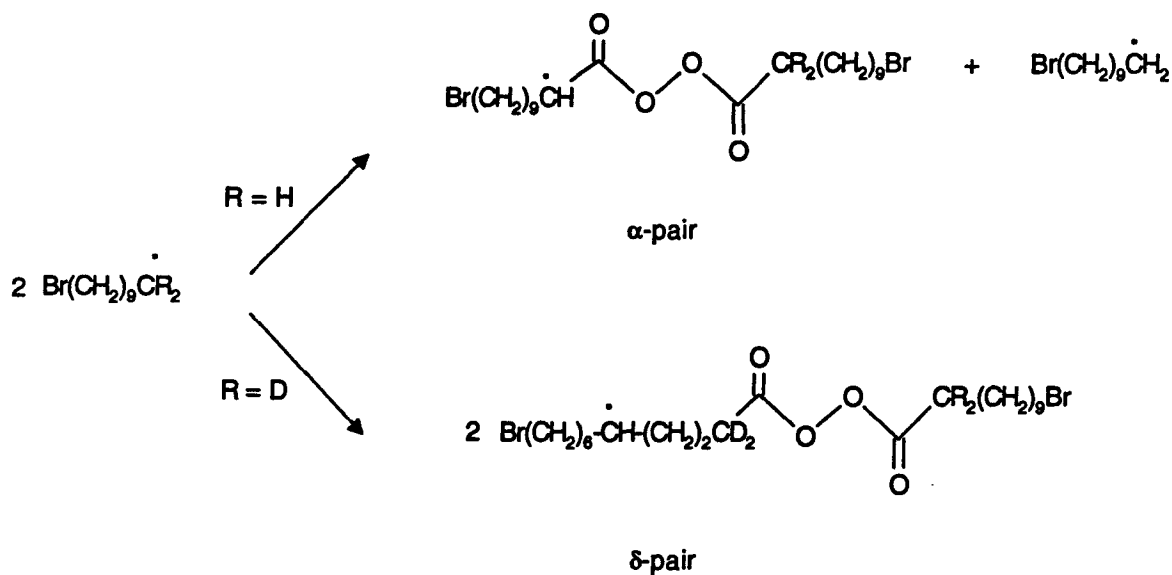
30c

Figure 1-11   Solid State Hydrogen Abstraction for Compound **30**

When the molecules crystallize in the space group $P4_32_12$, all protiums of the chiral center reside in the equatorial position and are in close proximity to the primary radical. Photolyses of these crystals and ESR studies confirmed that the α-pair of radicals is formed, presumably as the α-hydrogens are in a position favorable for abstraction. When compound **30c** crystallizes in the space group $P4_12_12$, the hydrogen and deuterium atoms exchange positions. In this enantiomorph, the protium is in the axial position which is not in close contact with the primary radical and is therefore not expected to be abstracted. On the other hand the deuterium in the equatorial position is not abstracted due to the isotope effect, which changes the preferred site of abstraction and, as the authors predicted, formation of the δ–pair is observed.

These examples illustrate that asymmetric phototransformations in the solid state are practical. The potential for asymmetric photosynthesis in the solid state is intimately connected to progress in the general field of solid state organic photochemistry. Further, it is noteworthy that asymmetric oxidation[38] has been achieved from molecules that crystallize in non-chiral space groups, provided that the crystals contain a polar axis. No asymmetric photochemical reaction has yet been reported from such crystals.

1.5 The Di-π-methane Rearrangement

The reaction under investigation in this thesis is the so-called di-π-methane rearrangement, one of the most thoroughly studied photochemical reactions.[39] As its name implies, the di-π-methane rearrangement is the rearrangement of a system of two π-bonds connected via a saturated carbon atom. The commonly accepted mechanism is shown in Figure 1-12. This mechanism was first proposed by Zimmerman[40] in 1967 and has been successful in predicting the results for a large number of reactions, although the

discrete existence of the initial 1,4-biradical remains questionable. Both aliphatic and aromatic π-bonds are capable of participating in this reaction. The chemoselectivity and regioselectivity of the di-π-methane rearrangement have been studied intensively.[41] Several processes are known to be capable of competing with the di-π-methane rearrangement. These include photocycloadditions, cis-trans isomerizations and sigmatropic shifts. The regioselectivity that arises from unsymmetrically substituted dienes depends on the system under investigation, but generally the regioselectivity can be interpreted as favoring the most stable biradical intermediate in the Zimmerman mechanism.

1,4 - diene   vinylcyclopropane
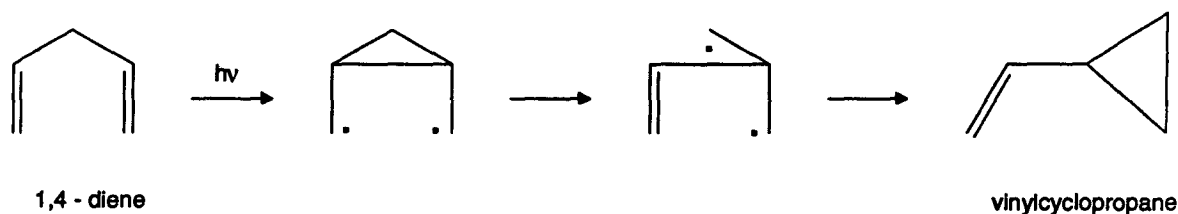
Figure 1-12   Representation of a Di-π-methane Rearrangement

Recently Scheffer et al.[8j, l, m, 42] have carried out studies on the solid state di-π-methane rearrangement. This research has concentrated mainly on dibenzobarrelene and its various derivatives, which rearrange to form the corresponding semibullvalene derivatives. When the Zimmerman mechanism for the di-π-methane rearrangement is applied to dibenzobarrelene bearing different substituents on the vinyl bond, two regioisomeric products are possible. Scheffer et al.[42] discovered that the regioselectivity is affected by the reaction medium when they investigated the photobehavior of esters 31a, 31b, 31c and 31d (Figure 1-13). Solution photolyses afforded photoproducts 32 and 33. Regioisomer 33 in which the smaller ester group occupies the more sterically

congested position, was slightly favored. In contrast, the solid state irradiations were much more selective for each compound but without any general trend. Two explanations were considered to interpret the regioselectivity in the solid state.

Figure 1-13   Regioselectivity of the Di-π-methane Rearrangement in Esters 31a to 31d
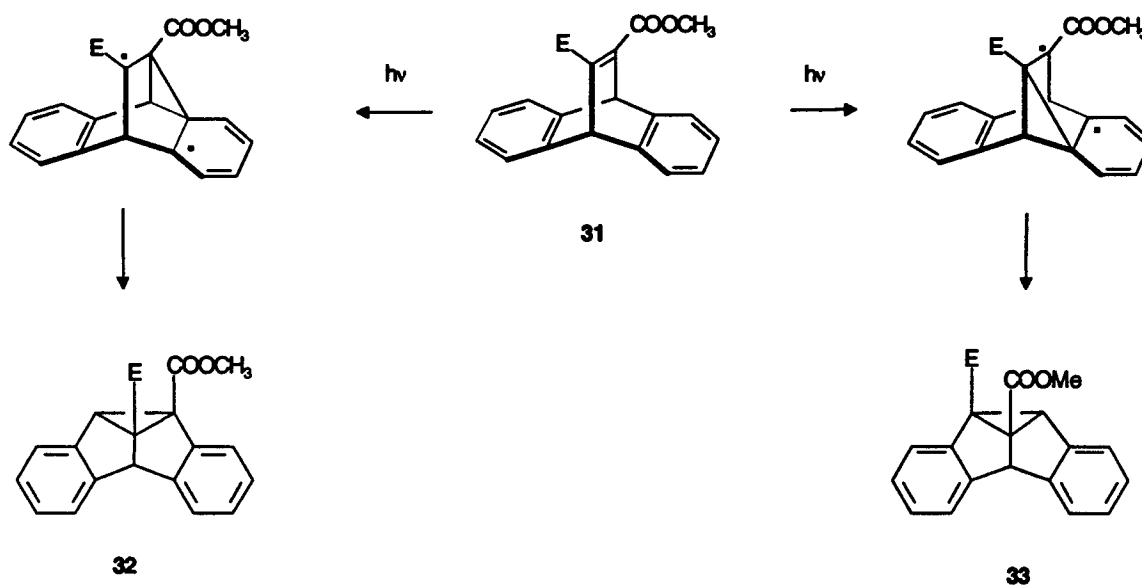
Compound	E	32:33 Ratio	
		Solution	Solid State
31a	COOCH$_2$CH$_3$	47:53	55:45
31b	COOCH(CH$_3$)$_2$	45:55	7:93
31c	COOC(CH$_3$)$_3$	40:60	85:15
31d	COOCH(CH$_3$)CH$_2$CH$_3$	40:60	1:99

First, attempts were made to explain the regioselectivity by comparing which of the two ester groups was better capable of stabilizing the initial radical on the vinyl bridge. The ester group which has a more coplanar arrangement to the vinyl bond in the crystals is more conjugated and is better capable of stabilizing the radical by resonance.

23

Therefore initial vinyl bridging should occur at the less conjugated ester group. X-ray structure analysis of the starting materials revealed that this theory does not explain the observed regioselectivity.

The second explanation suggested that steric effects between the reacting molecule and its neighbors controlled the regioselectivity. The authors hypothesized that the ester group attached to the bridging vinyl atom must move considerably during the benzo-vinyl bridging process and is therefore most likely to experience unfavorable steric interaction with the crystal lattice. Based on the crystal structure data, non-bonded contacts between the moving ester group and the crystal surroundings were estimated by a computer simulation of the benzo-vinyl bridging process and used to obtain potential packing energy calculations, which showed the increase in potential energy of the lattice was much smaller for the pathways observed experimentally in all cases.

One of the most interesting results in these studies done by Scheffer et al.[35,43] was the mapping of the absolute steric course for a reaction in the solid state. They discovered that the achiral dibenzobarrelene derivative **34** crystallizes in two dimorphic forms, Pbca and $P2_12_12_1$, where the latter is a chiral space group. Irradiation of **34** in solution and in the Pbca dimorph yielded photoproduct **35** as a racemic mixture. In comparison, irradiation of the $P2_12_12_1$ crystals gave quantitative optical yields of compound **35**. In solution, the di-π-methane rearrangement of compound **34** is four fold degenerate. Figure 1-14 depicts the four possible pathways, where pathways I and II lead to one enantiomer and pathways III and IV to the other. There must be complete discrimination between paths (I + II) and (III + IV) in the solid state because quantitative enantiomeric excess was obtained in the photoproducts. In order to differentiate between these pathways, the absolute configurations of the starting material and its photoproduct were determined by using the Bijovet method.[44] The absolute configurations were found to be (11M, 12P) and (4bS, 8bS, 8cS, 8dS) for the starting material and the photoproduct, respectively.
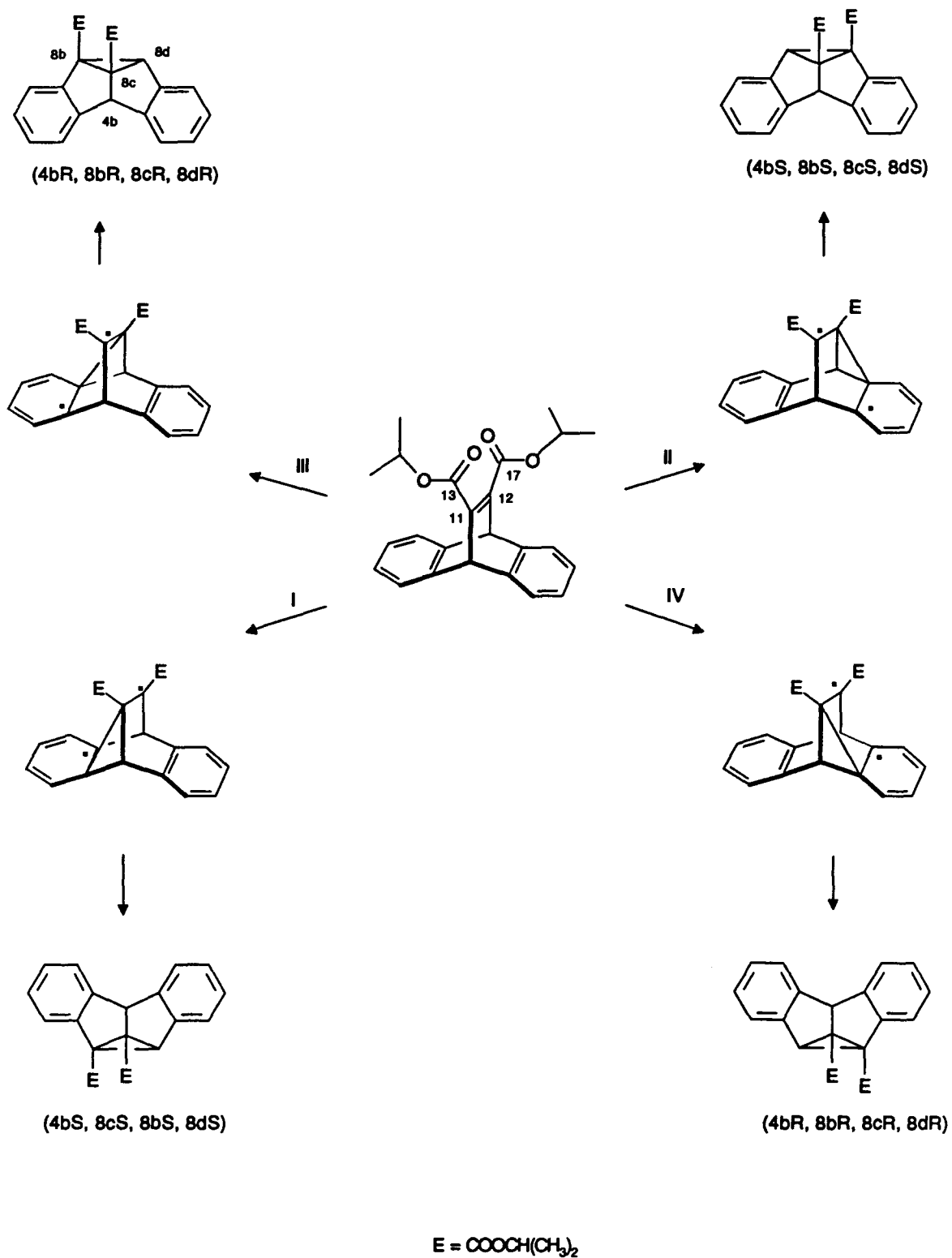
Figure 1-14   Four Different Pathways for the Di-π-methane Rearrangement in Ester 34

The designation 11M, 12P for ester **34** focuses on the site of dissymmetry around the ester groups in the molecule and uses the conformational chirality formalism for assigning absolute configuration.[45] The absolute configuration is specified around the single bonds, C11-C13 and C12-C17, by determining the smallest torsion angle between the groups of highest priority attached to each end of these single bonds. M stands for a negative torsion angle and P for a positive one. Comparison of the absolute configuration of the photoproduct and the starting material indicates that pathways I and or II are followed in the rearrangement.

34   **35**
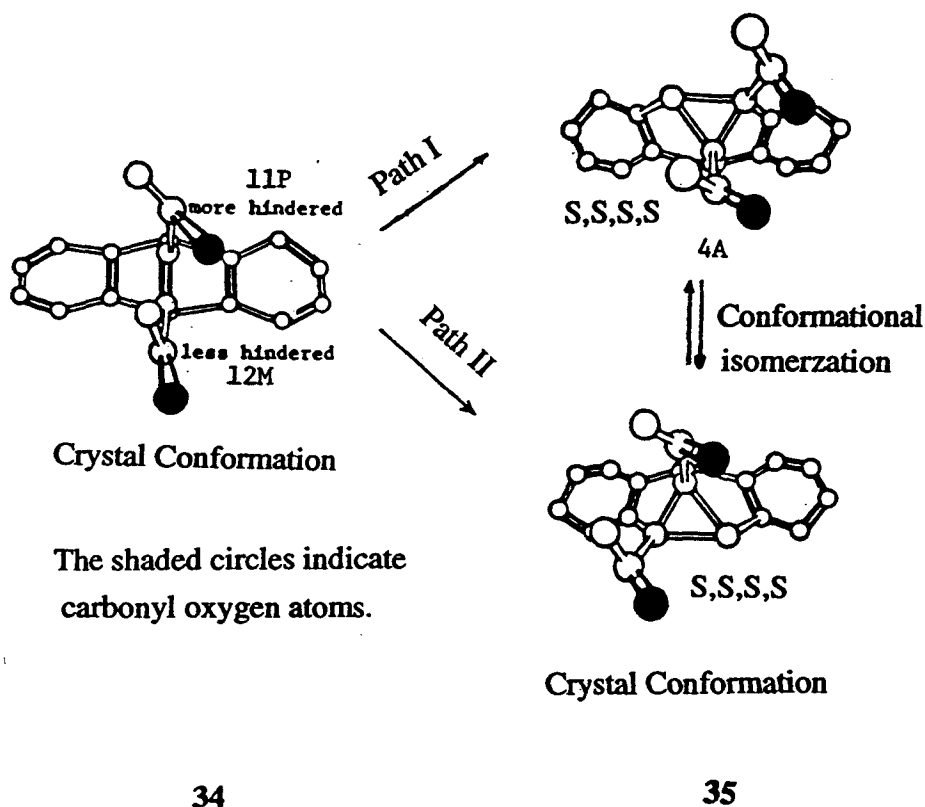
Figure 1-15   Crystal Conformation of Compounds **34** and **35**

Furthermore the authors suggested that pathway II is favored over pathway I by comparing the X-ray conformation of photoproduct **35** with the X-ray conformation of

the starting material. Assuming a least motion process, pathway II produces photoproduct 35 directly in its final crystal conformation whereas topochemical reaction via pathway I would lead to the unobserved conformer of product 35 (Figure 1-15). Further support for this interpretation came from inspection of the local lattice environment of the starting material, which shows that the free space surrounding the ester group at C12 is greater than the free space around C11.

1.6 Research Objectives

The central theme of this thesis is photochemistry in the solid state. The main emphasis will be on reactions that utilize crystal chirality for asymmetric induction. As discussed previously, achiral molecules can, though rarely, crystallize in chiral space groups and undergo chemical processes that transfer the chirality of the crystals to molecular chirality of the products. Introducing a resolved chiral handle onto the reactant ensures chiral crystals, since chiral compounds must crystallize in chiral space groups. A chiral handle can be introduced conveniently onto a substrate by salt formation with an optically active counterpart. When such a salt undergoes a solid state reaction at least one new chiral center must be formed in the achiral part of the salt so that the enantiomeric excess in the photoproducts can be used to measure the extent of the asymmetric induction by the crystalline medium.
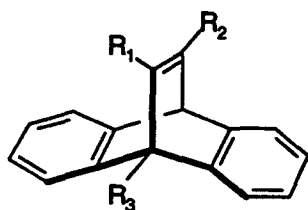
	R₁	R₂	R₃
36:	COOH	COOEt	H
37:	COOH	Me	H
38:	COOMe	COOMe	COOH
39:	COOMe	COOMe	NH₂

Figure 1-16   Dibenzobarrelene   Derivatives   Selected   for   Studying   Asymmetric
Induction in Chiral Salt Crystals

Dibenzobarrelene derivatives show the characteristics needed for studying asymmetric induction in chiral salt crystals. First of all dibenzobarrelene derivatives bearing functional groups such as carboxylic acids or amines which are necessary to form salts with chiral counterions can easily be synthesized. Four unsymmetrically substituted dibenzobarrelene derivatives were selected for this study: three carboxylic acids, **36**, **37** and **38**, and one amino compound, **39** (Figure 1-16). Secondly, as mentioned earlier, photolysis of unsymmetrically substituted dibenzobarrelene derivatives in solution and in the solid state yields chiral dibenzosemibullvalenes, where four new chiral centers are generated. Such dibenzobarrelene derivatives are excellent for studying both the regio- and the enantioselectivity of the di-π-methane rearrangement because the dibenzobarrelene skeleton has four different 1,4-diene systems (Figure 1-17). Each of these four systems is associated with a pathway that leads to a different product. As shown in Figure 1-17 pathways I and II lead to regioisomer A while pathways III and IV give regioisomer B. Furthermore pathways I and II lead to different enantiomers of isomer A. Similarly, pathways III and IV yield the opposite enantiomers of isomer B. It should be mentioned that enantioselectivity is only expected under conditions where a resolved dissymmetric influence affects the reaction.

The approach taken in this work to investigate unsymmetrically substituted dibenzobarrelene derivatives allows the regioselectivity of the di-π-methane rearrangement to be studied. The first part of this thesis will deal mainly with the regioselectivity exhibited by the starting materials prior to salt formation. The photochemistry of the esters of the carboxylic acids will also be investigated. This allows the regioselectivity of the acids to be compared with the regioselectivity of their corresponding esters giving better insight into the effect of hydrogen bonding on the regioselectivity. Any observed differences between solution and solid state reactivities will be investigated further by X-ray structure analysis of the reactants in an attempt to establish structure-reactivity correlations.

The second part of this thesis will investigate photoreactions of salts of the dibenzobarrelene starting materials formed with optically active counterparts. The extent of asymmetric induction in the chiral crystalline phase will be studied by measuring the enantiomeric excess of the photoproducts. The chiral crystals make it possible to study the effects of the crystal lattice on the four different pathways followed by the di-π-methane rearrangement of the dibenzobarrelene derivatives (Figure 1-17). Regioselectivity verifies which two pathways, (I+II) or (II+IV), are favored. Enantioselectivity can then indicate which of the two pathways are followed for a given regioisomer, but to distinguish between these pathways the absolute configurations of the photoproduct and the reactant must be known. The main goal of studying asymmetric induction is to design a salt that produces only one regioisomer in high optical yield. This would allow mapping of the reaction pathway and consequently X-ray structure analysis of the reactant has the potential to identify the crystal forces controlling regio- and enantioselectivity. Studying optically active salts of different dibenzobarrelene derivatives makes it possible to compare these crystal forces in different systems and search for a general explanation for the stereoselective pathways the di-π-methane rearrangement follows in these dibenzobarrelene systems
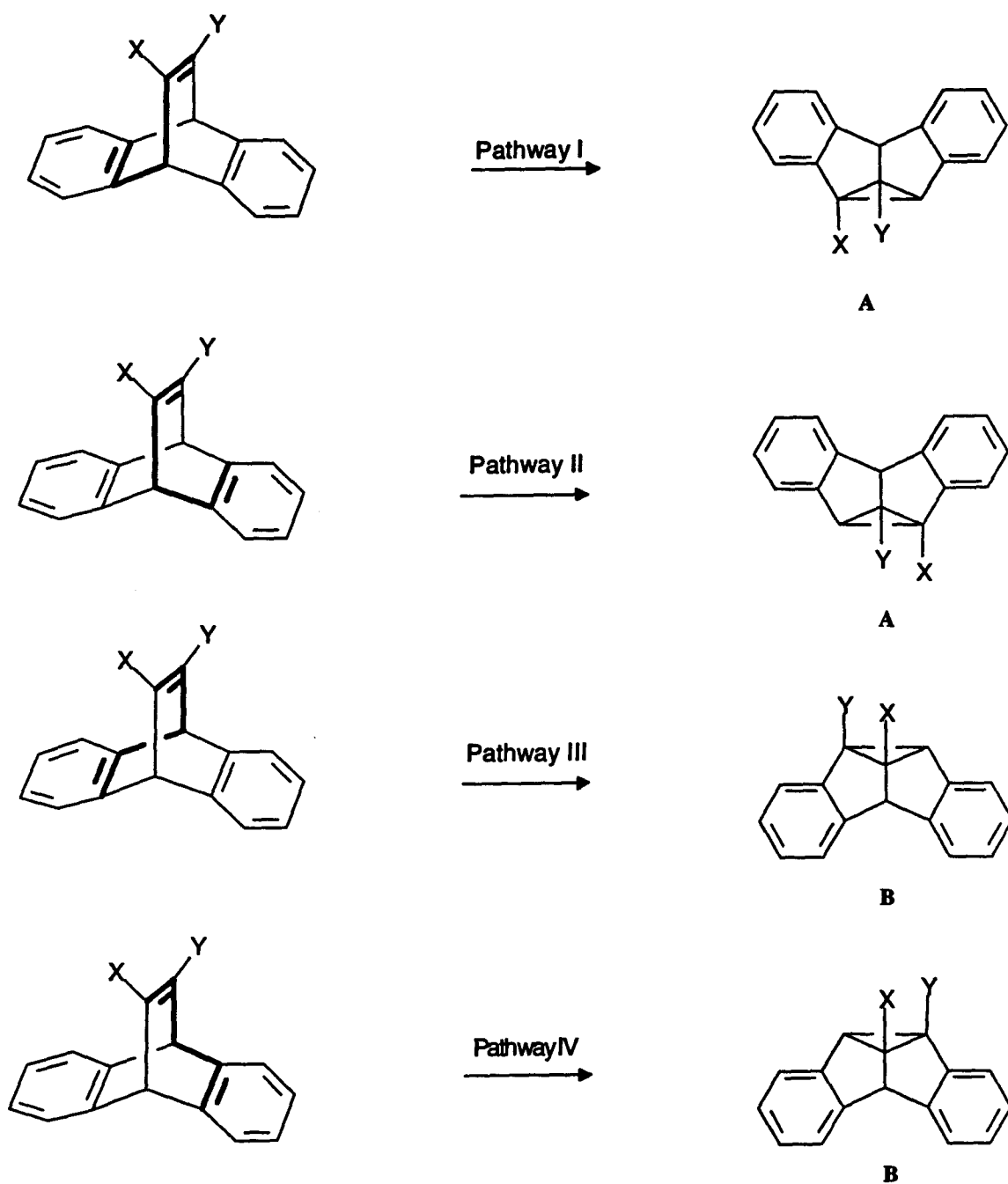
Figure 1-17   The Four Di-π-methane Systems in the Dibenzobarrelene Skeleton

A property of organic salt crystals is the strong lattice forces which bind them and lead to high melting points. This reduces the likelihood of crystal melting during reaction and may increase the probability of observing topotactic reaction. The final part of this thesis will concentrate on efforts made to observe single crystal-to-single crystal reactions for dibenzobarrelene acid **40** (Figure 1-18).

40
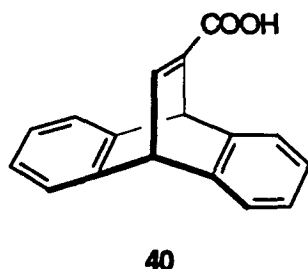
Figure 1-18   Dibenzobarrelene Derivative **40**

CHAPTER 2 RESULTS AND DISCUSSION

2.1 Preparation of Substrates

Dibenzobarrelene ester derivatives **39** to **46** were prepared by addition of an acetylenic ester derivative to the corresponding anthracene derivative according to the method of Diels and Alder[46] (Figure 2-19).

Compound	R_1	R_2	R_3
39	NH_2	$COOCH_3$	$COOCH_3$
41	H	CH_3	$COOCH_3$
42	H	H	$COOCH_2CH_3$
43	$COOCH_3$	$COOCH_3$	$COOCH_3$
44	$COOCH_2CH_3$	$COOCH_3$	$COOCH_3$
45	H	$COOCH_3$	$COOCH_3$
46	CHO	$COOCH_3$	$COOCH_3$
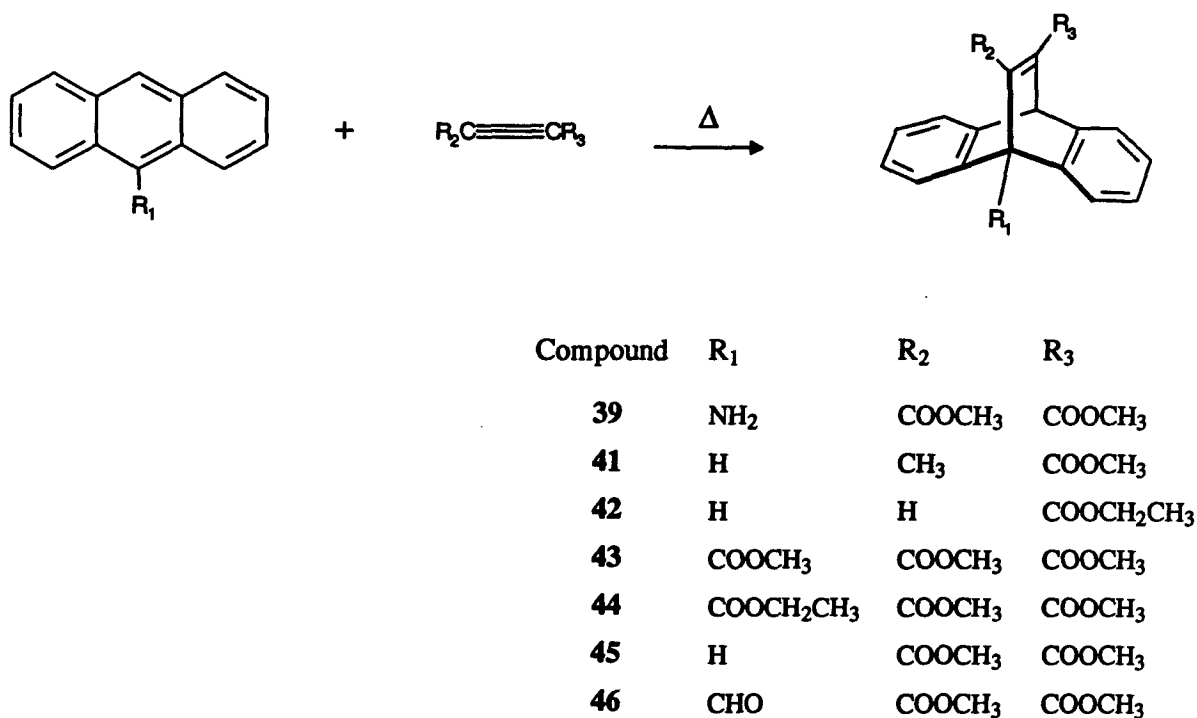
Figure 2-19   Preparation of Dibenzobarrelene Derivatives via the Diels-Alder Reaction

All of the acetylenic ester derivatives and anthracene itself are commercially available. 9-Anthraldehyde is also commercially available, but the other 9-substituted anthracenes were synthesized as follows: 9-amino anthracene was obtained by reduction of 9-nitroanthracene with stannous chloride.[47] The methyl[48] and the ethyl[49] esters of 9-anthracene carboxylic acid were made via the 9-anthracene acid chloride obtained by reaction of the 9-anthracene carboxylic acid with thionyl chloride.

12-Methyl-9,10-dihydro-9,10-ethenoanthracene-11-carboxylic acid (37) was obtained by hydrolysis of methyl 12-methyl-9,10-dihydro-9,10-ethenoanthracene-11-carboxylate (41) with aqueous NaOH.[50] Similarly, hydrolysis of the Diels-Alder adduct 42 with aqueous NaOH yielded 9,10-dihydro-9,10-ethenoanthracene-11-carboxylic acid (40, Figure 2-20).[50]

41: R₁ = CH₃, R₂ = CH₃
42: R₁ = H, R₂ = CH₂CH₃

1. NaOH
2. H⁺

37: R₁ = CH₃
40: R₁ = H
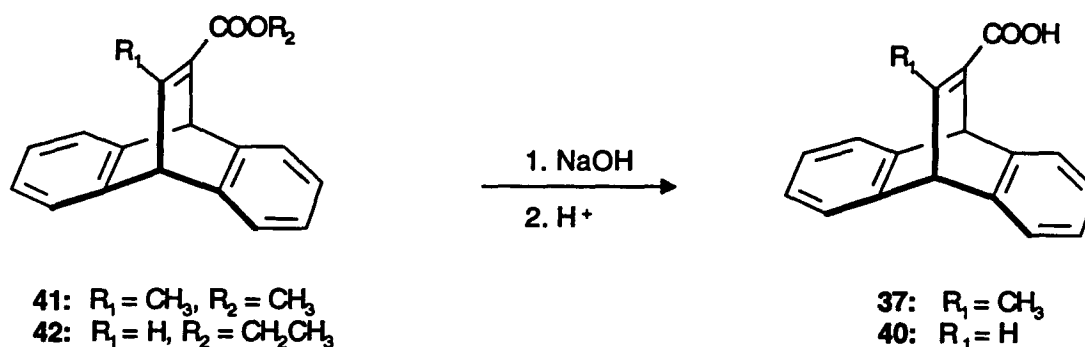
Figure 2-20   Preparations of Acids 37 and 40

The sequence followed to prepare ester acid 36 is illustrated in Figure 2-21. The initial step is the Diels-Alder addition of dimethyl acetylenedicarboxylate to anthracene to yield ester 45. Hydrolysis of ester 45 with aqueous NaOH gives the di-acid 47.[50] The acid anhydride 48[50] was formed by refluxing the di-acid 47 with oxalyl chloride. Finally addition of ethanol to anhydride 48 afforded the desired ethyl 9,10-dihydro-9,10-ethenoanthracene-11-carboxylate-12-carboxylic acid (36).
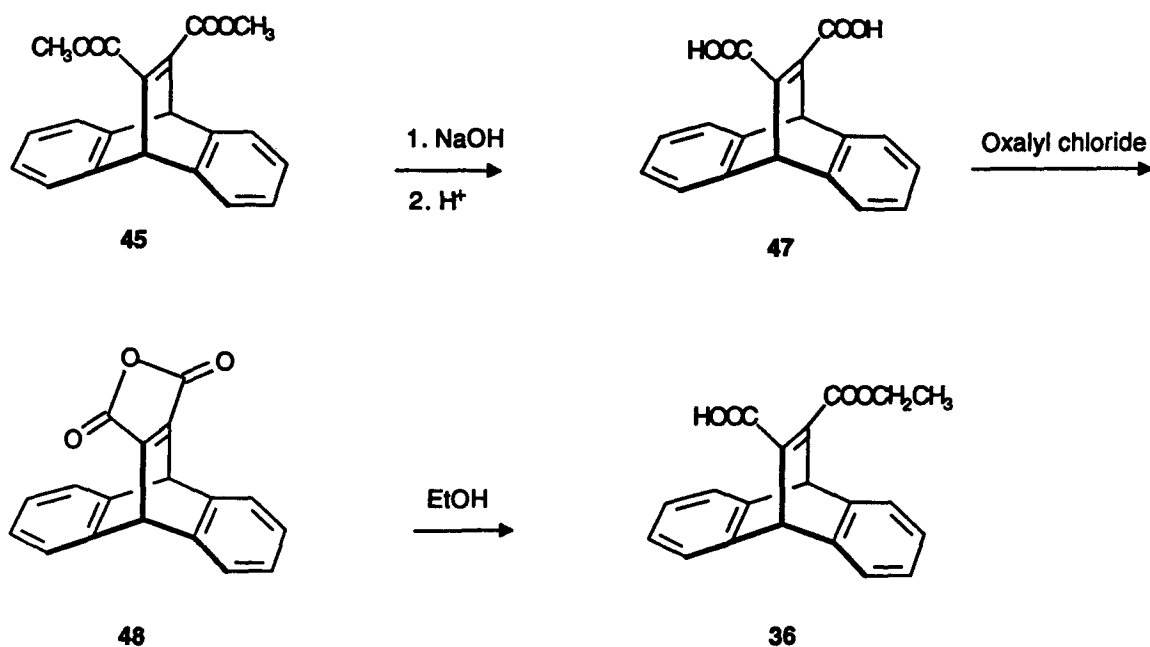
Figure 2-21   Preparation of Ester-Acid **37**

Dimethyl   9-carboxy-9,10-dihydro-9,10-ethenoanthracene-11,12-dicarboxylate acid (**38**) was obtained in the following manner: aldehyde **46** was formed by Diels-Alder addition of dimethyl acetylenedicarboxylate to 9-anthraldehyde.[51] Oxidation of aldehyde **46** with NaClO$_2$ according to the method of Lindgren et al.[52] yielded ester-acid **38**.
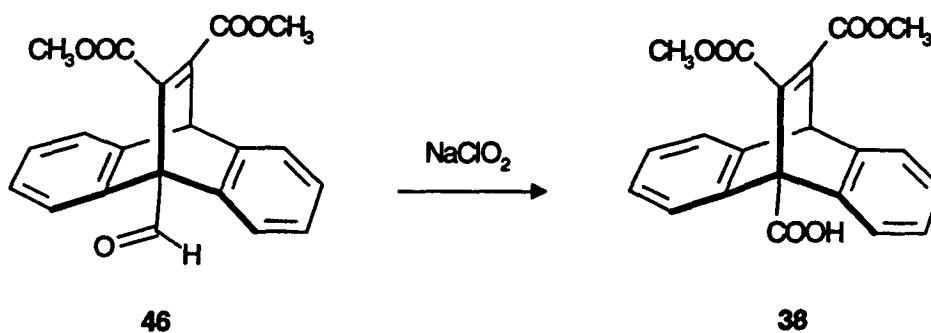
Figure 2-22   Preparation of Ester-Acid **38**

All compounds prepared were fully characterized by spectroscopic and analytical methods and X-ray structure analyses in some cases. The spectra of previously reported compounds were identical to those reported in the literature. The syntheses and characterizations are described in greater detail in the Experimental Section (Chapter 3).

2.2 Photochemical Studies of the Starting Materials Prior to Salt Formation

2.2.1 Photolyses of Ethyl 9,10-Dihydro-9,10-ethenoanthracene-11-carboxylate-12-carboxylic acid (36)

As mentioned earlier, Scheffer et al.[42] studied the photochemistry of the di-ester **31a**, which is the methyl ester of ester-acid **36**. Photolysis of ester **31a** yielded photoproducts **32a** and **33a**, with no selectivity in solution or in the solid state (Figure 2-23). According to Zimmerman's mechanism,[53] initial vinyl benzo bridging is the product-determining step. The initial radical on the vinyl bond is formed next to the vinyl substituent that can better stabilize it. The lack of preference for either product was explained in terms of both ester groups having the same radical stabilizing ability.
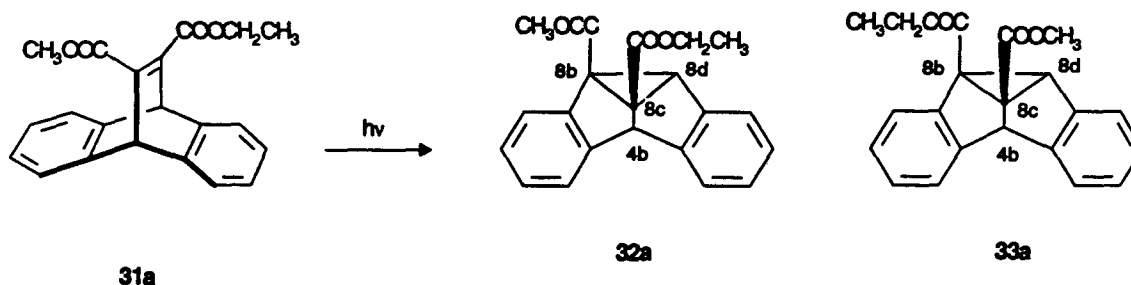
Figure 2-23   Photolysis of Di-Ester **31a**

The authors characterized photoproducts **32a** and **33a** from ^{1}H-NMR analyses. One of the isomers has a methyl singlet at $\delta = 3.87$ ppm and a methylene quartet at $\delta = 4.18$ ppm. The other has the methyl singlet at $\delta = 3.73$ ppm and the methylene quartet at $\delta = 4.35$ ppm. The **8b** benzylic position is more deshielded than the **8c** position, therefore the more deshielded methyl singlet was assigned to isomer **32a** which has the methyl ester in the **8b** position. The same holds true for the methylene signals of the ethyl ester groups. The more deshielded signal is assigned to regioisomer **33a** where the ethyl ester is in the **8b** position. These chemical shift differences seem to be characteristic of regioisomers of these kinds and their use in assigning structure is also supported by correlations of ^{1}H-NMR spectral interpretation to X-ray crystal structures done by Scheffer et al.[42]
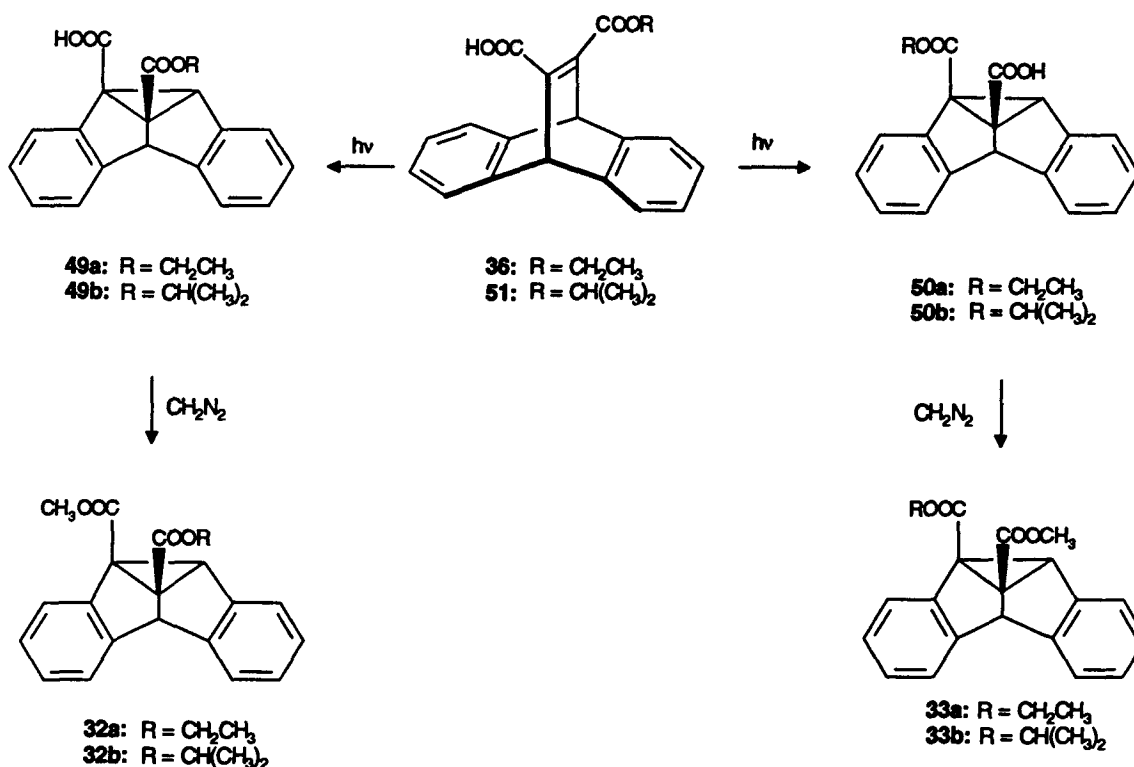
Figure 2-24   Photolysis and Work-up of Ester-Acid **36** and **51**

The photochemistry of ester-acid **36** was studied in solution and in the solid state. The results are listed in Table 2-1. Photoproducts **49a** and **50a** (Figure 2-24) were not isolated but were converted into products **32a** and **33a** by treating the reaction mixture with excess diazomethane. This allowed each photoproduct to be isolated by column chromatography. Product ratios were determined by GC analysis of the reaction mixture.

Table 2-1 illustrates that the photochemical behavior of ester-acid **36** is different from that of di-ester **31a**. The regioselectivity of the di-π-methane rearrangement of ester-acid **36** is strongly influenced by the photolysis medium. In the solid state isomer **33a** was the only product obtained, whereas solvents such as acetone and acetonitrile give mixtures of photoproducts **32a** and **33a**. In contrast, photolyses in benzene and aqueous $NaHCO_3$ solutions give quantitative yields of **32a**.

Table 2-1   Medium Dependent Photochemistry of Ester-Acids **36** and

51

Solvent	Ester-acid **36**		Ester-acid **51**[54]	
	Concentration	Ratio **32a:33a**[a]	Concentration	Ratio **32b:33b**[a]
Aqueous $NaHCO_3$	0.01[b]	100:0	0.01[b]	90:10
MeCN	0.01[b]	57:43	0.01[b]	50:50
Benzene	0.05	100:0	0.06	60:40
"	0.001	100:0	0.01	72:28
"	0.0005	100:0	0.001	83:17
Crystals		0:100		5:95
Acetone	0.01	60:40		

[a] The estimated error in the GC analysis is ±5%. [b] The product ratio is unaffected when the concentration is changed from 0.1 to 0.001M. [c] Conversion was kept below 10%.

These photochemical results for **36** are similar to those observed when Garcia-Garibay et al.[54] studied the photochemical behavior of ester-acid **51** The regioselectivity for ester-acid **51** in different media is listed in Table 2-1 as well. The main difference between the reactivities of **36** and **51** is in benzene solution. The regioselectivity for ester-acid **51** in benzene is concentration dependent, whereas no such effect was observed for **36**.

Garcia-Garibay et al.[54] suggested that the regioselectivity is controlled by different hydrogen bonded forms of ester-acid **51** in different media. They identified and studied three hydrogen bonded forms, **51A**, **51B**, **51C** of ester-acid **51**.[54b] Species **51A** is a monomer which is hydrogen bonded to a solvent molecule; **51B** is an intramolecular hydrogen bonded form of ester-acid **51**; and **51C** is an intermolecular hydrogen bonded dimer (Figure 2-25). The authors showed that structure **51C** is predominant in concentrated solutions in non-polar solvents and in the solid state, whereas structure **51A** is dominant in polar solvents and **51B** in non-polar solvents at low concentrations.

36: $R_1 = CH_2CH_3$
51: $R_1 = CH(CH_3)_2$
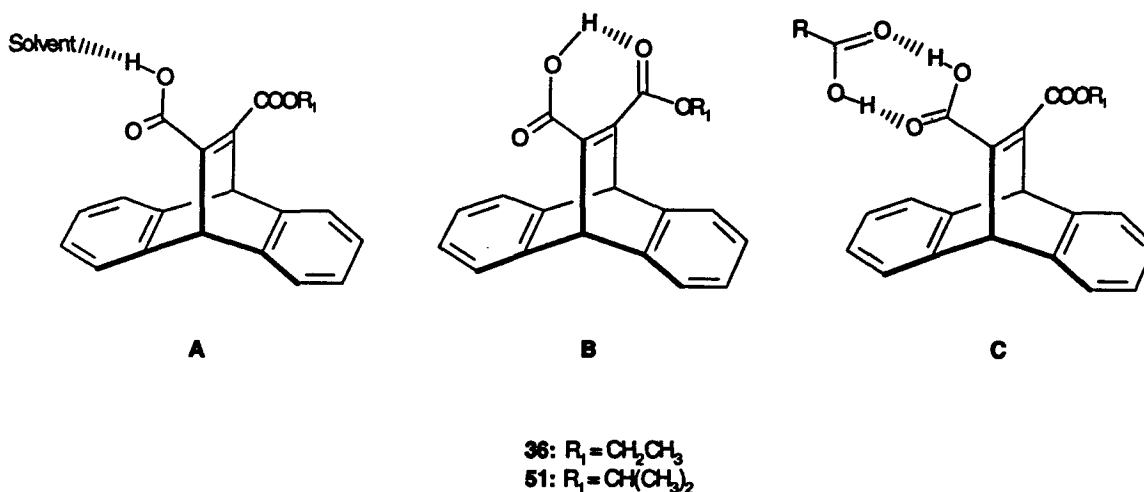
Figure 2-25   Different Hydrogen Bonded Forms of Ester-Acids **36** and **51**

The predominance of form **51A** in polar solvents such as acetone and acetonitrile explains the lack of regioselectivity in these media. Neither product **32b** or **33b** is favored since the solvent bonded acid group has a similar radical stabilizing ability as the ester group. In aqueous $NaHCO_3$ solution, however, ester-acid **51** exists as an anion and Garcia-Garibay et al.[54] hypothesized that a radical center adjacent to an ester substituent is better stabilized than one next to a carboxylate anion, since only product **32b** is observed.

X-ray structural analysis of ester-acid **51** showed that **51C** is the only species present in the crystal. The authors rationalized that the dimeric hydrogen bonding in the carboxylic acid group keeps it tightly "frozen" in the crystal lattice and hinders the motions necessary to form the initial vinyl benzo bridging next to the acid group. On the other hand, formation of photoproduct **33b** leaves the hydrogen bond relatively undisturbed and is thus favored.

Garcia-Garibay et al.[54] showed that structure **51B** dominates in benzene solutions at low concentrations where product **32b** is favored. The authors proposed an excited state proton transfer interaction for species **51B** in which a proton is transferred from one oxygen to the other to form species **51D** (Figure 2-26). Cristol et al.[55] have shown that dibenzobarrelene with carbocation in the 11 position represents the condition necessary for a positive charge initiated 1,2-aryl shift which would favor regioisomer **32b**. With increased concentration, species **51C** becomes more ubiquitous and hence formation of product **33b**. The authors concluded that the product ratio seemed to be determined by the relative amounts of **51B** and **51C** at a given concentration.

The explanation used to interpret the regioselectivity of the di-π-methane photorearrangement of ester-acid **51** can also be applied to ester-acid **36**. Infrared spectroscopy can be utilized to explore the different hydrogen bonded forms of ester-acid **36** in different reaction media.
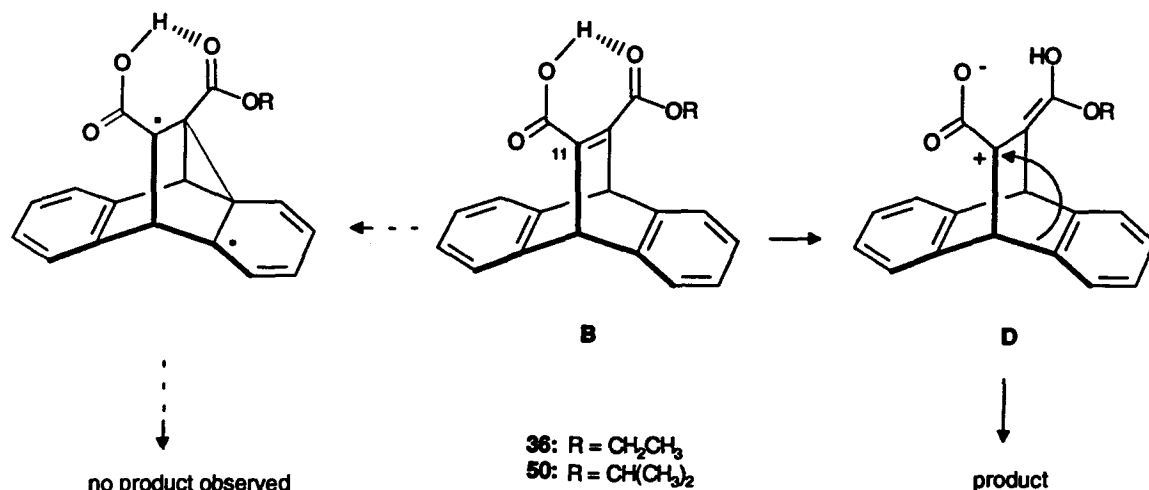
Figure 2-26   1,2 Aryl Shift of Ester-Acids **36** and **51**

The X-ray crystal structure of ester-acid **36** has not been obtained, but the solid state infrared spectrum suggests a dimeric carboxylic acid structure. The O-H stretching absorption was obtained as a very broad and relatively structureless band in the region 3500-2400 cm⁻¹ which is characteristic for carboxylic acid dimers.[56] The carbonyl bonds are observed at 1734 and 1678 cm⁻¹. The latter can be assigned to the acid carbonyl which is shifted to low frequency owing to the intermolecular hydrogen bonding (Figure 2-27). This is in good agreement with the solid state infrared spectrum for ester-acid **51** (3400-2200, 1724, 1680 cm⁻¹).

In acetonitrile, only one broad absorption band at 1714 cm⁻¹ is observed for the acid and the ester carbonyls. The O-H absorption in the region 3600-3500 cm⁻¹ indicates RC(O)O-H···solvent interaction (Figure 2-27). This is very similar to the infrared spectrum of ester-acid **51** in acetonitrile (3632, 3544, 1727 cm⁻¹). Hence a solvent bonded structure analogous to **51A** can be proposed for ester-acid **36** in polar solvent.

Spectrum recorded in C_6H_6

Spectrum recorded in CH_3CN

Spectrum recorded in KBr

3200   1600   400

1/cm
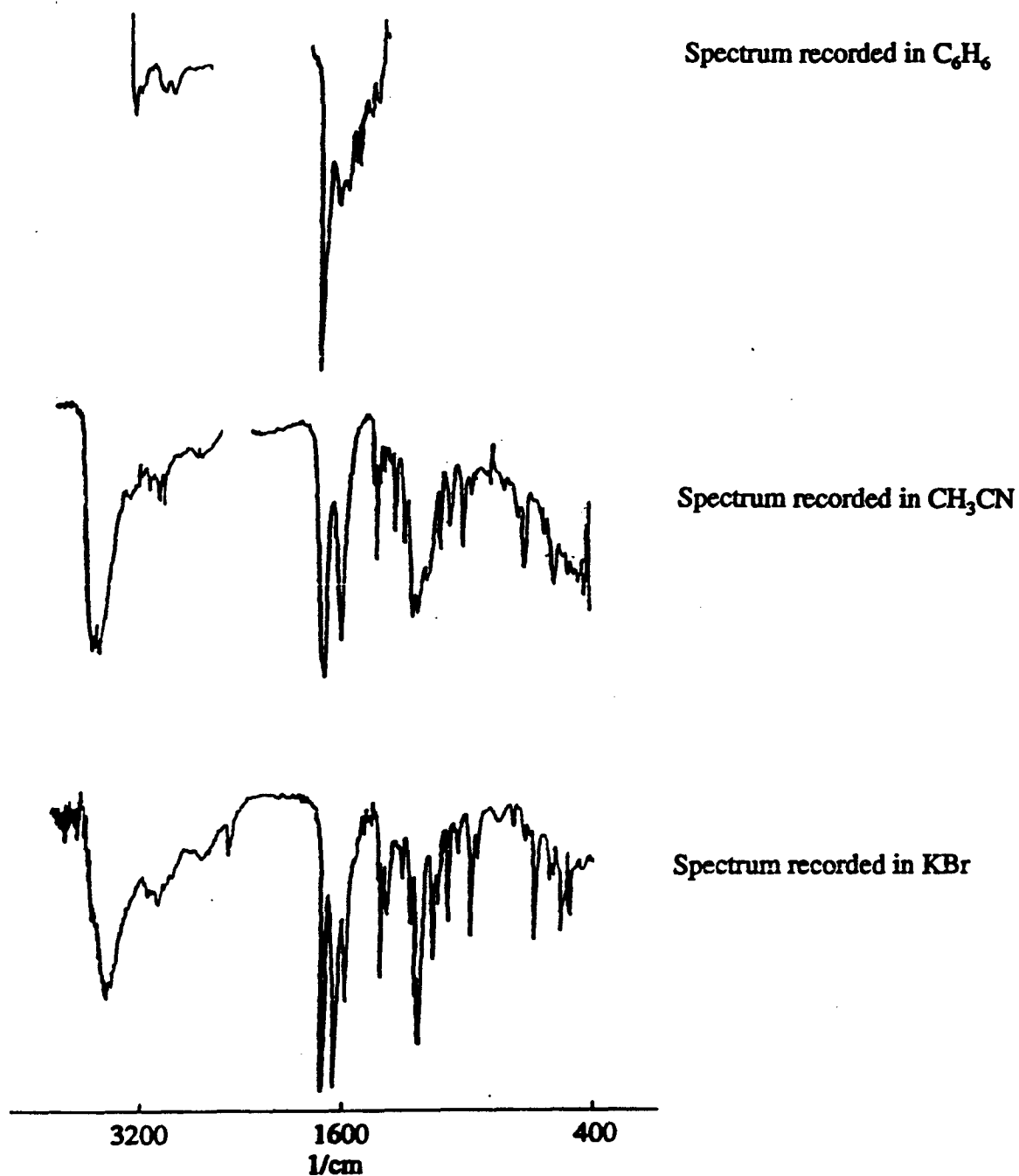
Figure 2-27   Medium Dependent Infrared Spectra of Ester-Acid 36

The infrared spectra of ester-acid **36** in C_6H_6 did not change when the concentration was increased from 0.005 M to 0.05 M. These spectra show an O-H band at low frequency (2800-2600 cm-1) which corresponds to intramolecular O-H bonding. The carboxylic acid band is observed at 1731 cm-1. A relatively weak carbonyl band is observed at 1673 cm-1 which is appropriate for an intramolecular hydrogen bonded ester. This infrared spectrum is very similar to the low concentration spectrum of ester-acid **51** in benzene (2780-2749, 1730, 1660 cm-1).

The carbonyl stretch of the ester group in ester-acid **36** is observed at higher frequencies in all spectra compared to ester-acid **51**. This difference can be attributed to the isopropyl substituent being capable of decreasing the stretching frequency of the carbonyl ester group relative to an ethyl substituent. Such a substituent effect is normally attributed to the inductive stabilization of the polar resonance form of the carboxylate group. This is illustrated very well in the frequency of the carbonyl resonance in the infrared spectra of a variety of alkyl benzoates[57] (Figure 2-28).

R	C=O (cm-1)
Me	1727
Et	1720
CH(CH₂)₃	1708
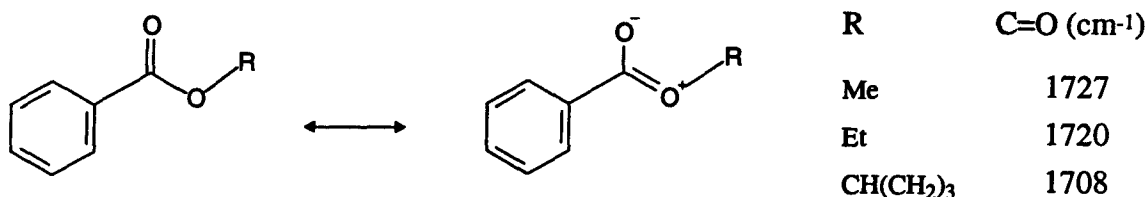
Figure 2-28   Inductive Effect of the Alkyl Substituent on the Infrared Carbonyl Stretching Frequency of Alkyl Benzoates

The infrared spectrum of ester-acid **36** in benzene suggests that the intramolecular hydrogen bonded structure **36B** is predominant at all concentrations in benzene solution. This is consistent with the results of the photochemical reaction of ester-acid **36** in benzene since only product **32a** is formed. For unknown reasons the equilibrium between

36C and **36B** is not shifted towards **36C** with increased concentration as is observed for ester acid **51**, at least over the concentration range tested.

2.2.2 Photolyses of 12-Methyl-9,10-dihydro-9,10-ethenoanthracene-11-carboxylate (37) and Methyl 12-Methyl-9,10-dihydro-9,10-ethenoanthracene-11-carboxylic acid (41)

Crystals of ester **41** exist in two different crystalline morphologies. Crystals grown from ethanol solutions melt at 137°C with immediate resolidification to form crystals which melt at 146°C.[50] Infrared spectra of the high and low melting crystals are different, which further supports that the idea these crystals are dimorphs.
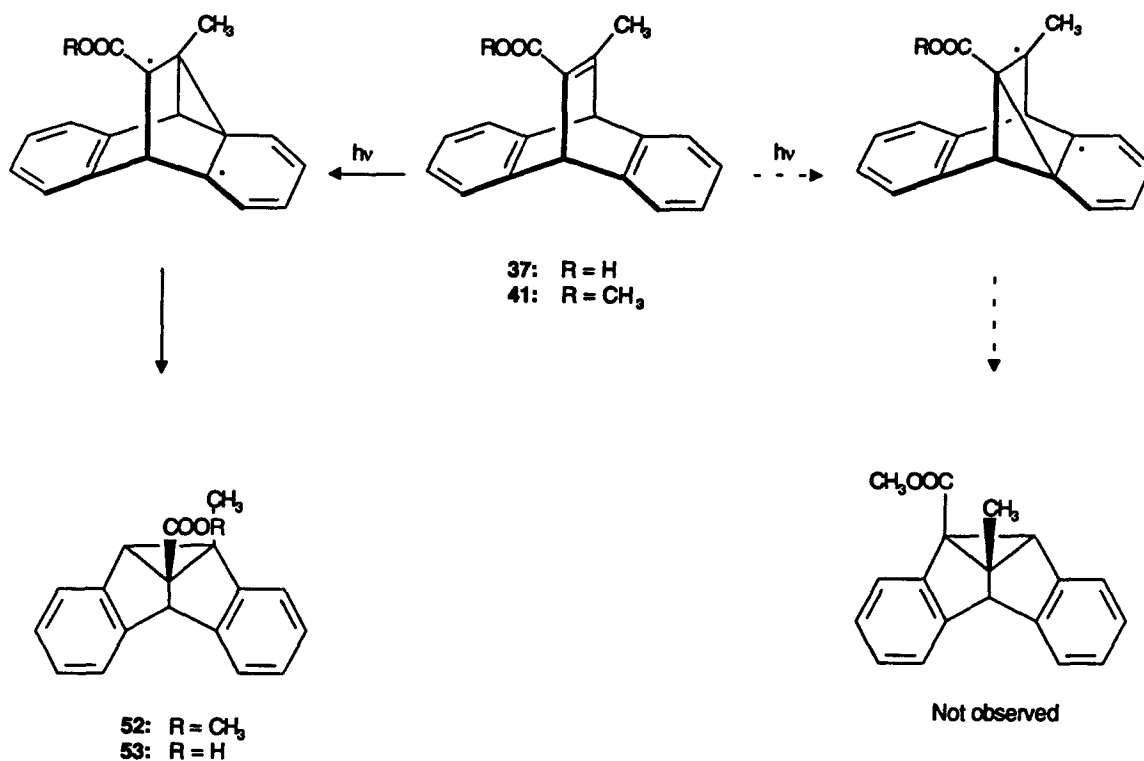
Figure 2-29   Photolysis of Compounds **37** and **41**

The photochemical behavior of both dimorphs is similar, and the only photoproduct formed is compound **52**. Direct and acetone-sensitized photolyses of ester **41** in solutions yielded only the photoproduct **52**.

The di-π-methane rearrangement of ester **41** can give two isomeric photoproducts, and determining which one of the two isomers is formed (Figure 2.29) can be achieved by analyzing the ^{1}H-NMR spectra of compound **52** in a similar way as for products **32a** and **33a**. The ^{1}H-NMR spectrum of the observed product can be compared to the spectra of the known analogs **54** and **55** (Figure 2-30).[58] Compound **54** has the ester group in the more deshielded **8b** position while compound **55** has the ester group in the **8c** position. The methyl singlet for ester **54** is at δ = 3.77 ppm while the methyl singlet for ester **55** is at δ = 3.72 ppm. Photoproduct **52** has the methyl ester signal at δ = 3.72 ppm in the ^{1}H-NMR which suggests that the ester is in the **8c** position. The structure of photoproduct **52** was confirmed with an X-ray diffraction analysis of a crystalline derivative of photoproduct **52**. The X-ray crystal structure of photoproduct **52** was obtained after a chiral handle was introduced into the molecule. This is discussed in detail in Section 2.4.2.

54   **55**
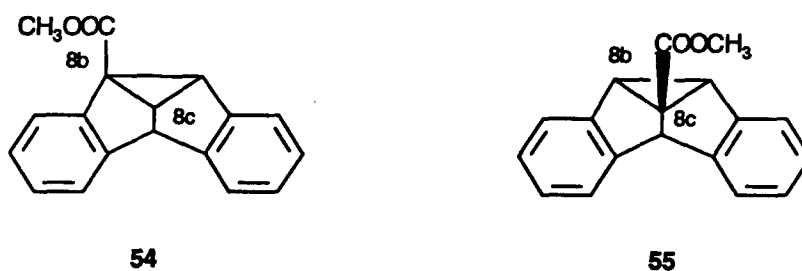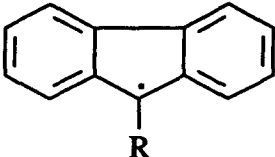
Figure 2-30   Structure of Compounds **54** and **55**

The photochemistry of acid **37** was studied in solution as well as in the solid state. The reaction mixtures were treated with excess diazomethane and analyzed by GC. Compound **52** was the only product formed under the various conditions.

The photochemistry of compounds **37** and **41** is similar in that the rearrangement is not affected by the reaction medium and only one di-π-methane photoproduct with the methyl substituent in the **8b** position is observed. The regioselectivity of the di-π-methane rearrangement of dibenzobarrelenes with substituents at the bridgehead positions has been investigated thoroughly, but little is known concerning the effect of substituents located on the vinyl bond.[59] Zimmerman[53] has suggested that the radical termini of the cyclopropyldicarbinyl biradical become electron rich during the di-π-methane rearrangement. Consequently, the regioselectivity of the di-π-methane rearrangement is controlled by the polar nature as well as the radical-stabilizing ability of the substituents. In order to explain the regioselectivity for compounds **37** and **41** the radical stabilization ability and the polar effects of the substituents must be compared.

Bordwell et al.[60] have developed a semiempirical method for estimating relative radical stabilization energies. They compared the radical stabilizing ability of various groups in the 9-substituted fluorenyl radical with the substituted methyl radical (Figure 2-31). In the methyl radical a carboxylic acid group is a slightly better stabilizer than a methyl group. In contrast, a methyl group stabilizes the 9-fluorenyl radical slightly better than an ester group. It was suggested that intramolecular steric inhibition of resonance between the ester group and the fluorenyl moiety decreased the radical stabilizing affect of the ester group compared to the methyl group. However, the authors came to the conclusion that methyl, acid and ester groups have very similar radical stabilizing effects. Clearly the relative radical stabilizing effects of the substituents in compounds **37** and **41** will not explain the regioselectivity.

R	9-Substituted Fluorenyl	R	Substituted Methyl Radical
CH_3	4.5 kcal/mol	CH_3	3.3 kcal/mol
$COOCH_3$	3.9 kcal/mol	COOH	5.7 kcal/mol

Figure 2-31   Comparison of Radical Stabilization Energies of 9-Substituted Fluorenyl
and Substituted Methyl Radicals

Even though a methyl group has a similar radical stabilizing effect as an ester group, it is electron donating whereas the ester group is electron withdrawing.[61] If, as Zimmerman suggests,[53] the radical center is electron rich, we may suggest that photoproduct 52 is formed exclusively owing to the preference of the radical to be formed next to the electron withdrawing ester group rather than the electron donating methyl substituent. Formation of photoproduct 53 (Figure 2.29) can be explained in a similar way.

It is interesting to apply the hypothesis used above to explain the regioselectivity of the di-π-methane photorearrangement of the monosubstituted dibenzobarrelenes 56 and 57 (Figure 2-32). Ciganek[58] demonstrated that dibenzobarrelene 56 gave only product 55 when irradiated. The initial radical is formed next to the ester group which is both a better radical stabilizer and a better electron withdrawing group than a hydrogen. Cristol et al.[62] studied the photochemistry of compound 57 and found that regioisomers 58 and 59 were formed in the ratio 6:4. The radical stabilization ability of the methyl group favors formation of product 58 whereas the electron donating effect favors formation of product 59 and hence a mixture of both products is formed.

56: R = COOCH₃
57: R = CH₃

55: R = COOCH₃
58: R = CH₃

59
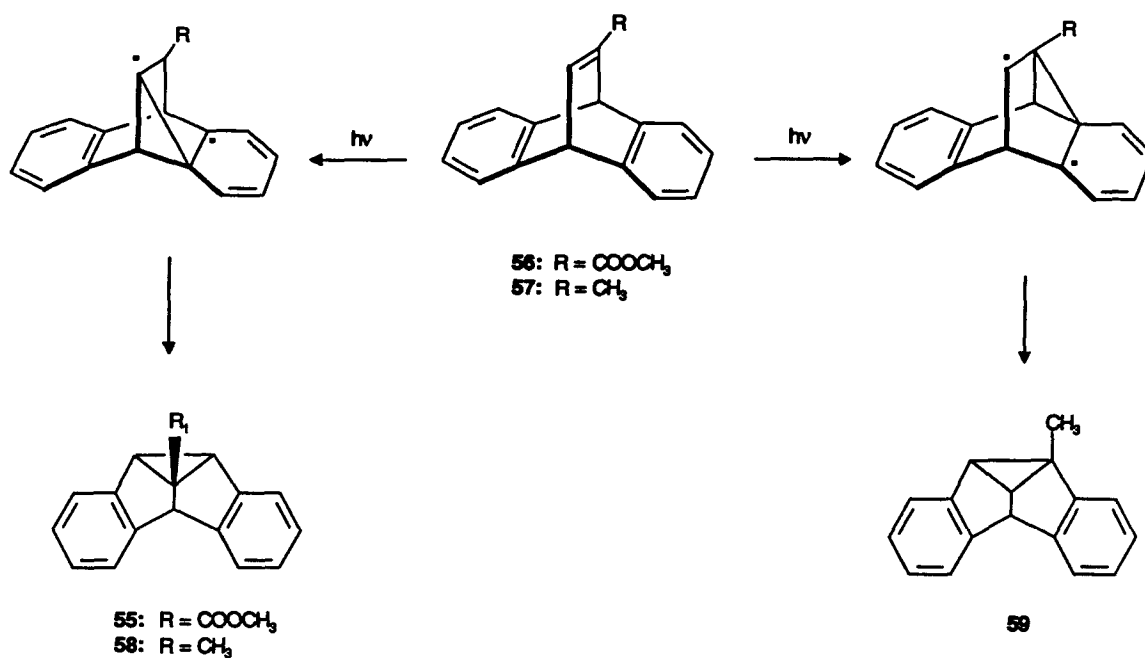
Figure 2-32   Photolysis of Monosubstitued Dibenzobarrelenes **56** and **57**

2.2.3 Photolyses of Dimethyl 9-Amino-9,10-dihydro-9,10-ethenoanthracene-11,12-dicarboxylate (39)

Earlier studies by Paddick et al.[63] on the photochemistry of amine **39** showed that it rearranges to the keto-diester **62** in acetone. This result was interpreted as being due to the di-π-methane rearrangement to the unstable amino-diester **61** followed by ring opening and hydrolysis under the photolysis conditions.

The solution photochemistry of amine **39** was repeated in acetone. This afforded amino-diester **61** as the major product, which was sufficiently stable to be isolated, although it did undergo conversion to keto-diester **62** upon attempted silica gel column chromatography. A significant amount of the alternative di-π-methane regioisomer **60**

was also isolated from the photolysis, although no mention of this compound was made in the original report by Paddick et al.[63] Unlike **61**, compound **60** could be purified without difficulty by column chromatography. GC analysis showed that compounds **60** and **61** were formed in the ratio 3:7. Photolyses of crystals of amine **39** yielded compounds **60** and **61** in the ratio 14:86. No rearrangement product **62** could be detected.
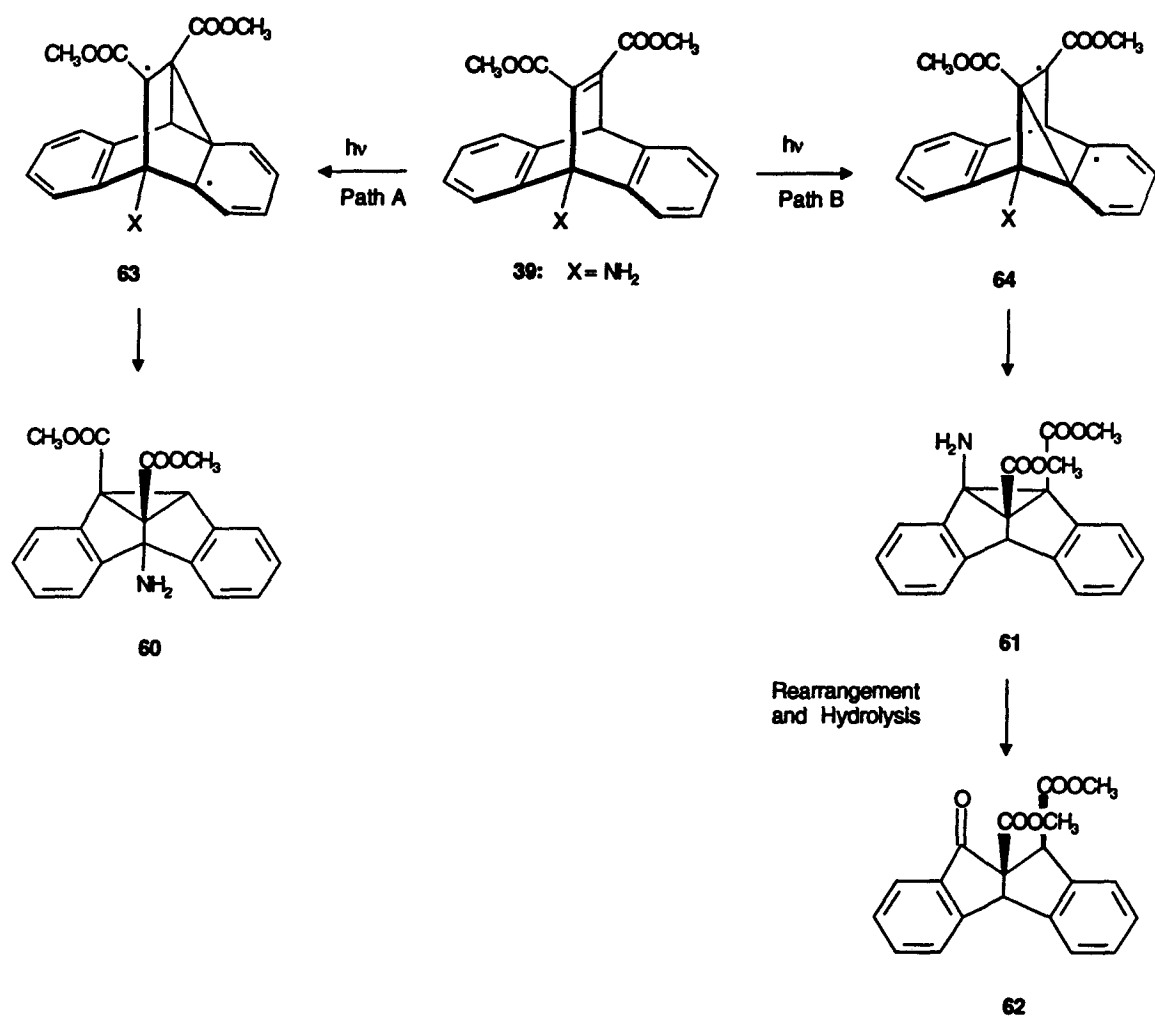
Figure 2-33   Photolysis of Amine **39**

The structures of compounds **60** and **61** are based on their spectra. The ^{1}H-NMR spectra are particularly informative. In the spectrum assigned to product **60**, a one proton

singlet at $\delta = 4.40$ ppm is attributed to the cyclopropyl methine. In contrast, the spectrum

of 61 contains a one proton singlet at $\delta = 5.45$ ppm, which can be assigned to the

hydrogen at the doubly benzylic position. These chemical shift differences appear to be

characteristic of regioisomers of this type, and their use in assigning structure rests

ultimately on correlating ^{1}H-NMR spectral interpretations to X-ray crystal structures.[42]

The spectroscopic data of 62 matched those reported by Richards et al.[64]

Paddick et al.[63] and Iwamura et al.[65] investigated the regioselectivity of the di-π-

methane rearrangement of bridgehead-substituted dibenzobarrelene derivatives with ester

groups on the vinyl bond. These authors suggested that the regioselectivity is controlled

by the stabilizing effect of the bridgehead substituents on intermediates 63 and 64

(Figure 2-33), in a similar way as the substituents R affect the equilibrium between

norcaradiene and cycloheptatriene[66] (Figure 2-34). Electron-accepting groups strengthen

the opposite bond in the cyclopropyl ring and the equilibrium is shifted towards

norcaradiene, whereas electron-donating groups weaken the same bond and favor the

cycloheptatriene.

Norcaradiene   Cycloheptatriene
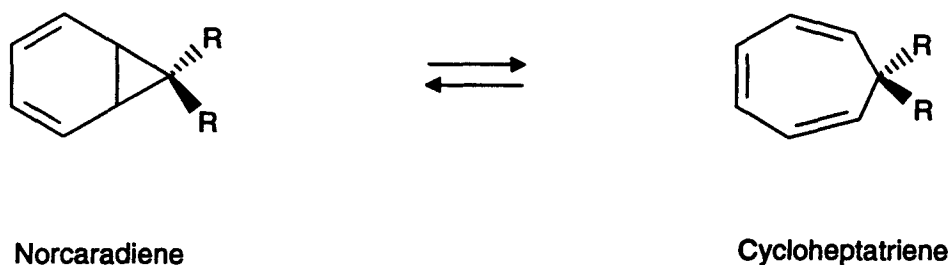
Figure 2-34   Equilibrium between Norcaradiene and Cycloheptatriene

Iwamura[65] did find experimentally that electron-donating and electronegative

bridgehead substituents such as OCH_3 favor path A whereas electron-accepting groups

such as Ph favor path B (Figure 2-33). Opposing electron-accepting and electronegative

effects of the same group can operate simultaneously to determine which regioisomer is

formed. For example the electron accepting nature of the NO_2 group favors path **B** but its high electronegativity destabilizes biradical **64**. The latter effect dominates and only path **A** is observed.

Solution photolyses of amine **39** favored product **61** or path B, in spite of the electronegative and electron donating effect of the amine group. Paddick et al.[63] explained the observed regioselectivity by proposing that there is intramolecular hydrogen bonding between the amino group and the nearest ester group. The authors suggested that this intramolecular hydrogen bond diminishes the stabilizing effect of the ester group on the adjacent radical. In other words, the intramolecular hydrogen bond is supposed to make intermediate **63** less stable. Furthermore they suggested that the destabilizing effect of the intramolecular hydrogen bonding in intermediate **63** dominates the stabilizing effect of the electron donating amine group, and as a result pathway **B** is favored (Figure 2-33).

The regioselectivity observed for amine **39** in the solid state is similar to that in solution, product **61** is the major one. The X-ray crystal molecular structure[67] of amine **39** and the crystal packing diagram are shown in Figure 2-35. There are two independent molecules in the asymmetric unit, **39A** and **39B**. The crystal structure reveals that there is intramolecular hydrogen bonding between the NH_2 group and the nearest carbonyl oxygen (O2 in molecule **39A** and O4 in molecule **39B**). There is one intermolecular hydrogen bond between the amino group in **39B** and the other carbonyl oxygen (O4) in molecule **39A** and another one between the NH_2 group in **39A** and the carbonyl oxygen O2 in **39B**. These intermolecular hydrogen bonds make an infinite chain between molecules **39A** and **39B** in the crystal lattice. Furthermore the carbonyl oxygen, O2, in **39A** is intermolecularly hydrogen bonded to the NH group in an another molecule of **39A**. The hydrogen bonds destabilize the radical stabilizing effect of both ester groups in molecules **39A** and **39B** and also hinder their movement. However, the hydrogen bonding affects the formation of photoproducts **60** and **61** similarly.

Molecule 39A
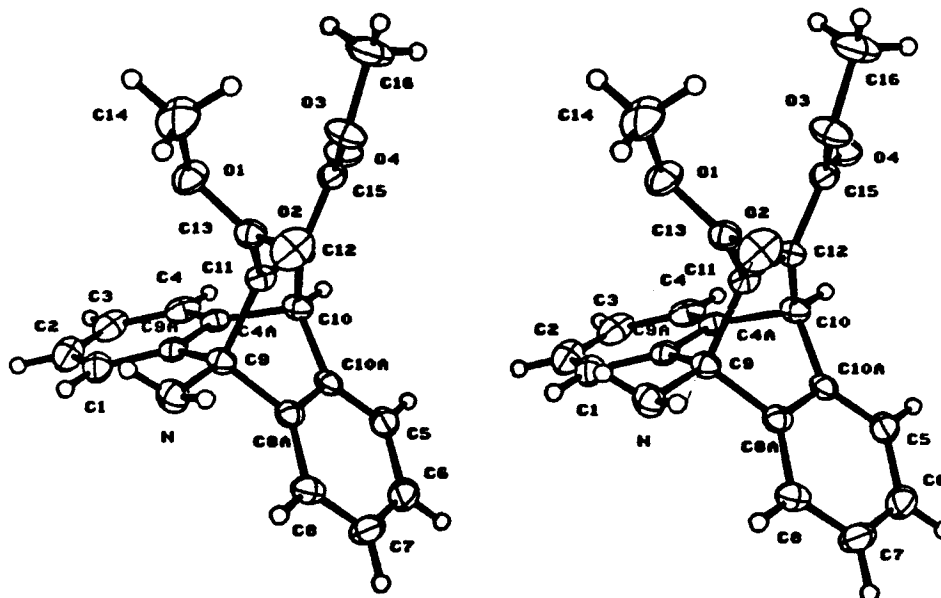
Molecule 39B
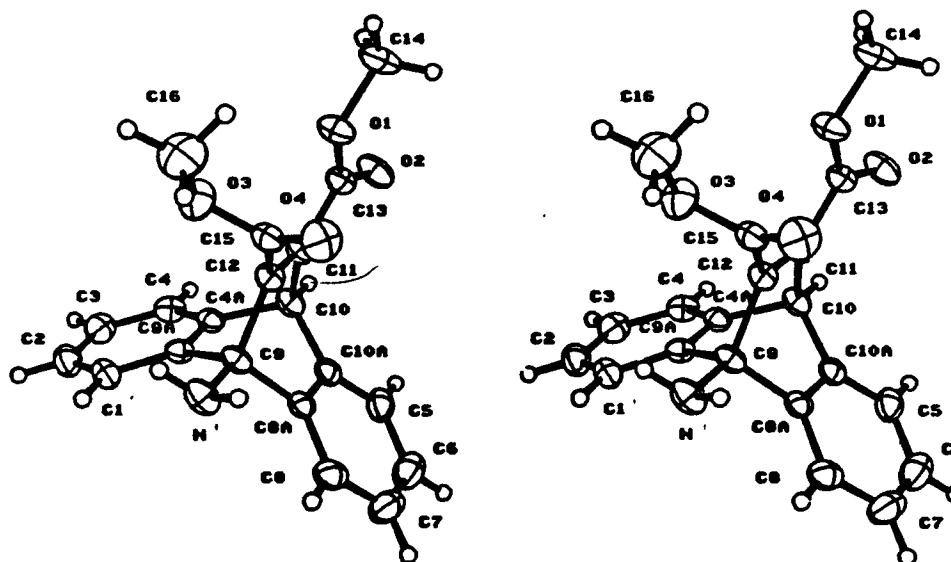
Figure 2-35   Crystal Structure of Amine 39
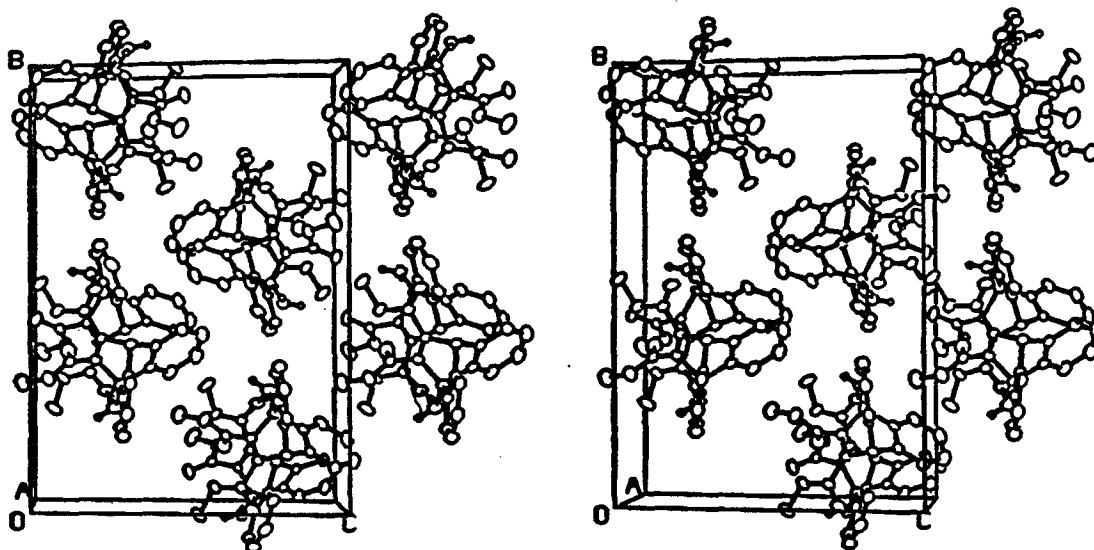
Figure 2-35 Crystal Structure of Amine **39** (continued)

As discussed earlier in this thesis, the steric effects of the crystal lattice can be a key factor in controlling the regioselectivity of the di-π-methane rearrangement. Scheffer et al.[42] suggested that the ester group attached to the bridging vinyl atom must move considerably during the benzo-vinyl bridging process and is therefore most likely to experience unfavorable steric interactions. Both ester groups in molecules **39A** and **39B** are tightly packed which affects the formation of both the di-π-methane rearrangement products similarly.

The crystal lattice enforces varying degrees of conjugation between the different ester groups and the double bonds between them. Initial benzo-vinyl bridging at the vinyl

carbon atom that is less conjugated to the attached ester group is favored since bonding at this side leads to the more highly resonance-stabilized biradical intermediate. Analyzing the intramolecular features of amine **39** illustrates that the torsion angles between the carbonyl next to the bridgehead substituent and the vinyl bond are -101° in **39A** and -87° in **39B**. This illustrates that these carbonyls (O2 in **39A** and O4 in **39B**) are largely un-conjugated. In contrast, the carbonyls farther away from the bridgehead substituent are in conjugation; their torsion angles (O4 in **39A** and O2 in **39B**) with the vinyl bonds are 158° for **39A** and 164° for **39B**. Formation of **61** is therefore favored, which is consistent with the observed regioselectivity.

Examples exist in the literature where the degree of conjugation of the vinyl bonds with a radical stabilizing group is thought to affect the di-π-methane rearrangement. Such an example comes from Schaffner and co-workers[68] who studied the photochemistry of ketone **65**. The infrared spectrum of ketone **65** in glassy solvent matrices showed two carbonyl bands at 1633 and 1644 cm^{-1}. These bands were assigned to two rotamers **65A** and **65B**, one with the carbonyl in conjugation with the vinyl bond, **65A** (1633 cm^{-1}), and the other with the benzoyl group out of conjugation, **65B** (1644 cm^{-1}, Figure 2-36). Irradiation led to disappearance of the band assigned to the conjugated benzoyl group at 1633 cm^{-1} and formation of a carbonyl band which corresponds to the photoproduct **66**. The carbonyl band assigned to unconjugated rotamer **65B** at 1644 cm^{-1} was unaffected. The author suggested that rotamer **65B** did not react due to lack of radical stabilization by the benzoyl group.

IR: 1633 cm⁻¹; conjugated C=O

65A

IR: 1644 cm⁻¹; unconjugated C=O

65B

hv

66
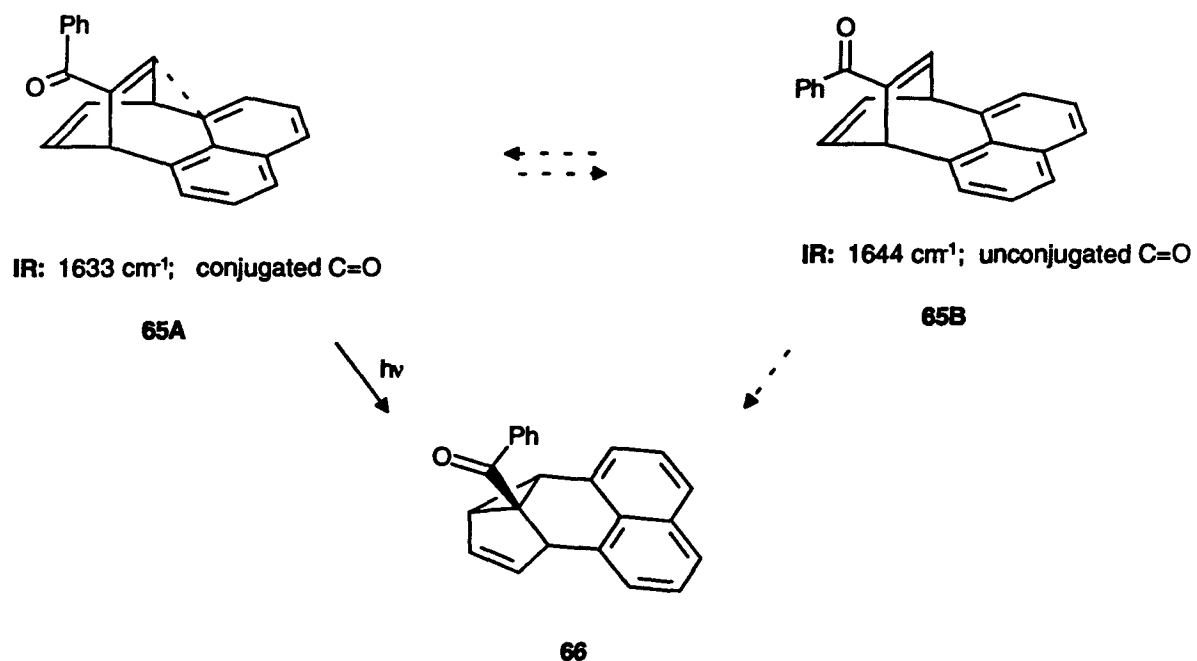
Figure 2-36   Photolysis of Ketone **65**

2.2.4 Photolyses of Trimethyl 9,10-Dihydro-9,10-ethenoanthracene-9,11,12-tricarboxylate (43) and Dimethyl 9-Ethoxycarbonyl-9,10-dihydro-9,10-ethenoanthracene-11,12-dicarboxylate (44)

Acetone-sensitized photolyses of tri-ester **43** gave product **67** as the major product and small amounts of the other di-π-methane rearrangement product **68**. Similarly, acetone solution photolyses of tri-ester **44** yielded the major product **69** and the minor product **70** (Table 2-2, Figure 2-37).

67: R = CH₃
69: R = CH₂CH₃

68: R = CH₃
70: R = CH₂CH₃

43: R = CH₃
44: R = CH₂CH₃

71: R = CH₃
72: R = CH₂CH₃

73

E = COOCH₃
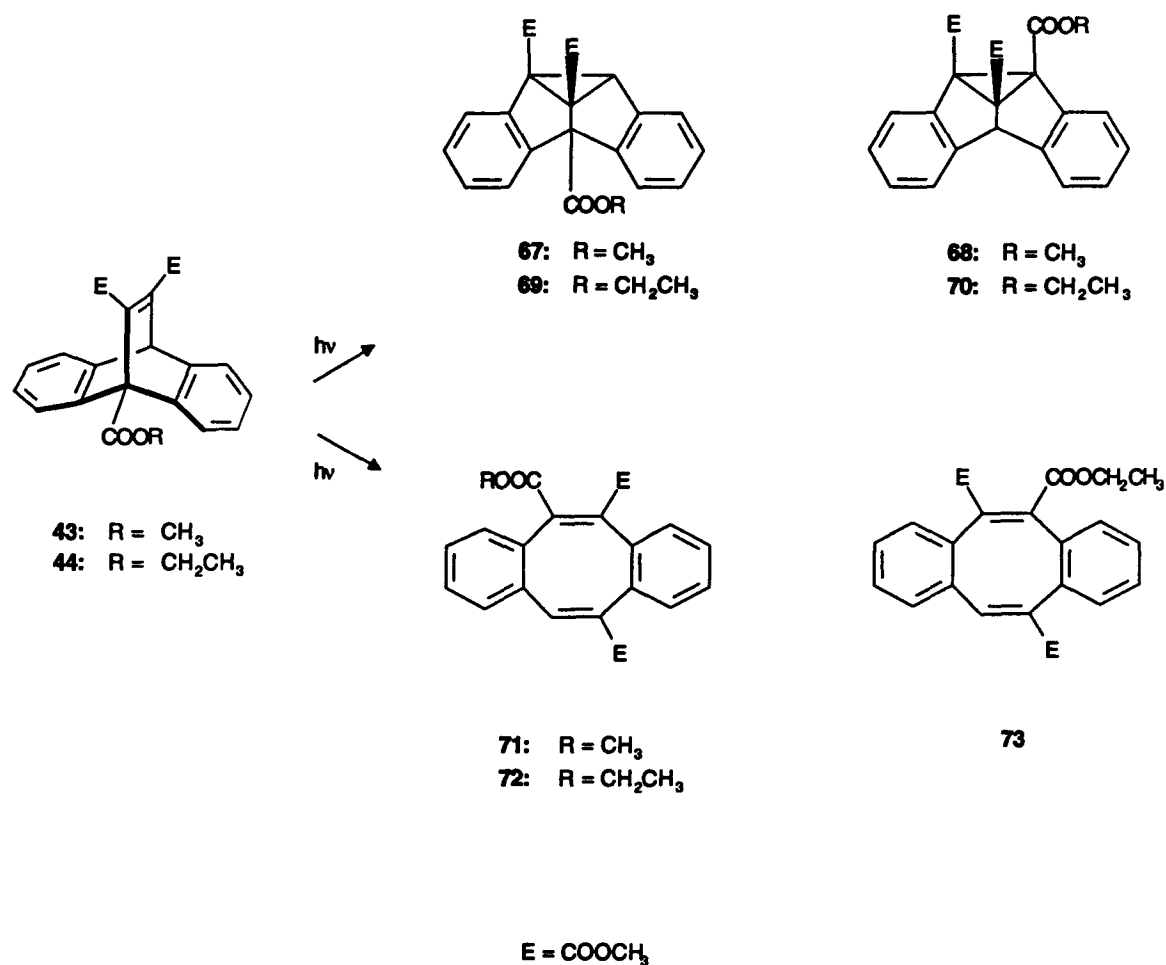
Figure 2-37   Photolysis of Tri-Esters 43 and 44

Irradiation of tri-ester **43** in chloroform (direct irradiation) gave an additional cyclooctatetraene product **71** as well as products **67** and **68**. Direct photolyses of tri-ester **44** in chloroform gave two new compounds, **72** and **73**, in addition to products **69** and **70** (Table 2-2, Figure 2-37).

Crystals of tri-ester **44** exist in two dimorphic forms which have similar melting points, 149°C, but their infrared spectra demonstrate that they are different. Irradiation of both crystal forms yielded significant amounts of all of the four photoproducts formed in chloroform solution. Photolyses of crystals of tri-ester **43** also yielded significant

55

amounts of all the chloroform solution products (Table 2-2, Figure 2-37). The crystals of tri-esters **43** and **44** are photochromic; irradiation results in colors which fade in the dark. The photochromism of these compounds is discussed in Section 2.5.3.

Table 2-2   Medium Dependent Photochemistry of Tri-Esters **43** and **44**

Medium	Tri-ester **43**[a]		Tri-ester **44**[a]		
	(67+68):71[b]	67:68[c]	(69+70):(72+73)[b]	69:70[c]	72:73[d]
Acetone	100:0	91:9	100:0	93:7	
Chloroform	66:34	90:10	44:54	80:20	58:42
Crystals (prisms)	74:26	49:51	61:39	48:52	22:77
Crystals (needles)			68:32	38:62	33:66

[a] The estimated error in the GC analysis is ±5%. [b] Ratio between S_1 and T_1 products. [c] Regioselectivity for the di-π-methane reactions. [d] Ratio for the S_1 products.

The structures of the di-π-methane products were determined from their spectroscopic data, and as before, the ¹H-NMR spectra were most useful.[42] The methine protons on the cyclopropyl ring appear at $\delta = 4.5$ ppm in **67** and **69**. The more deshielded protons in the 4b-position in products **68** and **70** give rise to signals at $\delta = 5.1$ ppm. The structural assignment of cyclooctatetraene product **71** is based on its spectroscopic data. For cyclooctatetraenes **72** and **73** the spectroscopic data are strikingly similar, so it is impossible to assign the structures based on spectroscopic data alone. Crystal structure analyses of these compounds allowed their structures to be assigned unambiguously.[67, 69]

Di-π-methane rearrangements of dibenzobarrelene derivatives are thought to take place from the triplet excited state, presumably due to rapid intersystem crossing of the initially formed singlet excited state.[39] The literature cites examples of dibenzobarrelene derivatives which react from the S_1 excited state to form dibenzocyclooctatetraene.[39] The

sensitization studies of tri-esters **43** and **44** demonstrate that the dibenzosemibullvalene products form from the triplet excited state, whereas the dibenzocyclooctatetraenes come from the singlet excited state.

In solution the di-π-methane rearrangement of tri-esters **43** and **44** favored formation of the 4b-substituted products, **67** and **69** respectively. As described earlier, electron-accepting groups on the bridgehead favor formation of the 8b-substituted semibullvalene whereas electronegative and electron-donating groups stabilize the biradical leading to formation of the 4b-substituted semibullvalene. The electronegative effect of the ester group must overwhelm the electron-accepting effect resulting in formation of the 4b-substituted products.

The regioselectivity observed for tri-esters **43** and **44** in solution is similar to that observed by Ciganek[58] for ester **74** (Figure 2-38). Irradiation of ester **74** yielded photoproducts **75** and **76** in the ratio 66:33, respectively. Paquette et al.[70] suggested that the photobehavior of ester **74** can be interpreted in terms of reluctance to position the electronegative ester group at the cyclopropane in the biradical intermediate that leads to product **76** (Figure 2-38).
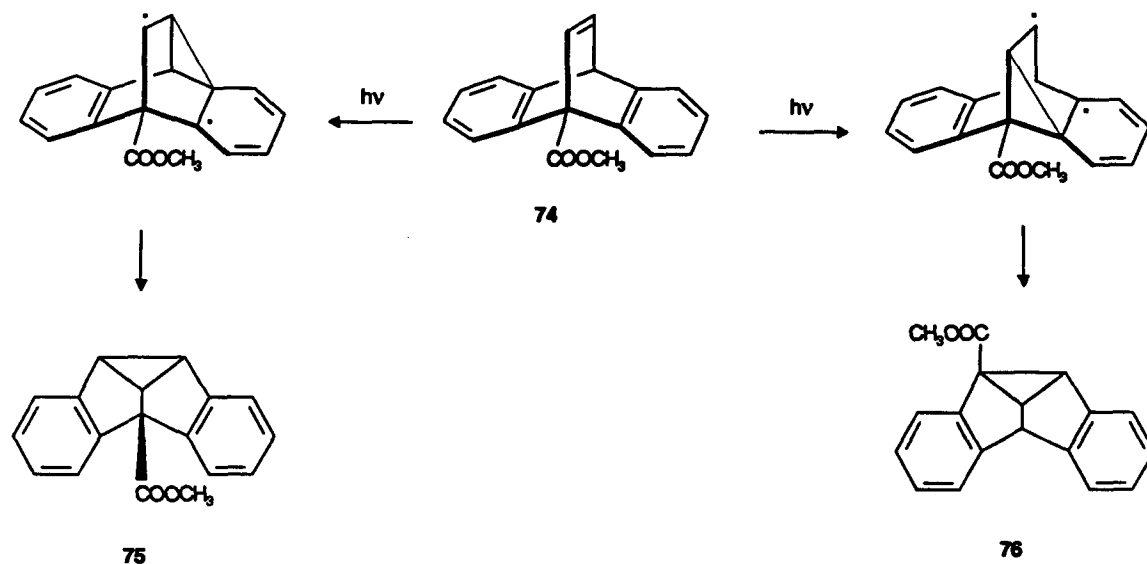
Figure 2-38   Di-π-methane Rearrangement of Ester 74

The di-π-methane rearrangement of tri-esters 43 and 44 in the solid state is not regioselective; similar amounts of both the 4b- and the 8b-substituted semibullvalenes are formed (Table 2-2). This differs from the regioselectivity in solution where the 4b-substituted products are favored. The reactivity must therefore be modified to some degree by the crystal lattice.

An X-ray structure[67] was obtained of the tri-ester 43 (Figure 2-39) and analyses of the packing arrangement indicate that there is some steric crowding around both vinyl ester groups, which presumably affects the formation of both di-π-methane products in similar ways. When the molecular conformation is analyzed, however, it shows that the ester group next to the bridgehead substituent is out of conjugation with the vinyl bond, whereas the other ester group is conjugated. The torsion angle between the carbonyl ester group (O2) next to the bridgehead substituent and the vinyl bond is 102°, whereas the torsion angle for the other carbonyl ester group (O6) and the vinyl band is 160°. As mentioned earlier, the initial biradical is better stabilized next to the ester group that is in

conjugation, and thus based on this assumption, formation of photoproduct **68** is favored. We suggest that since the electronic stabilizing effect of the bridgehead substituent and the radical stabilization capability of the different ester groups on the vinyl bond work in opposing directions in the solid state and neither one is dominant, no regioselectivity is observed.
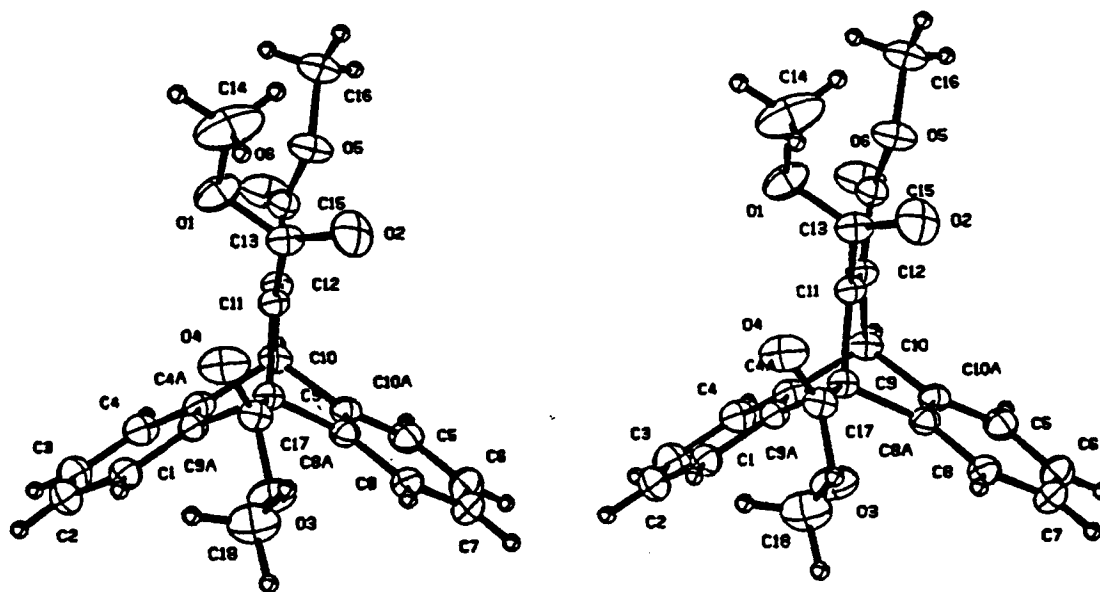
Figure 2-39   Crystal Structure of Tri-Ester **43**

It is a general trend for dibenzobarrelenes with ester groups on the vinyl bond and one bridgehead substituent, that the ester group on the vinyl bond next to the bridgehead

substituent is out of conjugation.[71] Presumably this occurs to relieve steric interactions between the ester group and the bridgehead substituent. It can be suggested that the same factors control the solid state regioselectivity for the di-π-methane rearrangement of tri-ester **44** as tri-ester **43**. There are only slight differences between the regioselectivities of the di-π-methane rearrangement of the two dimorphs of tri-ester **43**, which suggests they have similar packing arrangements.

Before discussing the singlet state photoreactivity of tri-esters **43** and **44**, a brief review of the literature is necessary. Photolysis of dibenzobarrelene via its singlet excited state yields dibenzocyclooctatetraene as the major product.[72] The commonly accepted mechanism involves [2+2] cycloaddition which is followed by thermal reorganization of the resulting cage compound (Figure 2-40). Deuterium labeling experiments were carried out by Zimmerman to support this mechanism.[73] Monobenzobarrelenes with deuterium on the bridgeheads gave cyclooctatetraene with C_2 symmetry (Figure 2-40).
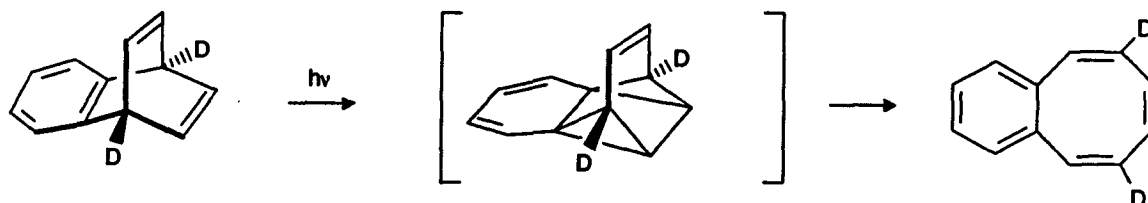
Figure 2-40   Photorearrangement of Labeled Benzobarrelene via the S_1

Recently, Scheffer et al.[8m, 74] and George et al.[75] have demonstrated that tetra- and tri-substituted dibenzobarrelenes form abnormal dibenzocyclooctatetraenes possessing C_2 symmetry rather than C_s symmetry. Scheffer et al.[74] suggested a mechanism for the formation of the abnormal cyclooctatetraene after studying the photochemistry of dibenzobarrelene derivative **77** (Figure 2-41). Acetone-sensitized irradiation of **77** yielded di-π-methane product **78**, whereas direct photolysis give **78** and cyclooctatetraene **79**. Solid state photolyses resulted in formation of compound **80** as the

60

major product with small amounts of products **78** and **79**. The authors suggested that compounds **79** and **80** are products of the singlet excited state and that the initial step is the so called tri-π-methane[76] interaction of both aromatic rings with the vinyl bond to form biradical **81**. Migration of both the carbomethoxy groups in biradical **81** leads to product **80** whereas Grob fragmentation results in cyclooctatetraene **79**.

77: R = COOCH₃
82: R = COPh
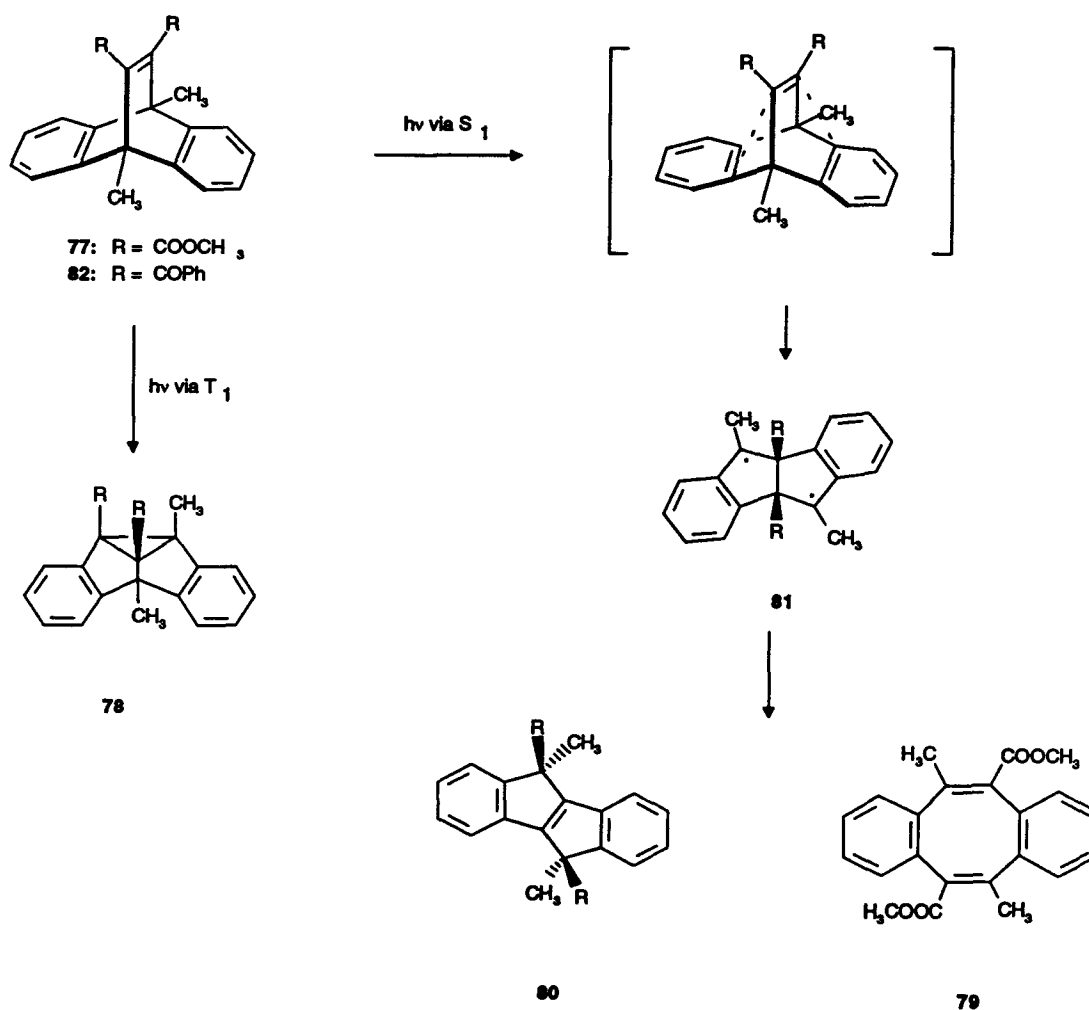
Figure 2-41   Photolysis of Compound **77**

There are only a few instances of abnormal cyclooctatetraene formation in the literature.[8m] Photolysis of dibenzobarrelene derivative **82**[75] yields photoproducts

analogous to compounds **79** and **80** (Figure 2-41). Dibenzobarrelene derivatives **83** and **84**[8m,74] also yielded abnormal cyclooctatetraenes (Figure 2-42). It is very difficult to distinguish whether a cyclooctatetraene is normal or abnormal based on spectroscopic data alone, and it is possible that some abnormal cyclooctatetraenes have been incorrectly assigned as normal cyclooctatetraenes in the literature. Some corrections have been reported.[74,75,77,78]

83: R = CH₃
84: R = Ph
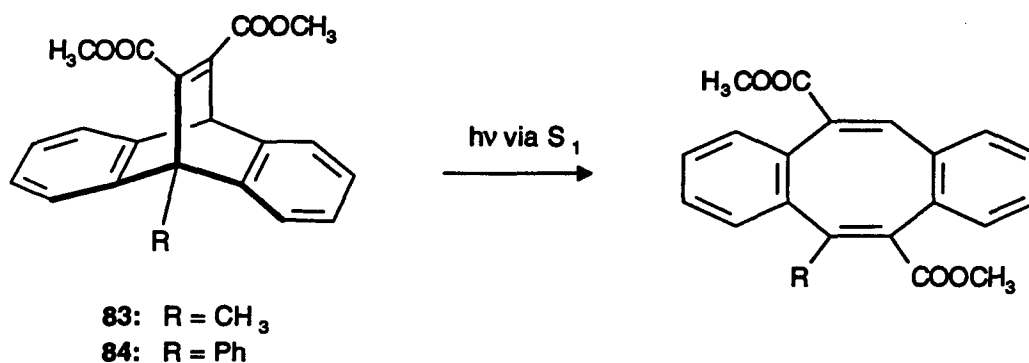
Figure 2-42   Singlet State Photorearrangement of Dibenzobarrelene Derivatives **83** and

84

Tri-ester **44** is the first compound reported to give both normal and abnormal cyclooctatetraenes. The cyclooctatetraene produced from tri-ester **43**, however, can be formed through the [2+2] derived mechanism, the Grob fragmentation or a combination of both, because these mechanisms lead to the same product. This leads to the question of what factors control the competition between formation of the normal and abnormal cyclooctatetraenes. Substitution at position 9, 10, 11 and 12 on the dibenzobarrelene nucleus is a significant factor, since these are the only compounds that have yielded cyclooctatetraenes with abnormal symmetry. Scheffer et al.[8m, 74] suggested that the reluctance of dibenzobarrelene derivatives **77**, **83** and **84** to undergo [2+2] photocycloaddition to produce normal cyclooctatetraenes may be attributed to steric

factors resulting from the presence of the bridgehead substituents. In other words, there are more unfavorable intramolecular steric interactions developed in the [2+2] pathway than in the tri-π-methane process. The bridgehead substituent(s) also give additional stability to the intermediate 1,4-biradical (e.g., **81**), which may be the driving force for the alternative rearrangement observed.

Interestingly, the solution photolyses of tri-ester **44** give similar amounts of both cyclooctatetraenes **72** and **73**, whereas the abnormal cyclooctatetraene **73** is slightly favored in the solid state for both the dimorphs of tri-ester **44** (Table 2-2, page 56).

Further studies of this type should provide the possibility of studying steric effects as well as the electron withdrawing and donating effects of different bridgehead substituents on the formation of cyclooctatetraenes. This would give valuable information about the reaction mechanism for forming abnormal and normal cyclooctatetraenes.

2.2.5 Photolyses of Dimethyl 9-Carboxy-9,10-dihydro-9,10-ethenoanthracene-11,12-dicarboxylate (38)

Acid **38** forms different crystals depending on the solvent used for crystallization. Crystals grown from ethanol and acetonitrile contain one equivalent of the solvent in the crystal lattice, whereas crystallization from ethyl acetate or *sec*-butanol solution yields crystals without solvent molecules. All three crystal forms were found to be photochromic when irradiated in the solid state. The photochromism is discussed in Section 2.5. After photolysis the reaction mixture was treated with diazomethane, which transformed the di-π-methane products to methyl esters **67** and **68**. Unreacted acid **38** was transformed into tri-ester **43** which underwent further reaction with diazomethane to form a pyrazoline derivative. This simplified the chromatographic separation of the

starting material from products **67** and **68** (Figure 2-43). The disadvantage of this method is that the dibenzocyclooctatetraene derivatives also undergo pyrazoline formation with diazomethane and cannot be separated from the derivatized starting material. As the di-π-methane rearrangement is the main focus of this thesis, it was decided to study only the triplet reactivity of acid **38**, even though it undergoes some singlet state reactivity as well. The regioselectivity of the di-π-methane rearrangement of acid **38** in the solid state and in acetone is listed in Table 2-3.
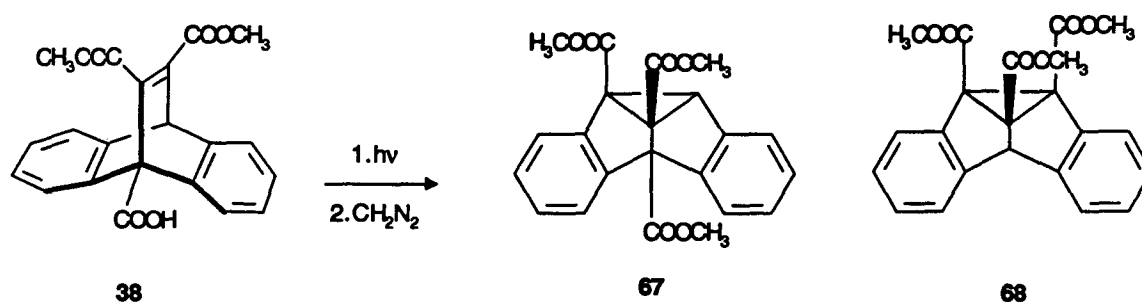
Figure 2-43   The Di-π-methane Rearrangement of Acid **38**

The regioselectivity of the di-π-methane rearrangement of acid **38** in acetone solution is the same as for tri-esters **43** and **44**, presumably because the ester and acid groups have similar electronegativities.

Table 2-3   Regioselectivity of the Di-π-methane Rearrangement of Acid **38**

Medium	Regioselectivity of the di-π-methane 67:68
Acetone	100:0
Crystals without solvent molecules	No reaction
Crystals containing ethanol	40:60
Crystals containing acetonitrile	10:90

Irradiations of crystals containing ethanol formed products **67:68** in the ratio 40:60, which is similar to that observed for solid state reactions of tri-esters **43** and **44**. The crystals grown from acetonitrile gave much better regioselectivity for the di-π-methane rearrangement, specifically compounds **67** and **68** in the ratio 1:9 respectively. Crystals of acid **38** without any solvent molecules were found to be photostable. The crystal structure has been obtained only of crystals that contain ethanol in the crystal lattice.[79]

The crystal structure of acid **38** confirms that crystals grown from an ethanol solution contain one equivalent of solvent (Figure 2-44). The methyl group in the ethanol was disordered with two equally occupied positions. The ethanol serves as a bridge between two molecules of **38** via hydrogen bonding, forming an infinite chain. The hydrogen bonds are between the ester carbonyl O2 and the OH group of the ethanol and between the oxygen of the ethanol and the OH group of the carboxylic acid.

Analyzing the intermolecular features of the X-ray structure reveals that both ester groups are sterically crowded which affects the formation of products **67** and **68** similarly. The intermolecular hydrogen bonding of carbonyl O2 does not favor formation of either product **67** or **68**. The hydrogen bonding of carbonyl oxygen O2 decreases its ability to stabilize an adjacent radical but this does not favor formation of product **68** because formation of product **68** also requires movement of this carbonyl oxygen (O2) which would interrupt the hydrogen bonding.

Inspection of the intramolecular features of acid **38** shows that, as before, the carbonyl group next to the bridgehead substituent is out of conjugation, whereas the other ester group is conjugated to the vinyl bond and therefore better capable of stabilizing an adjacent radical. This hypothesis would favor formation of product **68**.

The low regioselectivity of the di-π-methane photorearrangement of the ethanol-containing crystals of acid **38** can be attributed to the fact that the intramolecular

arrangement of acid **38** and the electronic effect of the carboxylic acid on the bridgehead work in opposing directions and neither factor dominates. This is similar to what was observed for tri-esters **43** and **44** in the solid state.
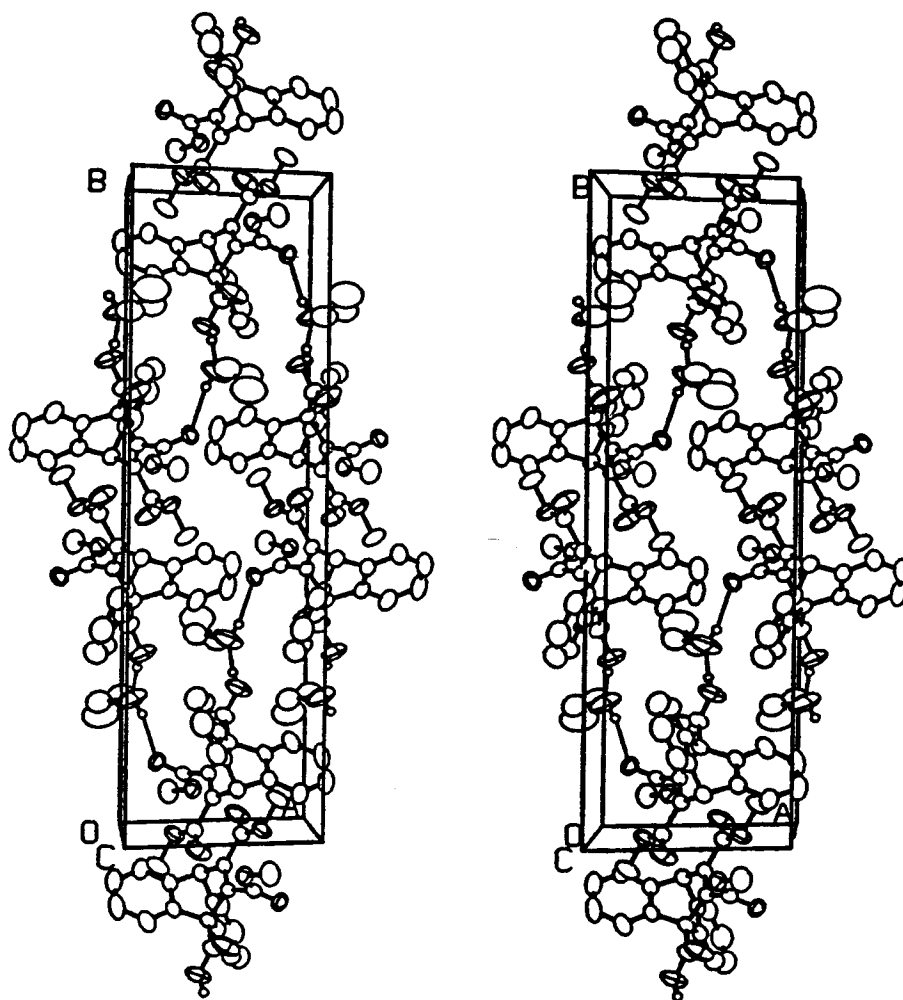
Figure 2-44   Crystal Structure of the Ethanol Solvate of Acid **38**
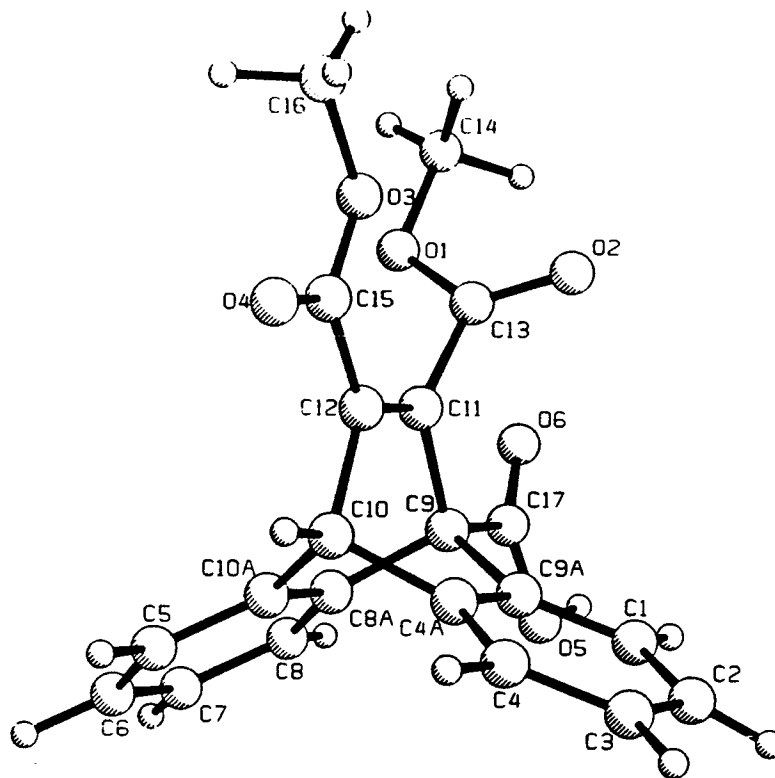
Figure 2-44   Crystal Structure of the Ethanol Solvate of Acid 38 (Continued)

X-ray structure analyses of the two other crystal forms of acid 38 are not available, and the solid state infrared spectra are too complicated to interpret the structural arrangement of acid 38 in these crystals. The crystals without solvent molecules became dark green when they were photolyzed and the color faded upon storing in the dark. This confirms that photons were absorbed but no products were

formed. It can be suggested that in these crystals the carboxylic acid groups form dimers resulting in very crowded crystal packing and therefore no reaction is observed. There are examples in the literature of other benzobarrelene carboxylic acid derivatives that are not photoreactive in the solid state although they are reactive in solutions.[22]
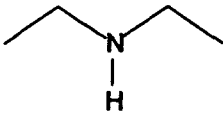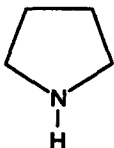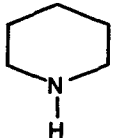
Any speculation on the high regioselectivity of the acetonitrile-containing crystals of acid 38 must await an X-ray crystal structure analysis.

2.3 Photochemistry of Salts of Starting Materials

2.3.1 Photolyses of Salts of Ethyl 9,10-Dihydro-9,10-ethenoanthracene-11-carboxylate-12-carboxylic acid (36)

Initially, salts of ester-acid 36 were formed with simple non-chiral bases to gain insight into their characterization and photochemical behavior. The non-chiral salts formed with ester-acid 36 are listed in Table 2-4.

Table 2-4   Photoproduct Mixture Composition for Salts **85** to **89**

Counterion	Salt	Crystal forms	Photoproduct ratio **32a:33a**	
			CH$_3$OH	Solid State
Na+	**85**	Powder	100:0[a, b]	100:0[b]
Ca+2	**86**	Powder	100:0[b]	100:0[b]
	87	Needles	100:0[b]	100:0[b]
	88	Plates	100:0[b]	100:0[b]
	89	Plates	100:0[b]	100:0[b]

[a] Photolyses carried out in water. [b] Compound **33a** was not detectable within the limits of this method. The estimated error is ±5%.

Salts **85** to **89** were formed by mixing equimolar quantities of acid and base in ethanol or diethyl ether and filtering the resulting precipitate. The amine salts were recrystallized from acetonitrile. These salts were shown to be simple 1:1 complexes (1:2 for salt **86**) by infrared and ^{1}H-NMR spectroscopy, mass spectrometry and elemental analysis. The infrared spectra of the salts were most informative. The carbonyl stretch of the acid group of ester-acid **36** at 1678 cm^{-1} was replaced by two bands for the carboxylate anion CO_2^-; a strong one in the 1650 - 1550 cm^{-1} region and a weaker one near 1400 cm^{-1}. For the salts formed with amine counterions, the OH band of the carboxylic acid in the region 3500-2400 cm^{-1} is replaced with multiple combination

bands for NH_2^+ in the 3200-2200 cm^{-1} region. The ^{1}H-NMR spectra and elemental analyses confirmed the ratio of the acid to the base.
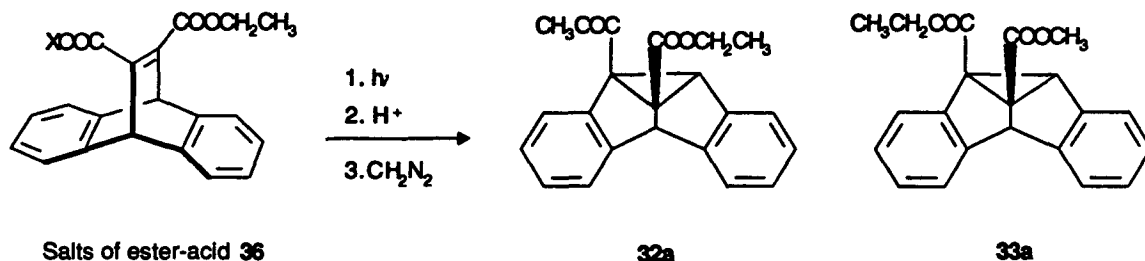
Figure 2-45   Photolysis of Salts of Ester-Acid 36

Salts **85** to **89** were photolyzed in solution and in the solid state. The reaction mixtures were acidified, treated with excess diazomethane to produce the corresponding methyl/ethyl diesters, and analyzed by GC. In all instances the major product was **32a** (Figure 2-45). The photoreactions follow the same mechanism as those discussed previously for ester-acid **36** in aqueous NaHCO$_3$ solutions. The initial benzo-vinyl bridging is favored at the carboxylate anion-bearing vinyl carbon, a result that can be attributed to preferential radical formation at the ester-bearing vinyl carbon.

In this project, the main aim was to find salts of acid **36** in which the di-π-methane rearrangement is very regio- and enantioselective. These initial studies showed that the salts of ester-acid **36** with passive counterions underwent the di-π-methane rearrangement with good regioselectivity, both in solution and in the solid state. It remained to find optically active bases which form salts with ester-acid **36**. These salts must be crystalline so that the chirality of the crystals can be transferred via the di-π-methane rearrangement into the photoproducts. The degree of asymmetric induction will then depend on the molecular arrangement in the crystals. A decision was made to utilize natural chiral amines and their simple derivatives as a chiral resource. No special preferences were made in selecting amines for these studies other than they had to be

70

readily available. It did turn out that it was easier to form salts with secondary amines than with primary or tertiary amines. It can be speculated that secondary amines give the best results since they are stronger bases than primary amines but not as sterically hindered as tertiary amines.

The initial studies[80] of chiral salts of acid **36** were done with the S-(-)-proline salt **90a**. This salt formed as a white powder, and attempted recrystallizations resulted in deposition of the parent acid. The spectroscopic data demonstrate that a 1:1 complex was formed between the S-(-)-proline and ester-acid **36**. Generally, simple carboxylic acids are weaker acids than amino acids and therefore ester-acid **36** is not expected to be capable of protonating the proline.[81] Due to poor crystal quality, it was not possible to obtain information about the structural arrangement of salt **90a** by X-ray analysis. However in our laboratory,[82] X-ray structure analysis of a 1:1 complex of proline with acid **91** shows that proline is in its zwitterionic form and acid **91** is in its neutral form (Figure 2-46). The complex is held together by a hydrogen bond between the OH group in acid **91** and the CO_2^- anion in proline. It can therefore be suggested that proline "salt" **90a** is a complex which is held together by hydrogen bonding between the neutral form of ester-acid **36** and the zwitterionic form of proline.
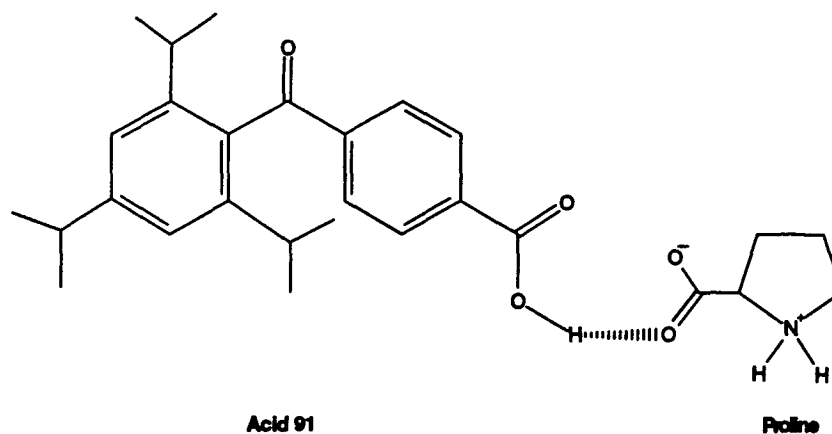
Acid 91   Proline

Figure 2-46   Hydrogen Bonded Complex of Proline and Acid **91** in the Solid State

The S-(-)-proline complex **90a** was photolyzed in the solid state at room temperature. The reaction mixture was acidified, treated with excess diazomethane, and subjected to silica gel column chromatography to isolate the photoproducts. The regioisomeric and enantiomeric compositions of the products were determined by 400 MHz ^{1}H-NMR spectroscopy. For the enantiomeric excess determination use was made of the chiral shift reagent (+)-Eu(hfc)$_3$. The signals monitored were the methyl singlets at δ = 3.9 ppm for **32a** and δ = 3.7 ppm for **33a**. These studies revealed that products **32a** and **33a** were formed in the ratio 83:17. Product **32a** was formed in 43% enantiomeric excess whereas product **33a** was formed without enantioselectivity. The optical rotation of the product mixture was measured at the sodium D line and found to be positive.

Determining enantiomeric excess with chiral shift reagents requires large chemical shift nonequivalence of the enantiomeric signals. When baseline separation of the enantiomeric signals under investigation is obtained, integrating the signals gives a direct measure of the enantiomeric composition.[83] Caution is required for enantiomeric values above 90% where the error in the measurement has been reported to be of the order of 10%.[83, 84] Figure 2-47 illustrates that the enantiomeric methyl ester signals of both compounds **32a** and **33a** are well resolved in CDCl$_3$ solutions.

¹H-NMR Spectra of Photoproducts **32a** and **33a**

in CDCl₃ after Addition of (+)-Eu(hfc)₃.
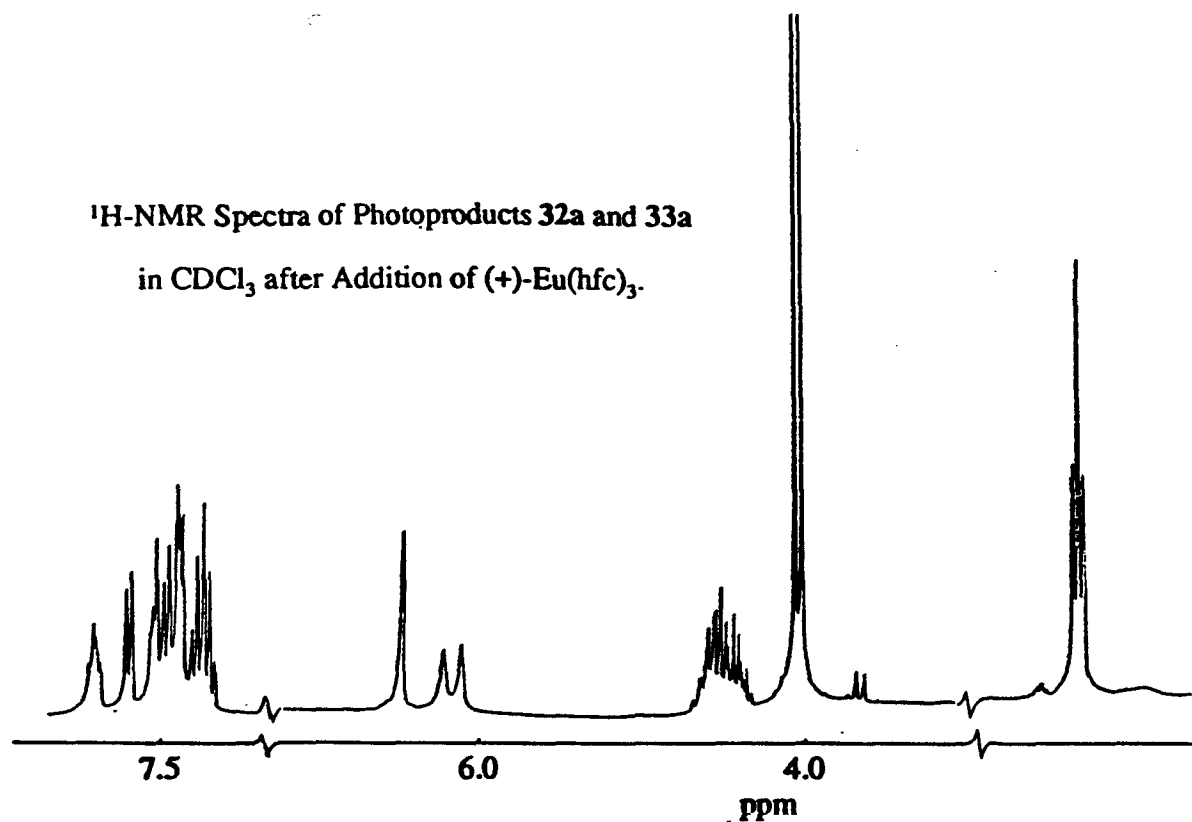
¹H-NMR Spectra of Photoproducts **32a** and **33a**

in CDCl₃.
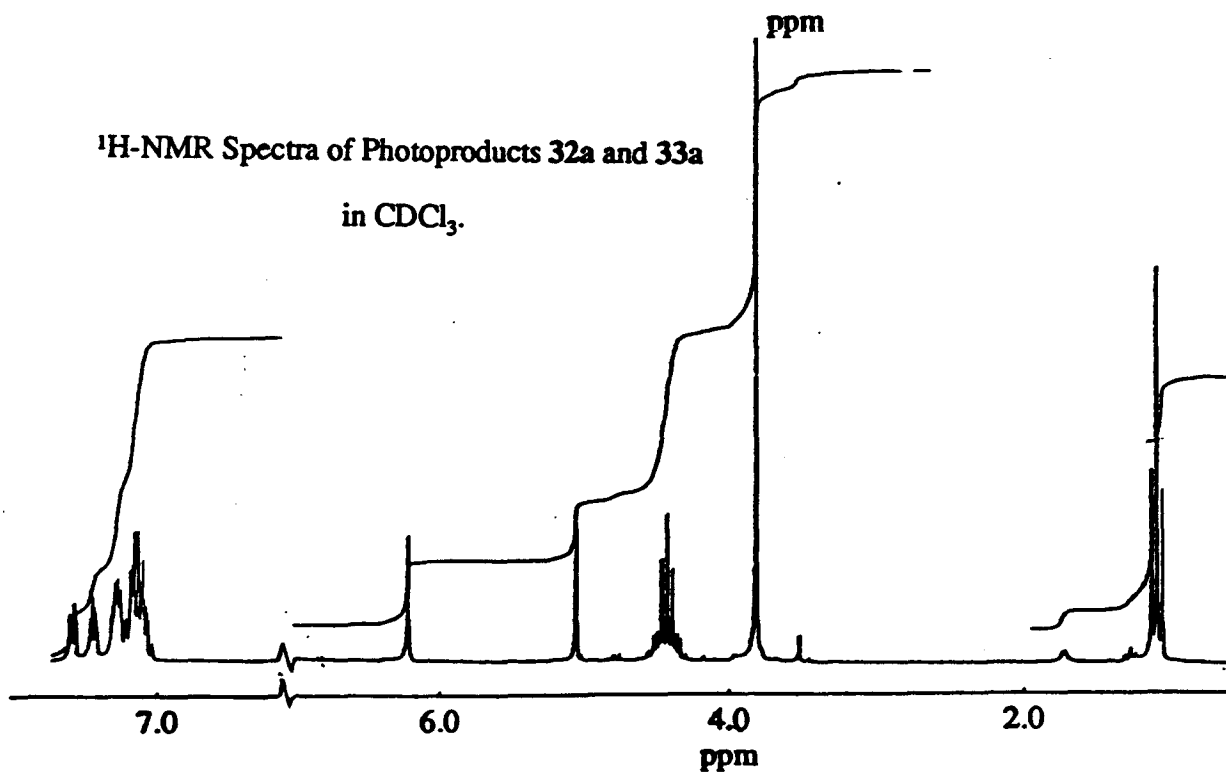
Figure 2-47   ¹H-NMR Spectra of a Mixture of Photoproducts **32a** and **33a**

73

After demonstrating that photolyses of the complex of acid **36** with a chiral base do indeed lead to optical activity in the product, the next step was to try to optimize the optical yields. First of all, the dissymmetric influences of the proline moiety on the reaction pathways of S-(-)-proline salt **90a** result in diastereomeric transition states for the different enantiomers of products **32a** and **33a**. Lowering the temperature should therefore increase the formation of the enantiomer which has lower activation energy. Secondly, although molecular motion is restricted in the solid state it is not completely eliminated and molecules in a crystal do undergo thermal motions.[8a] There are examples in the literature where the entire molecule undergoes a rotation in the crystal lattice.[85] Upon lowering the reaction temperature some of these movements are frozen out and this can increase the selectivity of solid state reactions.
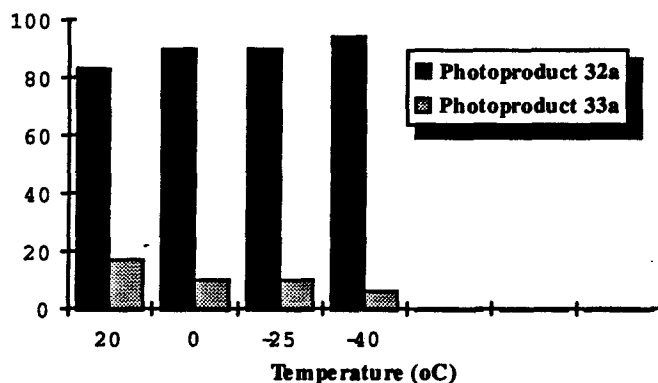
Figure 2-48   Product Ratio of Photolyses of S-(-)-Proline Salt **90a** at Different

Temperatures

Figures 2-48 and 2-49 illustrate that the di-π-methane rearrangement of S-(-)-proline complex **90a** becomes more regio- and enantioselective at low temperatures. Low temperature photolyses have the disadvantage of taking a considerably longer time. As a compromise, no reaction was carried out at temperatures below -40°C. The

regioselectivity improved from 83:17 at room temperature to 94:6 at -40°C for products 32a and 33a respectively. The enantiomeric excess increased from 43% to 76% for product 32a when the temperature was lowered to -40°C. No enantioselectivity was observed for product 33a in any instance.
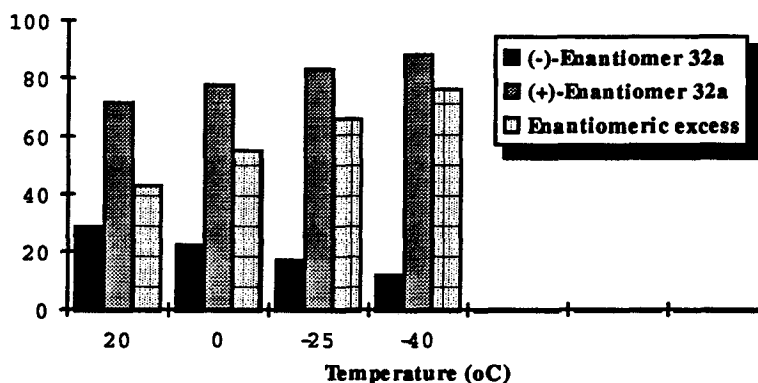
Figure 2-49   Enantiomeric Excess of Photoproduct 32a at Different Temperatures

The R-(+)-proline complex of ester-acid 36 (90b) was prepared as well as the-(±)-proline complex, 90c. Irradiations of the R-(+)-proline complex 90b at -40°C yielded similar product ratios as the S-(-)-proline complex 90a, but the enantioselectivity was reversed. In other words, product 32a was formed in 80% enantiomeric excess but the optical rotation was negative. The fact that the sign of rotation of photoproduct 32a can be reversed by using the optical antipode of the chiral induction agent indicates that the system is well behaved. Ester-acid 36 must have enantiomeric arrangements in the solids of the R-(+) and S-(-)-proline complexes. Solid state photolysis of the racemic (±)-proline complex 90c at -25°C gave optically inactive product 32a and 33a in the ratio 84:16.

The regioselectivity of the solid state di-π-methane rearrangement of proline complexes **90a** to **90c** is the same as for the non-chiral salts **85** to **89**. It can be suggested that there is intermolecular hydrogen bonding between the OH group in ester-acid **36** and the proline moiety, similar to that observed for the proline complex of acid **91** (Figure 2-46). The carboxylic acid in ester-acid **36** would then have considerable anionic character which would explain the observed regioselectivity.

Photolyses of proline complexes **90a** to **90c** in ethanol yielded products **32a** and **33a** in a 1:1 ratio without optical activity. This can be interpreted as being a result of the complex between acid **36** and proline dissociating in solution. Similar photochemical behavior was observed for the proline complexes **90a** to **90c** and ester-acid **36** in acetone solutions.

Salts **92** to **101** were prepared and characterized as described for the non-chiral salts of acid **36** (**85** to **89**). These salts were photolyzed in solutions at room temperature and in the solid state at -40°C. The solid state photolyses were stopped before 20% conversion to minimize melting of the crystals. The regioisomeric and enantiomeric compositions of the photoproducts were studied in the same way as for the photolysis of S-(-)-proline complex **90a**. The results are listed in Table 2-5.

Table 2-5   Photoproduct Mixture Composition for Complexes and Salts **90a** to **90c** and
92 to **98**
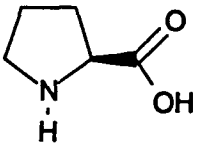
Optically Active Amine	Salt or Complex	Medium	Product 32a		Product 33a	
			Yield (%)[a]	ee[a,b]	Yield (%)[a]	ee[a,b]
S-(-)-Proline	**90a**	Solid State	96	(+)-76	4	nil
		Ethanol	47	nil	53	nil

Table 2-5 (Continued)   Photoproduct Mixture Composition for Complexes and Salts
90a to **90c** and **92** to **98**
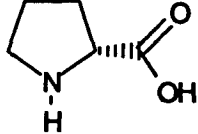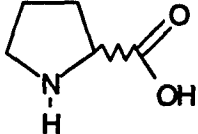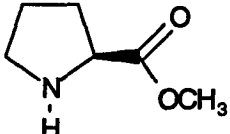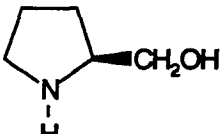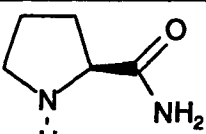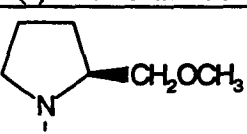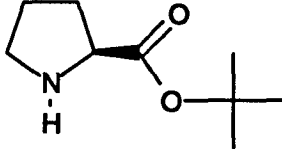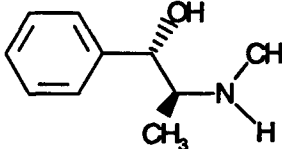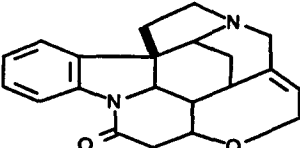
Structure / Name	No.	Condition				
R-(+)-Proline	90b	Solid State	96	(-)-80	4	nil
		Ethanol	50	nil	50	nil
(±)-Proline	90c	Solid State^c	84	nil	16	nil
		Ethanol	50	nil	50	nil
S-(-)-Proline Methyl Ester	92	Solid State	93	(+)-58	7	nil
		Benzene	95	nil	5	nil
S-(+)-2-Prolinol	93	Solid State	100	(-)-37	-	-
S-(-)-Prolineamide	94	Solid State	100	(-)-24	-	-
S-(+)-2-(Methoxymethyl)-pyrrolidine	95	Solid State	100	(-)-16	-	-

77

Table 2-5 (Continued)   Photoproduct Mixture Composition for Complexes and Salts
90a to 90c and 92 to 98

				≥ (+)-		
S-(-)-Proline *tert*-butyl ester	96	Solid State	100	95	-	-
		Acetone	50	nil	50	nil
S,S-(+)-Pseudoephedrine	97	Solid State	87	(-)-87	13	73
(-)-Strychnine	98	Solid State	65	(+)-14	35	nil
		Acetone	60	nil	40	nil

ᵃ The estimated error is ±5%. ᵇ The sign of the rotation of the predominant enantiomer is shown in parentheses. ᶜ Solid state photolysis carried out at -20°C.

Several interesting conclusions can be drawn from the results in Table 2-5. Solution photolysis of the chiral salts yielded racemic products. The product ratio depended on the solvent and corresponded to the regioselectivity of the photoreaction of ester-acid 36 in the same solvent. This indicates that the salts of acid 36 dissociate in solution and explains why no enantiomeric excess is observed in the photoproducts.

In contrast, solid state photolysis of the chiral salts favored formation of photoproduct 32a in all instances; only minor amounts of product 33a were formed from some of the salts. The enantioselectivity of the di-π-methane rearrangement in the solid

state varied from poor to good. Photoproduct **32a** was formed in a range of 14% to more than 95% enantiomeric excess, whereas no optical activity was observed for isomer **33a** except in the case of S,S-(+)-pseudoephedrine salt **97**, where it was formed in 73% enantiomeric excess. The degree of asymmetric induction depends on the nature of the chiral amine which modifies the crystal packing of ester-acid **36**. The enantioselectivity of the solid state photoreaction was not affected by the conversion when it was kept below 20%.

It is interesting to compare the regio- and enantioselectivity for the di-π-methane rearrangement of chiral salts and complexes **90a** to **90c** and **92** to **98** with the result of a study by Scheffer et al.[86] on dibenzobarrelene derivatives **99** and **100** which contain chiral substituents. These compounds were photolyzed in solution and in the solid state and the regio- and diastereoselectivities of the di-π-methane rearrangements were determined. Different chiral handles yielded different regio- and diastereoselectivities, both in the solid state and in solutions. The diastereomeric selectivity was not always increased in the solid state. The authors suggested that the molecular and environmental effects of the chiral substituents either reinforce or oppose one another in the solid state. Depending on the relative magnitude of the opposing effects, it could lead to either reduced or strongly reversed selectivity in the solid state compared to the liquid state.

Figure 2-50   Photolysis of Dibenzobarrelene Derivatives **99** and **100**
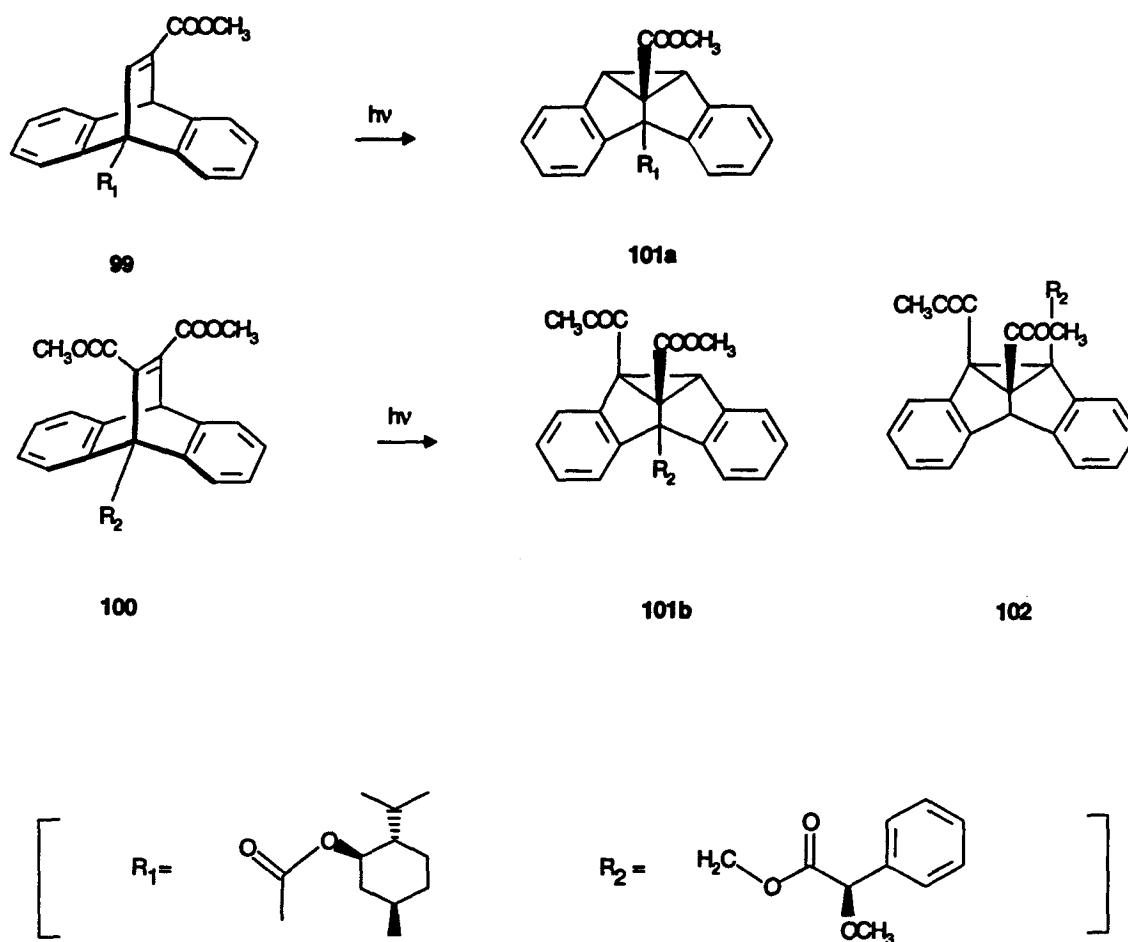
Compound	Medium	Product 101		Product 102	
		Yields (%)	de[a]	Yield (%)	de[a]
99	Solid State	100	80:20	-	-
	Solution	100	40:60	-	-
101	Solid State	80	61:39	20	50:50
	Solution	90	66:33	10	75:25

[a] Diastereomeric excess

In general, photolyzing chiral salt crystals of ester-acid **36** is an effective way to obtain photoproducts in high optical yields. The conversion of the solid state photolyses was limited to 20% in order to minimize melting of the crystals. Within this range, the enantiomeric excess in the photoproducts was not affected by the degree of conversion. The different chiral amines used for salt formation did not affect the regioselectivity of the di-π-methane rearrangement but controlled the enantioselectivity. This is a more effective method than introducing chiral substituents into ester-acid **36**, which requires tedious synthetic routes and complicated separations of isomers.

2.3.2 Photolyses of Salts of 12-Methyl-9,10-dihydro-9,10-ethenoanthracene-11-carboxylic acid (37)

Chiral salts **103** to **105** were prepared from acid **37** by mixing equimolar quantities of acid and base in diethyl ether and filtering the resulting precipitates. The salts were shown to be simple 1:1 complexes by infrared and ^{1}H-NMR spectroscopy, mass spectrometry and elemental analysis. These salts were photolyzed in acetone solutions at room temperature and in the solid state at -40°C. The reaction mixtures were acidified, treated with excess diazomethane and subjected to silica gel column chromatography, which resulted in the isolation of photoproduct **52**. The enantiomeric composition of the photoproduct was determined from 400 MHz ^{1}H-NMR spectra utilizing the chiral shift reagent (+)-Eu(hfc)$_3$. The signal monitored was the methyl singlet at $\delta = 1.90$ ppm. The optical rotation of photoproduct **52** was also measured at the sodium D line. The results are listed in Table 2-6.

Table 2-6   Photoproduct Mixture Composition for Salts **103** to **105**

Chiral Amine	Salt	Enantiomeric excess in Product 52[a,b]	
		Acetone	Solid State
 S-(+)-Prolinol	**103**	nil	(+)-38
 S-(-)-Proline *tert*-butyl ester	**104**	nil	(+)-26
 (S,S)-(+)-Pseudoephedrine	**105a**	nil	≥ (+)-95%
 (R,R)-(-)-Pseudoephedrine	**105b**	nil	≥ (-)-95%

[a] The estimated accuracy in these values is ±10%. [b] The sign of rotation of the predominant enantiomer is shown in parentheses.

Salts of acid 37 → 1. hv → 2. H⁺ → 3. CH₂N₂ → 52
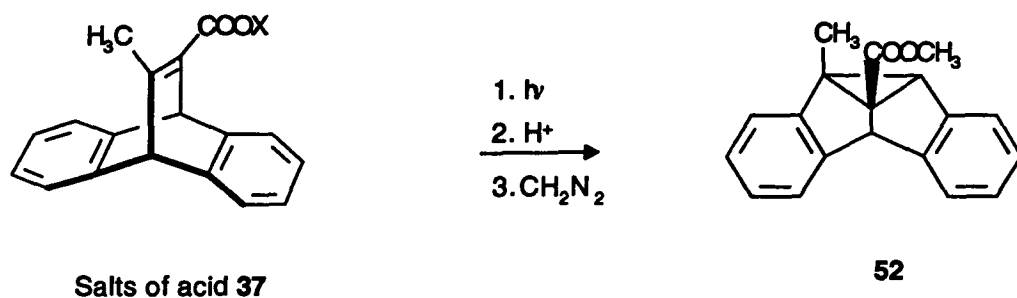
Figure 2-51   Photolysis of Salts of Acid 37

Addition of the chiral shift reagent to a ^{1}H-NMR sample of photoproduct **52** in C_6D_6 led to splitting of the methyl singlet at $\delta = 1.90$ ppm, but baseline separation of these signals could not be obtained (Figure 2-52). Nevertheless this method allowed the enantiomeric excess of the photoproduct **52** to be determined in instances where the enantiomeric excess is low, for example in the cases of irradiation of salts **103** and **104** (Table 2-6). When this method was used to determine the enantiomeric excess of photoproduct **52** formed by the solid state photolysis of pseudoephedrine salts **105**, only one enantiomer was observed within the limits of this method. As described earlier, when enantiomeric excess is determined by use of chiral shift reagents, the accuracy of the method decreases with increasing enantiomeric excess.

^{1}H-NMR Spectra of Photoproduct 52 in C_6D_6 after addition of (+)-Eu(hfc)$_3$

1.9

7   6   5   4   3   2   1   0

ppm

^{1}H-NMR Spectra

of Photoproduct 52 in C_6D_6

7   6   5   4   3   2   1   0

ppm
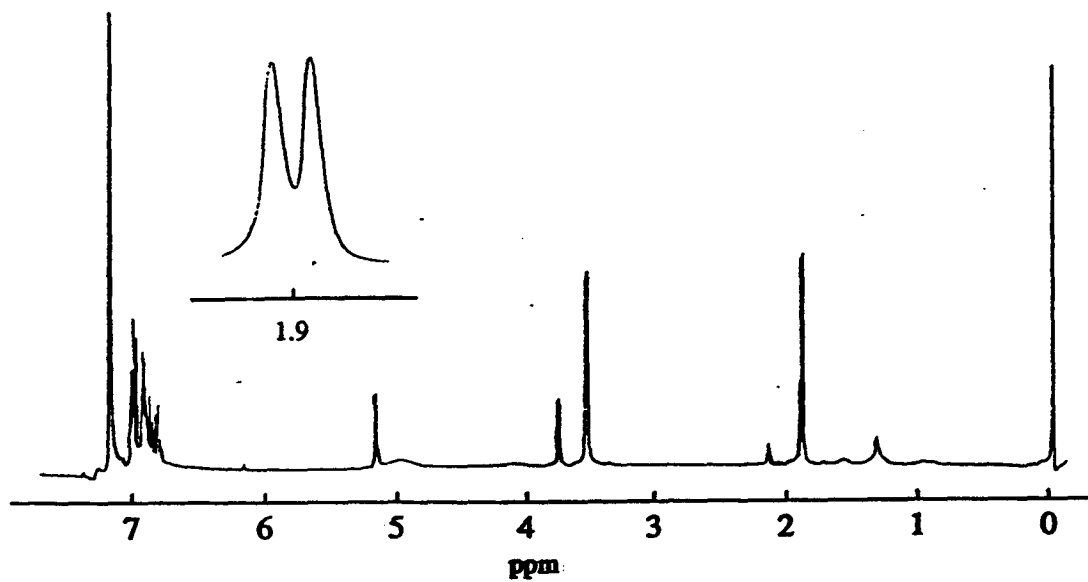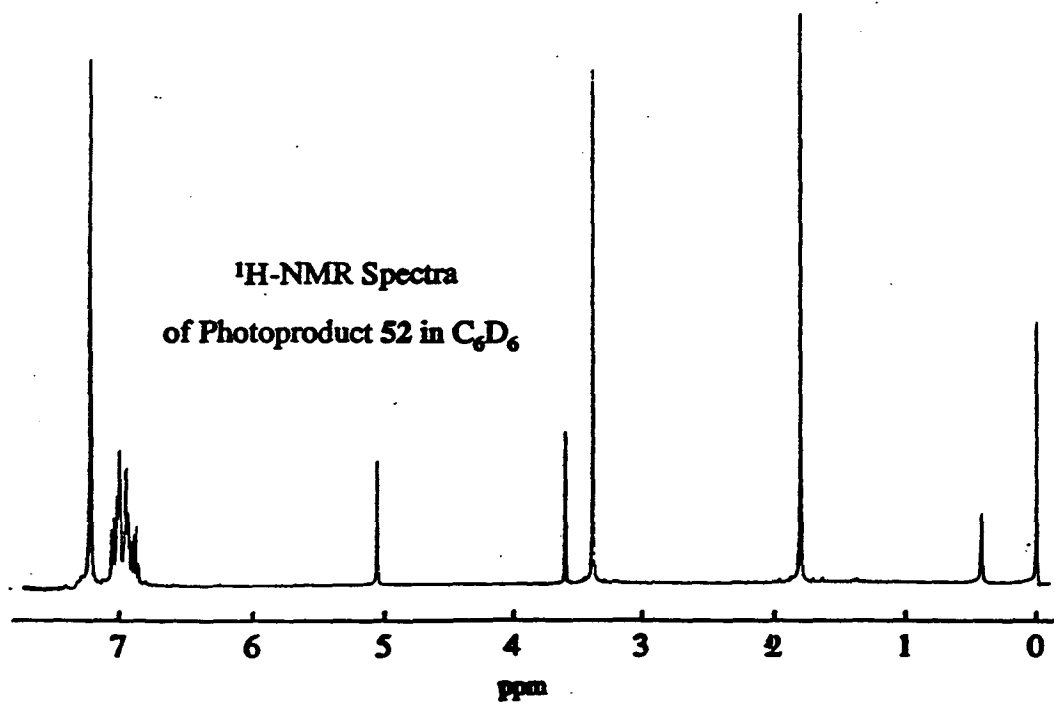
Figure 2-52 ^{1}H-NMR of Photoproduct 52

106   **107**
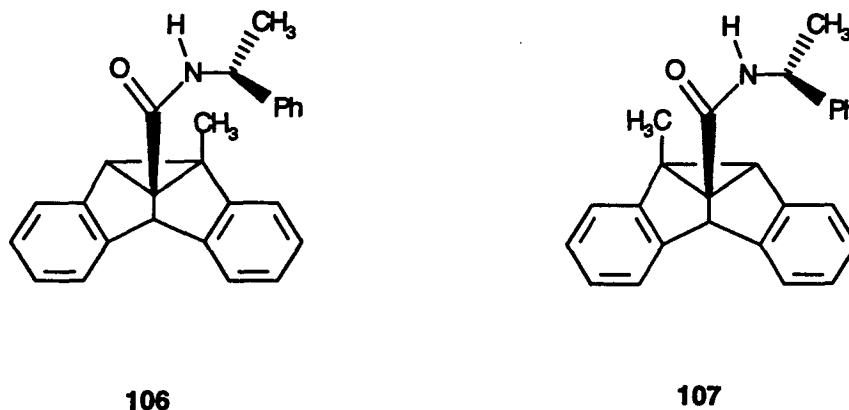
Figure 2-53   Diastereomers **106** and **107**

A second method was used to determine the enantiomeric excess of photoproduct **52** from the solid state photolysis of pseudoephedrine salts **105a** and **105b**. Photoproduct **52** was isolated as before, hydrolyzed with K_2CO_3 and refluxed with S-(-)-α-methylbenzylamine to yield compound **106**. The same procedure was applied to photoproduct **52** which was isolated from the solution photolysis of acid **37**. This yielded diastereomers **106** and **107** in the ratio 1:1. The ^{1}H-NMR spectra of diastereomers **106** and **107** are shown in Figure 2-54. The signals for the proton on the cyclopropane rings are at δ = 4.68 ppm and δ = 4.72 ppm for compounds **106** and **107** respectively. These signals are well resolved. ^{1}H-NMR spectra of compound **106** formed by solid state photolysis of (S,S)-(+)-pseudoephedrine salt **105a** showed no sign of diastereomer **107**. This experiment confirms that photolysis of pseudoephedrine salts **105** yields product **52** in over 95% enantiomeric excess.

¹H-NMR Spectra of 1:1 Mixture of Diastereomers **106** and **107**

4.8 4.7 4.6

7.0   ppm   0.0

¹H-NMR Spectra of Compound **106**

4.8 4.7 4.6

7.0   ppm   0.0
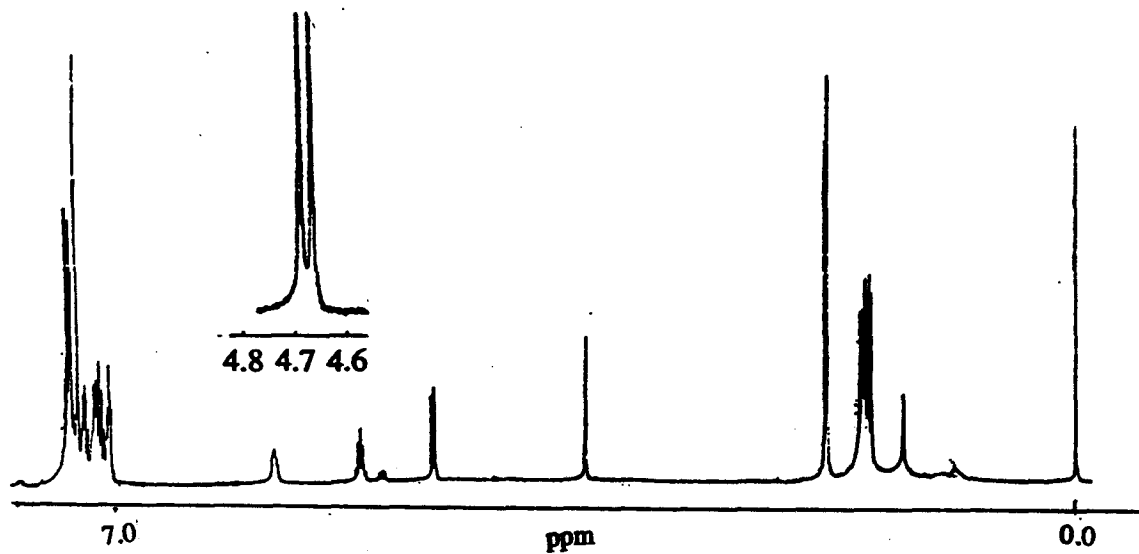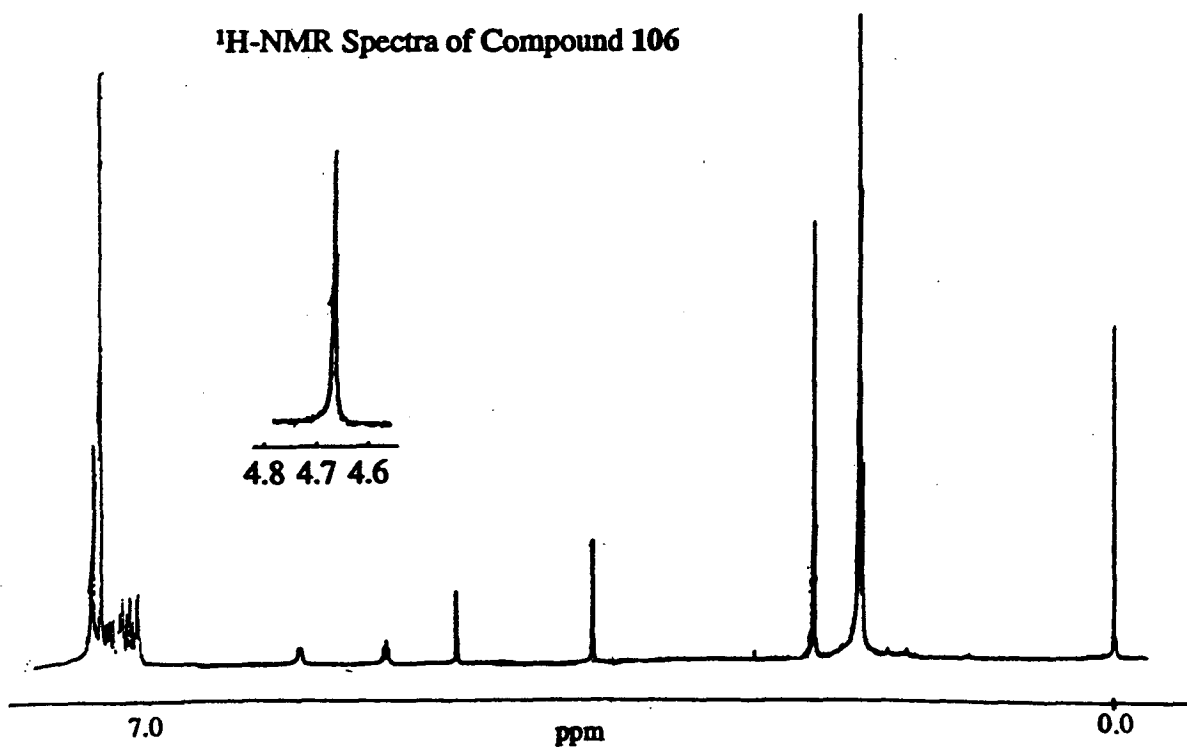
Figure 2-54   ¹H-NMR Spectra of Diastereomers **106** and **107**
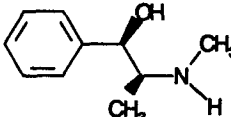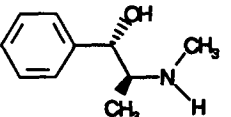
The results in Table 2-6 illustrate that the regioselectivity of the di-π-methane rearrangement of acid **37** is not affected by the salt formation. The only observed photoproduct is compound **52**. The regioselectivity of the rearrangement of acid **37** can be explained in terms of the initial radical forming adjacent to the acid group which is a better radical stabilizer and a more electron withdrawing group, than the methyl functionality. It is interesting that salt formation does not affect the di-π-methane rearrangement, although a carboxylate anion is a poorer electron withdrawing group than a carboxylic acid.

No enantioselectivity was observed for the di-π-methane rearrangement of salts of acid **37** in solution, presumably because the salts have dissociated. In contrast the solid state photolyses led to optical activity in the photoproduct **52**. The enantiomeric excess observed was in the range of 26% to more than 95%. The enantioselectivity of the di-π-methane rearrangement depends on the chiral base used in each instance. In general, these results corroborate those observed for the salts of ester-acid **36**. The solid state photolyses could be carried out to 40% conversion without effecting the enantiomeric excess in the photoproduct.

2.3.3 Photolyses of Salts of Dimethyl 9-Carboxy-9,10-dihydro-9,10-ethanoanthracene-11,12-dicarboxylate (38)

Optically active salts of acid **38** (Figure 2-55) were prepared by mixing equimolar quantities of acid and base in diethyl ether and filtering the resulting precipitate. These salts were shown to be simple 1:1 complexes by infrared and ^{1}H-NMR spectroscopy, mass spectrometry and elemental analysis. Elemental and X-ray structure analyses of salts **108** and **109** demonstrated that they crystallize with half an equivalent of water.

Table 2-7   Photoproduct Mixture Composition for Salts **108** and **109**

Optically Active Amine	Salt	Medium	Work-up with CH_2N_2			Work-up with CH_3CHN_2			
			67		68	69		70	
			Yield (%)[a]	ee[a]	Yield (%)[a]	Yield (%)[a]	ee[a]	Yield (%)[a]	ee[a]
(R,S)-(-)-Ephedrine	108	Acetone	81	nil	19				
		Solid state	10	-	90	10	24	90	≥(-)-95[b]
(S,S)-(+)-Pseudoephedrine	109	Acetone	90	nil	10				
		Solid state				80	16	20	18

[a] The estimated error is ± 5%. [b] The sign of the rotation of the predominant enantiomer is shown in parentheses.

Salts **108** and **109** were photolyzed in acetone solutions at room temperature. The reaction mixtures were acidified, treated with excess diazomethane and subjected to silica gel column chromatography to yield the photoproducts. Solution photolyses of salts **108** and **109** gave compound **67** as the major product with small amounts of product **68** (Table 2-7, see Figure 2-55 for structures).

38: X = H
108: X = (R,S)-(-)-Ephedrine
109: X = (S,S)-(+)-Pseudoephedrine
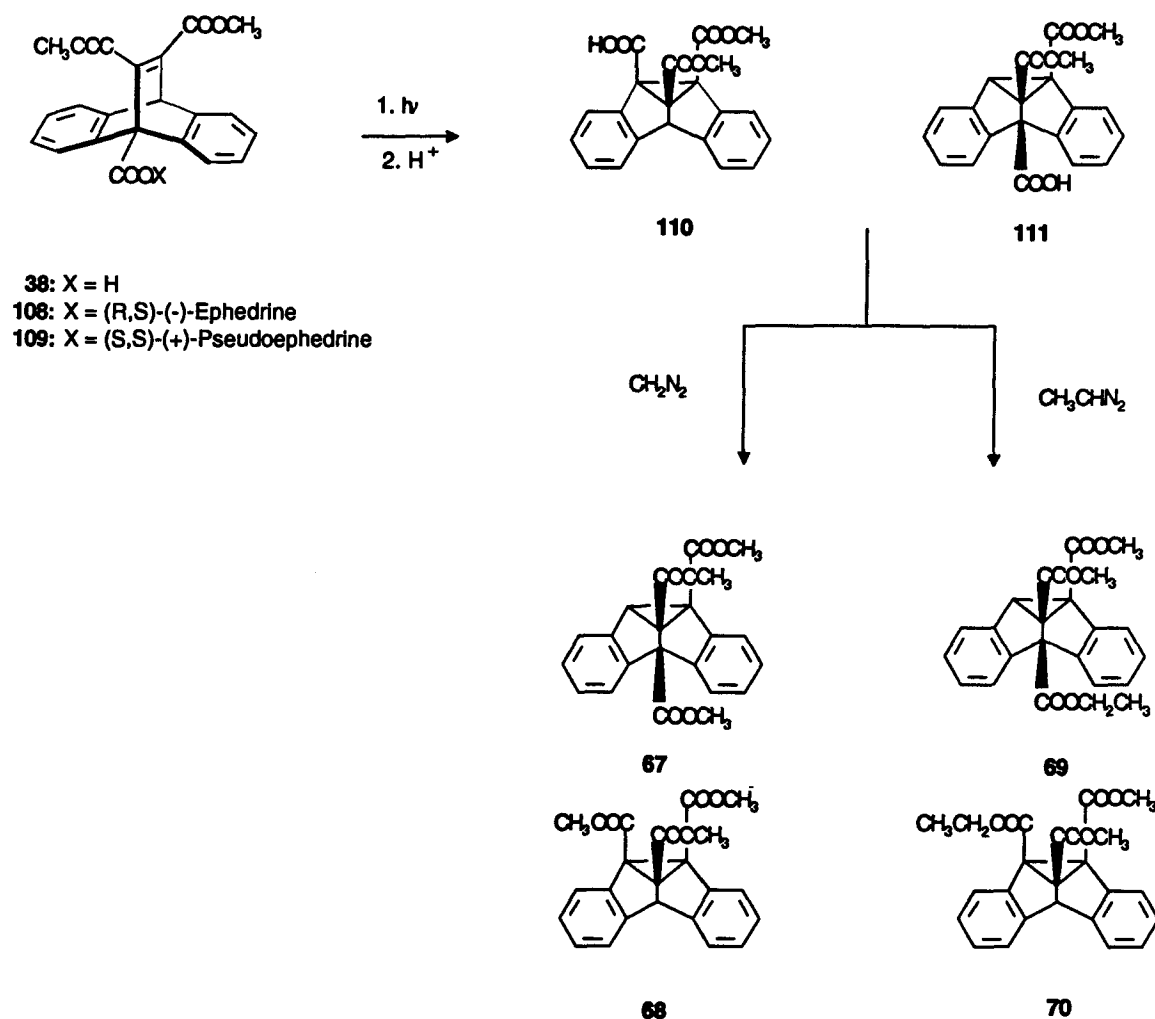
Figure 2-55 Photolysis and Workup of Salts **108** and **109**

(R,S)-Ephedrine salt **108** was photolyzed in the solid state and the photoproducts were isolated following the same procedure as was used for the isolation of the products

of solution photolyses of salts **108** and **109**. As described earlier, the possible dibenzocyclooctatetraene product cannot be isolated using this method and therefore only the di-π-methane rearrangement products of (R,S)-ephedrine salt **108** were isolated. Solid state photolysis of salt (R,S)-ephedrine **108** yielded photoproducts **67** and **68** in the ratio 1:9. The regioselectivity of the di-π-methane rearrangement has been completely reversed in the solid state compared to solutions. Although product **68** is achiral, its precursor, photoproduct **110**, is chiral (Figure 2-55). The solid state photoreactions of salts **108** and **109** were repeated and worked up with diazoethane instead of diazomethane. The product ratios of the solid state photolyses were determined by 400 MHz ^{1}H-NMR spectroscopy. For enantiomeric excess determination, use was made of the chiral shift reagent (+)-Eu(hfc)$_3$. The signals monitored were the methyl singlets at δ = 3.4 ppm and δ = 3.5 ppm for compounds **69** and **70**, respectively. Large chemical shift nonequivalences were observed for the enantiomeric signals (Figure 2-56). In addition the signs of rotation of the predominant enantiomer were measured at the sodium D line by polarimetry. The results of these experiments are summarized in Table 2-7.

Several conclusions can be drawn from the results summarized in Table 2-7. No optical activity was observed in the photoproducts of photolysis of salts **108** and **109** in acetone solutions. The product ratios are the same as observed for the photolysis of acid **38** in acetone. This can be attributed to dissociation of the salts in solution.
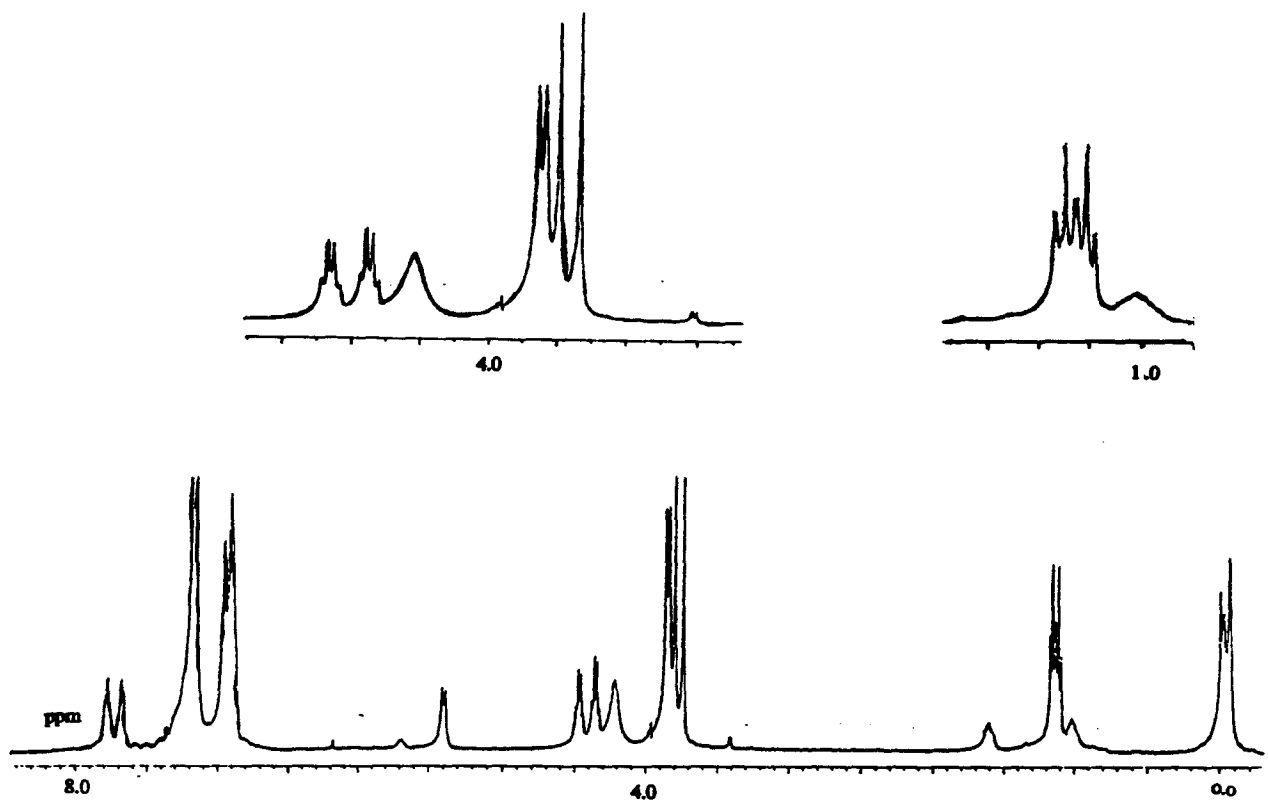
¹H-NMR Spectra of Photoproduct **70** in C₆D₆ after Addition of (+)-Eu(hfc)₃
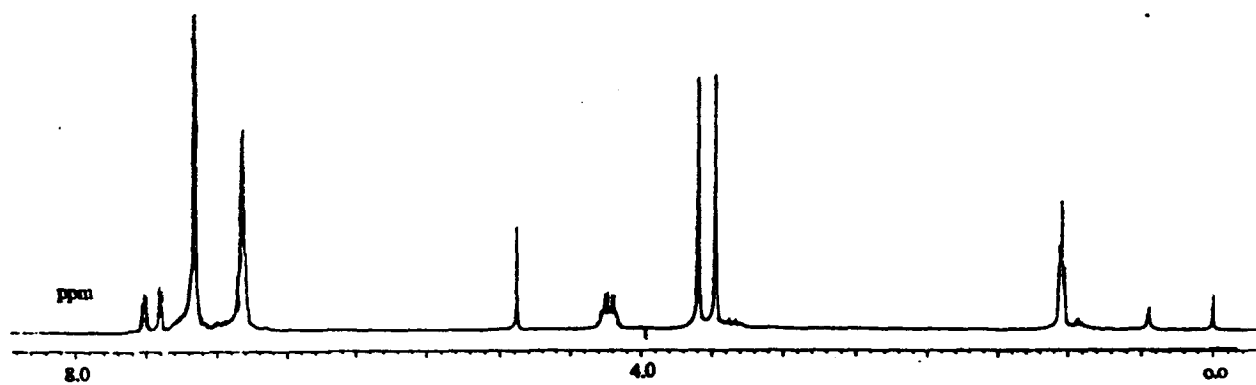
¹H-NMR Spectra of Photoproduct **70** in C₆D₆

Figure 2-56   ¹H-NMR Spectra of Product **70**

The product ratios for the photolysis of salts **108** and **109** in the solid state gave different results (Table 2-7). The product ratio for the solid state irradiation of (R,S)-(-)-ephedrine salt **108** is reversed from the product ratio in solution reactions, whereas the product ratio for photolysis of (S,S)-(+)-pseudoephedrine salt **109** in solution and the solid state is the same. It can be concluded that the crystal lattice controls the reactivity of salt **108**. The enantiomeric excess in the photoproducts of salts of acid **38** depended on the nature of the chiral handle and was poor for salt **109** but good for salt **108**. The solid state photolyses all stopped before 25% conversion. Within this range, the enantioselectivity of these reactions was not affected by the degree of conversion.

In order to explain the regioselectivity of the photoreaction of salt **108**, an X-ray structure analysis was obtained (Figure 2-57). This confirmed that salt **108** crystallizes with half of an equivalent of water. Furthermore it illustrated that acid **38** exists as its anionic form, whereas the amine group in the ephedrine counterion is protonated. There is a hydrogen bond between the carboxylic anion oxygen (O2) of acid **38** and the hydroxy group of the ephedrine moiety. There are also five other intermolecular hydrogen bonds. As expected, the ester group on the vinyl bond next to the bridgehead substituent in acid **38** is out of conjugation, whereas the other ester carbonyl is conjugated to the vinyl bond. This favors formation of the observed product **110** (Figure 2-55).

As mentioned earlier the motions associated with the ester group attached to the vinyl bond are considered to be the most important determinants of regioselectivity in the solid state di-π-methane rearrangement.[42] Both carbonyl groups are involved in hydrogen bonding which should affect their capability to stabilize an adjacent radical similarly.
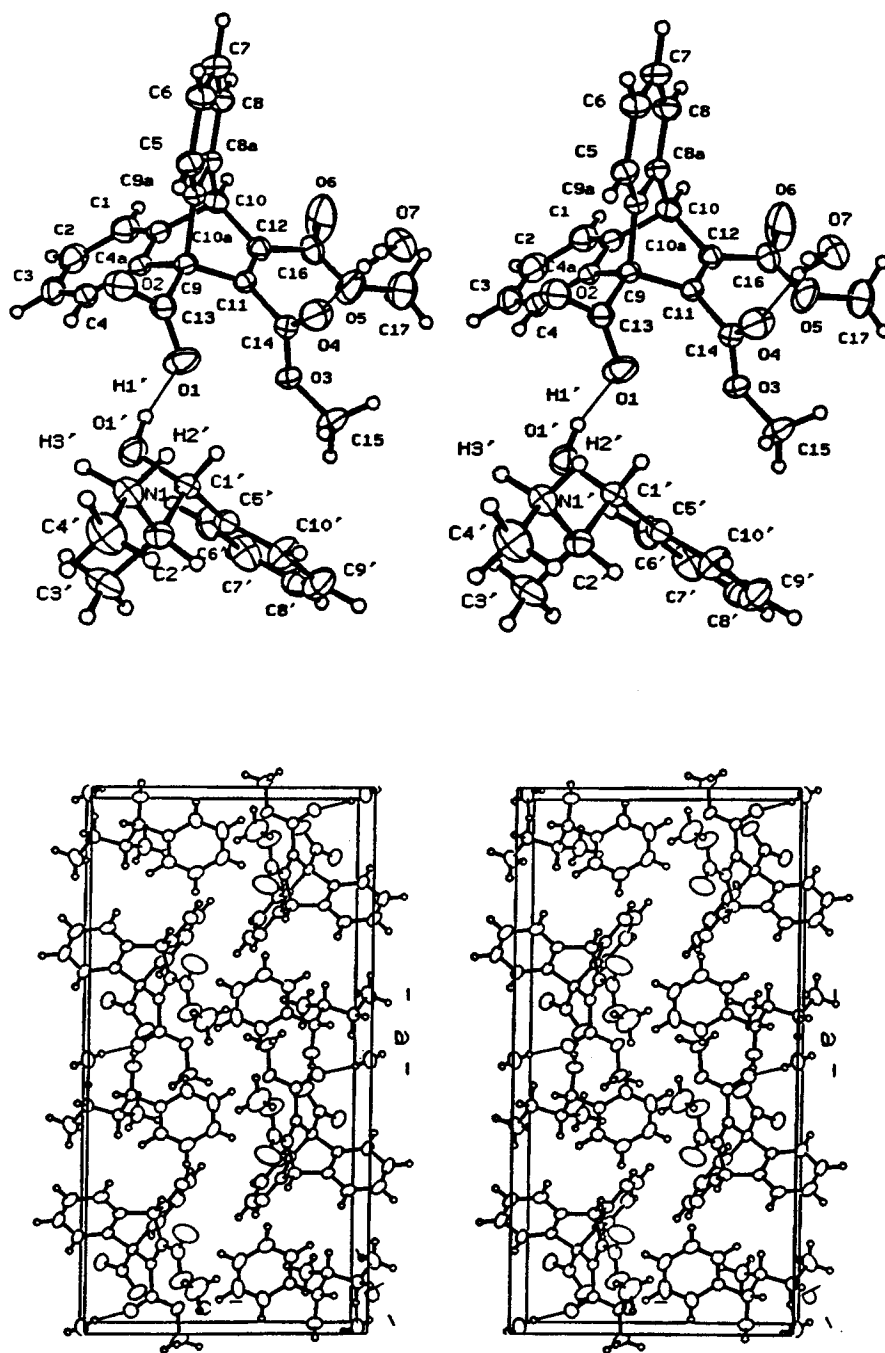
Figure 2-57   Crystal Structure of (S,S)-Ephedrine Salt **108**

When the intermolecular features of the crystal structure are analyzed it becomes clear that the movement of the ester group on C12 is hindered because of the aromatic ring on an adjacent molecule in the crystal lattice. The carbonyl oxygen, O6, is weakly hydrogen bonded to one of the hydrogens on this aromatic ring. For the other ester group on C11 there is close contact between O3 and a methyl group on an adjacent molecule. It can be suggested that the initial vinyl benzo bridging takes place between C9a and C11, which requires the ester group to swing away from the methyl group on the adjacent molecule. The space around the carbonyl oxygen O4 is free of any intermolecular contacts except to a water molecule, which is hydrogen bonded to O4. However, it can be expected that the water molecule is better able to move around in the crystal lattice, presumably because of its small size.

There are few known examples in the literature of co-crystallized water molecules affecting solid state reactivity. As discussed earlier, Jones et al.[21] studied the [4+4] photodimerization of the acridizinium salt 11 (Figure 1-5). They observed that for salts that co-crystallize with water molecules, the majority of reactions were topotactic. In contrast, for the same salts crystallized without water molecules the reactions stopped at 80% conversion. Although the source of this effect is still unclear, apparently the incorporation of water molecules affects reactivity.

Similarly Hasegawa et al.[87] found that photodimerization of p-formylcinnamic acid crystals with incorporated water gives much higher yields of the photodimer than anhydrous crystals.

2.3.4 Photolyses of Salts of Dimethyl 9-Amino-9,10-dihydro-9,10-ethenoanthracene-11,12-dicarboxylate (39)

Hydrochloride salt **112** was prepared by mixing a solution of amine **39** in ethanol with concentrated hydrochloric acid (Figure 2-58). The crystals that formed were shown to be a simple 1:1 salt by ^{1}H-NMR spectroscopy, infrared spectroscopy and elemental analysis. Salt **112** was irradiated in acetonitrile and in the solid state. The reaction mixtures were made basic and the samples analyzed by GC, which showed that photoproduct **60** was the only product formed.

The results represent a striking reversal of the regioselectivity of the di-π-methane rearrangement of the hydrochloride salt **112** compared with amine **39**. As described earlier, irradiation of amine **39** gave predominantly the photoproduct **61**. Paddick et al.[63] explained the regioselectivity of this reaction by suggesting that intramolecular hydrogen bonding between the amine group and its nearest ester group renders the ester group less capable of stabilizing an adjacent radical and therefore product **61** is favored over product **60** (Figure 2-58). The regioselectivity of the di-π-methane rearrangement of salt **112** is not affected by the reaction medium; the major photoproduct is **60** both in solution and in the solid state. Since the ammonium ion is more electronegative than the amino group, we propose that the electronegativity of the ammonium ion destabilizes intermediate **63** more than the intramolecular hydrogen bonding destabilizes intermediate **64**, and consequently product **60** is favored for irradiation of the hydrochloride salt **112**.[88]
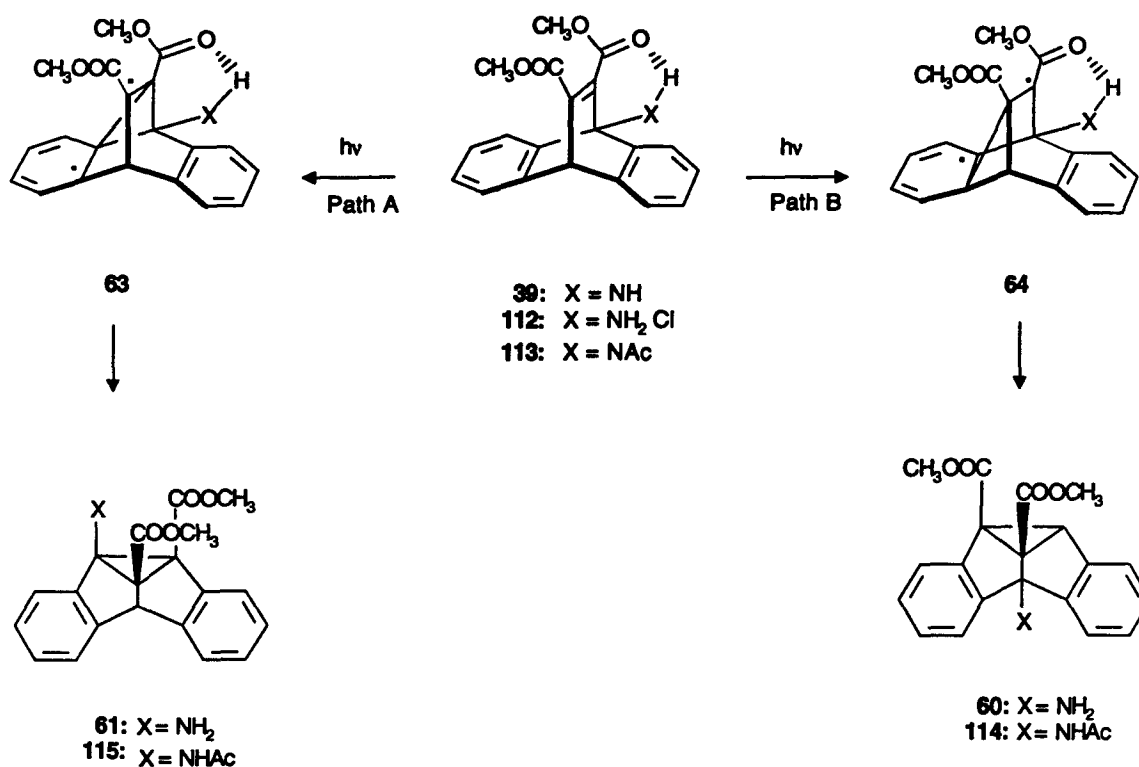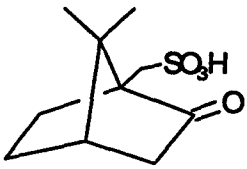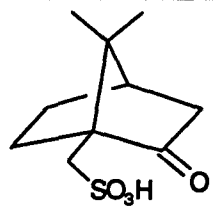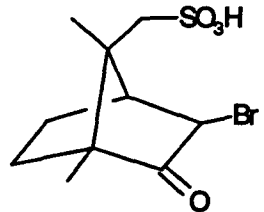
Figure 2-58   Photolysis of Compounds **39**, **112** and **113**

It is interesting to compare the above results with the regioselectivity of the di-π-methane rearrangement of acetamide **113** (Figure 2-58). Paddick et al.[63] found that solution photolysis of acetamide **113** yields a mixture of di-π–methane rearrangement products **114** and **115** in the ratio 70:30. The authors suggested that the electronegativity effect in acetamide **113** outweighs the hydrogen bonding effect and consequently product **114** is favored. The regioselectivity is the same as observed for the di-π-methane rearrangement of hydrochloride salt **112** but reversed compared with amine **39**.

Chiral salts of amine **39** were prepared by mixing equimolar quantities of base and acid in a suitable solvent and filtering off the crystals that formed upon standing. The salts **116a**, **116b** and **117** were shown to be simple 1:1 salts by infrared and ¹H-NMR spectroscopy, mass spectrometry and elemental analysis. Camphorsulfonic acid salts

116a and **116b** co-crystallized with one equivalent of H_2O as shown by elemental analysis. This was confirmed by X-ray structure analysis of salt **116a**. Elemental analysis and FAB-MS indicated that crystals of salt **117** contained one equivalent of HCl. Attempts to prepare salts of amine **39** with various optically active carboxylic acids were not successful.

Table 2-8   Enantiomeric Excess in Photoproduct **60** from Salts **116a** to **117**

Acid	Salt	Solid State ee[a]	Solution Phase ee[a]
R-(-)-Camphorsulfonic acid	**116a**	(-)-68	nil
S-(+)-Camphorsulfonic acid	**116b**	(+)-64	nil
(-)-3-Bromocamphor-8-sulfonic acid	**117**	(-)-30[b]	nil

[a] The estimated accuracy in these values is ±5%; The sign of the rotation of the predominant enantiomer is shown in parentheses. [b] Only in the case of salt **117** was a small amount of photoproduct **61** detectable (ca. 15%).

¹H-NMR Spectra of Photoproduct **60** in

CDCl₃ after Addition of (+)-Eu(hfc)₃

3.9

7 ppm   6   5   4   3   2   1   0

¹H-NMR Spectra of

Photoproduct **60** in CDCl₃

7 ppm   6   5   4   3   2   1   0
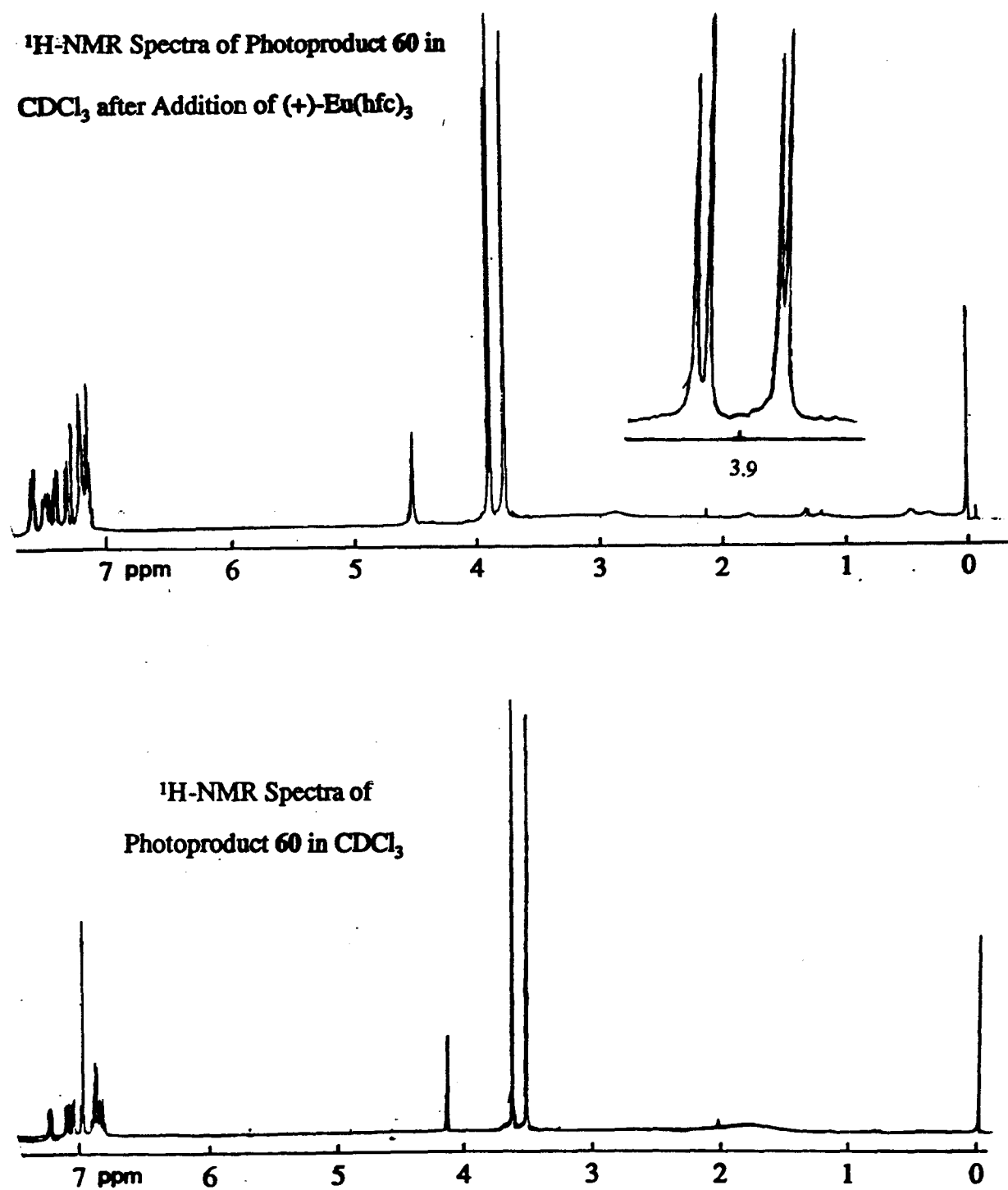
Figure 2-59   ¹H-NMR Spectra of Photoproduct **60**

Salts **116a, 116b** and **117** were irradiated in solution at room temperature and in the solid state at -40°C. After photolysis the samples were dissolved in ethyl acetate, washed thoroughly with 10% aqueous sodium hydroxide, dried, and analyzed by GC. This revealed that compound **60** was the sole product formed, except in the case of solid state irradiation of salt **117**, where a small amount of photoproduct **61** was detected (ca. 15%). The photoproducts of the chiral salts **116a, 116b** and **117** were isolated by silica gel chromatography and analyzed by polarimetry and ^{1}H-NMR chiral shift reagent analysis: for the latter, use was made of the chiral shift reagent (+)-Eu(hfc)$_3$. The signal monitored was the methyl singlet at $\delta = 3.83$ ppm, which showed almost full baseline separation of the enantiomers (Figure 2-59). The results are listed in Table 2-8.

The results in Table 2-8 show that good enantiomeric excess can be achieved for the di-π-methane rearrangement of salts of amine **39** in the solid state, but that in solution negligible asymmetric induction is observed. The degree of asymmetric induction depends on the nature of the chiral acid. The fact that the sign of rotation of the photoproduct can be reversed by using the optical antipode of the chiral induction agent indicates that the system is well behaved. The solid state photolyses could be carried out to 60% conversion without affecting the enantiomeric excess in the photoproduct.

This demonstrates that asymmetric induction in the solid state photochemistry of amines with optically active acids works as well as the opposite approach, i.e., asymmetric induction in the solid state photochemistry of carboxylic acids complexed with optically active amines.

99

2.4 Absolute Steric Course of Solid State Di-π-methane Rearrangements

In salts of dibenzobarrelene derivatives **36, 37** and **39**, the electronic effects control the regioselectivity of the di-π-methane rearrangement or at least the electronic effects and the crystal lattice reinforce each other. In contrast, the regioselectivity of the di-π-methane rearrangement of salts of acid **38** was affected by the crystal lattice, and different regioselectivity was observed in solution compared with the solid state. Photolyses of optically active salts of the four dibenzobarrelene derivatives investigated yielded low to good enantiomeric excesses in the photoproducts. The results depended on the nature of the chiral counterion, however a counterion leading to high enantiomeric excess in the photoproducts of one dibenzobarrelene derivative does not necessarily give good results for the others. The chiral counterions ensure chiral crystals, but the crystal lattice alone is accountable for asymmetric induction and salts of different dibenzobarrelene derivatives crystallize in different crystal packing arrangements.

As described earlier, there are four different di-π-methane systems in the dibenzobarrelene skeleton and each of these four systems is associated with a pathway that leads to a different product (Figure 1-14). That is, two pathways lead to the same regioisomer and the other two to a different regioisomer. However, pathways that lead to the same regioisomer yield opposite enantiomers of the product. In dibenzobarrelene derivatives for which the di-π-methane rearrangement is both regio- and enantioselective, it is possible to specify which of these pathways is followed by comparing the absolute configurations of the starting material and the photoproduct.

For each dibenzobarrelene derivative the absolute configuration of the chiral salt which gave the best results and its photoproduct were determined. The solid state

reaction pathways were determined by comparing the absolute configuration of the starting material with that of its product. Knowing which pathway is followed makes it possible in principle to identify the crystal forces that control the enantioselectivity of the photorearrangement in the solid state. Salts of dibenzobarrelene derivatives **36, 37** and **39**, were investigated. Furthermore, by studying salts of different dibenzobarrelene derivatives, the crystal forces in different systems can be compared in order to propose a general explanation of factors that control asymmetric induction in dibenzobarrelene systems.

2.4.1 Absolute Configurations of S-(-)-Proline *tert*-Butyl Ester Salt 96 and Photoproduct 32a

Photolysis of S-(-)-proline *tert*-butyl ester salt **96** yielded photoproduct **32a** in over 95% enantiomeric excess. The absolute configuration of salt **96** can be easily obtained since the absolute configuration of the proline moiety is known. The absolute configuration of S-(-)-proline *tert*-butyl ester salt **96** was obtained by X-ray structure analysis[89] which demonstrated that the dibenzobarrelene moiety in salt **96** has the absolute configuration 11M, 12M (Figure 2-60). The designation 11M, 12M focuses on the conformational dissymmetry conferred on the molecule by the carboxylic groups on C11 and C12. The absolute configuration was obtained by determining the smallest torsion angle between the groups of highest priority, or fiduciary groups, attached to each end of the single bond for which the conformation is specified.[45] If two of the groups are identical, that which provides the smallest angle is fiducial. A positive torsion angle (clockwise rotation) is designated P (plus) and a negative torsion angle (counter-clockwise rotation) is designated M (minus). The torsion angles O4-C14-C12-C11 and

O1-C13-C11-C12 of S-(-)-proline *tert*-butyl ester salt 96 were analyzed and both were found to be negative.
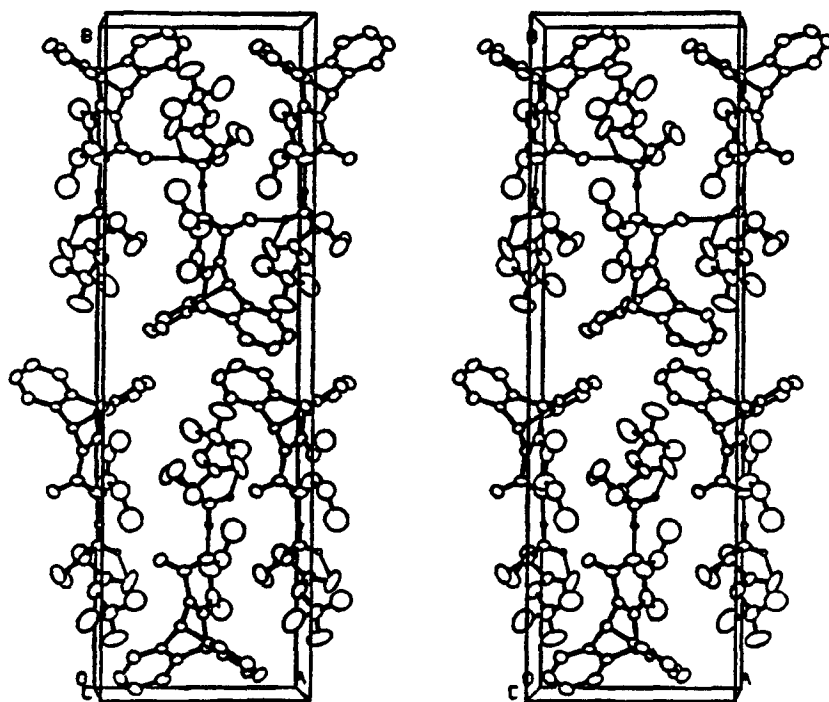
Figure 2-60   Crystal Structure of Proline *tert*-Butyl Ester Salt 96
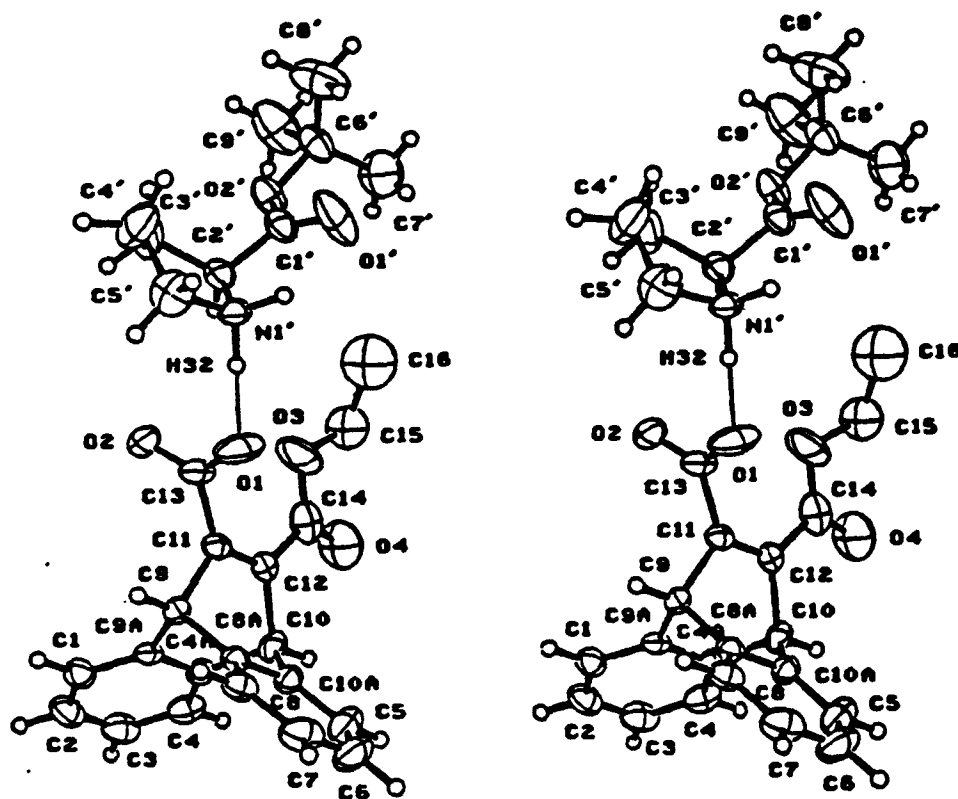
Figure 2-60   Crystal Structure of S-(-)-Proline *tert*-Butyl Ester Salt 96 (continued)

The crystal structure of S-(-)-proline *tert*-butyl ester salt 96 revealed that the amine group of the proline moiety is protonated whereas the carboxylic acid functionality in the dibenzobarrelene moiety is in its anion form. The oxygens of the carboxylic anion are hydrogen bonded to different proline moieties. It was suggested earlier that the regioselectivity of the di-π-methane rearrangement of salt 96 is controlled by electronic

effects. There is considerably more steric influence from the crystal lattice around the carboxylate anion than in the vicinity of the ester group, mainly because of the hydrogen bonding of the carboxylate anion to the proline moiety. The intramolecular packing arrangement of the dibenzobarrelene reinforces the electronic effects since the oxygens of the carboxylate anion are almost completely out of conjugation with the vinyl bond whereas the ester carbonyl is nearly fully conjugated to the vinyl bond. This favors formation of the observed product 32a.
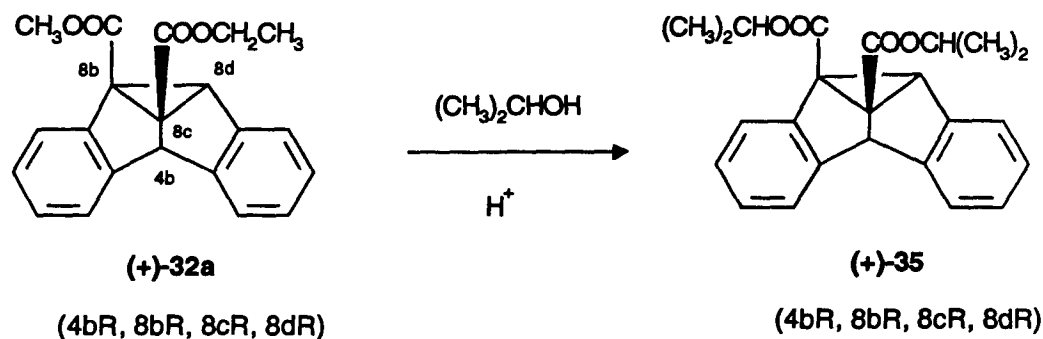
Figure 2-61   Transesterification of Di-Ester 32a into Di-Ester 35

Photoproduct 32a from the solid state photolysis of S-(-)-proline tert-butyl ester salt 96 was isolated as described before. The circular dichroism spectrum of 32a is shown in Figure 2-62; the sign of the optical rotation was positive at the sodium D line (589 nm). Photoproduct 32a was refluxed in sec-butanol to yield the (+)-enantiomer of di-ester 35 (Figure 2-61). Scheffer et al.[42] showed that the (+)-enantiomer of di-ester 35 has the absolute configuration (4bR, 8bR, 8cR, 8dR) and therefore the (+)-enantiomer of product 32a must have the same absolute configuration. The circular dichroism spectrum for di-ester 35 is shown in Figure 2-62; as expected the circular dichroism spectra for di-esters 32a and 35 are almost identical.[90]
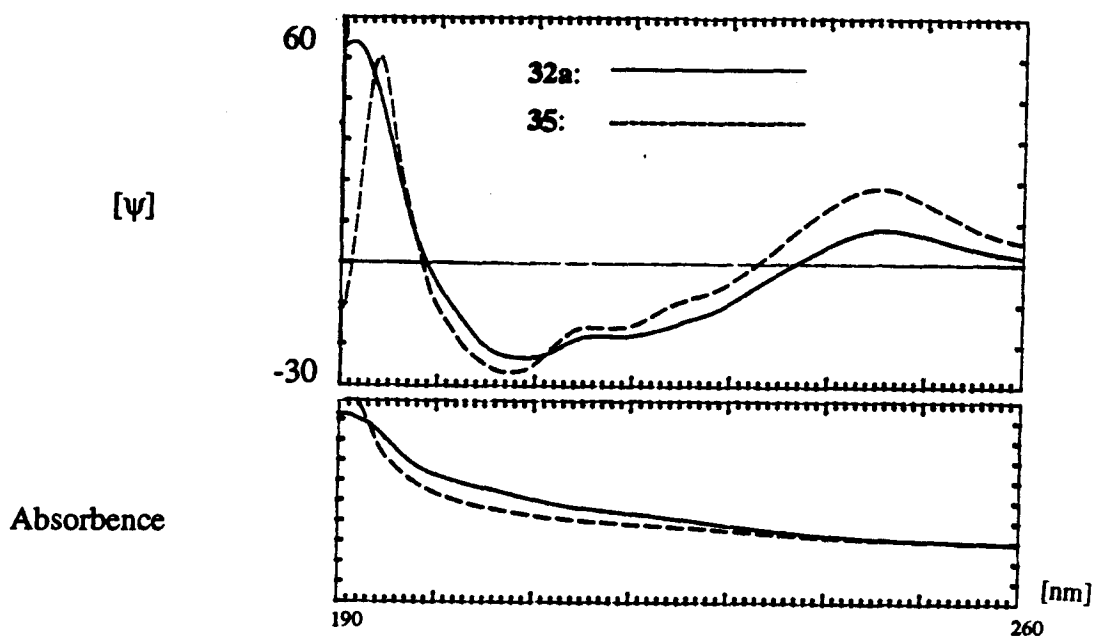
Figure 2-62   Circular Dichroism Spectra for Compounds **32a** and **35**

Comparison of the absolute configurations of S-(-)-proline *tert* butyl ester salt **96** and its photoproduct (+)-**32a** demonstrates that the initial benzo-vinyl bridging of the solid state di-π-methane rearrangement in salt **96** is formed between C8a and C11. In order to identify the factors that favor initial vinyl bonding between C8a to C11 over C9a to C11, the intramolecular arrangement of the dibenzobarrelene system was investigated. The vinyl bond substituents are frozen in non-C_{2v} orientation which gives the molecule a chiral conformation. The motions associated with the vinyl substituents are considered to be most important in determining the regio- and enantioselectivity of the di-π-methane rearrangement.[42] The carbonyl group in the ester is almost completely conjugated with the vinyl bond (O4-C14-C12-C11 = -171°) whereas the oxygens of the carboxylate anion are almost completely out of conjugation with the double bond (O1-C13-C11-C12 = -81°, O2-C13-C11-C12 = +104°). This suggests that moving C11 towards C8a would cause similar steric interactions between the vinyl substituents, as moving C11 towards C9a, that is neither initial benzo-vinyl bridging between C11 and C8a or C11 and C9a should be favored. However, when the -9° torsion angle between C13-C11-C12-C14 (Figure 2-

105

63) is taken into account it can be suggested that the initial benzo vinyl bridging between C8a and C11 should be favored because it involves movement of the C11-C13 bond away from the C12-C14 bond. In contrast, initial benzo-vinyl bonding between C9a and C11 requires eclipsing of the C11-C13 bond with the C12-C14 bond, which brings the substituents on C11 and C12 closer together causing steric interactions between them and would thus be expected to be unfavorable.

The intramolecular distance between C8a and C11, 2.44(8) Å, is the same as the distance between C9a and C11, 2.44(7) Å. The torsion angle between C13-C11-C12-C14 suggests that the p orbital on C11 is better aligned to form a bond with C8a than C9a (Figure 2-63). In other words if the initial excited state has a similar conformation as the starting material it requires less movement of C11 to form a bond with C8a than C9 because the p orbital on C11 is tilted towards C8a.

Torsion Angles

O1-C13-C11-C12 = - 81°
O2-C13-C11-C12 = + 104°

O3-C14-C12-C11 = + 6°
O4-C14-C12-C11 = - 171°

C13-C11-C12-C14 = - 9°
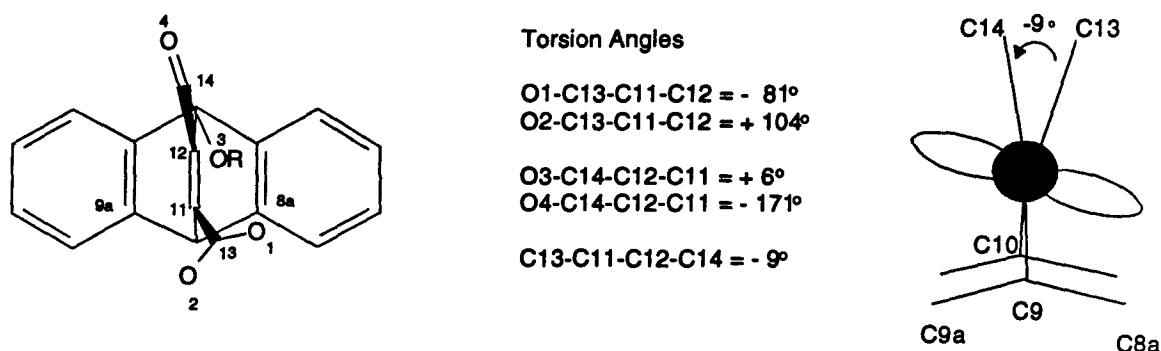
Figure 2-63   Some Torsion Angles of S-(-)-Proline *tert*-Butyl Ester Salt 96

Analyzing the intermolecular packing arrangement of salt **96** reveals that carboxylate anion O1 is hydrogen bonded to a proline moiety above it in the crystal lattice whereas carboxylate anion O2 is hydrogen bonded to a proline moiety beside it in the crystal lattice (Figure 2-60). These intermolecular hydrogen bonds result in intermolecular steric crowding between the carboxylate anion and the proline moieties. However, it can be proposed that the intermolecular arrangement of the dibenzobarrelene

106

moiety in salt **96** does not favor either formation of the (+) or the (-)-enantiomer of product **32a**. This suggests that the intramolecular packing arrangement of salt **96** controls the enantioselectivity in the di-π-methane rearrangement.

Scheffer et al.[91] studied type II photoreactions of macrocyclic di-ketones in the solid state. Irradiation of these ketones yielded either *cis* or *trans*-cyclobutanols. The authors explained the regioselectivity of the type II reaction from the X-ray crystal structure of the starting materials. They proposed that the *cis* or *trans*-cyclobutanol which was favored required less movement of the 1,4 biradical intermediate for ring closure. That is the p orbitals in the biradical intermediate were better aligned for ring closure to form the favored cyclobutanol.

n = 5, 7	85%	13%
n = 6, 8	3%	88%
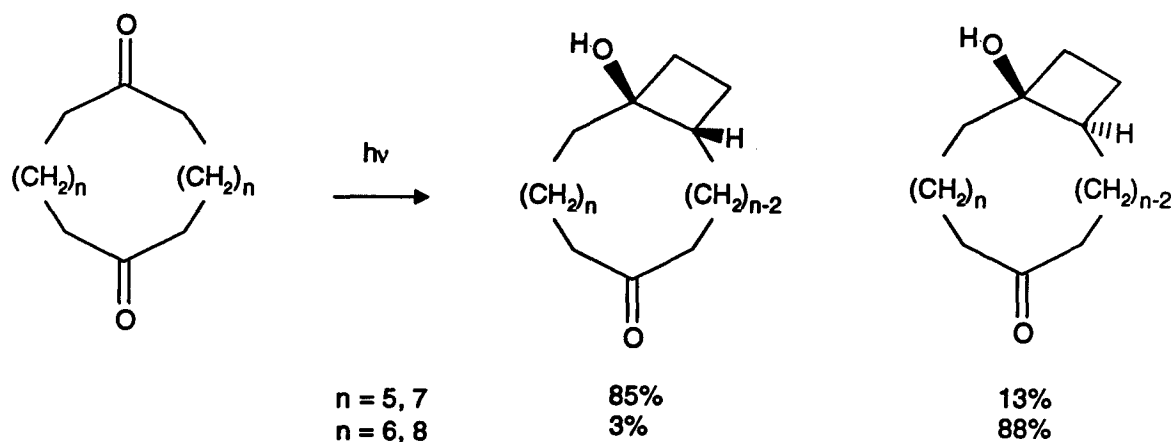
Figure 2-64   Type II Reaction of Macrocyclic Di-ketones

As described earlier, Scheffer et al.[43] explained the enantioselectivity of the di-π-methane rearrangement of di-ester **34** by suggesting that paths I and II shown in Figure 1-14 were favored because they caused the ester groups to move away from each other in the initial stage of the reaction. Paths III and IV, on the other hand, were thought to lead to severe steric interactions between the ester groups. Both the ester carbonyls are

partially conjugated with the vinyl bond (Figure 2-65) which makes it easier to visualize an interaction between the two ester groups in the initial step of the di-π-methane rearrangement. The torsion angle between the ester substituents on the vinyl bond is +5° (C13-C11-C12-C17), which suggests that pathways I and II in Figure 1-14 are favored as they will not cause eclipsing of the C11-C13 bond with the C12-C17 bond. This hypothesis does not discriminate between the two pathways which both lead to the (-)-enantiomer of product 35.
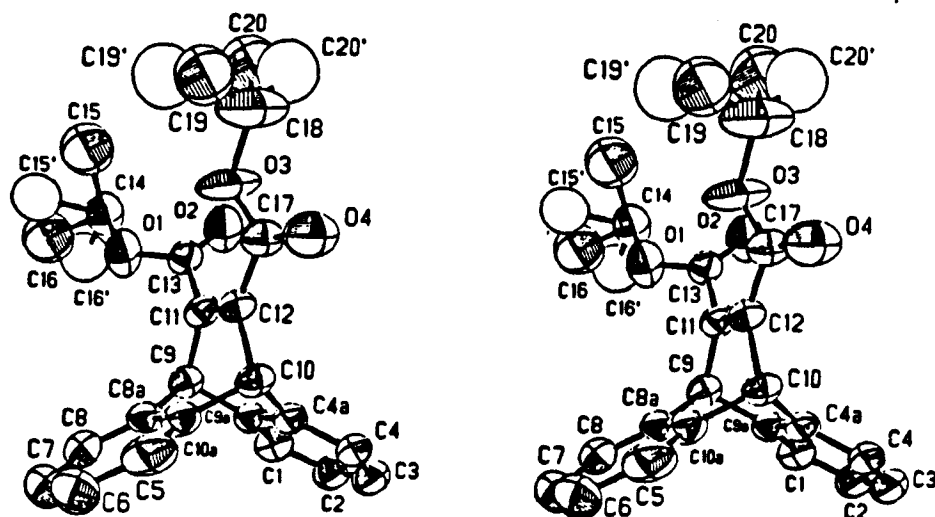
Figure 2-65   Crystal Structure of Di-ester 34

2.4.2 Absolute Configurations of Salts 103, 105a and Photoproduct 52

Photolysis of (S,S)-(+)-pseudoephedrine salt **105a** yielded the (+)-enantiomer of photoproduct **52** in over 95% enantiomeric excess. The absolute configuration of the dibenzobarrelene moiety in the (S,S)-(+)-pseudoephedrine salt **105a** was determined by X-ray crystal structure analysis and shown to be 12P (Figure 2-66). The X-ray structure revealed that acid **37** is in its anionic form whereas the amine group in the pseudoephedrine moiety is protonated. Both oxygens in the dibenzobarrelene moiety are involved in hydrogen bonding. The space around the methyl group on the vinyl bond is relatively free from interaction with the neighboring molecules, whereas the space around the carboxylate anion is very crowded due to hydrogen bonding with the pseudoephedrine moiety.
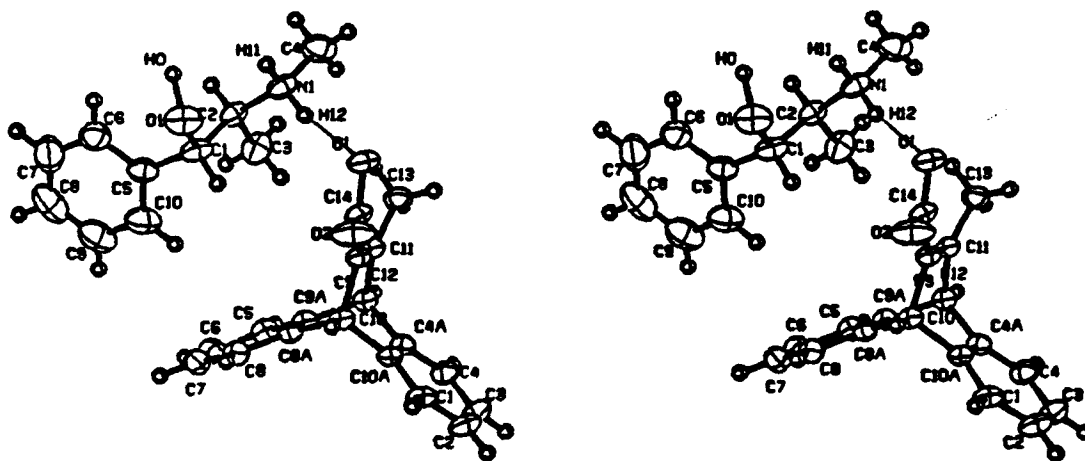
Figure 2-66   Crystal Structure of (S,S)-(+)-Pseudoephedrine Salt **105a**.

109
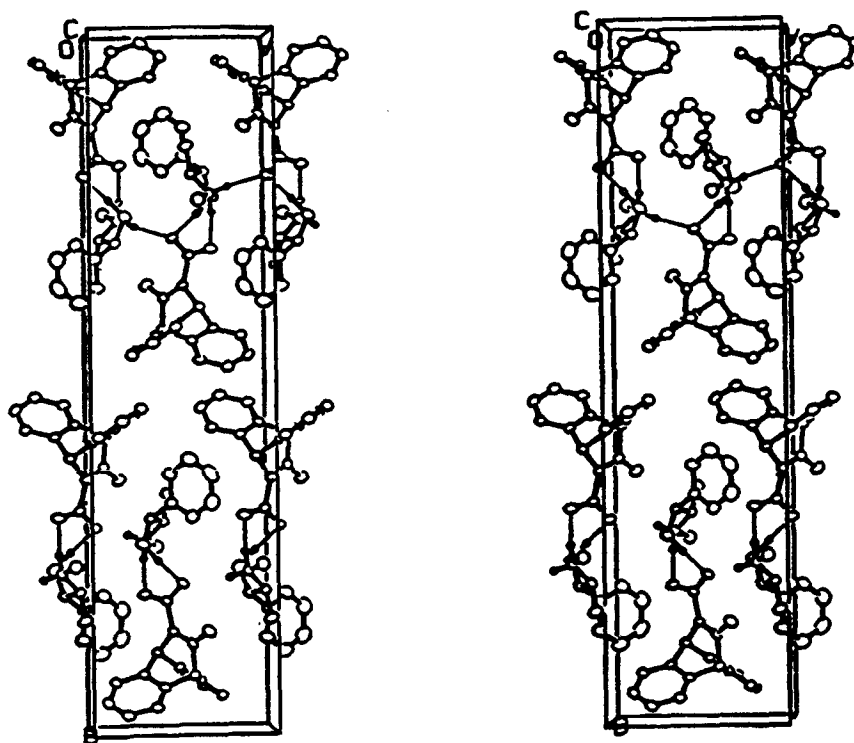
Figure 2-66   Crystal Structure of (S,S)-(+)-Pseudoephedrine Salt 105a (continued)

The photoproduct 52 (the (+)-enantiomer) of the solid state irradiation of (S,S)-
(+)-pseudoephedrine salt 105a was worked up as before and hydrolyzed with K_2CO_3 to
yield acid 115. Refluxing acid 115 with oxalyl chloride gave acid chloride 116 which
was refluxed with S-(-)-α-methylbenzylamine to yield compound 106 (Figure 2-67).

110
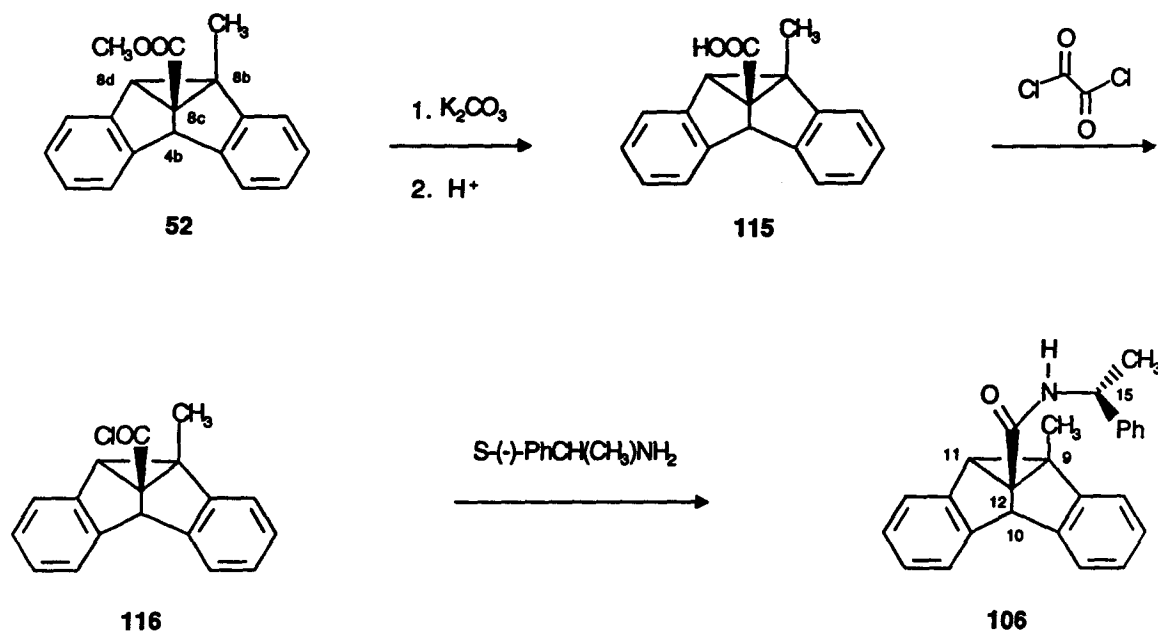
Figure 2-67   Synthesis of Compound **106**

The absolute configuration of compound **106** was determined by X-ray analysis (Figure 2-68). There are two independent molecules in the unit cell and both have the absolute configuration (C9R, C10S, C11S, C12S, C15S) (Figure 2-68, The crystallographer used a different numbering system). Consequently it can be concluded that the (+)-enantiomer of product **52** has the absolute configuration (4bS, 8bR, 8cS, 8dS).
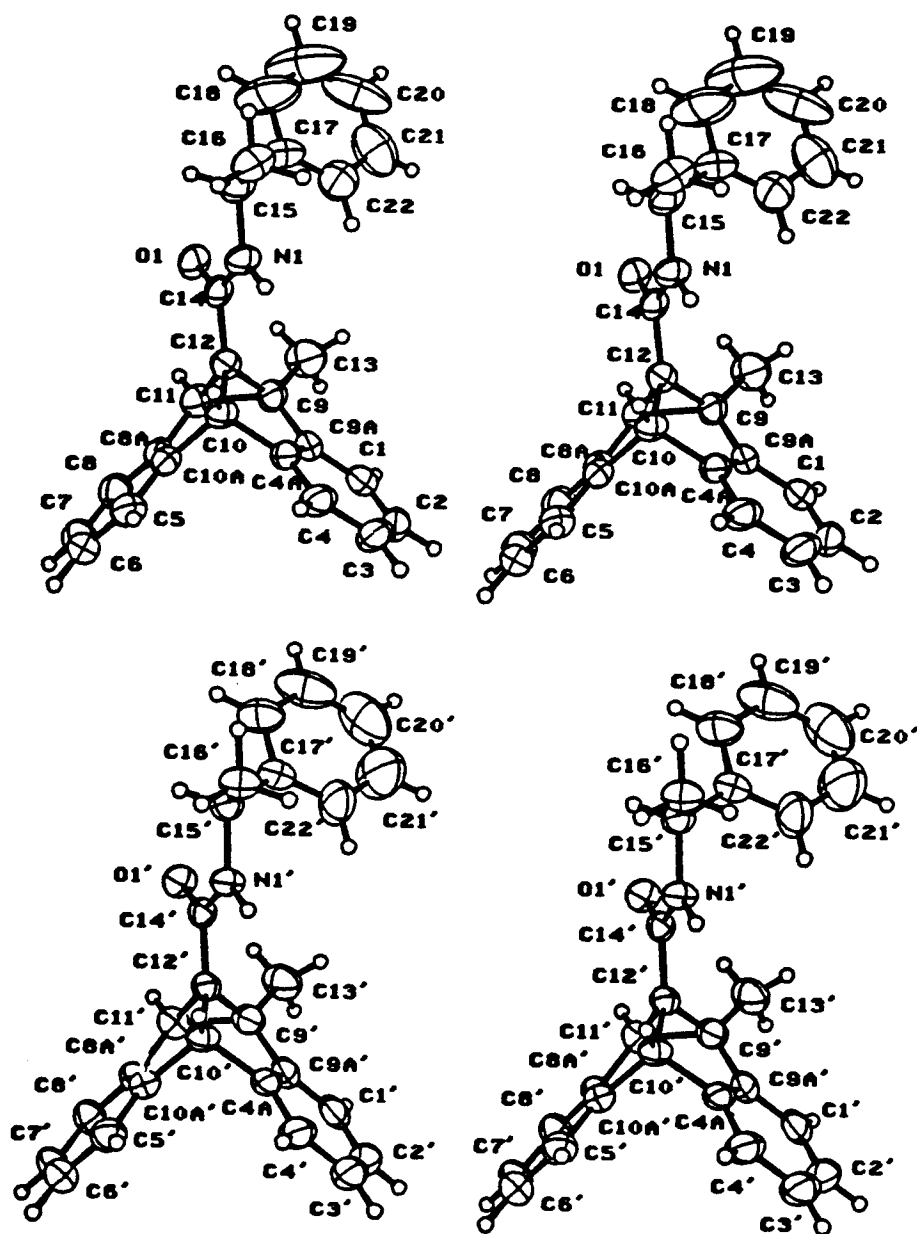
Figure 2-68   Crystal Structure of Compound **106**

112

A comparison of the absolute configurations of (S,S)-(+)-pseudoephedrine salt 105a and its photoproduct 52 illustrates that the initial vinyl benzo bridging takes places between C4a and C11. The hypothesis used to explain the enantioselectivity of S-(-)-proline *tert*-butyl ester salt 96 can also be applied the enantioselectivity of salt 105a. The torsion angle between the acid and methyl substituents (C13-C11-C12-C14) is +8° and is shown along with the torsion angles between the carboxylic oxygens and the vinyl bond in Figure 2-69. This suggests that the initial vinyl benzo bridging is favored between C4a and C11 as this does not involve the eclipsing of the C11-C13 bond with the C12-C14 bond. It can be suggested, as before, that the p orbital on C11 is better aligned for bond formation with C4a than C9a.

Torsion Angles

O1-C14-C12-C11 = + 12°
O2-C14-C12-C11 = - 167°

C13-C11-C12-C14 = + 8°
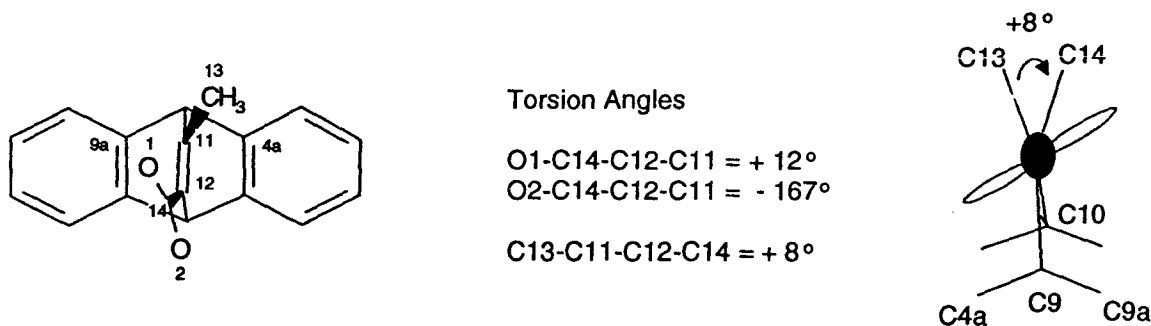
Figure 2-69   Some Torsion Angles in (S,S)-(+)-Pseudoephedrine Salt 105a

The packing diagram of salt 105a reveals that the space around the methyl group on the vinyl bond is relatively free from interaction with the neighboring molecules. This suggests that the intermolecular packing arrangement of salt 105a does not favor either enantiomer of product 52.

To further test this hypothesis, the X-ray structure of S-(+)-prolinol salt 103 was obtained. The X-ray structure, which is shown in Figure 2-70, reveals that the asymmetric unit contains two independent molecules, 103A and 103B, with the absolute configurations 12P and 12M, respectively. The enantioselectivity of the photoreaction of

S-(+)-prolinol salt **103** is 38% and the (+)-enantiomer of product **52** is favored. There are steric interactions between the crystal lattice and the acid groups in molecule **103A** and **103B**, mainly as the acid groups are hydrogen bonded to the prolinol moieties. The methyl group attached to the vinyl bond is relatively free of interaction with the crystal lattice in both molecules **103A** and **103B**.

Molecule 103B

Molecule 103A

Figure 2-70   Crystal Structure of S-(+)-Prolinol Salt **103**
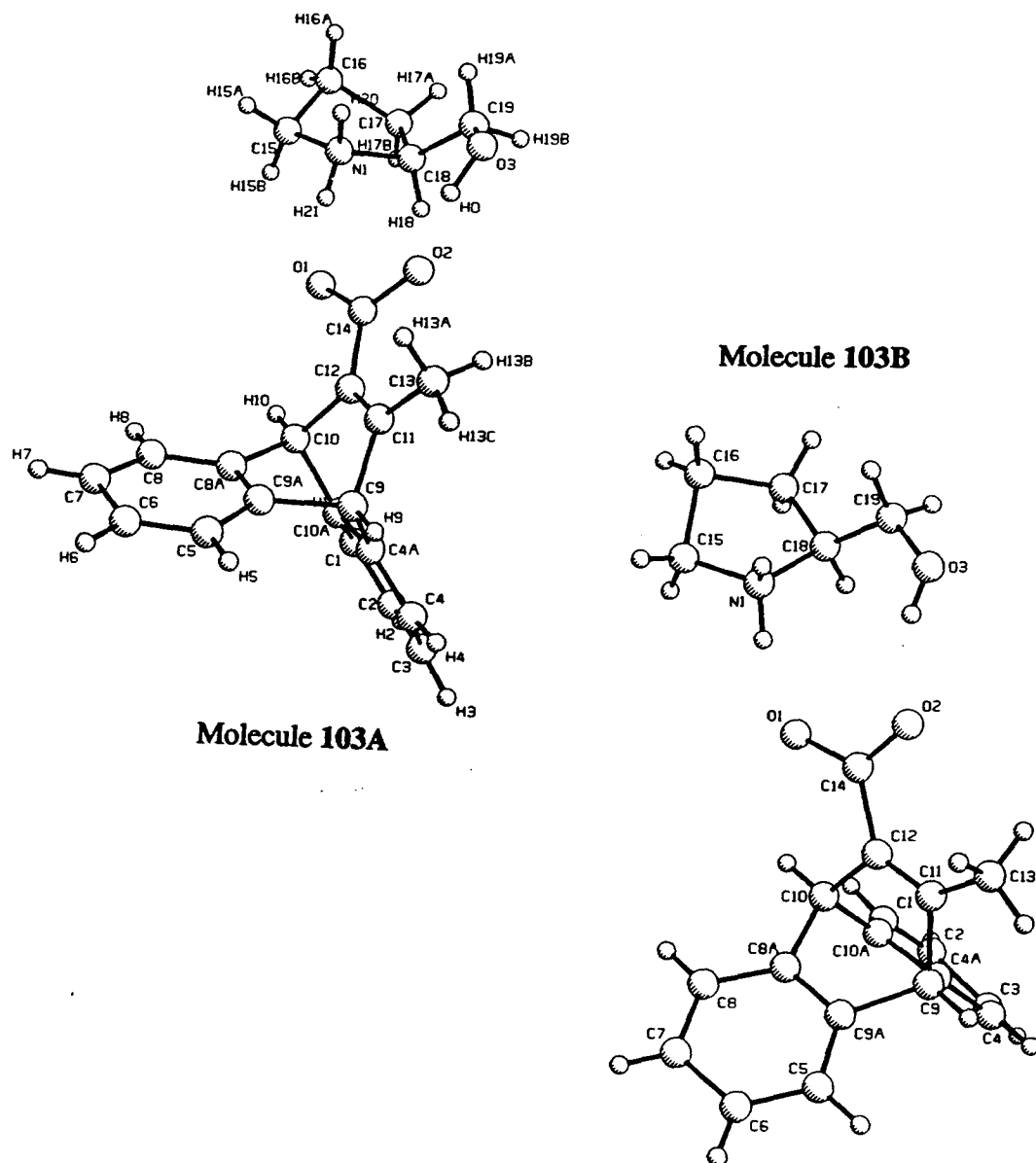
The carboxylate anion is in conjugation with the vinyl bond in both molecules **103A** and **103B** (Figure 2-71). The torsion angle between C13-C11-C12-C14 is +1° in **103A** and +5° in **103B**. Since the torsion angle between the vinyl substituents in molecule **103B** is greater, it can be proposed that molecule **103B** reacts enantioselectively to yield mainly the (+)-enantiomer of product **52**, that is via initial vinyl-benzo bridging between C11 and C9a. In contrast, it can be suggested that molecule **103A** reacts without extensive enantioselectivity because the conformation of **103A** does not strongly favor either initial vinyl benzo bridging between C4a and C11 or C9a and C11. The torsion angle between C13-C11-C12-C14 is very small and formation of either the (+) or the (-) enantiomer of product **52** will move the C11-C13 bond away from C12-C14 bond.

103A
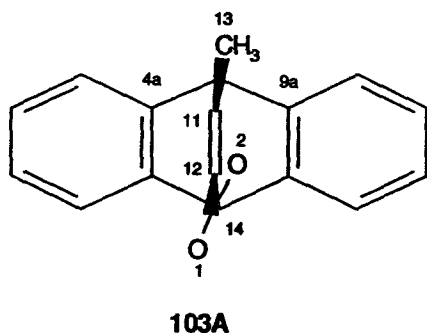
Torsion Angles

O1-C14-C12-C11 = + 173 °
O2-C14-C12-C12 = - 6 °

C13-C11-C12-C14 = + 1 °
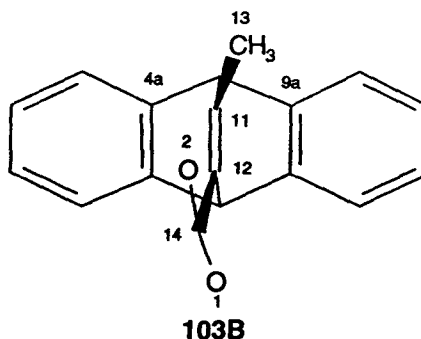
103B

Torsion Angles

O1-C14-C12-C11 = - 169 °
O2-C14-C12-C11 = + 14 °

C13-C11-C12-C14 = + 5 °

Figure 2-71   Some Torsion Angles in S-(+)-Prolinol Salt **103**

The packing diagram of salt **103** shows that the space around the methyl group on the vinyl bond in both molecules **103A** and **103B** is relatively free from interaction with

the neighboring molecules. Consequently, it can be suggested that the intermolecular packing arrangement of salt **103** does not favor either enantiomer of product **52**.

Yang et al.[92] studied the photochemistry of salt **117** which exists in dimorphic forms: needles and plates (Figure 2-72). Irradiation of the needle dimorph of salt **117** in the solid state yielded the major product **118** in over 95% enantiomeric excess with a small amount of the minor product **119**. In contrast irradiation of the plates gave the major product **118** in 12% enantiomeric excess. The authors explained these results from X-ray structure analyses of both dimorphs of salt **117**. In the needle-like crystals the carboxylate anions adopt a single homochiral conformation whereas in the plate form there are two independent carboxylate anions in the asymmetric unit that have opposite absolute configurations. It was suggested that the needles react stereospecifically to form one stereoisomer of the photoproduct, whereas in the plates there are competing stereospecific photoreactions that yield photoproducts of low overall enantiomeric excess.
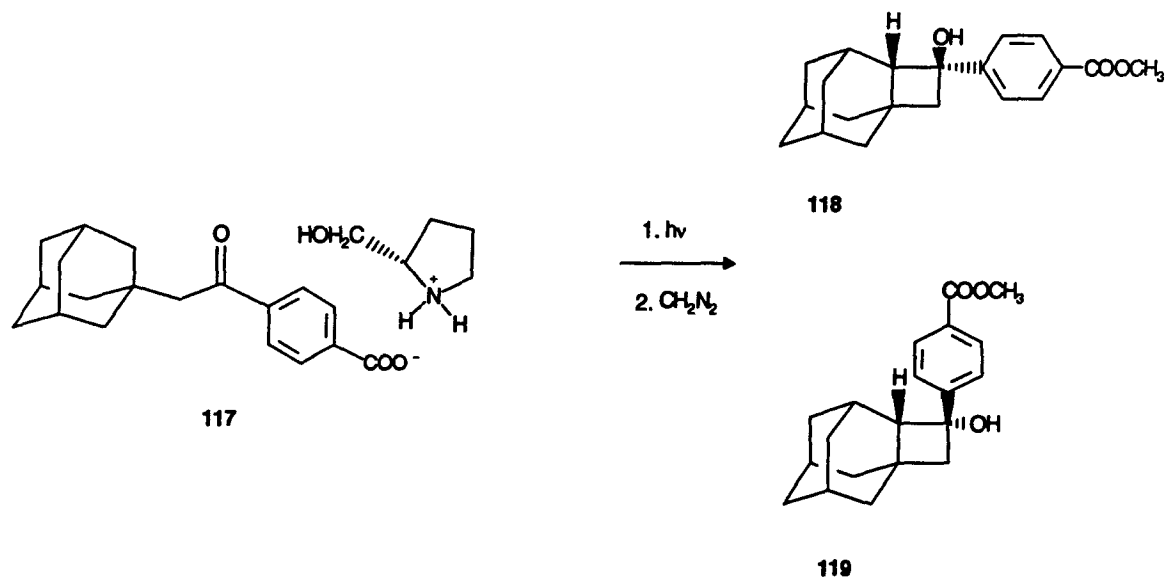
Figure 2-72   Photochemistry of Salt **117**

116

2.4.3 Absolute Configurations of R-(-)-Camphorsulfonic Acid Salt 116a and Photoproduct 60

Photolysis of R-(-)-camphorsulfonic acid salt **116a** in the solid state yielded the photoproduct **60** in 70% enantiomeric excess. The absolute configuration of salt **116a** was obtained by X-ray structure analysis (Figure 2-73). The dibenzobarrelene moiety was shown to have the absolute configuration 11P, 12P. It was suggested earlier that the regioselectivity of the solid state photoreaction of salt **116a** was controlled by electronic effects. The crystal packing arrangement reinforces the electronic effect since the ester group on C12 is almost out of conjugation with the vinyl bond whereas the ester group on C11 is in conjugation with the vinyl bond. The packing arrangement favors formation of the observed product **60**.
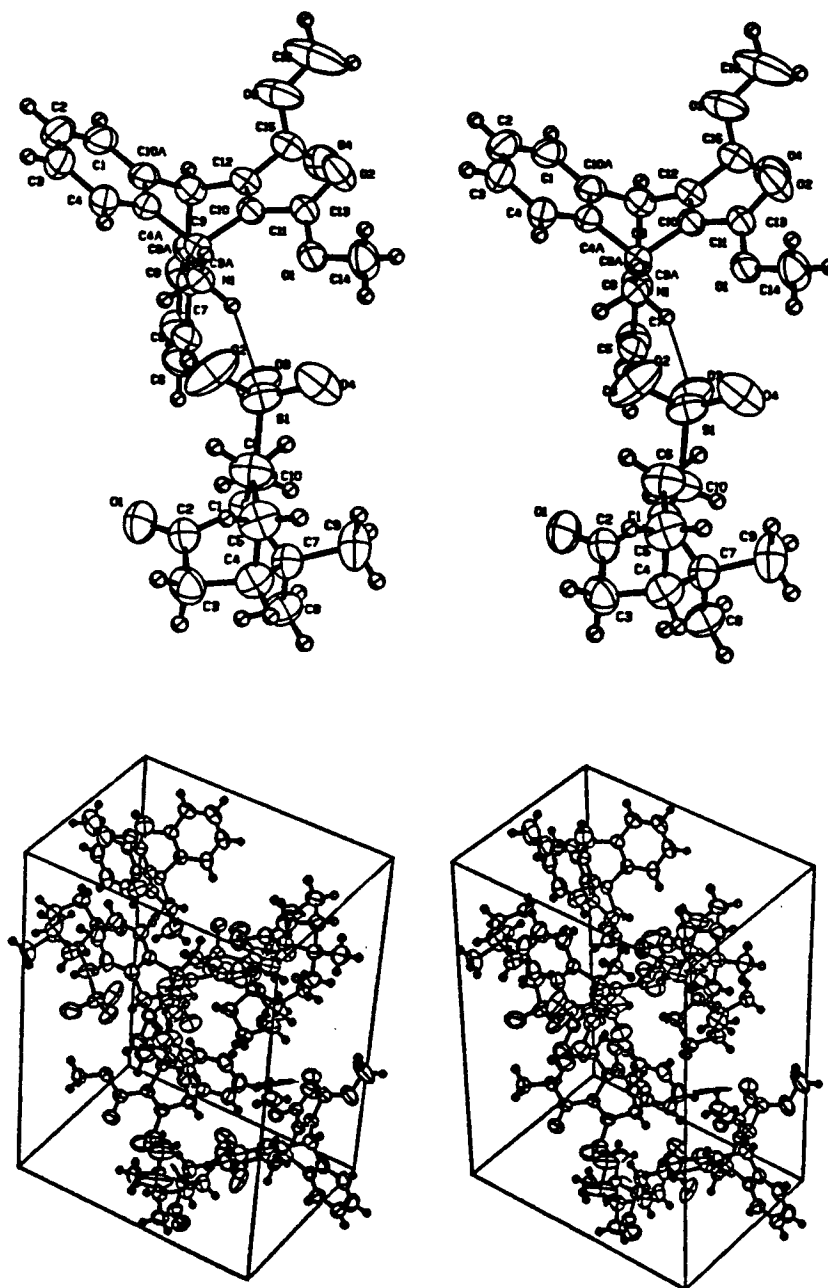
Figure 2-73   Crystal Structure of R-(-)-Camphorsulfonic Acid Salt 116a

The circular dichroism spectrum of the (-)-enantiomer of photoproduct **60** of the solid state irradiation of R-(-)-camphorsulfonic acid salt **116a** is shown in Figure 2-74. Photoproduct **60** was formed with 70% excess of the (-)-enantiomer.
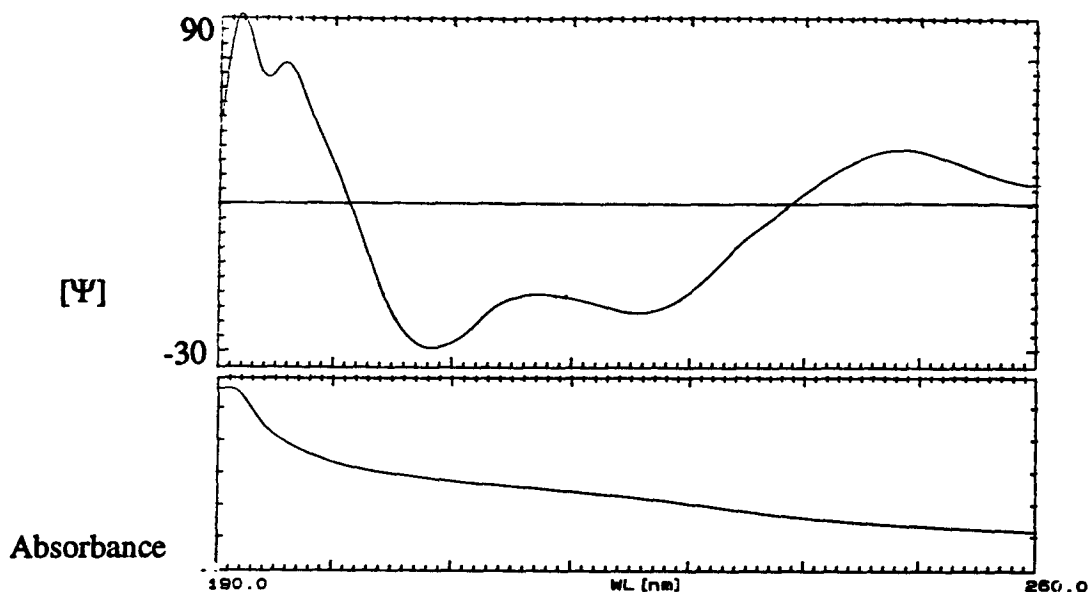
Figure 2-74   Circular Dichroism Spectrum of Photoproduct **60**

This spectrum is very similar to the circular dichroism spectra of compounds (+)-**32a** and (+)-**34** (Figure 2-74). It can be suggested that the (-)-enantiomer of product **60** has the same absolute configuration as the (+)-enantiomers of compounds **32a** and **34**. A chiral handle was introduced into product **60** allowing confirmation of the absolute configuration by X-ray structure analysis. Refluxing a racemic mixture of product **60** and R-(-)-α-methoxyphenylacetic acid chloride yielded diastereomers **120** and **121** in the ratio 1:1. Diastereomers **120** and **121** were separated by HPLC chromatography. Diastereomer **120** was crystallized from an acetone and n-hexane solution to give crystals containing one equivalent of acetone. X-ray structure analysis of these crystals showed that compound **120** has the absolute configuration (9R, 10S, 11S, 12R, 18R).

119
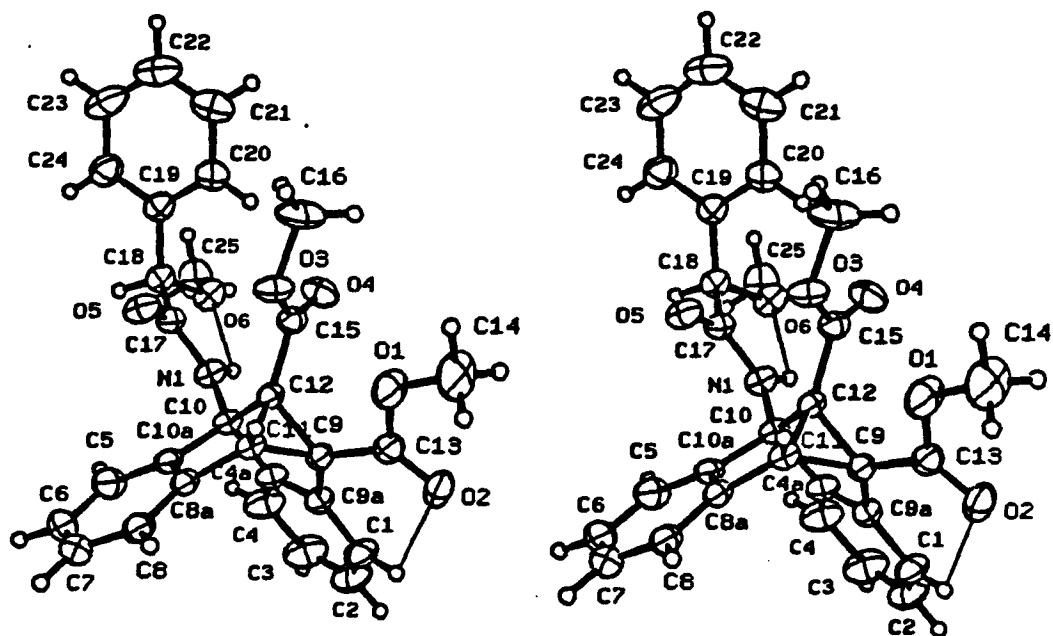
Figure 2-75   Crystal Structure of Compound 120

Photoproduct 60 from the solid state irradiation of salt 116a was refluxed with R-
(-)-α-methoxyphenylacetic acid chloride. GC analysis of the reaction mixture
demonstrated that diastereomers 120 and 121 were formed in the ratio 86:14. It can be
concluded that the (-)-enantiomer of product 60 has the absolute configuration (4bS,
8bR, 8cR, 8dS) as shown in Figure 2-76 (Crystallographer used a different numbering

120

system). Furthermore, this does agree with the absolute configuration suggested after analyzing the circular dichroism spectrum of product **60**.

CH$_3$OOC COOCH$_3$

9   11
12
10
NH

C=O
H$_3$CO 18

120

(9R, 10S, 11S, 12R, 18R)

CH$_3$OOC COOCH$_3$

8b   8d
8c
4b
NH$_2$

60

(4bS, 8bR, 8cR, 8dS)
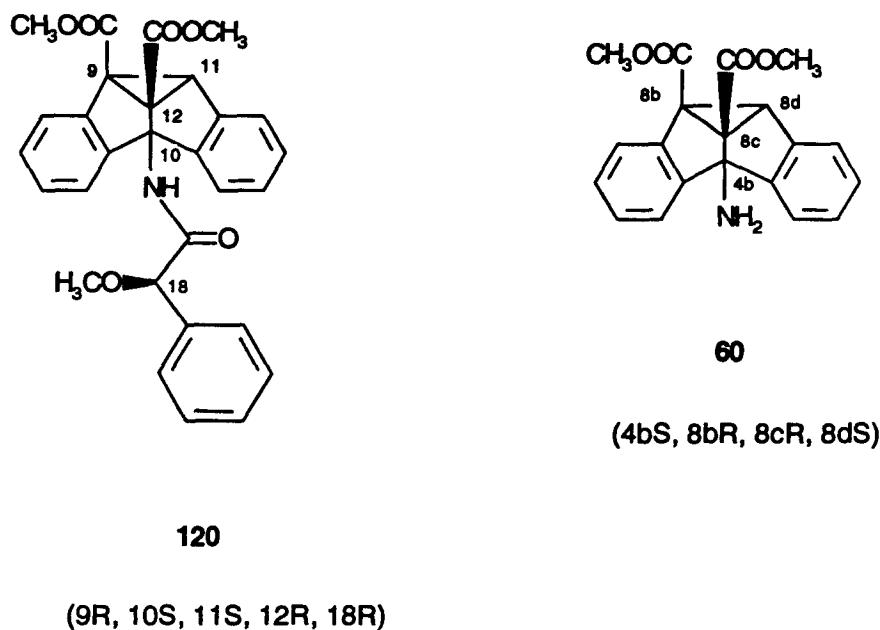
Figure 2-76   Absolute Configuration of (-)-Enantiomer of Product **60** and Compound

120

Comparison of the absolute configurations of salt **116a** with the (-)-enantiomer of product **60** reveals that initial vinyl benzo bridging between C10a and C12 is favored. The torsion angles between the vinyl substituents, C13-C11-C12-C15, is +1° and is shown in Figure 2-77 along with the torsion angles between the ester groups and the vinyl bond. According to our hypothesis that the torsion angle between the vinyl substituents controls the enantioselectivity of the di-π-methane rearrangement, salt **116a** is not expected to react enantioselectively, since the torsion angle between the vinyl group substituents is very small. This theory favors formation of the (+)-enantiomer product of **60** (initial bonding between C12 and C8a) and is opposed to what is observed.
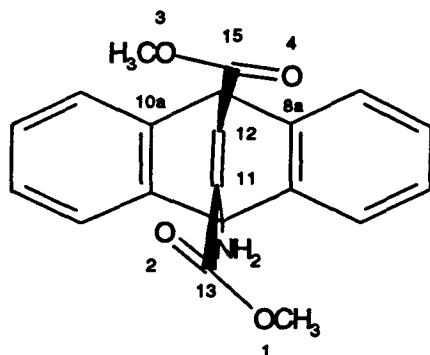
Torsion Angles

O1-C13-C11-C12 = - 156°
O2-C13-C11-C12 = + 22°

O3-C15-C12-C11 = - 102°
O4-C15-C12-C11 = + 84°

C13-C11-C12-C14 = + 1°

Figure 2-77   Some Torsion Angles in R-(-)-Camphorsulfonic Acid Salt **116a**

Considering that there is an intermolecular steric interaction between O4 and an adjacent aromatic ring which hinders the movement of the ester group on C12 towards C8a, it can be proposed that the intramolecular and the intermolecular arrangements of salt **116a** affect the asymmetric induction in opposite ways. That is to say, the intramolecular arrangement slightly favors formation of an initial vinyl benzo-bridge between C8a and C12. In contrast the crystal lattice favors formation of an initial benzo vinyl bridge between C10a and C12 since steric interaction between O4 and an adjacent aromatic ring disfavors formation of an initial vinyl benzo bridging between C8a and C12.

2.5 Solid State Photochromism of Dibenzobarrelene Derivatives 38, 43 and 44

Photochromism is a phenomenon whereby a substance undergoes a color change upon absorption of light. By definition, this process must be reversible either thermally or photochemically.[93] Photochromic compounds have been studied in a sporadic manner

since the end of the last century.[94] Photochromism has been observed for various compounds in different media and some of these systems have been studied intensively. Several compounds that are photochromic in the solid state have been reported.[8j,m]

38: R = H

43: R = CH₃

44: R = CH₂CH₃
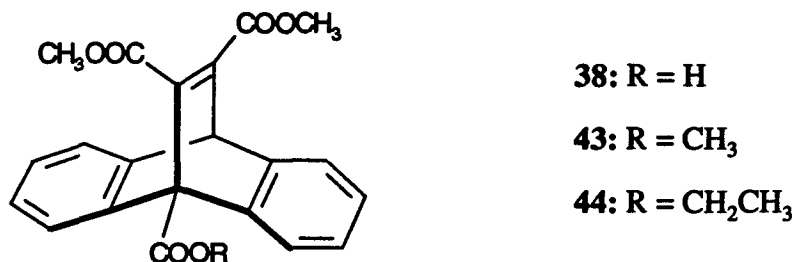
Figure 2-78   Dibenzobarrelene Derivatives **38**, **43** and **44** which Display Solid State Photochromism

Compounds **38**, **43** and **44** (Figure 2-78) exist as white crystals. Upon irradiation the crystals of these compounds turn dark blue or blue-green. Tri-ester **44** exists as dimorphs and both forms show very similar photochromism. Acid **38** is trimorphic and all the crystal forms show a color change to green-blue upon irradiation. Salts **108** and **109**, ephedrine and pseudoephedrine salts of acid **38**, were photochromic at low temperatures (-40°C); they turned a pink color. No such color change was observed for these salts at room temperature. None of these compounds are photochromic in solution. The intensity of color developed in these compounds was approximately proportional to the irradiation time. The photolyzed crystals lose their color after a few hours to a few days in the dark. Heating the colored crystals or dissolving them removed the color much more effectively. GC analysis of the colored crystals showed no sign of reaction. The coloring and bleaching process could be repeated several times without damaging the crystals. Prolonged irradiation of the colored crystals did eventually turn them colorless and photoreaction was observed. Exposure of the crystals to UV light under aerobic conditions or pure oxygen has no deleterious effect on the photochromism.

Tri-ester **43**

1: Before irradiation.

2: After irradiation.

Acid **38**.

1: Before irradiation.

2: After irradiation.
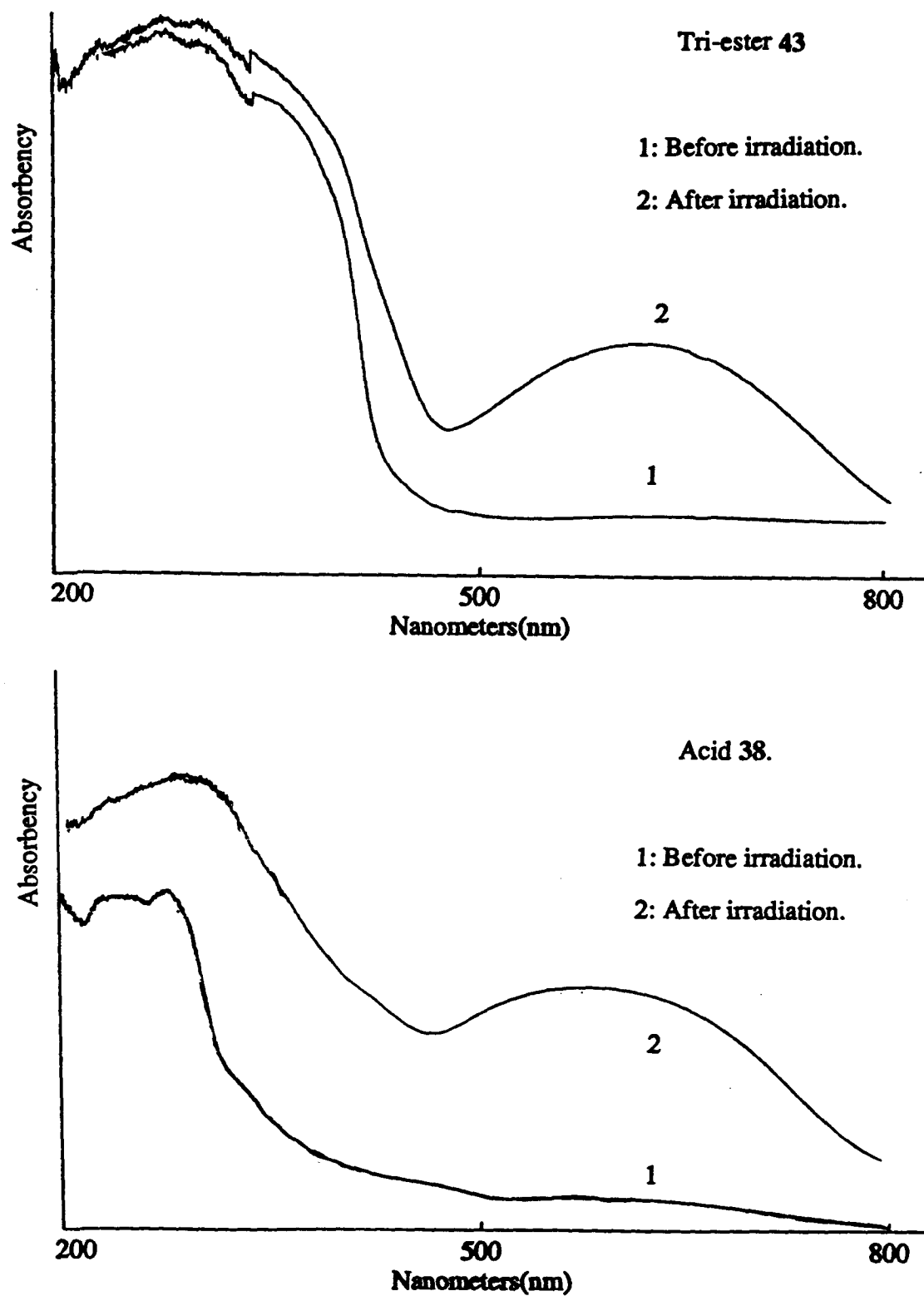
Figure 2-79   Solid State UV-Visible Absorption Spectra for Compounds **38** and **43**

The solid state UV-visible absorption spectra[95] for the colored crystals of dibenzobarrelenes **38** and **43** are shown in Figure 2-79 along with the spectra of the crystals before irradiation. The spectra of the irradiated crystals display absorption in the 500-800 nm range which is absent before irradiation and was not detected after the color had faded.

The ESR spectrum[95] of colored crystals of tri-ester **43** is shown in Figure 2-80. The g-value indicates that the radical species is organic in nature.[96] The ESR signal fades with time and is absent when the crystals have returned to their original color. The solid state UV and ESR spectra of tri-ester **43** suggest that a radical species which absorbs in the 400-800 nm range is responsible for the photochromic behavior.

$g = 1.99413$

| 3340 | 3380 | 3420 |

[G]
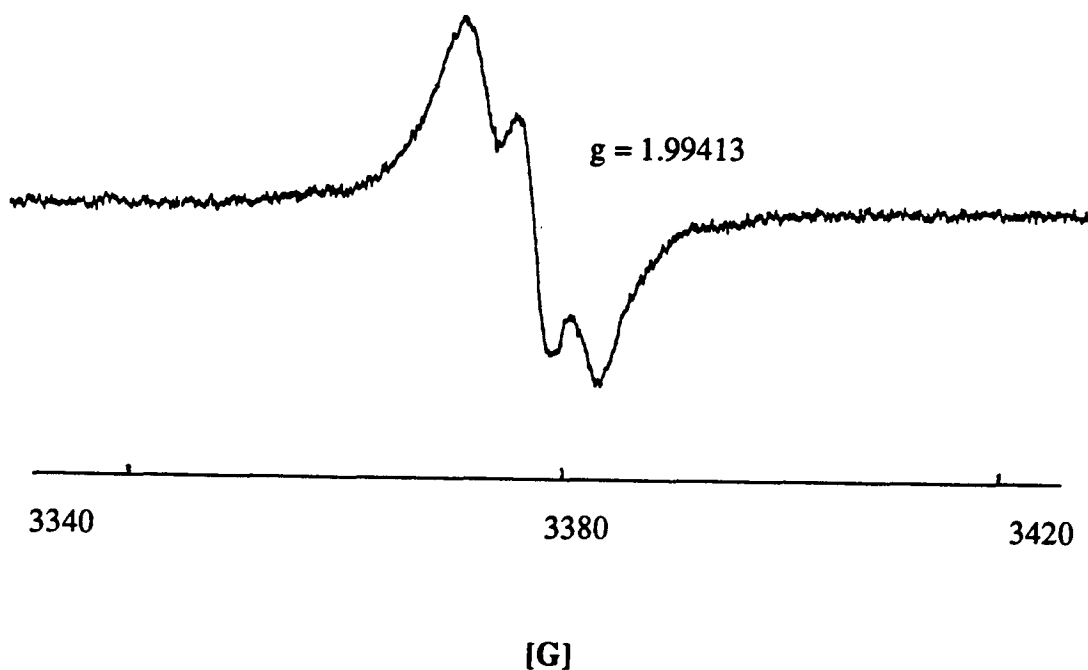
Figure 2-80   ESR Spectra of Irradiated Crystals of Tri-ester **43**

In our laboratory, similar solid state photochromic behavior has been found for other dibenzobarrelene derivatives. Dibenzobarrelene 122[71] is dimorphic and both crystal forms turn purple when irradiated at room temperature. Dibenzobarrelene 123[51] is trimorphic and two of the crystal forms exhibit blue photochromism at room temperature, whereas the other crystal form showed a color change to pink only at low temperatures (-40°C). The UV and ESR spectra of the blue colored crystals of dibenzobarrelene 122 and 123 are very similar to the ones recorded for tri-ester 43.

Compound	R$_1$	R$_2$	Photochromic
39	NH$_2$	H	no
46	CHO	H	at low T
80	CH$_3$	CH$_3$	at low T
122	Cl	Cl	at RT
123	CH$_2$Cl	H	at RT
124	CH$_3$	H	no
125	Cl	H	no

Figure 2-81   Bridgehead   Substituted   Dibenzobarrelene   Derivatives   and   their Photochromism

Dibenzobarrelenes 46 and 80[74] (Figure 2-81) turn green and pink, respectively when irradiated at low temperatures (-40°C). No such color change is observed for irradiations at room temperature.

Generally, only dibenzobarrelene-11,12-diester derivatives with either one or two bridgehead substituents have shown photochromism. It should be mentioned that not all compounds that have this structure are photochromic. For example, dibenzobarrelene

derivatives **39**, **124**[97] and **125**[97] are not photochromic. No photochromism has been observed for dibenzobarrelene-11,12-diesters lacking bridgehead substituents. The photochromism is not observed in solution or polymer films and therefore it can be proposed that the crystal lattice must play a key factor in the photochromism. Observations of different photochromism for different dimorphs of the same compound also support this theory. X-ray structures have been obtained for most of these bridgehead substituted dibenzobarrelene derivatives, both the photochromic and the non-photochromic ones. Correlation of crystal packing arrangements and photochromism has been attempted, however no final conclusions have been drawn. Some possible explanations for this unusual solid state phenomenon are presented below, but these theories are speculative. Much more information about the photochromic compounds is needed before the nature of colored state is known.
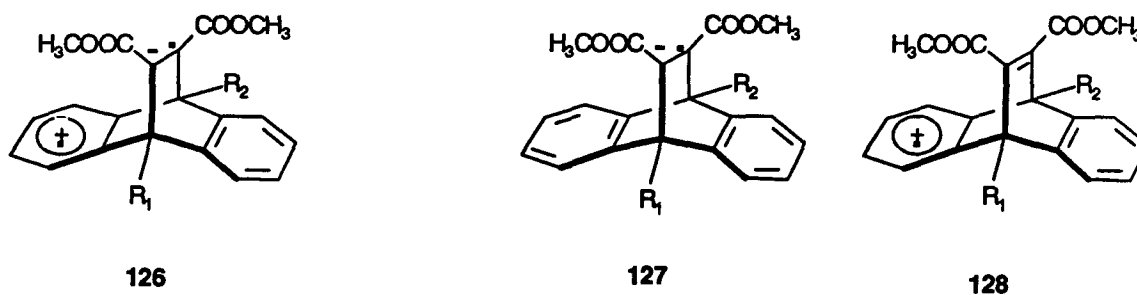
Figure 2-82   Radical Ions **126-128**

The first theory suggests that a radical ion species, such as structures **126-128** (Figure 2-82) which are formed via either an intra- or intermolecular photoinduced electron-transfer process, might be responsible for the observed photochromism. The feasibility of photochemical electron transfer in polar solvents can be predicted on the basis of the Weller[98] equation, in which the free-energy change for the electron transfer is calculated from the redox potentials and the excitation energy. Our estimation of ΔG

obtained from this equation gives ΔG as negative. This is based on the known oxidation and reduction potentials for dimethylbenzene and maleic anhydride which can serve as a model for the photochromic dibenzobarrelenes. The oxidation potential for dimethylbenzene is 44 kcal/mol and the reduction potential for maleic anhydride is -21 kcal/mol.[98b] The excitation energy of the photochromic dibenzobarrelenes can be estimated to be approximately 100 kcal/mol.

$$A + D \xrightarrow{h\nu} A^{\cdot -} + D^{\cdot +}$$
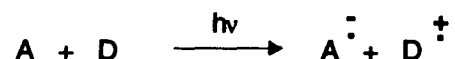
$$\Delta G = E^{ox} - E^{red} - E^{excit}$$

(Weller equation)

E^{ox}: Oxidiation Potential
E^{red}: ReductionPotential
E^{excit}: Excitation energy

This is similar to what Sakaguchi et al.[99] found when they studied the solid state photochromism of styrylpyridinium tetraphenylborate **129** (Figure 2-83). They discovered that the yellow salt turned blue upon irradiation. The photochromism was assigned to photoinduced electron transfer from the tetraphenylborate anion to the styrylpyridinium cation in the solid state to form a styrylpyridinium radical.
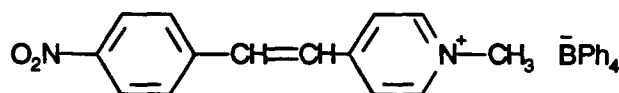
129

Figure 2-83   Styrylpyridinium Tetraphenylborate Complex, **129**

Returning to the dibenzobarrelene photochromism, it is possible that breaking of the C9-C12 bond of the dibenzobarrelene ring results in the formation of a zwitterion **130** (Figure 2-84), thus leading to the observed photochromism. Zwitterion **130** is then stabilized through resonance. This is consistent with the fact that only bridgehead-substituted dibenzobarrelenes are photochromic, since R_1 should stabilize the cation at C9 (Figure 2-82). The electron transfer theory fails to account for the effect of the bridgehead substituents.

130
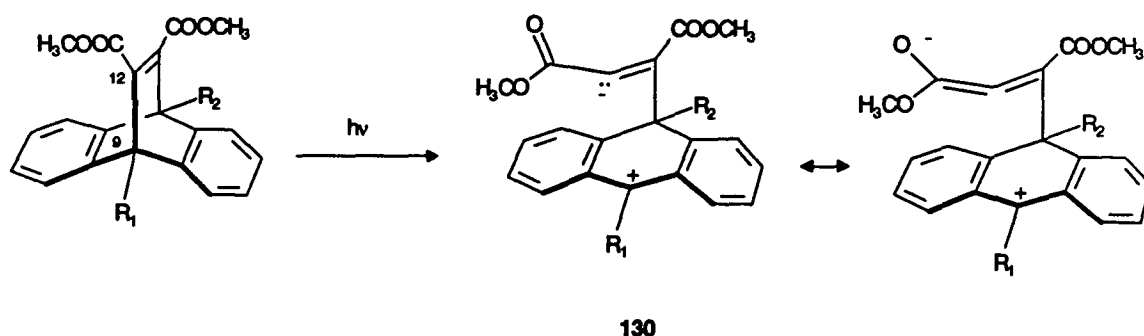
Figure 2-84   Zwitterion **130**

Another possible explanation involves the biradical intermediate **131** produced by initial benzo-vinyl bridging during the photorearrangement (Figure 2-85). The biradical species resembles structure **132**, which is known to absorb at 560 nm in the visible region.[100] However, radical **132** shows a weak absorption in the visible region whereas the photochromic dibenzobarrelene derivatives show a strong broad absorption in the same region. Another drawback of this theory is that it does not take into account that only bridgehead substituted dibenzobarrelenes are photochromic.
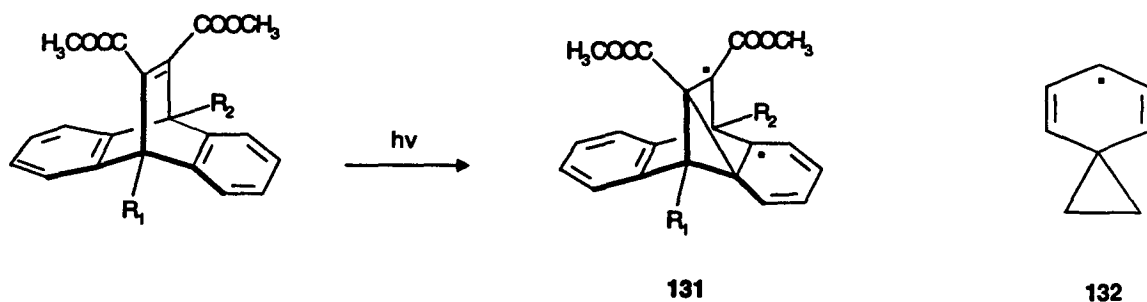
Figure 2-85   Biradicals 131 and 132

It is interesting to compare the photochromism of the dibenzobarrelenes with the solid state photochromism of compound **133** (Figure 2-86). Wudl et al.[101] discovered that colorless crystals of compound **133** turn pink when irradiated in the solid state with UV-light or X-rays. However, no color change was produced when solutions of these compounds were irradiated. Heating of the colored crystals returned them to their original white color. ESR studies of the pink crystals of **133** indicated the presence of two radical species, one with an unpaired electron localized on a sulfur atom and the other with an electron localized on a carbon atom. The X-ray crystal structure revealed intramolecular phenyl-thiobenzene contacts as well as intermolecular phenyl-phenyl contacts. The authors were unable to identify the nature of the colored state. However they proposed three hypotheses to explain the photochromism. They suggested that intermolecular charge transfer between thiobenzenes or intermolecular charge transfer between thiobenzene and phenyl rings are possible explanations for the pink crystals. Alternatively, homolytic cleavage of benzyl-sulfur bonds can also explain the photochromism.

130

PhCH$_2$S—⟨structure⟩—SCH$_2$Ph

PhCH$_2$S—⟨structure⟩—SCH$_2$Ph
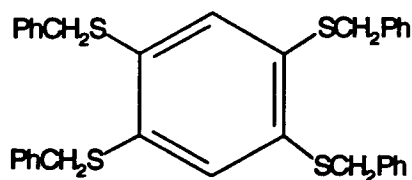
133

Figure 2-86   Compound **133**

2.5.1 γ–Ray Irradiation of Salt 134

A notable property of organic salt crystals is the strong lattice forces which bind them and translate into high melting points. Consequently the likelihood of the crystal melting during reaction is reduced and the probability of observing a topotactic reaction is increased. It was decided to look for a single crystal-to-crystal reaction of a salt of a dibenzobarrelene derivative, and acid **40**[58] was selected for this study. The piperidine salt (**134**) of acid **40** was prepared (Figure 2-88).[102] Salt **134** was photolyzed in acetone. The reaction mixture was made acidic and treated with excess diazomethane to yield product **135**.[58] Crystals of the piperidine salt **134** were irradiated through a Pyrex filter. GC analysis of single crystals indicated 60% conversion to product **135**. The crystals had turned yellow and were no longer transparent.

134   **135**
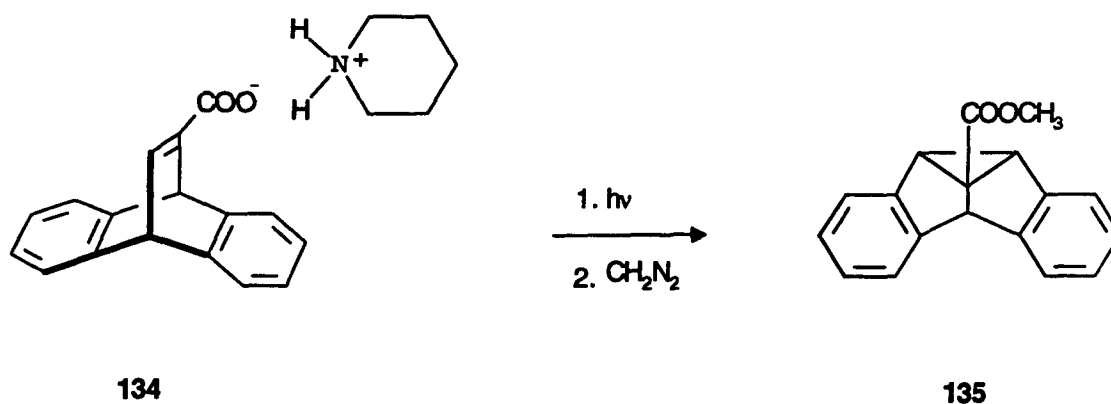
Figure 2-88   Photolysis of Piperidine Salt **134**

There are examples in the literature in which solid state γ-ray irradiation yields cleaner reactions than UV irradiation.[103] An understanding of the nature of the interaction of γ-rays with organic molecules in crystals is very limited, however.[104]

Crystals of piperidine salt **134** were irradiated with γ-rays from a ^{60}Co source for one week. The crystals looked undamaged, but slightly yellow, and they were almost indistinguishable from their non-irradiated counterparts. GC analysis indicated 10-25% conversion to product **135** for single crystals. This was repeated with an another sample of piperidine salt **134**, but this time the crystals were irradiated for a month. As before the crystals looked undamaged after irradiation but slightly yellow. GC analysis of single crystals showed conversion in the range 10-25% as before. No further attempts were made to achieve topotactic reaction for piperidine salt **134**.

Although topotactic reactions were not observed for piperidine salt **134**, it would be most interesting to study γ-irraditions as well as solid state reactions induced by UV irradiation.

CHAPTER 3 EXPERIMENTAL

3.1 General

Melting Points (MP). Melting points were determined on a Fisher-Johns melting point apparatus and are not corrected.

Infrared Spectra (IR). A Perkin Elmer 1710 Fourier transform infrared spectrometer was used for obtaining infrared spectra. The positions of the absorption maxima are reported in cm^{-1}. The spectra of liquid samples were recorded without solvent as thin films between two sodium chloride pellets. Solid samples (2-5 mg) were ground in KBr (100-200 mg) and pelleted in an evacuated die (Perkin-Elmer 186-0002) with a laboratory press (Carver, model B) at 15,000 psi.

Mass Spectra (MS). Low and high resolution electron ionization (EI) mass spectra were obtained on a Kratos MS 50 mass spectrometer. Coupled gas chromatography-mass spectral (EI) analysis was performed on a Kratos MS 80 spectrometer attached to a Carlo-Erba chromatogram. Fast atom bombardment (FAB) mass spectra were registered on an AEI MS 9 mass spectrometer.

Nuclear Magnetic Resonance Spectra. Proton nuclear magnetic resonance spectra (^{1}H-NMR) were recorded on Bruker AC-200 (200 MHz), Varian XL-300 (300 MHz) and Bruker WP-400 (400 MHz) spectrometers. Signal positions are reported as

chemical shifts (δ) in parts per million (ppm) with tetramethyl silane (TMS) as an internal reference. The multiplicity of the signals, number of protons, coupling constants (J) in Hz and assignments are given in parentheses following the chemical shifts.

Carbon nuclear magnetic resonance spectra (^{13}C-NMR) were recorded at 100.6 Hz on Bruker Am-400 spectrometer, at 75.4 MHz on Varian XL-300 and at 50.3 MHz on Bruker AC-200 spectrometers. Chemical shifts (δ) are reported under broad band proton decoupling in ppm and are followed by their assignments, which were determined in part by the attached proton test (APT) experiment.

Ultraviolet Spectra (UV). Ultraviolet spectra were recorded on a Perkin Elmer Lambda-4B UV/Vis spectrometer. The wavelength (λ) in nanometers (nm) and the extinction coefficient (ε (l/mol/cm)) of each absorption maximum are given.

Elemental Analysis. All elemental analyses reported were performed by Mr. P. Borda, Department of Chemistry, University of British Colombia.

Chromatography. Gas liquid chromatography (GC) analyses were performed on a Hewlett Packard 5890A gas chromatograph fitted with a flame ionization detector, and the instrument was equipped with a Hewlett Packard 3392A integrator. All the chromatographic analyses were carried out on a 15 m x 0.25 mm DB-1 and a 15 m x 0.25 mm DB-17 columns from J&W Scientific Inc.

Gravity column chromatographic separations were carried out by using 230-400 mesh gel (E. Merck) with a suitable solvent or solvent combinations.

Thin layer chromatographic analyses were performed on pre-coated silica gel plates (type 5554 from E. Merck).

High performance liquid chromatography (HPLC) was performed on a Waters 600E system equipped with a Waters 486 UV detector and a Waters fraction collector.

Radial-Pak cartridge (μ Porasil, particle size 10 μ), with 8 mm x 100 mm from Millipore (cat# 85720) was used for analytical studies. For preparative scale work, a similar column with an internal diameter of 25 mm (cat # 38504) was used.

Optical rotations and Circular dichroism. Circular dichroism spectra were obtained on a Jasco-J710/ORD-M polarimeter. Specific ellipticity, $[\psi]_\lambda^t$, was calculated by the following equation:

$$[\psi]_\lambda^t = \frac{\psi}{l\,c}100$$

Where   t = the temperature at which the optical rotation was measured

λ = the wavelength

ψ = the angle of ellipticity in degrees

l = the path length in decimeters

c = the concentration of the sample solution in milligrams per 10 mL

Optical rotations were measured on a Jasco-J710/ORD-M and a Perkin Elmer 141 polarimeter at the sodium D line (589 nm) at room temperature. Specific rotation, $[\alpha]_D^t$, was calculated by the following equation:

$$[\alpha]_D^t = \frac{\alpha}{l\,c}100$$

Where   t = the temperature at which the optical rotation was measured

D = the sodium D line at 589 nm

α = the recorded optical rotation in degrees

l = the path length in decimeters

c = the concentration of the sample solution in milligrams per 10 mL

Solvents and Reagents: Unless otherwise specified, all the solvents and reagents were used directly without any further purification. When further purification was needed, known methods and procedures were followed in each case.[105]

Crystallographic Analyses: All crystal structures were determined on a Rigaku 4-circle diffractometer by the following people M. Kaftory, A.D. Guðmundsdóttir, W. Li, S.J. Rettig, J. Trotter of the University of British Columbia Chemistry Department.

3.2 Preparation of Starting Materials

3.2.1 Synthesis of Starting Materials

Dimethyl 9,10-Dihydro-9,10-ethenoanthracene-11,12-dicarboxylate (45)[46]

In a round bottom flask equipped with a condenser, a mixture of anthracene (7 g, 39 mmol, Eastman) and dimethyl acetylenedicarboxylate (6 mL, 49 mmol, Aldrich) was heated to 190°C. After 30 min of heating, the mixture was cooled and the resulting dark solid recrystallized three times from a chloroform-ethanol solution to yield diester **45** (18 g, 56 mmol, 72% yield).

MP: 160-161°C (lit.[46] 160-161°C).

IR (KBr) v_{max}: 1729, 1713 (C=O), 1632 (C=C), 1273 (C-O) cm^{-1}.

MS m/e (relative intensity): 320 (M$^+$, 22), 261 (62), 202 (25), 178 (83), 28 (100).

Exact mass calculated for $C_{20}H_{16}O_4$: 320.1049. Found: 320.1041

^{1}H-NMR (400 MHz, CDCl$_3$) δ 7.4 -7.3 (m, 4H, aromatic H), 7.1-7.0 (m, 4H, aromatic

H), 5.48 (s, 2H, bridgehead H), 3.76 (s, 6H, CO$_2$CH$_3$) ppm.

^{13}C-NMR (50 MHz, CDCl$_3$) δ 165.9 (C=O), 147.0 (vinyl C), 143.8 (aromatic C), 125.4,

123.8 (aromatic C-H), 52.5, 52.3 (CO$_2$CH$_3$ and bridgehead C-H) ppm.

9,10-Dihydro-9,10-ethenoanthracene-11,12-dicarboxylic acid (47) [50, 106]

Diester 45 (18 g, 56 mmol) was dissolved in ethanol (65 mL) and aqueous NaOH

(30%, 110 mL) added. This solution was refluxed for 24 h, cooled to room temperature

and washed two times with diethyl ether to remove all unreacted starting material. The

aqueous fraction was cooled to 0°C, conc. HCl added until acidic and then extracted

twice with diethyl ether. The combined organic fractions were dried over MgSO$_4$ and

evaporated to dryness. The resulting powder was recrystallized from n-hexane-acetone

solution to yield di-acid 47 (15 g, 52 mmol, 92%).

MP: 214-215°C (lit.[106] 215-216°C).

IR (KBr) v$_{max}$: 3600-2400 (OH and CH), 1696 (C=O) cm^{-1}.

MS m/e (relative intensity): 292 (M+, 0.8), 274 (21), 248 (33), 230 (30), 202 (100), 178

(40).

Exact mass calculated for C$_{18}$H$_{12}$O$_4$: 292.0736. Found 292.0737.

^{1}H-NMR (300 MHz, CDCl$_3$) δ: 7.5 -7.4 (m, 4H, aromatic H), 7.1-7.0 (m, 4H, aromatic

H), 6.03 (s, 2H, bridgehead H) ppm, no O-H signals detectable.

^{13}C-NMR (100 MHz, CD$_3$OD) δ 167.1 (C=O), 147.7 (vinyl C), 143.7 (aromatic C),

124.6, 123.0 (aromatic C-H), 52.4 (bridgehead C-H) ppm.

9,10-Dihydro-9,10-ethenoanthracene-11,12-dicarboxylic acid anhydride (48)[46]

A mixture of di-acid **47** (6 g, 20 mmol) and oxalyl chloride (3.5 mL, 40 mmol) in anhydrous methylene chloride (60 mL) was refluxed for 24 h. The excess oxalyl chloride and solvent were removed under vacuum. The resulting solid was recrystallized from a chloroform-ethyl acetate solution to yield anhydride **48** (4.5 g, 16 mmol, 82%).

MP: 252-254°C (lit.[46] 247°C).

IR (KBr) v_{max}: 1843 (C=O asym.), 1787, 1767 (C=O sym.), 1636 (C=C) cm^{-1}.

MS m/e (relative intensity): 274 (M$^+$, 15), 230 (22), 202 (100), 178 (17).

Exact mass calculated for $C_{18}H_{10}O_3$: 274.0630. Found 274.0633.

^{1}H-NMR (400 MHz, CDCl$_3$) δ 7.5-7.0 (m, 8H, aromatic H), 5.55 ppm (s, 2H, bridge-head H) ppm.

^{13}C-NMR (50 MHz, CDCl$_3$) δ 160.3, 159.5 (C=O and vinyl C), 142.8 (aromatic C), 126.1 124.9 (aromatic C-H), 47.9 (bridgehead C-H) ppm.

Ethyl 9,10-Dihydro-9,10-ethenoanthracene-11-carboxylate-12-carboxylic acid (36)

A solution of anhydride **48** (4.5 g, 16 mmol) in ethanol (75 mL) was refluxed for 6 h, after which the solvent was removed under vacuum and the remaining solid recrystallized from acetonitrile to give acid **36** (4.0 g, 13 mmol, 76% yield).

MP: 224-226°C.

IR (KBr) v_{max}: 3500-3400 (OH), 1734, 1678 (C=O), 1629 (C=C), 1282 (C-O) cm^{-1}.

MS m/e (relative intensity): 320 (M$^+$, 3.5), 276 (22), 247 (23), 230 (22), 202 (100), 178 (32).

Exact mass calculated for $C_{20}H_{16}O_4$: 320.1049. Found: 320.1041.

^{1}H-NMR (400 MHz, CDCl$_3$) δ 7.5-7.4 (m, 4H, aromatic H), 7.1-7.0 (m, 4H, aromatic H), 6.19 (s, 1H, bridgehead H), 5.83 (s, 1H, bridgehead H), 4.45 (q, 2H, J=7 Hz, CO$_2$CH$_2$CH$_3$), 1.48 (t, 3H, J=7 Hz, CO$_2$CH$_2$CH$_3$) ppm, no O-H signal detectable.

^{13}C-NMR (75 MHz, CDCl$_3$) δ 168.2, 163.0 (C=O), 153.0, 145.9 (vinyl C), 143.7, 143.1 (aromatic C), 126.0, 125.1, 124.5, 123.4 (aromatic C-H), 64.3 (CO$_2$CH$_2$CH$_3$), 54.3, 52.8 (bridgehead C-H), 14.0 (CO$_2$CH$_2$CH$_3$) ppm.

UV (Acetonitrile) λ_{max}: 212 (ε 19,000), 278 (ε 1,600) nm.

Anal. calculated for $C_{20}H_{16}O_4$: C, 74.99; H, 5.03. Found: C, 74.79; H, 5.11.

Methyl 12-Methyl-9,10-dihydro-9,10-ethenoanthracene-11-carboxylate (41)

A Carius tube containing methyl 2-butynoate (5 mL, 4.9 g, 50 mmol, Aldrich) and anthracene (5 g, 28 mmol) was sealed and heated at 175°C for 60 h. The resulting yellow oil was purified by column chromatography (silica gel, petroleum ether:ethyl acetate, 80:20) and then recrystallized twice from ethanol to yield ester 41 (6.8 g, 25 mmol, 88%).

MP: 135-137°C (lit.[50] 136.9-137.3°C) with immediate resolidification and remelting at 145-146°C (lit.[50] 146.1-146.5°C).

IR (KBr) v_{max}: Crystals from ethanol; 1704 (C=O), 1633 (C=C), 1225 (C-O) cm^{-1}, crystals from melt; 1699 (C=O), 1625 (C=C), 1228 (C-O) cm^{-1}.

MS m/e (relative intensity): 276 (M+, 49), 217 (100), 202 (32), 178 (42).

Exact mass calculated for $C_{19}H_{16}O_2$: 276.1151. Found: 276.1152.

¹H-NMR (400 MHz, CDCl₃) δ 7.4-7.3 (m, 4H, aromatic H), 7.1-6.9 (m, 4H, aromatic H), 5.68 (s, 1H, bridgehead H), 4.90 (s, 1H, bridgehead H), 3.75 (s, 3H, CO₂CH₃) 2.45 (s, 3H, vinyl CH₃) ppm.

¹³C-NMR (50 MHz, CDCl₃) δ 166.4 (C=O), 162.4 (vinyl C), 145.4, 144.0 (aromatic C), 135.3 (vinyl C), 125.3, 124.9, 123.32, 123.28 (aromatic C-H), 60.0 (bridgehead C-H), 51.5, 51.4 (bridgehead C-H and CO₂CH₃), 19.56 (vinyl CH₃) ppm.

UV (Ethanol) λ_max: 214 (ε 10,000), 271 (ε 1,200), 279 (ε 1,300) nm.

12-Methyl-9,10-dihydro-9,10-ethenoanthracene-11-carboxylic acid (37)[50]

The procedure used for the hydrolysis of ester **45** was applied to ester **41** (1.44 g, 5.35 mmol), yielding acid **37** (0.85 g, 3.23 mmol, 62%), which was recrystallized from ethanol to give prism like crystals.

MP: 278-280°C (lit.[50] 279.8-280.0°C).

IR (KBr) v_max: 3400-3000 (OH), 1679 (C=O), 1638 (C=C), 1193 (C-O) cm⁻¹.

MS m/e (relative intensity): 262 (M+, 61), 217 (100), 202 (87), 178 (48).

Exact mass calculated for C₁₈H₁₄O₂: 262.0994. Found: 262.0996.

¹H-NMR (400 MHz, CDCl₃) δ 7.4-7.3 (m, 4H, aromatic H), 7.0-6.9 (m, 4H, aromatic H), 5.68 (s, 1H, bridgehead H), 4.94 (s, 1H, bridgehead H), 2.42 (s, 3H, vinyl CH₃) ppm, no O-H signal detectable.

¹³C-NMR (50 MHz, CDCl₃) δ 171.6 (C=O), 165.7 (vinyl C), 145.2, 143.5 (aromatic C), 134.7 (vinyl C), 125.4, 124.8, 123.31, 123.28 (aromatic C-H), 60.2, 51.0 (bridgehead C-H), 19.8 (vinyl CH₃) ppm.

UV (Ethanol) λ_max: 219 (ε 9,800), 271 (ε 2,300), 279 (ε 2,600) nm.

Ethyl 9,10-Dihydro-9,10-ethenoanthracene-11-carboxylate (42)[50]

A Carius tube containing anthracene (5.0 g, 28 mmol) and ethyl propiolate (2.8 mL, 2.7 g, 28 mmol, Aldrich) was sealed and heated at 175°C for 2.5 h. Unreacted starting materials were removed from the Diels Alder adduct by column chromatography on silica gel eluted with 20% ethyl acetate in petroleum ether. The crude product was recrystallized from ethanol to yield crystals of ester 42 (3.0 g, 11 mmol, 40%).

MP: 103-104°C (lit.[50] 111.5-112.5°C).

IR (KBr) v_{max}: 1699 (C=O), 1619 (C=C) cm-1.

MS m/e (relative intensity): 275 (M+, 38), 203 (100), 178 (47), 89 (39).

Exact mass calculated for $C_{19}H_{16}O_2$: 276.1151. Found: 276.1151.

1H-NMR (400 MHz, CDCl3) δ 7.86 (dd, 1H, J=2 Hz and J=7 Hz, vinyl C-H), 7.4-7.3 (m, 4H, aromatic H), 6.9-7.0 (m, 4H, aromatic H), 5.68 (d, 1H, J=2 Hz, bridgehead H), 5.21 (d, 1H, J=7 Hz, bridgehead H), 4.18 (q, 2H, J=7 Hz, CO2CH2CH3), 1.25 (t, 3H, J=7 Hz, CO2CH2CH3) ppm.

13C-NMR (50 MHz, CDCl3) δ 164.8 (C=O), 149.3 (vinyl C-H), 145.4 (aromatic C), 144.8 (vinyl C), 144.5 (aromatic C), 125.1, 124.9, 123.8, 123.5 (aromatic C-H), 60.7 (CO2CH2CH3) 51.6, 50.4 (bridgehead C-H), 14.3 (CO2CH2CH3) ppm.

UV (Ethanol) λ_{max}: 222 (ε 6,400), 271 (ε 2,400), 279 (ε 2,800) nm.

9,10-Dihydro-9,10-ethenoanthracene-11-carboxylic acid (40)[50]

The same procedure was followed as in the saponification of ester 45. Starting with ester 42 (2.8 g, 10 mmol), acid 40 (0.7 g, 2.8 mmol, 28% yield) was obtained and recrystallized from acetonitrile to give transparent prisms.

MP: 253-254°C (lit.[50] 249.2-250.0°C.).

IR (KBr) v_{max}: 3400-2600 (OH), 1675 (C=O), 1611 (C=C), 1233 (C-O) cm-1.

MS m/e (relative intensity): 248 (M+, 53), 203 (100), 178 (11), 101 (21).

Exact mass calculated for $C_{17}H_{12}O_2$: 248.0838. Found: 248.0838.

1H-NMR (400 MHz, DMSO-d6) δ 12.48 (s, 1H, D2O exchangeable), 8.84 (dd, 1H, J=2 Hz and J=7 Hz, vinyl C-H), 7.5-7.4 (m, 4H, aromatic H), 7.0-6.9 (m, 4H, aromatic H), 5.63 (d, 1H, J=2 Hz, bridgehead H), 5.42 (d, 1H, J=7 Hz, bridgehead H) ppm.

13C-NMR (50 MHz, DMSO-d6) δ 165.8 (C=O), 149.4 (vinyl C-H), 145.6, 144.9 (aromatic C), 144.0 (vinyl C), 124.84, 124.77, 123.76, 123.6 (aromatic C-H), 50.7, 49.9 (bridgehead C-H) ppm.

UV (Ethanol) λ_{max}: 224 (ε 5,400), 271 (ε 1,700), 279 (ε 2,100) nm.

9-Aminoanthracene (136)[47]

A suspension of 9-nitroanthracene (2.0 g, 8.7 mmol, Aldrich) and $SnCl_2 \cdot H_2O$ (14 g, 62 mmol) in conc. HCl (14 mL) was refluxed for 1 h. The solution was cooled to 0°C, made basic by the addition of 60% aqueous NaOH and extracted three times with diethyl ether. The combined organic fractions were washed with saturated NaCl solution and dried over MgSO4. The solvent was removed under vacuum to yield 9-aminoanthracene (1.5 g, 7.9 mmol, 88%).

MP: 140-145°C (lit.[107] 148-51°C).

IR (KBr) v_{max}: 3600-3400 (N-H), 1623 (N-H) cm-1.

MS m/e (relative intensity): 193 (M+, 100), 179 (39), 165 (55), 152 (44).

Exact mass calculated for $C_{14}H_{11}N$: 193.0892. Found: 193.0884.

1H-NMR (200 MHz, CDCl3) δ 7.5-7.0 (m, 9H, aromatic C-H) ppm, no detectable N-H.

^{13}C-NMR (50 MHz, CDCl$_3$) δ 137.9, 132.1 (aromatic C), 128.4, 125.2, 123.8, 121.1 (aromatic C-H) 118.2 (aromatic C), 116.3 (aromatic C-H) ppm.

Dimethyl 9-Amino-9,10-dihydro-9,10-ethenoanthracene-11,12-dicarboxylate (39)[63]

An excess of dimethyl acetylenedicarboxylate (2 mL, 16 mmol) was added to a solution of 9-aminoanthracene (1.5 g, 7.8 mmol) in benzene at 0°C (15 mL). The resulting white precipitate was filtered and recrystallized from ethanol to give needles of compound **39** (1.8 g, 5.3 mmol, 68% yield).

MP: 220-222°C (lit.[63] 220-222°C).

IR (KBr) ν_{max}: 3382, 3324 (N-H), 1747, 1738, 1719, 1698 (C=O), 1638 (C=C), 1297 (C-O) cm^{-1}.

MS m/e (relative intensity): 335 (M$^+$, 15), 276 (34), 244 (12), 216 (21), 193 (100).

Exact mass calculated for C$_{20}$H$_{17}$NO$_4$: 335.1158. Found: 335.1166.

^{1}H-NMR (400 MHz, CDCl$_3$) δ 7.5-7.3 (m, 4H, aromatic H), 7.1-7.0 (m, 4H, aromatic H), 5.62 (s, 1H, bridgehead H), 3.83 (s, 3H, CO$_2$CH$_3$), 3.76 (s, 3H, CO$_2$CH$_3$), 2.45 (br. s, 2H, D$_2$O exchangeable, N-H$_2$) ppm.

^{13}C-NMR (50 MHz, CDCl$_3$) δ 166.9, 163.8 (C=O), 155.4 (vinyl C), 145.3, 144.0 (aromatic C), 141.0 (vinyl C), 125.6, 125.2, 123.6, 119.8 (aromatic C-H), 66.4 (bridgehead C), 52.7, 52.4 (CO$_2$CH$_3$), 49.6 (bridgehead C-H) ppm.

UV (Acetonitrile) λ_{max}: 219 (ϵ 16,000), 270 (ϵ 2,600), 278 (ϵ 2,800) nm.

143

Methyl 9-Anthracenecarboxylate (137)[48]

A suspension of 9-anthracenecarboxylic acid (7.0 g, 32 mmol, Aldrich) and SOCl₂ (10 mL) in anhydrous chloroform (100 mL) was refluxed for 0.5 h. The solvent and excess SOCl₂ were removed under vacuum to yield a yellow solid assumed to be the corresponding acyl chloride. The acyl chloride was dissolved in anhydrous chloroform (100 mL) and anhydrous methanol (30 mL) was added. This solution was refluxed for 20 h and the solvent removed under vacuum. The residue was dissolved in diethyl ether, washed three times with 10% aqueous NaOH, two times with a saturated aqueous NaCl solution and dried over MgSO₄. Evaporation of the solvent resulted in a yellow solid which was recrystallized from ethanol to yield ester 137 (6.2 g, 26 mmol, 84%).

MP: 110-112°C (lit.[48] 112-113°C).

IR (KBr) v_{max}: 1729 (C=O), 1625 (C=C), 1209 (C-O) cm⁻¹

MS m/e (relative intensity): 236 (M⁺, 83), 205 (100), 177 (86).

Exact mass calculated for $C_{16}H_{12}O_2$: 236.0838. Found: 236.0846.

¹H-NMR (400 MHz, CDCl₃) δ 8.52 (m, 1H, aromatic H), 8.1-8.0 (m, 4H, aromatic H), 7.6-7.4 (m, 4H, aromatic H), 4.18 (s, 3H, CO₂CH₃) ppm.

¹³C-NMR (50 MHz, CDCl₃) δ 170.1 (C=O), 131.0 (aromatic C), 129.5, 128.6 (aromatic C-H), 128.5, 127.8 (aromatic C), 127.0, 125.5, 125.0 (aromatic C-H), 52.6 (CO₂CH₃) ppm.

Trimethyl   9,10-Dihydro-9,10-ethenoanthracene-9,11,12-tricarboxylate   (43)   and Trimethyl 1,4-Dihydro-1,4-ethenoanthracene-9,11,12-tricarboxylate (138)

In a round bottom flask equipped with a condenser, ester **137** (2.0 g, 8.5 mmol) and dimethyl acetylenecarboxylate (3 mL, 3.5 g, 24 mmol) were refluxed for 15 min. The resulting brown oil was chromatographed on silica gel eluted with 30% ethyl acetate in petroleum ether. Two crude isomeric Diels-Alder adducts were obtained from the separated fractions; 959 mg (25 mmol, 30% yield) of compound **43** and 106 mg (2.8 mmol, 3% yield) of compound **138**. Both isomers were purified further by recrystallization from ethanol and characterized as follows:

Compound **43** was characterized as trimethyl 9,10-dihydro-9,10-ethenoanthracene-9,11,12-tricarboxylate. This was further supported with X-ray crystal structure.[67]

MP: 174-176°C

IR (KBr) v_{max}: 1737, 1712 (C=O), 1629 (C=C), 1286, 1263 (C-O) cm^{-1}.

MS m/e (relative intensity): 378 (M$^+$, 26), 260 (100), 201 (85), 177 (55).

Exact mass calculated for $C_{22}H_{18}O_6$: 378.1103. Found: 378.1112.

^{1}H-NMR (400 MHz, CDCl$_3$) δ 7.6-7.4 (m, 4H, aromatic H), 7.1-7.0 (m, 4H, aromatic H), 5.62 (s, 1H, bridgehead H), 4.08 (s, 3H, CO$_2$CH$_3$), 3.85 (s, 3H, CO$_2$CH$_3$), 3.75 (s, 3H, CO$_2$CH$_3$) ppm.

^{13}C-NMR (50 MHz, CDCl$_3$) δ   168.8, 167.1, 163.8 (C=O), 150.34 (vinyl C), 144.1 (aromatic C), 143.6 (vinyl C), 142.0 (aromatic C), 126.0, 125.4, 123.8, 123.4 (aromatic C-H), 64.1 (bridgehead C), 52.5, 52.5, 52.4 (CO$_2$CH$_3$), 51.1 (bridgehead C-H) ppm.

UV (Ethanol) λ_{max}: 219 (ε 14,000), 277 (ε 2,800) nm.

Anal. calculated for $C_{22}H_{18}O_6$: C, 69.84; H, 4.80. Found C, 69.75; H, 4.70.

Compound **138** was characterized as trimethyl 1,4-dihydro-1,4-ethenoanthracene-9,11,12-dicarboxylate.

MP: 117-118°C.

IR (KBr) v_{max}: 1729, 1713 (C=O), 1643 (C=C), 1276, 1249 (C-O) cm^{-1}.

MS m/e (relative intensity): 378 (M+, 49), 346 (37), 318 (100), 287 (78), 177 (21).

Exact mass calculated for $C_{22}H_{18}O_6$: 378.1103. Found: 378.1097.

¹H-NMR (400 MHz, CDCl$_3$) δ 8.0-7.9 (m, 2H, aromatic H), 7.8-7.7 (m, 2H, aromatic H), 7.5-7.4 (m, 2H, aromatic H), 7.0-6.9 (m, 2H, vinyl H), 5.65 (m, 1H, bridgehead H), 5.30 (m, 1H, bridgehead H), 4.10 (s, 3H, CO$_2$CH$_3$), 3.81 (s, 3H, CO$_2$CH$_3$), 3.80 (s, 3H, CO$_2$CH$_3$) ppm.

¹³C-NMR (100 MHz, CDCl$_3$) δ 168.3 165.9, 165.4 (C=O), 147.2, 145.5 140.7, 140.4 (aromatic C-H and or vinyl C), 138.8, 137.8 (vinyl C-H), 131.0 (aromatic C or vinyl C), 128.0 (aromatic C-H), 127.8 (aromatic C or vinyl C), 127.0, 126.5, 125.22, 125.16, 123.8 (aromatic C-H), 52.41, 52.37, 52.3 (CO$_2$CH$_3$), 49.7, 47.4 (bridgehead C-H) ppm.

Anal. calculated for $C_{22}H_{18}O_6$: C,69.84; H, 4.80 Found; C, 69.68; H, 4.82.

Ethyl 9-Anthracenecarboxylate (139)[49]

The procedure used to prepare methyl 9-anthracenecarboxylate (**137**) was modified by using anhydrous ethanol instead of anhydrous methanol. Starting with 9-anthracenecarboxylic acid (3.0 g, 14 mmol), crude ethyl 9-anthracenecarboxylate (**139**) was obtained in 91% yield (3.2g, 13 mmol) and purified further by recrystallization from ethanol.

MP: 112-114°C (lit.[49] 102°C).

IR (KBr) v_{max}: 1714 (C=O), 1625 (C=C), 1217 (C=O) cm^{-1}

MS m/e (relative intensity): 250 (M+, 92), 222 (41), 205 (100), 177 (89).

Exact mass calculated for $C_{17}H_{14}O_2$: 250.0994. Found: 250.0994.

^{1}H-NMR (400 MHz, CDCl$_3$) δ 8.50 (s, 1H, aromatic H), 8.1-8.0 (m, 4H, aromatic H), 7.6-7.4 (m, 4H, aromatic H), 4.70 (q, 2H, J=7 Hz, CO$_2$CH$_2$CH$_3$), 1.50 (t, 3H, J=7 Hz, CO$_2$CH$_2$CH$_3$) ppm.

^{13}C-NMR (50 MHz, CDCl$_3$) δ 169.7 (C=O), 131.0 (aromatic C) 129.2, 128.6 (aromatic C-H), 128.7, 128.4 (aromatic C), 126.9, 125.4, 125.0 (aromatic C-H), 61.8 (CO$_2$CH$_2$CH$_3$), 14.5 (CO$_2$CH$_2$CH$_3$) ppm.

Dimethyl 9-ethoxycarbonyl-9,10-dihydro-9,10-ethenoanthracene-11,12-dicarboxylate (44)

In a round bottom flask fitted with a condenser, ester **139** (3.0 g, 14 mmol) and dimethyl acetylenecarboxylate (2 mL, 2.3 g, 16 mmol) were refluxed for 15 min. The resulting yellow oil was crystallized from ethanol three times to yield ester **44** (3.0 g, 7.7 mmol, 67%). Crystallization from ethanol gave two forms of crystals; prisms and needles.

MP: Prisms 147-149°C, needles 145-149°C.

IR (KBr) ν_{max}: Needles 1746, 1735, 1714 (C=O), 1630 (C=C), 1279, 1256 (C-O); prisms 1732, 1703 (C=O), 1627 (C=C), 1290, 1262 (C-O) cm^{-1}.

MS m/e (relative intensity): 392 (M+, 65), 364 (40), 287 (43), 260 (100), 177 (23).

Exact mass calculated for $C_{23}H_{20}O_6$: 392.1260. Found: 392.1256.

^{1}H-NMR (400 MHz, CDCl$_3$) δ 7.6-7.4 (m, 4H, aromatic H), 7.1-7.0 (m, 4H, aromatic H), 5.64 (s, 1H, bridgehead H), 4.62 (q, 2H, J=7 Hz, CO$_2$CH$_2$CH$_3$), 3.82 (s, 3H, CO$_2$CH$_3$), 3.78 (s, 3H, CO$_2$CH$_3$), 1.48 (t, 3H, J=7 Hz, CO$_2$CH$_2$CH$_3$) ppm.

147

^{13}C-NMR (50 MHz, CDCl$_3$) δ 168.3, 167.1, 163.9 (C=O), 150.5 (vinyl C), 144.2 (aromatic C), 143.6 (vinyl C), 142.2 (aromatic C), 125.9, 125.4, 123.8, 123.5 (aromatic C-H), 63.8 (bridgehead C), 62.0 (CO$_2$CH$_2$CH$_3$), 52.5, 52.3 (CO$_2$CH$_3$), 51.1 (bridgehead C-H), 14.2 (CO$_2$CH$_2$CH$_3$) ppm.

UV (Ethanol) λ_{max}: 216 (ε 17,800) nm.

Anal. calculated for C$_{23}$H$_{20}$O$_6$: C, 70.40; H, 5.14. Found: for plates C, 70.19; H, 5.17; for needles C, 70.36; H, 5.05.

Dimethyl 9-Formyl-9,10-dihydro-9,10-ethenoanthracene-11,12-dicarboxylate (46)[51]

A mixture of 9-anthraldehyde (5.0 g, 24 mmol, Aldrich) and dimethyl acetylenedicarboxylate (4 mL, 4.4 g, 32 mmol) was refluxed for 1.5 h. The resulting yellow oil was purified on silica gel eluted with 25% ethyl acetate in petroleum ether and recrystallized from an ether-ethanol solution to yield aldehyde 39 (5.0 g, 14 mmol, 60% yield).

MP: 171-172°C (lit.[51] 171-173°C).

IR (KBr) v_{max}: 2755 (CH=O), 1728 (C=O), 1630 (C=C) cm^{-1}.

MS m/e (relative intensity): 348 (M$^+$, 31), 316 (19), 290 (17), 260 (100), 202 (67).

Exact mass calculated for C$_{21}$H$_{16}$O$_5$: 348.0998. Found: 348.0991.

^{1}H-NMR (200 MHz, CDCl$_3$) δ 10.93 (s, 1H, CH=O), 7.5-7.0 (m, 8H, aromatic H), 5.64 (s, 1H, bridgehead H), 3.85 (s, 3H, CO$_2$CH$_3$), 3.80 (s, 3H, CO$_2$CH$_3$) ppm.

^{13}C-NMR (100 MHz, CDCl$_3$) δ 197.3 (CH=O), 166.39, 163.7 (C=O), 148.6 (vinyl C), 144.4 (aromatic C), 144.2 (vinyl C), 144.0 (aromatic C), 126.1, 125.3, 124.4, 122.2 (aromatic C-H), 64.1 (bridgehead C), 52.5, 51.7 (CO$_2$CH$_3$), 50.9 (bridgehead C-H) ppm.

Dimethyl 9-Carboxy-9,10-dihydro-9,10-ethenoanthracene-11,12-dicarboxylate (38)[52]

Aldehyde **46** (1.1 g, 3.2 mmol) and resorcinol (1.5 g, 14 mmol) were dissolved in *tert*-butanol (40 mL). A solution of $NaClO_2$ (1.1 g, 14 mmol) and $Na_2HPO_4 \cdot 7H_2O$ (1.1 g, 4 mmol) in water (10 mL) was added. This was allowed to stand for 24 h and then the aqueous layer was removed. The organic layer was extracted three times with 5% aqueous $NaHCO_3$, the combined aqueous fractions were made acidic with conc. HCl and extracted with diethyl ether three times. The organic fractions were washed twice with saturated NaCl solution, dried over $MgSO_4$ and the solvent was removed under vacuum. The residue was recrystallized from ethanol to give crystals of acid **38** (964 mg, 2.35 mmol, 74%). ^{1}H-NMR and ^{13}C-NMR showed that these crystals contained a 1:1 ratio of acid **38** and ethanol. Recrystallization from acetonitrile gave crystals which contained solvent molecules in the crystal lattice, while recrystallization from ethyl acetate and *sec*-butanol gave crystals without any solvent molecules. The structure of the crystals recrystallized from ethanol was further supported by X-ray analysis.[79]

MP: Crystals from ethyl acetate 210-212°C, crystals from acetonitrile 208-212°C, crystals from ethanol 210-212 °C.

IR (KBr) v_{max}: Crystals from ethyl acetate 3600-3200 (O-H), 1751, 1716, 1699 (C=O), 1625 (C=C), 1296 (C-O) cm^{-1}.

Crystals from acetonitrile 3200-2600 (O-H), 1724, 1702 (C=O), 1624 (C=C), 1290, 1252 (C-O) cm^{-1}.

Crystals from ethanol 3500-2500 (O-H and C-H), 1703 (C=O), 1621 (C=C), 1296, 1261 (C-O) cm^{-1}.

MS m/e (relative intensity): 364 (M$^+$, 17), 332 (34), 260 (100), 229 (42), 201 (43).

Exact mass calculated for $C_{21}H_{16}O_6$: 364.0947. Found: 364.0938.

149

¹H-NMR (200 MHz, CDCl₃) Crystals from ethyl acetate δ 8.8 (br s, 1H, D₂O exchangeable) 7.8-7.7 (m, 2H, aromatic H), 7.5-7.4 (m, 2H, aromatic H), 7.2-7.0 (m, 4H, aromatic H), 5.65 (s, 1H, bridgehead H), 3.82 (s, 3H, CO₂C$\underline{H}$₃), 3.78 (s, 3H, CO₂C$\underline{H}$₃) ppm.

Crystals from acetonitrile δ 7.7-7.6 (m, 2H, aromatic H), 7.4-7.3 (m, 2H, aromatic H), 5.50 (s, 1H, bridgehead H), 5.40 (br s, D₂O exchangeable), 3.78 (s, 3H, CO₂C$\underline{H}$₃), 3.70 (s, 3H, CO₂C$\underline{H}$₃), 1.98 (s, 3H, CNC$\underline{H}$₃) ppm.

Crystals from ethanol; δ 7.8-7.7 (m, 2H, aromatic H), 7.5-7.4 (m, 2H, aromatic H), 7.1-7.0 (m, 4H, aromatic H), 6.15 (br s, D₂O exchangeable), 5.64 (s, 1H, bridgehead H), 3.82 (s, 3H, CO₂C$\underline{H}$₃), 3.80 (q, 2H, J=7 Hz, CH₃C$\underline{H}$₂OH), 3.78 (s, 3H, CO₂C$\underline{H}$₃), 1.38 (t, 3H, J=7 Hz, C$\underline{H}$₃CH₂OH) ppm.

¹³C-NMR (50 MHz, CDCl₃) Crystals from ethyl acetate δ 173.3, 167.4, 163.9 (C=O), 150.1 (vinyl C), 144.0 (aromatic C), 143.8 (vinyl C), 141.4 (aromatic C), 126.2, 125.6, 124.0 123.6 (aromatic C-H), 64.2 (bridgehead C), 52.7, 52.6 (CO₂C$\underline{H}$₃), 51.1 (bridgehead C-H) ppm.

UV (Ethanol) λ$_{max}$: 216 (ε 39,900), 277 (ε 4,800) nm.

Anal. calculated for crystals recrystallized from ethyl acetate C₂₁H₁₆O₆: C, 69.23; H, 4.43. Found: C, 69.47; H, 4.39.

3.2.2 Salt Formation of Starting Materials

3.2.2.1 Salt Formation of Ethyl 9,10-Dihydro-9,10-ethenoanthracene-11-carboxylate-12-carboxylic acid (36)

Sodium salt of acid 36 (85)

To a solution of acid **36** (339 mg, 1.06 mmol) in ethanol (9 mL) was added NaOH (54 mg, 1.06 mmol) in water (1 mL). This solution was stirred until clear, the solvent removed under vacuum and the resulting white solid dried at 100°C at 10^{-2} mm Hg.

MP: Does not melt below 300°C.

IR (KBr) v_{max}: 1708 (C=O ester), 1615 (COO⁻ asym.), 1391 (COO⁻ sym.) cm⁻¹.

Calcium salt of acid 36 (86)

Acid **36** (333 mg, 1.04 mmol) was dissolved in ethanol (10 mL) and CaO (27.9 mg, 0.50 mmol) added. This solution was stirred for 10 min. The white precipitate that formed was filtered (230 mg, 0.339 mmol, 65% yield) and dried at 100°C under vacuum.

MP: does not melt below 300°C.

IR (KBr) v_{max}: 1719 (C=O ester), 1579 (COO⁻ asym.), 1402 (COO⁻ sym.) cm⁻¹.

Diethylamine salt of acid 36 (87)

Acid 36 (242 mg, 0.756 mmol) was dissolved in 10 mL of diethyl ether and 5 mL (3.5 g, 48 mmol) of diethylamine added. The resulting precipitate was filtered and recrystallized from acetonitrile to yield colorless needles of salt **87** (299 mg 0.761 mmol, 99%).

MP: 168-173°C.

IR (KBr) v_{max}: 3100-2400 (N-H,), 1711 (C=O ester), 1631 (COO⁻ asym.), 1386 (COO⁻ sym.) cm⁻¹.

MS FAB: 394 (M+1).

^{1}H-NMR (400 MHz, CDCl$_3$) δ 7.4-7.3 (m, 4H, aromatic H), 7.0-6.9 (m, 4H, aromatic H), 5.54 (s, 1H, bridgehead H), 5.30 (s, 1H, bridgehead H), 4.15 (q, 2H, J=7 Hz, CO$_2$CH$_2$CH$_3$), 2.16 (q, 4H, J=7 Hz, HN(CH$_2$CH$_3$)$_2$), 1.26 (t, 3H, J=7 Hz, CO$_2$CH$_2$CH$_3$), 1.12 (t, 6H, J=7 Hz, HN(CH$_2$CH$_3$)$_2$) ppm, no O-H or N-H signals detectable.

UV (Ethanol) λ_{max}: 217 (ε 13,000), 272 (ε 2,200), 279 (ε 2,500) nm.

Anal. calculated for C$_{24}$H$_{27}$NO$_4$: C, 73.26; H, 6.92; N, 3.56. Found: C, 73.32; H, 7.06; N, 3.65.

Pyrrolidine salt of acid 36 (88)

Pyrrolidine (0.5 mL, 0.43 g, 6.0 mmol) was added to a solution of acid 36 (168 mg, 0.53 mmol) in diethyl ether (15 mL). The precipitate which formed was filtered and recrystallized from acetonitrile to yield colorless plates of salt **88** (152 mg 0.390 mmol, 73%). The elemental analysis and infrared spectra of salt **88** suggest that it crystallizes with one equivalent of H$_2$O.

MP: 134-140°C.

IR (KBr) v_{max}: 3600-2800 (N-H, C-H, O-H), 1696 (C=O ester), 1621 (COO⁻ asym.), 1386 (COO⁻ sym.) cm⁻¹.

MS FAB: 392 (M+1).

¹H-NMR (400 MHz, CDCl₃) δ 7.4-7.3 (m, 4H, aromatic H), 7.0-6.9 (m, 4H, aromatic H), 5.49 (s, 1H, bridgehead H), 5.29 (s, 1H, bridgehead H), 4.16 (q, 2H, J=7 Hz, CO₂_CH₂_CH₃), 2.89 (m, 4H, -N(_CH₂_)₂-), 1.58 (m, 4H, -N(CH₂_CH₂_)₂-), 1.28 (t, 3H, J=7 Hz, CO₂CH₂_CH₃_) ppm, no O-H or N-H signals were detectable.

UV (Ethanol) λ_{max}: 221 (ε 13,000), 272 (ε 3.500), 279 (ε 4,100) nm.

Anal. calculated for C₂₄H₂₅NO₄·H₂O: C, 70.40; H, 6.65; N, 3.42. Found: C, 70.60; H, 6.60; N 3.42.

Piperidine salt of acid 36 (89)

To a solution of acid **36** (0.43 g, 1.3 mmol) in diethyl ether (45 mL) was added piperidine (1.75 mL, 1.5 g, 18 mmol) and the solution stirred for 20 min. The resulting precipitate was filtered and recrystallized from an acetonitrile-acetone solution to yield colorless plates of salt **89** (0.42 g, 1.0 mmol, 77%).

MP: 160-162°C.

IR (KBr) v_{max}: 3100-2400 (N-H, C-H), 1708 (C=O ester), 1626 (C=C), 1581 (COO⁻ asym.), 1386 (COO⁻ sym.), 1217 (C-O) cm⁻¹.

MS FAB: 406 (M+1).

¹H-NMR (400 MHz, CDCl₃) δ 7.4-7.3 (m, 4H, aromatic H), 7.0-6.9 (m, 4H, aromatic H), 5.52 (s, 1H, bridgehead H), 5.35 (s, 1H, bridgehead H), 4.17 (q, 2H, J=7 Hz, CO₂_CH₂_CH₃), 2.66 (t, 4H, J=6 Hz, -N(_CH₂_)₂-), 1.38 (m, 4H, -N(CH₂_CH₂_)₂-), 1.18 (m,

2H, -N(CH$_2$CH$_2$)$_2$CH$_2$), 1.18 (t, 3H, J=7 Hz, CO$_2$CH$_2$CH$_3$) ppm, no O-H or N-H signals detectable.

UV (Ethanol) λ_{max}: 223 (ϵ 12,000), 272 (ϵ 3,700), 279 (ϵ 4,200) nm.

Anal. calculated for C$_{25}$H$_{27}$NO$_4$: C, 74.05; H, 6.71; N, 3.45. Found: C, 73.89; H, 6.78; N, 3.33.

S-(-)-Proline complex of acid 36 (90a)

Acid **36** (275 mg, 0.858 mmol) and S-(-)-proline (98.2 mg, 0.854 mmol, Sigma) were dissolved in 50 mL of ethanol. Approximately half of the solvent was removed under vacuum and the remaining solution was stirred for 0.5 h, yielding a white precipitate of complex **90a** (299 mg, 0.687, 80%) which was filtered and dried over P$_2$O$_5$ (100°C, 10^{-2} mmHg). All attempts to recrystallize complex **90a** from different solvents failed.

MP: 173-175°C.

IR (KBr) ν_{max}: 3400-2400 (O-H, N-H, C-H), 1706 (C=O ester), 1633 (C=C), 1579 (COO$^-$ asym.), 1391 (COO$^-$ sym.), 1289, 1224 (C-O) cm^{-1}.

MS FAB: 436 (M+1).

^{1}H-NMR (400 MHz, CDCl$_3$) δ 7.5-7.4 (m, 4H, aromatic H), 7.1-7.0 (m, 4H, aromatic H), 6.18 (s, 1H, bridgehead H), 5.79 (s, 1H, bridgehead H), 4.44 (q, 2H, J=7 Hz, CO$_2$CH$_2$CH$_3$), 4.2-4.1 (m, 1H, -NCH(CO$_2$)-), 3.4-3.3 (m, 2H, (-NCH$_2$-), 2.4-2.2 (m, 1H), 2.2-2.0 (m, 1H), 2.0-1.9 (m, 2H), 1.45 (t, 3H, J=7 Hz, CO$_2$CH$_2$CH$_3$) ppm, no O-H or N-H signals were detectable.

UV (Ethanol) λ_{max}: 214 (ϵ 13,000), 271 (ϵ 1,500), 279 (ϵ 1,600) nm.

Anal. calculated for C₂₅H₂₅NO₆: C, 68.95; H, 5.79; N, 3.22. Found: C, 68.82; H, 5.83; N, 3.29.

R-(+)-Proline complex of acid 36 (90b)

Complex **90b** was prepared in 80% yield (267 mg, 0.613 mmol) from acid **36** (246 mg, 0.768 mmol) and R-(+)-proline (88.9 mg, 0.773 mmol, Sigma) exactly as described above; complexes **90a** and **90b** exhibited identical spectroscopic properties.

MP: 173-174°C.

Anal. calculated for $C_{25}H_{25}NO_6$: C, 68.95; H, 5.79; N, 3.22. Found C, 68.62; H, 5.87; N, 3.26.

(S,R)-(±)-Proline complex of acid 36 (90c)

Complex **90c** was formed in 72% yield from acid **36** (140 mg, 0.436 mmol) and (±)-proline (51.6 mg, 0.448 mmol, Sigma) exactly as described for complex **90a**.

MP: 183-186°C.

IR (KBr) v_{max}: 3200-2400 (O-H, N-H, C-H), 1704 (C=O ester), 1633 (C=C), 1582 (COO⁻ asym.), 1380 (COO⁻ sym.), 1289, 1222 (C-O) cm⁻¹.

MS FAB: 436 (M+1).

¹H-NMR (400 MHz, CDCl₃) δ 7.5-7.4 (m, 4H, aromatic H), 7.1-7.0 (m, 4H, aromatic H), 6.05 (s, 1H, bridgehead H), 5.77 (s, 1H, bridgehead H), 4.42 (q, 2H, J=7 Hz,

155

$CO_2\underline{CH}_2CH_3$), 4.1-4.0 (m, 1H, -N$\underline{CH}$-), 3.4-3.1 (m, 2H, -N$\underline{CH}_2$-), 2.3-2.2 (m, 1H), 2.15-2.05 (m, 1H), 1.80 (m, 2H), 1.45 (t, 3H, $CO_2CH_2\underline{CH}_3$) ppm, no O-H or N-H detectable.

UV (Ethanol) λ_{max}: 214 (ϵ 12,000), 271 (ϵ 2,000), 279 (ϵ 2,100) nm.

Anal. calculated for $C_{25}H_{25}NO_6$: C, 68.95; H, 5.79; N, 3.22. Found: C, 69.13; H, 5.85; N, 3.00.

S-(-)-Proline methyl ester salt of acid 36 (92)

A solution of acid **36** (245 mg, 0.764 mmol), the hydrochloride salt of S-(-)-proline methyl ester (127 mg, 0.765 mmol, Aldrich) and KOH (43.9 mg, 0.782 mmol) in anhydrous ethanol (30 mL) was stirred for 0.5 h and then centrifuged for 20 min. The white precipitate which formed was discarded and the solvent removed under vacuum. The residue was solidified in 2 mL of diethyl ether, filtered and recrystallized from ethanol to yield colorless prisms of salt **92** (205 mg 0.456 mmol, 60%).

MP: 126-130°C.

IR (KBr) v_{max}: 3000-2000 (C-H, N-H), 1746, 1723, 1708 (C=O), 1630 (COO$^-$ asym.), 1387 (COO$^-$ sym.), 1204 (C-O) cm^{-1}.

MS DCI: 450 (M+1).

^{1}H-NMR (400 MHz, CDCl$_3$) δ 7.4-7.3 (m, 4H, aromatic H), 7.1-7.0 (m, 4H, aromatic H), 5.80 (s, 1H, bridgehead H), 5.68 (s, 1H, bridgehead H), 4.34 (q, 2H, J=7 Hz, $CO_2\underline{CH}_2CH_3$), 4.16 (m, 1H, -N$\underline{CH}$-), 3.76 (s, 3H, $CO_2\underline{CH}_3$), 3.11 (m, 2H, -N$\underline{CH}_2$-), 2.25 (m, 1H), 2.0-1.8 (m, 3H), 1.38 (t, 3H, J=7 Hz, $CO_2CH_2\underline{CH}_3$) ppm, no O-H or N-H signals detectable.

UV (Ethanol) λ_{max}: 217 (ϵ 13,000), 271 (ϵ 2,500), 279 (ϵ 2,800) nm.

156

Anal. calculated for $C_{26}H_{27}NO_6$: C, 69.47; H, 6.05; N, 3.12. Found C, 69.30; H, 5.93; N, 2.90.

S-(+)-Prolinol salt of acid 36 (93)

Acid **36** (255 mg, 0.798 mmol) was dissolved in diethyl ether (30 mL) and S-(+)-prolinol (0.5 mL, 513 mg, 5.08 mmol, Aldrich) was added. The precipitate which formed was filtered and recrystallized from ethanol to yield colorless prisms of salt **93** (296 mg 0.673 mmol, 84%). The elemental analysis and infrared spectra of salt **93** suggested that it crystallizes with half an equivalent of water.

MP: 158-165°C.

IR (KBr) v_{max}: 3600-2400 (O-H, N-H, C-H), 1699 (C=O ester), 1625 (C=C), 1609 (COO$^-$ asym.), 1387 (COO$^-$ sym.), 1289, 1225, 1207 (C-O) cm^{-1}.

MS FAB: 422 (M+1).

^{1}H-NMR (400 MHz, CDCl$_3$) δ 7.4-7.3 (m, 4H, aromatic H), 7.0-6.9 (m, 4H, aromatic H), 5.50 (s, 1H, bridgehead H), 5.30 (s, 1H, bridgehead H), 4.20 (q, 2H, J=7 Hz, CO$_2$C̲H̲$_2$CH$_3$), 3.70 (dd, 1H, J=1 and J=10 Hz), 3.45 (dd, 1H, J=6 and J=10 Hz), 3.25 (m, 1H), 2.93 (m, 1H), 2.80 (m, 1H), 1.8-1.4 (m, 4H), 1.30 (t, 3H, CO$_2$CH$_2$C̲H̲$_3$) ppm, no O-H or N-H signals detectable.

UV (Ethanol) λ_{max}: 215 (ϵ 10,000), 272 (ϵ 1,400), 279 (ϵ 1,600) nm.

Anal. calculated for $C_{25}H_{27}NO_5 \cdot \frac{1}{2}H_2O$: C, 69.75; H, 6.56; N,3.25. Found: C, 69.67; H, 6.55; N, 3.50.

157

S-(-)-Prolineamide salt of acid 36 (94)

S-(-)-Prolineamide (64.3 mg, 0.564 mmol) was dissolved in ethanol (5 mL) and added to a solution of acid **36** (179 mg, 0.559 mmol) in diethyl ether (20 mL). The resulting white precipitate was filtered and recrystallized from acetonitrile to yield flakes of salt **94** (220 mg 0.506 mmol, 91%).

MP: 200-204°C.

IR (KBr) v_{max}: 3400-2800 (N-H, C-H), 1694, 1674 (C=O), 1623 (C=C), 1583 (COO⁻ asym.), 1382 (COO⁻ sym.), 1288, 1226, 1207 (C-O) cm⁻¹.

MS FAB: 435 (M+1).

¹H-NMR (400 MHz, D₂O) δ 7.5–7.4 (m, 4H, aromatic H), 7.1-7.0 (m, 4H, aromatic H), 5.66 (s, 1H, bridgehead H), 5.38 (s, 3H, bridgehead H), 4.35 (m, 1H, -NCH-), 4.16 (q, 2H, J=7 Hz, CO₂ CH₂CH₃), 3.4-3.3 (m, 2H), 2.42 (m, 1H), 2.12 (m 3H), 1.20 (t, 3H, J=7 Hz, CO₂CH₂CH₃) ppm.

UV (Ethanol) λ_{max}: 218 (ε 13,000), 271 (ε 2,500), 279 (ε 2,800) nm.

Anal. calculated for C₂₅H₂₆N₂O₅: C, 69.11; H, 6.03; N, 6.45. Found: C, 68.88; H, 5.90; N, 6.56.

S-(+)-2-(Methoxymethyl)pyrrolidine salt of acid 36 (95)

Acid **36** (523 mg, 1.63 mmol) was dissolved in diethyl ether (50 mL) and S-(+)-2-(methoxymethyl)pyrrolidine (200 μL, 1.69 mmol, Aldrich) added. This solution was stirred for 10 min and the white precipitate which formed was filtered and recrystallized from an acetone-petroleum ether solution to yield prisms of salt **95** (615 mg, 1.41 mmol, 86%).

MP: 164-170°C.

IR (KBr) v_{max}: 3200-2400 (N-H, C-H) 1708 (C=O ester), 1620 (C=C), 1578 (COO⁻ asym.), 1377 (COO⁻ sym.), 1287, 1212 (C-O) cm⁻¹.

MS FAB. 436 (M+1).

¹H-NMR (400 MHz, CDCl₃) δ 7.4-7.3 (m, 4H, aromatic H), 6.9-7.0 (m, 4H, aromatic H), 5.52 (s, 1H, bridgehead H), 5.40 (s, 1H, bridgehead H), 4.22 (q, 2H, J=7 Hz, CO₂CH₂CH₃), 3.50 (m, 1H), 3.42 (m, 2H), 3.16 (s, 3H, CH₂OCH₃), 3.05 (m, 2H), 1.9-1.6 (m, 3H), 1.58 (m, 1H), 1.28 (t, 3H, J=7 Hz, CO₂CH₂CH₃) ppm, no O-H or N-H signals detectable.

UV (Ethanol) λ_{max}: 219 (ε 10,000), 252 (ε 3,200), 272 (ε 2,200), 279 (ε 2,500) nm.

Anal. calculated for C₂₆H₂₉NO₅: C, 71.70; H, 6.71; N, 3.21. Found: C, 71.44; H, 6.75; N, 3.32.

S-(-)-Proline *tert*-Butyl ester salt of acid 36 (96)

Acid 36 (658 mg, 2.06 mmol) was dissolved in diethyl ether (50 mL) and S-(-)-proline *tert*-butyl ester (372 mg, 2.17 mmol, Sigma) was added and the solution was stirred for 10 min. The resulting precipitate was filtered and recrystallized from acetone to give colorless needles of salt 96 (872 mg, 1.78 mmol, 86%). The structure of this salt was further studied by X-ray diffraction analysis.[89]

MP: 154-169°C.

IR (KBr) v_{max}: 3200-3000 (N-H, C-H), 1728 (C=O *tert*-butyl ester), 1698 (C=O ethyl ester), 1626 (C=C), 1589 (COO⁻ asym.), 1372 (COO⁻ sym.), 1252, 1155 (C-O) cm⁻¹.

MS FAB: 492 (M+1).

^{1}H-NMR (400 MHz, CDCl$_3$) δ 8.0 (s, 2H, D$_2$O exchangeable), 7.4-7.3 (m, 4H, aromatic H), 7.0-6.9 (m, 4H, aromatic H), 5.55 (s, 1H, bridgehead H), 5.50 (s, 1H, bridgehead H), 4.22 (q, 2H, J=7 Hz, CO$_2$CH$_2$CH$_3$), 4.10 (m, 1H, -NCH-), 3.18 (m, 1H), 3.08 (m, 1H), 2.22 (m, 1H), 1.88 (m, 2H), 1.72 (m, 1H), 1.46 (s, 9H, CO$_2$C(CH$_3$)$_3$), 1.28 (t, 3H, J=7 Hz, CO$_2$CH$_2$CH$_3$) ppm.

UV (Ethanol) λ$_{max}$: 222 (ε 19,000), 252 (ε 9,600), 271 (ε 4,700), 279 (ε 4,800) nm.

(S,S)-(+)-Pseudoephedrine salt of acid 36 (97)

Acid 36 (339 mg, 1.06 mmol) was dissolved in diethyl ether (40 mL) and (S,S)-(+)-pseudoephedrine (175 mg, 1.06 mmol, Sigma) was added. The resulting solution was stirred for 10 min and the white precipitate which formed was filtered to give salt 97 (471 mg, 0.972 mmol, 92%). All attempts to recrystallize this compound from various solvents failed.

MP: 153-169°C.

IR (KBr) ν$_{max}$: 3600-2400 (O-H, N-H, C-H), 1703 (C=O ester), 1626 (C=C), 1587 (COO$^-$ asym.), 1387 (COO$^-$ sym.), 1292, 1224 (C-O) cm^{-1}.

MS FAB: 486 (M+1).

^{1}H-NMR (400 MHz, CDCl$_3$) δ 7.4-7.2 (m, 9H, aromatic H), 7.0-6.9 (m, 4H, aromatic H), 5.52 (s, 1H, bridgehead H), 5.38 (s, 1H, bridgehead H), 4.78 (d, 1H, J=8 Hz, PhCH-), 4.16 (q, 2H, J=7 Hz, CO$_2$CH$_2$CH$_3$), 3.05 (m, 1H, PhCH(OH)CH-), 2.38 (s, 3H, -NCH$_3$), 1.25 (t, 3H, J=7 Hz, CO$_2$CH$_2$CH$_3$), 0.78 (d, 3H, J=7 Hz, PhCH(OH)CH(CH$_3$)-) ppm, no O-H or N-H signals were detectable.

UV (Ethanol) λ$_{max}$: 210 (ε 16,000), 272 (ε 1,700), 279 (ε 1,900) nm.

160

Anal. calculated for $C_{30}H_{31}NO_5$: C, 74.21; H, 6.44; N, 2.88. Found: C, 73.86; H, 6.45; N, 2.88.

(-) Strychnine salt of acid 36 (98)

Acid 36 (325 mg, 1.02 mmol) and strychnine (340 mg, 1.02 mmol, Aldrich) were dissolved in diethyl ether (15 mL) and stirred for 30 min. The resulting precipitate was filtered, affording salt 98 (474 mg, 0.725 mmol, 73%). All attempts to recrystallize salt 98 from various solvents failed. The elemental analysis and infrared spectra of salt 98 suggest that it crystallizes with one equivalent of H_2O.

MP: 142-150°C.

IR (KBr) v_{max}: 3400-3200 (O-H), 1700 (C=O ester), 1673 (C=O amide), 1633 (C=C), 1598 (COO⁻ asym.), 1391 (COO⁻ sym.), 1288, 1219 (C-O) cm⁻¹.

MS FAB: 655 (M+1).

¹H-NMR (400 MHz, $CDCl_3$) δ 8.08 (m, 1H, aromatic H), 7.5-6.9 (m, 11H, aromatic H), 6.26 (m, 1H), 5.63 (s, 1H, bridgehead H), 5.61 (s, 1H, bridgehead H), 4.63 (s, 1H), 4.8-4.0 (m, 6H), 3.97 (m, 1H), 3.82 (m, 1H), 3.28 (m, 1H), 3.2-3.0 (m, 3H), 2.68 (m, 1H), 2.55 (m, 1H), 2.25 (m, 1H), 2.15 (m, 1H), 1.63 (m, 1H), 1.37 (m, 4H) ppm, no O-H signal was detectable.

UV (Ethanol) λ_{max}: 219 (26,000), 252 (17,000), 279 (7,400) nm.

Anal. calculated for $C_{41}H_{38}N_2O_6 \cdot H_2O$: C, 73.18; H, 5.99; N, 4.29. Found: C, 72.98; H, 6.10; N, 4.30.

3.2.2.2 Salt Formation of 9,10-Dihydro-9,10-ethenoanthracene-11-carboxylic acid (40)

Piperidine salt of acid 40 (134)[102]

To a solution of acid **40** (457 mg, 1.84 mmol) in diethyl ether (50 mL) was added 2.4 mL (1.80 mmol) of piperidine. This solution was stirred for 20 min and the resulting precipitate was filtered and recrystallized from acetonitrile to give colorless prisms of salt **134** (600 mg, 1.80 mmol, 98%).

MP: 195-208°C (lit.[102] 197-208°C).

IR (KBr) v_{max}: 3200-2400 (N-H, C-H), 1634 (C=C), 1548 (COO⁻ asym.), 1373 (COO⁻ sym.) cm⁻¹.

MS DCI: 334 (M+1).

¹H-NMR (400 MHz, CDCl₃) δ 8.8 (br s, 2H, D₂O exchangeable), 7.6-7.5 (m, 1H, vinyl H), 7.4-7.2 (m, 4H, aromatic H), 7.0-6.9 (m, 4H, aromatic H), 5.64 (m, 1H, bridgehead H), 5.16 (m, 1H, bridgehead H), 3.0-2.8 (m, 4H, -N(CH₂)₂-), 1.7-1.5 (m, 4H, -N(CH₂CH₂)₂-), 1.4-1.3 (m, 2H, -N(CH₂CH₂)₂CH₂) ppm.

UV (Ethanol) λ_{max}: 223 (ε 13,000), 272 (ε 4,100), 280 (ε 5,000) nm.

Anal. calculated for C₂₂H₂₃NO₄: C, 79.24; H, 6.95; N, 4.28. Found: C, 79.19; H, 6.85; N, 4.12.

3.2.2.3 Salt Formation of 12-Methyl-9,10-dihydro-9,10-ethenoanthracene-11-carboxylic acid (37)

S-(+)-Prolinol salt of acid 37 (103)

Acid **37** (307 mg, 1.17 mmol) was dissolved in diethyl ether (30 mL) and S-(+)-prolinol (133 mg, 1.32 mmol) was added. The precipitate which formed was filtered and recrystallized from acetonitrile to give colorless prisms of salt **103** (395 mg, 1.09 mmol, 93%). X-ray diffraction analysis[67] was performed on these crystals, which further proved the salt formation.

MP: 193-208°C.

IR (KBr) v_{max}: 3400-2200 (O-H, N-H, C-H), 1636 (C=C), 1527 (COO⁻ asym.), 1386 (COO⁻ sym.) cm⁻¹.

MS FAB: 364 (M+1).

¹H-NMR (400 MHz, CDCl₃) δ 7.4-6.9 (m, 8H, aromatic H), 5.58 (s, 1H, bridgehead H), 4.80 (s, 1H, bridgehead H), 3.65 (m, 1H), 3.55 (m, 1H), 3.45 (m, 1H), 3.00 (m, 2H), 2.36 (s, 3H, vinyl CH₃), 1.75 (m, 2H), 1.60 (m, 2H) ppm, no O-H or N-H detectable.

UV (Ethanol) λ_{max}: 215 (ε 11,400); 272 (ε 1,800); 280 (ε 2,100) nm.

Anal. calculated for C₂₃H₂₅NO₃: C, 76.04; H, 6.94; N, 3.86. Found C, 76.12; H, 6.91; N, 3.76.

S-(-)-Proline *tert*-butyl ester salt of acid 37 (104)

Salt **104** was prepared by dissolving acid **37** (231 mg, 0.882 mmol) in diethyl ether (40 mL) and adding S-(-)-proline *tert*-butyl ester (182 mg, 1.07 mmol). The resulting precipitate was filtered and dried to afford salt **104** (284 mg, 0.656 mmol, 74%). Crystallization from various solvents gave only an amorphous solid.

MP: 153-165°C.

IR (KBr) v_{max}: 3200-2200 (N-H, C-H), 1737 (C=O ester), 1688 (NH$_2^+$), 1631 (C=C), 1541 (COO⁻ asym.), 1370 (COO⁻ sym.), 1236 (C-O) cm⁻¹.

MS FAB: 434 (M+1).

¹H-NMR (400 MHz, CDCl₃) δ 7.6 (br s, 2H, D₂O exchangeable), 7.4-7.3 (m, 4H, aromatic H), 7.0-6.9 (m, 4H, aromatic H), 5.68 (s, 1H, bridgehead H), 4.90 (s, 1H, bridgehead H), 3.96 (m, 1H), 3.12 (m, 2H), 2.40 (s, 3H vinyl CH₃), 2.22 (m, 1H), 1.94 (m, 2H), 1.75 (m, 1H), 1.45 (s, 9H, CO₂C(CH₃)₃) ppm.

UV (Methanol) λ_{max}: 223 (ε 13,400); 271 (ε 4,700); 279 (5,500) nm.

(S,S)-(+)-Pseudoephedrine salt of acid 37 (105a)

Salt **105a** was prepared by dissolving acid **37** (362 mg, 1.38 mmol) and (S,S)-(+)-Pseudoephedrine (229 mg, 1.39 mmol) in diethyl ether (30 mL). The resulting white precipitate was filtered and recrystallized from acetonitrile to afford colorless prisms of salt **105a** (480 mg, 1.12 mmol, 81%). The structure of salt **105a** was studied in detail by X-ray diffraction analysis.[67]

MP: 174-183°C.

IR (KBr) v_{max}: 3600-2400 (O-H, N-H, C-H), 1629 (C=C), 1548 (COO⁻ asym.), 1376 (COO⁻ sym.) cm⁻¹.

MS FAB: 428 (M+1).

¹H-NMR (400 MHz, CDCl₃) δ 7.4-7.3 (m, 9H, aromatic H), 7.0-6.9 (m, 4H, aromatic H), 6.85 (br s, 2H, D₂O exchangeable), 5.68 (s, 1H, bridgehead H), 4.80 (s, 1H, bridgehead H), 4.42 (d, J=8 Hz, PhCH-), 2.94 (m, 1H, PhCH(OH)CH-), 2.45 (s, 3H, vinyl CH₃), 2.30 (s, 3H, -NCH₃), 0.85 (d, 3H, J=7 Hz, PhCH(OH)CHCH₃-) ppm.

UV (Ethanol) λ_{max}: 220 (ε 25,900); 258 (ε 6,000); 271 (ε 7,600); 280 (ε 8,700) nm.

Anal. calculated for C₂₈H₂₉NO₃: C, 78.66; H, 6.84; N, 3.28. Found: C, 78.94; H, 6.78; N, 3.05.

(R,R)-(-)-Pseudoephedrine salt of acid 37 (105b)

Salt 105b was prepared in 69% yield (235 mg, 0.550 mmol) from acid 37 (210 mg, 0.802 mmol) and (R,R)-(-)-pseudoephedrine (132 mg, 0.800 mmol) exactly as described above. Salts 105a and 105b exhibited identical spectroscopic properties.

MP: 174-183°C.

Anal. calculated for C₂₈H₂₉NO₃: C, 78.66; H, 6.84; N, 3.28. Found: C, 78.62; H, 7.00; N, 3.21.

3.2.2.4 Salt Formation of 9-Carboxy-9,10-dihydro-9,10-ethenoanthracene-11,12-dicarboxylate (38)

(R, S)-(-)-Ephedrine salt of acid 38 (108)

Acid **38** (145 mg, 0.333 mmol) and (R,S)-(-)-ephedrine (80.2 mg, 0.486 mmol) were dissolved in diethyl ether (30 mL) and the solution stirred. The resulting precipitate was filtered and recrystallized from acetonitrile to yield colorless flakes of salt **108** (167 mg, 0.316 mmol, 89%). X-ray diffraction analysis revealed that salt **108** crystallizes with half an equivalent of H_2O.[69]

MP: 155-160°C

IR (KBr) v_{max}: 3600-2400 (O-H, N-H, C-H), 1708 (C=O), 1631 (COO⁻ asym), 1392 (COO⁻ sym.), 1287 (C-O) cm⁻¹.

MS FAB: 530 (M+1).

¹H-NMR (400 MHz, $CDCl_3$) δ 8.04 (m, 1H, aromatic H), 7.90 (m, 1H, aromatic H), 7.5-7.0 (m, 11H, aromatic H), 5.63 (s, 1H, bridgehead H), 5.55 (s, 1H, PhC<u>H</u>-), 3.82 (s, 3H, CO₂C<u>H</u>₃), 3.80 (s, 3H, CO₂C<u>H</u>₃), 3.48 (m, 1H, PhCH(OH)C<u>H</u>-), 2.42 (s, 3H, NC<u>H</u>₃), 1.10 ppm (d, 3H, J=7 Hz, PhCH(OH)CHC<u>H</u>₃-) ppm, no O-H or N-H signals detectable.

UV (Ethanol) λ_{max}: 217 (ε 16,300); 278 (ε 2,500) nm.

Anal. calculated for $C_{31}H_{31}NO_7 \cdot \frac{1}{2} H_2O$: C, 69.13; H, 5.99; N, 2.60. Found C, 68.89; H, 6.08; N, 2.67.

(S,S)-(+)-Pseudoephedrine salt of acid 38 (109)

Salt **109** was prepared by dissolving acid **38** (115 mg, 0.281 mmol) and (S,S)-(+)-pseudoephedrine (47.1 mg, 0.286 mmol) in diethyl ether (50 mL), this solution was stirred for 24 h. The resulting precipitate was filtered and recrystallized from diethyl ether to afford fine needles of salt **109** (138 mg, 0.261 mmol, 93%). Elemental analysis revealed that salt **109** crystallizes with half an equivalent of H_2O.

MP: 164-168°C.

IR (KBr) v_{max}: 3600-2600 (O-H, N-H, C-H), 1713 (C=O), 1611 (COO$^-$ asym.), 1386 (COO$^-$ sym.), 1275 (C-O) cm^{-1}.

MS FAB: 530 (M+1).

^{1}H-NMR (400 MHz, $CDCl_3$) δ 8.0-7.9 (m, 2H, aromatic H), 7.5-7.3 (m, 7H, aromatic H), 7.1-7.0 (m, 4H, aromatic H), 5.62 (s, 1H, bridgehead H), 4.88 (d, 1H, J=8 Hz, PhCH-), 3.75 (s, 3H, CO$_2$CH$_3$), 3.74 (s, 3H, CO$_2$CH$_3$), 3.40 (m, 1H, PhCH(OH)CH-), 2.70 (s, 3H, NCH$_3$), 1.10 (d, 3H, J=7 Hz, PhCH(OH)CHCH$_3$-) ppm, no O-H or N-H signals detectable.

UV (Ethanol) λ_{max}: 215 (ε 15,300); 278 (ε 1,300) nm.

Anal. calculated for $C_{31}H_{31}NO_7\cdot\frac{1}{2}H_2O$: C, 69.13; H, 5.99; N, 2.60. Found: C, 68.87; H, 5.93; N, 2.56.

3.2.2.5 Salt Formation of Dimethyl 9-Amino-9,10-dihydro-9,10-ethenoanthracene-11,12-dicarboxylate (39)

Hydrochloride salt of amine 39 (112)

The hydrochloride salt **112** was prepared by mixing a solution of amine **39** (512 mg, 1.53 mmol) in ethanol (10 mL) with conc. hydrochloric acid (10 mL). Upon evaporation of the solvent, colorless crystals of salt **112** (495 mg, 87%) were formed. Recrystallization from ethanol-water gave platelets.

MP: 194-212°C

IR (KBr) v_{max}: 3600-2200 (N-H, C-H), 1718 (C=O), 1632 (C=C), 1584, 1528 (NH$_3^+$), 1275, 1224 (C-O) cm^{-1}.

^{1}H-NMR (400 MHz, acetone-d$_6$) δ 7.65 (m, 4H, aromatic H), 7.25 (m, 4H, aromatic H), 5.80 (s, 1H, bridgehead H), 3.82 (s, 3H, CO$_2$CH$_3$), 3.80 (s, 3H, CO$_2$CH$_3$) ppm, no N-H signals detectable.

UV (Acetonitrile) λ_{max}: 213 (ε 8,000) nm.

Anal. calculated for C$_{20}$H$_{18}$NO$_4$Cl: C, 64.61; H, 4.87; N, 3.77. Found C, 64.38; H, 5.12; N, 3.99.

R-(-)-10-Camphorsulfonic acid salt of amine 39 (116a)

Salt **116a** was prepared by dissolving a 1:1 mixture of R-(-)-10-camphorsulfonic acid (343 mg, 1.48 mmol, Aldrich) and amine **39** (503 mg, 1.50 mmol) in hot ethyl

acetate (55 mL) and allowing the solution to stand for 2 days. The resulting solid was filtered and dried to afford crystals of salt **116a** (721 mg, 1.27 mmol, 86%). X-ray diffraction analysis[67] of salt **116a** revealed that it crystallizes with inclusion of one equivalent of H_2O.

MP: 183-184°C.

IR (KBr) v_{max}: 3200-2200 (N-H, C-H), 1737 (C=O), 1634 (C=C), 1558 (NH_3^+), 1275 (C-O), 1177, 1043 (S=O).

MS FAB: 568 (M+1).

^{1}H-NMR (400 MHz, $CDCl_3$) δ 8.40 (m, 1H, aromatic H), 8.10 (m, 1H, aromatic H), 7.5-7.0 (m, 6H, aromatic H), 5.60 (s, 1H, bridgehead H), 4.05 (s, 3H, $CO_2\underline{CH_3}$), 3.80 (s, 3H, $CO_2\underline{CH_3}$), 3.35 (m, 1H), 2.50 (m, 1H), 2.35 (m, 1H), 2.10 (m, 1H), 1.8-1.5 (m, 3H), 1.25 (m, 1H), 1.0 (br m, 1H), 0.35 (br s, 3H), 0.10 (br s, 3H) ppm, no O-H or N-H signals detectable.

UV (Acetonitrile) λ_{max}: 215 (ε 20,000) nm.

Anal. calculated for dried powder $C_{30}H_{33}NO_8S$: C, 63.48; H, 5.86; N, 2.47. Found: C, 63.19; H, 6.03; N, 2.39. Anal. calculated for crystals $C_{30}H_{35}NO_9S \cdot H_2O$: C, 61.52; H, 6.02; N, 2.39. Found: C, 61.58; H, 6.06; N, 2.40.

S-(+)-10-Camphorsulfonic acid salt of amine 39 (116b)

Salt **116b** was prepared in 92% yield (407 mg, 0.717 mmol) from S-(+)-10-camphorsulfonic acid (181 mg, 0.780 mmol, Aldrich) and amine **39** (261 mg, 0.779 mmol) exactly as described above. Salts **116a** and **116b** exhibited identical spectroscopic properties.

MP: 183-185°C.

Anal. calculated for dried crystals $C_{30}H_{33}NO_8S$: C, 63.48; H, 5.86; N, 2.47. Found: C, 63.46; H, 6.00; N, 2.29.

(-)-3-Bromocamphor-8-sulfonic acid salt of amine 39 (117)

Salt **117** was prepared by dissolving a mixture of hydrochloride salt **112** (252 mg, 0.678 mmol) and ammonium (-)-3-bromocamphor-8-sulfonate (223 mg, 0.680 mmol, Aldrich) in hot ethanol (50 mL) and allowing the solution to stand at room temperature for 2 days. The resulting solid was filtered and dried to afford crystalline salt **117** (374 mg (0.648 mmol, 81%) which, according to mass spectra and elemental analysis, crystallizes with one equivalent of HCl.

MP: 210-212°C.

IR (KBr) v_{max}: 3200-2200 (N-H, C-H), 1755, 1718 (C=O), 1630 (C=C), 1573 (NH$_3^+$), 1291 (C-O), 1178, 1039 (S=O) cm^{-1}.

MS FAB: 684 (M+1).

^{1}H-NMR (400 MHz, CDCl$_3$) δ 10.6 (br s, 1H, D$_2$O exchangeable), 8.60 (m, 1H, aromatic H), 8.25 (m, 1H, aromatic H), 7.50 (m, 2H, aromatic H), 7.25-7.10 (m, 4H, aromatic H), 5.70 (s, 1H, bridgehead H), 4.10 (m, 1H), 3.95 (s, 3H, CO$_2$CH$_3$), 3.80 (s, 3H, CO$_2$CH$_3$), 2.6-2.5 (m, 3H), 1.85 (br s, 2H, D$_2$O exchangeable, N-H), 1.25 (m, 1H), 0.8 (m, 3H), 0.75 (br s, 3H), 0.70 (br s, 3H) ppm.

UV (Acetonitrile) λ_{max}: 212 (ε 18,000)

Anal. calculated for $C_{30}H_{32}NO_8SBr \cdot HCl$: C, 52.72; H, 4.87; N, 2.05. Found: C, 52.40; H, 4.85; N, 1.94.

3.3 Photochemical studies

3.3.1 General Procedures

All analytical photolyses, both in solution and in the solid state, were carried out using Pyrex (λ>290 nm) or quartz (λ>200 nm) filtered light from a 450W Hanovia medium pressure mercury lamp at room temperature unless otherwise stated. Spectral grade solvents (BDH) were used for solution phase photolyses and the concentration of the sample solution was kept at ca. 0.01 M. The samples were degassed by three freeze-pump-thaw cycles and sealed with paraffin film under a nitrogen atmosphere in each case prior to irradiation. Photolyses in the solid state were conducted either on single crystals in Pyrex or quartz tubes sealed under nitrogen or on powders sandwiched between two Pyrex or quartz glass plates. The photolyzed samples were normally analyzed by GC, GC-MS and ^{1}H-NMR.

For preparative scale photolyses in solution, 50 mg to 500 mg of the appropriate compound was dissolved in spectral grade solvent and put into a preparative photolysis apparatus.[108] Oxygen was purged by passing a steady flow of nitrogen through the solution for 30 min prior to and during irradiation. The light source used was a 450 W Hanovia medium pressure mercury lamp and the desired output wavelength was achieved using a Pyrex glass filter.

Samples were prepared for solid state photolysis by crushing crystals between two Pyrex or quartz glass plates and sliding the top and bottom plates back and forth so as to distribute the crystals over the surface in a thin, even layer. The sample plates were

then taped together at the top and bottom ends, placed in polyethylene bags and thoroughly degassed with nitrogen. The bags were sealed under a positive pressure of nitrogen with a heat-sealing device and irradiated with the output from a 450 W Hanovia medium pressure mercury lamp equipped with Pyrex or quartz glass filters.

Low temperature solid state photolyses were carried out by maintaining the sample in a cooling bath controlled by the Cryocool CC-100-II immersion cooling system from Neslab Instruments Inc. The temperature was kept within ± 2°C and the samples irradiated with a Hanovia medium pressure mercury lamp. The desired output wavelength was achieved using a Pyrex glass filter.

3.3.2 Diazomethane Workup

After irradiation of dibenzobarrelene acid derivatives **36**, **37**, **38** and **40**, the reaction mixtures were treated with an ethereal solution of diazomethane to esterify the starting materials as well as the photoproducts. The resulting solutions were left in the fume hood until the yellow diazomethane color had disappeared. At that time the methyl ester of dibenzobarrelene derivatives had undergone further derivatization to form pyrazoline cycloaddition products with diazomethane, while the corresponding methyl esters of the dibenzosemibullvalene photoproducts did not react further.[57, 109] This simplified the chromatographic separation of the starting materials and the photoproducts, because the pyrazoline derivatives were found to elute much faster from silica gel than the dibenzosemibullvalene compounds.

The disadvantage of this method is that the dibenzocyclooctatetraenes formed from unsensitized irradiation of acid **38** undergo cycloaddition with diazomethane and can not be separated from the derivatized starting material.

172

3.3.3 Photolyses of Starting Materials

Photolysis of Ethyl 9,10-Dihydro-9,10-ethenoanthracene-11-carboxylate-12-carboxylic acid (36)

A solution of acid **36** (80.6 mg, 0.252 mmol) in anhydrous benzene (50 mL) was photolyzed through a Pyrex filter for 12 h. The solvent was removed under vacuum and the remaining oil was treated with ethereal diazomethane. GC (DB-17) showed formation of photoproduct **32a** with no remaining starting material. The solvent was removed under vacuum and the residue purified on silica gel eluted with 10% ethyl acetate in petroleum ether. The resulting oil was recrystallized twice from ethanol-petroleum ether to give photoproduct **32a** (60.4 mg, 0.183 mmol, 73%).

Compound **32a** was characterized as 4b,8b,8c,8d-tetrahydro-dibenzo[a,f]cyclopropa[c,d]pentalene-8b,8c-dicarboxylic acid, 8b-ethyl 8c-methyl ester. The ^{1}H-NMR spectrum is identical to that reported by Garcia-Garibay.[57]

MP: 86-88°C.

IR (KBr) v_{max}: 1733, 1717 (C=O), 1246 (C-O) cm^{-1}.

MS m/e (relative intensity): 334 (M$^+$, 47), 274 (100), 261 (94), 202 (42).

Exact mass calculated for $C_{21}H_{18}O_4$: 334.1205. Found: 334.1204.

^{1}H-NMR (400 MHz, CDCl$_3$) δ 7.4-7.0 (m, 8H, aromatic H), 5.06 (s, 1H, benzylic H), 4.69 (s, 1H, cyclopropyl H), 4.18 (q, 2H, J=7 Hz, CO$_2$CH$_2$CH$_3$), 3.87 (s, 3H, CO$_2$CH$_3$), 1.26 (t, 3H, J=7 Hz, CO$_2$CH$_2$CH$_3$) ppm.

^{13}C-NMR (50 MHz, CDCl$_3$) δ 169.0, 168.6 (C=O), 150.04, 149.96, 134.89, 133.6 (aromatic C), 127.9, 127.8, 127.6, 126.9, 125.9, 125.8, 125.5, 121.4 (aromatic C-H),

67.4 (cyclopropyl), 61.3 (CO$_2$CH$_2$CH$_3$), 57.5 (cyclopropyl C), 55.7 (benzylic C-H), 52.7 (CO$_2$CH$_3$), 49.2 (cyclopropyl C-H), 14.2 (CO$_2$CH$_2$CH$_3$) ppm.

Crystals of acid **36** (252 mg, 0.788 mmol) were crushed between four microscopic plates and irradiated through a Pyrex filter for 36 h. The crystals, which had turned brown and sticky, were dissolved in diethyl ether and treated with excess diazomethane. CG (DB-17) indicated 20% conversion with formation of photoproducts **32a** and **33a** in the ratio 1:9. The solvent was removed under vacuum and the residue chromatographed on silica gel eluted with 20% ethyl acetate in petroleum ether to yield compounds **32a** and **33a** (52.4 mg, 0.157 mmol, 20%) in the ratio 1:9. No product separation could be achieved and compound **33a** was therefore analyzed in the mixture.

Photoproduct **33a** was characterized as 4b,8b,8c,8d-tetrahydro-dibenzo[a,f]cyclopropa[c,d]pentalene-8b,8c-dicarboxylic acid, 8b-methyl 8c-ethyl ester. The ^{1}H-NMR spectrum is identical to that reported by Garcia-Garibay.[57]

IR of mixture (CDCl$_3$) v_{max}: 1733 (C=O), 1247 (C-O) cm^{-1}.

MS m/e (relative intensity): 334 (M+, 30), 275 (24), 260 (43), 233 (21), 202 (69), 155 (35), 100 (20), 91 (100).

Exact mass calculated for C$_{21}$H$_{18}$O$_4$: 334.1205. Found: 334.1197.

^{1}H-NMR (400 MHz, CDCl$_3$) δ 7.4-7.0 (m, 8H, aromatic H), 5.05 (s, 1H, benzylic H), 4.67 (s, 1H, cyclopropyl H), 4.35 (q, 2H, J=7 Hz, CO$_2$CH$_2$CH$_3$), 3.73 (s, 3H, CO$_2$CH$_3$), 1.34 (t, 3H, J=7 Hz, CO$_2$CH$_2$CH$_3$) ppm.

^{13}C-NMR (50 MHz, CDCl$_3$) δ 169.4, 168.0 (C=O), 150.0, 149.9, 134.8, 133.6 (aromatic C), 127.9, 127.8, 127.6, 126.9, 125.9, 125.8, 125.5, 121.3 (aromatic C-H), 65.6 (cyclopropyl C), 61.8 (CO$_2$CH$_2$CH$_3$), 57.6 (cyclopropyl C), 55.8 (benzylic C-H), 52.2 (CO$_2$CH$_3$), 49.2 (cyclopropyl C-H), 14.3 (CO$_2$CH$_2$CH$_3$) ppm.

The regioselectivity of the di-π-methane rearrangement of acid **36** was studied in different solvents. Samples of acid **36** were irradiated through a Pyrex filter and afterwards the solvent was removed under vacuum. The residue was treated with ethereal diazomethane and analyzed by GC (DB-17). The results are listed in Table 3-9.

Table 3-9   Medium Dependent Photochemistry of Ester-Acid 36

Solvent	Concentration (M)	Photoproduct ratio[a] 32a:33a
Benzene	0.052	100:0
"	0.010	100:0
"	0.00054	100:0
Acetone	0.0095	60:40
Acetonitrile	0.012	57:43
DMSO	0.0091	41:59
Methanol	0.0090	46:59
NaHCO₃ (aq)	0.0083	100:0
Crystals[b]		0:100

[a] The estimated error in the GC analyses is ±5%.   [b] Conversion was kept below 10%.

Photolysis of Methyl 12-Methyl-9,10-dihydro-9,10-ethenoanthracene-11-carboxylate (41)

A solution of ester **41** (237 mg, 8.59 mmol) in acetone (350 mL) was purged with nitrogen for 25 min and then irradiated for 1.5 h through a Pyrex filter. GC (DB-17) indicated formation of photoproduct **52** with little remaining starting material. The

solvent was removed under vacuum and the residue chromatographed on a silica gel column eluted with 20% ethyl acetate in petroleum ether. The resulting oil was recrystallized from ethanol to yield crystals of photoproduct **52** (187 mg, 6.83 mmol, 80%).

Compound **52** was characterized as methyl 8b-methyl-4b,8b,8c,8d-tetrahydro-dibenzo[a,f]cyclopropa[c,d]pentalene-8c-carboxylate.

MP: 92-94°C.

IR (KBr) v_{max}: 1713 (C=O), 1231 (C-O) cm^{-1}.

MS m/e (relative intensity): 276 (M$^+$, 32), 217 (100), 202 (69).

Exact mas calculated for $C_{19}H_{16}O_2$: 276.1151. Found: 276.1150.

^{1}H-NMR (400 MHz, CDCl$_3$) δ 7.3-6.9 (m, 8H, aromatic H), 5.00 (s, 1H, benzylic H), 3.72 (s, 3H, CO$_2$CH$_3$), 3.62 (s, 1H, cyclopropyl H), 1.90 (s, 3H, cyclopropyl CH$_3$) ppm.

^{13}C-NMR (50 MHz, CDCl$_3$) δ 171.3 (C=O), 150.0, 149.1, 139.0, 136.8 (aromatic C), 127.2, 126.8, 126.7, 126.5 124.7, 123.9, 121.2, 121.1 (aromatic C-H), 66.6 (cyclopropyl C), 54.9 (cyclopropyl or benzylic C-H), 53.7 (cyclopropyl C), 51.8, 51.6 (cyclopropyl or benzylic C-H and CO$_2$CH$_3$), 16.3 (cyclopropyl CH$_3$) ppm.

Anal. calculated for $C_{19}H_{16}O_2$: C, 82.58; H, 5.84. Found: C, 82.58; H, 5.90.

Irradiation of ester **41** in anhydrous CH$_2$Cl$_2$ through a Pyrex filter gave **52** as the only observed photoproduct.

Photolyses of ester **41** in the solid state were performed on both the low melting crystals, crystallized from ethanol, and the high melting crystals from the melt. The reaction was found to be very slow when a Pyrex filter was used, so a quartz filter was substituted. After 18 h of irradiation, GC (DB-17) showed 30% conversion for the high melting crystals and 9% for the low melting crystals. The only photoproduct observed in both cases was compound **52**.

Photolysis of 12-Methyl-9,10-dihydro-9,10-ethenoanthracene-11-carboxylic acid (37)

Analytical solution photolyses of acid **37** were carried out in acetone and chloroform. The solutions were irradiated through a Pyrex filter. The solvents were removed under vacuum, the residues were dissolved in diethyl ether and treated with one equivalent of diazomethane. GC (DB-17) analyses of these solutions showed that compound **52** was the only photoproduct formed.

Crystals of acid **37** were photolyzed through a Pyrex filter for 20 h. The photolyzed crystals were dissolved in diethyl ether and one equivalent of diazomethane was added. GC (DB-17) indicated 11% conversion to form photoproduct **52**.

Photolysis of Dimethyl 9-Amino-9,10-dihydro-9,10-ethenoanthracene-11,12-dicarboxylate (39)

A solution of amine **39** (214 mg, 0.639 mmol) in acetone (300 mL) was purged with nitrogen for 30 min and irradiated. After 2 h, GC (DB-17) indicated the formation of photoproducts **60** and **61** in a 3:7 ratio with little starting material remaining. Removal of the solvent under vacuum afforded an oil which was crystallized from diethyl ether to afford photoproduct **61** (60 mg, 33%).

The mother liquor from above was chromatographed on silica gel with ethanol-petroleum ether (10:90) as the eluting solvent. The first band contained photoproduct **60** (45 mg, 21%) which was recrystallized from ethanol to give colorless crystals.

The second chromatographic fraction contained a mixture of compounds **61** and **62** (85 mg, 40%). Rechromatography of this mixture afforded the rearranged product **62e** (50 mg, 23%).

Photoproduct **60** was characterized as dimethyl 4b-amino-4b,8b,8c,8d-tetrahydro-dibenzo[a,f]cyclopropa[c,d]pentalene-8b,8c-dicarboxylate.

MP: 131-132°C.

IR (KBr) v_{max}: 3397, 3327 (N-H), 1731, 1714 (C=O), 1237, 1208 (C-O) cm^{-1}.

MS m/e (relative intensity): 335 (M+, 6), 276 (100), 244 (54), 216 (95), 193 (43), 189 (37).

Exact mass calculated for $C_{20}H_{17}NO_4$: 335.1158. Found: 335.1162.

^{1}H-NMR (400 MHz, CDCl$_3$) δ 7.55-7.05 (m, 8H, aromatic H), 4.40 (s, 1H, cyclopropyl H), 3.83 (s, 3H, CO$_2$CH$_3$), 1.70 (s, 2H, D$_2$O exchangeable, NH$_2$) ppm.

^{13}C-NMR (100 MHz, CDCl$_3$) δ 168.8, 167.5 (C=O), 152.0, 151.6, 132.8, 160.6 (aromatic C), 127.81, 127.77, 127.73, 127.65, 126.2, 125.3, 119.91, 119.88 (aromatic C-H), 76.9, 73.5, 54.2 (benzylic C and cyclopropyl C), 52.5, 52.1 (CO$_2$CH$_3$), 49.3 (cyclopropyl C-H) ppm.

Anal. calculated for $C_{20}H_{17}NO_4$: C, 71.63; H, 5.11; N, 4.17. Found: C, 71.55; H, 5.17; N, 4.19.

Photoproduct **61** was characterized as dimethyl 8d-amino-4b,8b,8c,8d-tetrahydro-dibenzo[a,f]cyclopropa[c,d]pentalene-8b,8c-dicarboxylate.

MP: 138-141°C.

IR (KBr) v_{max}: 3263 (N-H), 1730, 1713 (C=O), 1274, 1216 (C-O) cm^{-1}.

MS m/e (relative intensity): 335 (M+, 27), 276 (100), 244 (83), 216 (92), 189 (31).

Exact mass calculated for $C_{20}H_{17}NO_4$: 335.1158. Found: 335.1153.

^{1}H-NMR (400 MHz, CDCl$_3$) δ 7.8-7.1 (m, 8H, aromatic H), 5.45 (s, 1H, benzylic H), 3.75 (s, 6H, CO$_2$CH$_3$), 1.60 (s, 2H, D$_2$O exchangeable, NH$_2$) ppm.

^{13}C-NMR (50 MHz, CDCl$_3$) δ 179.3, 172.5 (C=O), 169.9, 151.3, 143.2 (aromatic C), 133.4, 128.9, 128.1, 127.8, 125.1, 124.92, 124.85, 123.3 (aromatic C-H), 69.8, 65.8 (cyclopropyl C), 55.6 (benzylic C-H), 53.0, 52.4 (CO$_2$CH$_3$) ppm.

Anal. calculated for $C_{20}H_{17}NO_4$: C, 71.63; H, 5.11; N, 4.17. Found: C, 71.44; H, 5.21;
N, 4.14.

Compound **62** was characterized as dimethyl 4b,10-dihydro-10-oxo-ideno[1,2-a]indene-
9,9a(9H)-dicarboxylate. All the spectra are identical to those reported by Richards et al.[64]
MP: 177-179 (lit.[64] 185°C).

IR (KBr) v_{max}: 1739, 1722 (C=O), 1240 (C-O) cm^{-1}.

MS m/e (relative intensity): 336 (M$^+$, 7), 304 (48), 276 (86), 249 (30), 234 (23), 217
(100), 189 (80).

Exact mass calculated for $C_{20}H_{16}O_5$: 336.0998. Found: 336.0990.

^{1}H-NMR (400 MHz, CDCl$_3$) δ 7.9-7.8 (m, 1H, aromatic H), 7.7-7.6 (m, 2H, aromatic
H), 7.4-7.1 (m, 5H, aromatic H), 5.64 (s, 1H, benzylic H), 4.81 (s, 1H), 3.71 (s, 3H,
CO$_2$CH$_3$), 3.70 (s, 3H, CO$_2$CH$_3$) ppm.

^{13}C-NMR (75 MHz, CDCl$_3$) δ 199.1, 172.3, 167.64 (C=O), 156.9, 143.0, 137.5
(aromatic C), 136.3 (aromatic C-H), 133.2 (aromatic C), 128.9, 128.4, 128., 125.5,
125.4, 125.3, 125.0 (aromatic C-H), 72.7 (tertiary C), 54.8, 53.9, 53.1, 52.5 (CO$_2$CH$_3$
and benzylic C-H) ppm.

Crystals of amine **39** were crushed between glass plates and photolyzed through a
Pyrex filter. The reaction was found to be very slow when Pyrex plates were used, so
quartz plates were used instead. After 24 h of irradiation, GC (DB-17) showed 20%
conversion and a 60:61 ratio of 14:86; no rearrangement product **62** could be detected.

Photolysis of Trimethyl 9,10-dihydro-9,10-ethenoanthracene-9,11,12-tricarboxylate (43)

A solution of ester **43** (120 mg, 0.317 mmol) in acetone (250 mL) was purged with nitrogen for 30 min and irradiated through a Pyrex filter for 0.5 h. GC (DB-17) indicated the formation of photoproduct **67** with little starting material remaining. The solvent was removed under vacuum and the residue was chromatographed on silica gel eluted with 20% ethyl acetate in petroleum ether. The resulting oil was crystallized from ethanol to yield photoproduct **67** (94.4 mg, 80%).

Compound **67** was characterized as trimethyl 4b,8b,8c,8d-tetrahydro-dibenzo[a,f]cyclopropa[c,d]pentalene-4b,8b,8c-tricarboxylate.

MP: 126-127°C

IR (KBr) v_{max}: 1743 with a shoulder at 1730 (C=O), 1274 (C-O) cm^{-1}.

MS m/e (relative intensity): 378 (M+, 51), 319 (74), 291 (100), 232 (35), 216 (27), 193 (56).

Exact mass calculated for $C_{22}H_{18}O_6$: 378.1103. Found: 378.1100.

^{1}H-NMR (400 MHz, CDCl$_3$) δ 7.5-7.0 (m, 8H, aromatic H), 4.48 (s, 1H cyclopropyl H), 3.88 (s, 6H CO$_2$CH$_3$), 3.70 (s, 3H, CO$_2$CH$_3$) ppm.

^{13}C-NMR (50 MHz, CDCl$_3$) δ 169.2, 168.2, 167.1 (C=O), 144.1, 148.3, 134.0, 132.2 (aromatic C), 128.1, 128.0, 127.74, 127.66, 126.5, 125.7, 121.7, 121.2 (aromatic C-H), 69.9, 69.6, 54.9 (cyclopropyl and benzylic C), 52.8, 52.6, 52.5 (CO$_2$CH$_3$), 49.1 (cyclopropyl C-H) ppm.

Anal. calculated for $C_{22}H_{18}O_6$: C, 69.83; H, 4.80. Found: C, 69.77; H, 4.86.

A solution of ester **43** (360 mg, 0.953 mmol) in anhydrous CHCl$_3$ (250 mL) was degassed for 0.5 h and irradiated for 0.5 h. GC (DB-17) indicated 63% conversion to

photoproducts **67** and **71** in the ratio 70:30 respectively. The solvent was removed under vacuum and the residue chromatographed on silica gel eluted with 20% ethyl acetate in petroleum ether. Two fractions were collected: The first one contained a 1:1 mixture of the starting material and photoproduct **67** (223 mg, 62%). The second fraction contained a mixture of compounds **43:67:71** (120 mg, 33%) in the ratio 38:42:21. Compound **71** was found to be somewhat unstable on silica gel, but after the second fraction had been rechromatographed several times, compound **71** (9.3 mg, 3%) was isolated as an oil.

Photoproduct **71** was characterized as trimethyl dibenzo[a,e]cyclooctene-5,6,11-tricarboxylate.

IR (CHCl$_3$) v_{max}: 1722 (C=O), 1634 (C=C), 1250 (C-O) cm^{-1}.

MS m/e (relative intensity): 378 (M+, 10), 318 (100), 287 (83), 201 (90).

Exact mas calculated for C$_{22}$H$_{18}$O$_6$: 378.1103. Found: 378.1103.

^{1}H-NMR (400 MHz, CDCl$_3$) δ 8.08 (s, 1H, vinyl H), 7.4-7.1 (m, 8H, aromatic H), 3.82 (s, 3H, CO$_2$CH$_3$), 3.75 (s, 6H, CO$_2$CH$_3$) ppm.

Photolyses of ester **43** in solutions were repeated and analyzed on a different GC column, DB-1, which revealed formation of an additional minor photoproduct. This photoproduct was later characterized as compound **68**. Photoproducts **67** and **68** were found to have the same retention time on GC column DB-17, while they were well separated on a column of the DB-1 type. GC (DB-1) analyses of photolyses of ester **43** in acetone indicated formation of photoproducts **67** and **68** in the ratio 91:9, while irradiation of ester **43** in chloroform showed formation of photoproducts **67:68:71** in the ratio 60:6:34.

Crystals of ester **43** (227 mg, 0.601 mmol) were crushed between four Pyrex plates and irradiated for 48 h. The photolyzed solid was recrystallized from ethanol to

yield unreacted starting material (150 mg, 66%). The mother liquor was chromatographed on silica gel eluted with 20% ethyl acetate in petroleum ether. The first band contained the starting material (24 mg, 11%). The second band contained a mixture of the starting material and three photoproducts (52.4 mg, 23%) in the ratio 28:72. The three photoproducts were compounds **67:68:71**, which were formed in the ratio 36:38:26 as determined by ^{1}H-NMR.

Photolysis of Dimethyl 9-Carboxy-9,10-dihydro-9,10-ethenoanthracene-11,12-dicarboxylate (38)

Acid **38** (49.8 mg, 0.137 mmol) was dissolved in acetone (15 mL) and irradiated for 2 h. The solvent was removed under vacuum and the resulting oil was dissolved in diethyl ether and treated with excess diazomethane. GC (DB-17) indicated 80% conversion to photoproduct **67**. The solvent was removed under vacuum and the residue chromatographed on silica gel with 20% ethyl acetate in petroleum ether as the eluting solvent. The resulting oil (41.6 mg, 0.1101 mmol, 80%) was analyzed by ^{1}H-NMR, which showed the only photoproduct formed was compound **67**.

Crystals of acid **38** (514 mg, 1.412 mmol) which had been recrystallized from acetonitrile were crushed between two quartz plates and photolyzed for 4 days. The solid was dissolved in diethyl ether and treated with excess diazomethane. CG (DB-1) indicated 10% conversion to form photoproducts **67** and **68** in the ratio 1:9 respectively. The solvent was removed under vacuum and the residue chromatographed on silica gel eluted with 15% ethyl acetate in petroleum ether. The resulting oil (33.8 mg, 0.0904 mmol, 7%) was recrystallized from ethanol to yield crystals of photoproduct **68** (28.6 mg, 5%).

Compound **68** was characterized as trimethyl 4b,8b,8c,8d-tetrahydro-dibenzo[a,f]cyclopropa[c,d]pentalene-8b,8c,8d-tricarboxylate.

MP: 184-186°C.

IR (KBr) v_{max}: 1737 (C=O), 1229 (C-O) cm^{-1}.

MS m/e (relative intensity): 378 (M+, 6), 350 (4), 318 (10), 260 (23), 202 (47), 57 (100).

Exact mass calculated for $C_{22}H_{18}O_6$: 378.1103. Found: 378.1106.

^{1}H-NMR (400 MHz, CDCl$_3$) δ 7.45 (m, 2H, aromatic H), 7.2-7.1 (m, 6H, aromatic H), 5.07 (s, 1H, benzylic H), 3.92 (s, 6H, CO$_2$CH$_3$), 3.78 (s, 3H, CO$_2$CH$_3$) ppm.

^{13}C-NMR (100 MHz, CDCl$_3$) δ 167.4, 167.2 (C=O), 150.2, 132.8 (aromatic C), 128.4, 127.0, 126.6, 121.2 (aromatic C-H), 67.5, 58.6 (cyclopropyl C), 58.0 (benzylic C-H), 52.8, 52.6 (CO$_2$CH$_3$) ppm.

Anal. calculated for $C_{22}H_{18}O_6$: C, 69.83; H, 4.80. Found: C, 69.92, H, 4.80.

Crystals of acid **38** crystallized from ethyl acetate were photostable and did not react when irradiated through a quartz filter.

Crystals of acid **38** (95.1 mg, 0.26 mmol) which had been recrystallized from ethanol were crushed between two Pyrex plates and irradiated for 25 h. Afterwards the solid was dissolved in diethyl ether and excess diazomethane was added. The solvent was removed under vacuum and the residue chromatographed on silica gel eluted with 40% ethyl acetate in petroleum ether, yielding photoproducts **67** and **68** (4.0 mg, 0.0106 mmol, 4%). ^{1}H-NMR revealed that compounds **67** and **68** were formed in the ratio 40:60.

Photolysis of Dimethyl 9-Carboxyethyl-9,10-dihydro-9,10-ethenoanthracene-11,12-dicarboxylate (44)

A solution of ester **44** (384 mg, 0.797 mmol) in acetone (350 mL) was purged with nitrogen for 20 min and irradiated for 0.5 h. GC (DB-17) indicated formation of photoproducts **69** and **70** in the ratio 93:7 respectively with little remaining starting material. The solvent was removed under vacuum and the residue chromatographed on silica gel eluted with 15% ethyl acetate in petroleum ether. The first band contained compound **69** (86 mg, 22%), which was recrystallized from ethanol to give colorless prisms. The second fraction contained a mixture of photoproducts **69** and **70** (201.5 mg, 54%).

Compound **69** was characterized as 4b,8b,8c,8d-tetrahydro-dibenzo-[a,f]cyclopropa[c,d]pentalene-4b,8b,8c-tricarboxylic acid, 4b-ethyl-8b-methyl-8c-methyl ester.

MP: 134-135°C.

IR (KBr) v_{max}: 1746, 1723, 1718 (C=O), 1298, 1274, 1184 (C-O) cm^{-1}.

MS m/e (relative intensity): 392 (M+, 100), 365 (10), 319 (36), 291 (22), 260 (38).

Exact mass calculated for $C_{23}H_{20}O_6$: 392.1260. Found: 392.1257.

^{1}H-NMR (400 MHz, CDCl$_3$) δ 7.5-7.1 (m, 8H, aromatic H), 4.48 (s, 1H, cyclopropyl H), 4.36 (q, 2H, J=7 Hz, CO$_2$CH$_2$CH$_3$), 3.88 (s, 3H, CO$_2$CH$_3$), 3.70 (s, 3H, CO$_2$CH$_3$), 1.32 (t, 3H, J=7 Hz, CO$_2$CH$_2$CH$_3$) ppm.

^{13}C-NMR (75 MHz, CDCl$_3$) δ 168.7, 168.4, 167.0 (C=O), 149.4, 148.3, 134.1, 132.0 (aromatic C), 128.0, 128.0, 127.68, 127.60 126.63 125.7, 121.8, 121.0 (aromatic C-H), 70.0, 69.5 (benzylic C and cyclopropyl C), 61.7 (CO$_2$CH$_2$CH$_3$), 54.4 (cyclopropyl C), 52.8, 52.3 (CO$_2$CH$_3$), 49.2 (cyclopropyl C-H), 14.2 (CO$_2$CH$_2$CH$_3$) ppm.

Anal. calculated for $C_{23}H_{20}O_6$: C, 70.40; H, 5.14. Found: C, 70.34; H, 5.16.

A solution of ester **44** (330 mg, 0.843 mmol) in chloroform (350 mL) was purged with nitrogen for 20 min and irradiated for 4 h. GC (DB-1) showed 80% conversion and formation of photoproducts **69** and **70** plus an additional peak in the ratio 35:9:56, respectively. The solvent was removed under vacuum and the resulting oil chromatographed on silica gel eluted with 15% ethyl acetate in petroleum ether. The first fraction contained the starting material (17 mg, 5%). The second band consisted of a mixture of the starting material and photoproducts **69** and **70** (118 mg, 36%). The third fraction contained a colorless oil (105 mg, 32%), which showed up as a single peak on the GC (DB-17). This oil was crystallized from ethanol to yield colorless prisms, which were characterized as photoproduct **72** (19 mg, 6%). The mother liquor was crystallized to give a compound (41.2 mg, 12%) with the same retention time on the GC (DB-17) as compound **72** but which was characterized as photoproduct **73**. ¹H-NMR revealed that the remaining mother liquor was a mixture of compounds **72** and **73** in the ratio 40:60. The structures of photoproducts **72** and **73** were further supported by X-ray analyses of crystals of both compounds.[67,69]

Photoproduct **72** was characterized as dibenzo[a,e]cyclooctene-5,6,12-tricarboxylic acid, 5-ethyl 6-methyl 12-methyl ester.

MP: 174-175°C.

IR (KBr) v_{max}: 1731, 1714 (C=O), 1638 (C=C), 1284, 1225, 1208 (C-O) cm⁻¹.

MS m/e (relative intensity): 392 (M⁺, 5), 364 (20), 287 (46), 260 (50), 229 (87), 201 (100).

Exact mass calculated for $C_{23}H_{20}O_6$: 392.1260. Found: 392.1262.

¹H-NMR (400 MHz, CDCl₃) δ 8.08 (s, 1H, vinyl H), 7.4-7.1 (m, 8H, aromatic H), 4.23 (q, 2H, J=7 Hz, CO₂CH₂CH₃), 3.82 (s, 3H, CO₂CH₃), 3.76 (s, 3H, CO₂CH₃), 1.25 (t, 3H, J=7 Hz, CO₂CH₂CH₃) ppm.

^{13}C-NMR (100 MHz, CDCl$_3$) δ 166.9, 166.8 (C=O), 141.8 (vinyl C-H), 140.2, 137.9, 136.0, 135.3, 134.5, 134.22, 133.5 (aromatic C), 129.4, 128.5, 128.2, 127.9, 127.8, 127.6, 127.5 127.2 (aromatic C-H), 61.7 (CO$_2$CH$_2$CH$_3$), 52.6, 52.4 (CO$_2$CH$_3$), 13.9 (CO$_2$CH$_2$CH$_3$) ppm.

Photoproduct 73 was characterized as dibenzo[a,e]cyclooctene-5,11,12-tricarboxylic acid, 5-ethyl 11-methyl 12-methyl ester.

MP: 123-125°C.

IR (KBr) ν$_{max}$: 1733, 1718 (C=O), 1635 (C=C), 1266, 1240, 1196 (C-O) cm^{-1}.

MS m/e (relative intensity): 392 (M$^+$, 5), 364 (23), 318 (28), 287 (44), 260 (54), 229 (78), 201 (100).

Exact mass calculated for C$_{23}$H$_{20}$O$_6$: 392.1260. Found: 392.1259.

^{1}H-NMR (400 MHz, CDCl$_3$) δ 8.09 (s, 1H, vinyl H), 7.4-7.1 (m, 4H, aromatic H), 4.23 (q, 2H, J=7 Hz, CO$_2$CH$_2$CH$_3$), 3.83 (s, 3H, CO$_2$CH$_3$), 3.76 (s, 3H, CO$_2$CH$_3$) 1.25 (t, 3H, J=7 Hz, CO$_2$CH$_2$CH$_3$) ppm.

^{13}C-NMR (100 MHz, CDCl$_3$) δ 167.0, 166.6, 166.5 (C=O), 141.9 (vinyl C-H), 139.0, 135.9, 135.3 134.4, 134.3, 133.5 (aromatic C and vinyl C), 129.4, 129.3, 128.29, 128.1, 127.8, 127.6, 127.5, 127.2 (aromatic C-H), 61.7 (CO$_2$CH$_2$CH$_3$), 52.5, 52.3 (CO$_2$CH$_3$), 13.9 (CO$_2$CH$_2$CH$_3$) ppm.

Crystals of the prism form of ester 46 (465 mg, 1.18 mmol) were crushed between 6 quartz plates and irradiated for 4 days. GC (DB-17) showed 18% conversion to photoproducts 69:70:(72+73) in the ratio 29:32:39. Compounds 72 and 73 were formed in the ratio 22:77 as determined by ^{1}H-NMR. The photolyzed crystals were recrystallized from ethanol to yield the starting material (238 mg, 58%). The mother liquor was chromatographed on silica gel eluted with 20% ethyl acetate in petroleum ether. The first band contained (40.2 mg, 7%) of the starting material. The second one

contained a mixture of the photoproducts and the starting material (58.6 mg, 13%), which was recrystallized from ethanol to yield crystals of compounds 43 and 69. The mother liquor, which contained 60% of photoproduct 70, was treated with excess diazomethane and rechromatographed to yield 80% pure compound 70 (16 mg, 4%). This compound was further purified by recrystallization from ethanol, yielding crystals of pure compound 70 (12 mg, 3%).

Photoproduct 70 was characterized as 4b,8b,8c,8d-tetrahydro-dibenzo-[a,f]cyclopropa[c,d]pentalene-8b,8c,8d-tricarboxylic acid, 8b-methyl 8c-methyl 8d-ethyl ester.

MP: 120-126°C.

IR (KBr) v_{max}: 1745, 1731, 1714 (C=O), 1277, 1224, 1200 (C-O) cm^{-1}.

MS m/e (relative intensity): 392 (M+, 12), 364 (3), 332 (12), 318 (12), 291 (12), 260 (19), 217 (19), 201 (20), 149 (100).

Exact mass calculated for $C_{23}H_{20}O_6$: 392.1260. Found: 392.1256.

^{1}H-NMR (400 MHz, CDCl$_3$) δ 7.5 (m, 2H, aromatic H), 7.2-7.1 (m, 6H, aromatic H), 5.06 (s, 1H, benzyl H), 4.47 (q, 2H, J=7 Hz, CO$_2$CH$_2$CH$_3$), 3.91 (s, 3H, CO$_2$CH$_3$), 3.88 (s, 3H, CO$_2$CH$_3$), 1.44 (t, 2H, J=7 Hz, CO$_2$CH$_2$CH$_3$) ppm.

^{13}C-NMR (100 MHz, CDCl$_3$) δ 167.5, 167.2, 166.7 (C=O), 150.3, 150.2, 133.0, 133.0 (aromatic C), 128.5, 128.4, 127.7, 127.6, 127.1, 127.0, 121.2, 121.0 (aromatic C-H), 67.6 (cyclopropyl C), 62.0 (CO$_2$CH$_2$CH$_3$), 62.0, 61.7 (cyclopropyl C), 58.1 (benzyl C-H), 52.8, 52.5 (CO$_2$CH$_3$), 14.0(CO$_2$CH$_2$CH$_3$) ppm.

Anal. calculated for $C_{23}H_{20}O_6$: C,70.40; H, 5.14. Found: C, 70.60; H, 5.05.

Needle-like crystals of ester 44 (57.0 mg, 0.145 mmol) were crushed between two quartz plates and irradiated for 8 h. GC (DB-1) indicated 30% conversion and formation

of photoproducts **69:70:(72+73)** in the ratio 26:42:32. GC analysis on DB-1 showed that photoproducts **72** and **73** were formed in the ratio 33:66 respectively.

3.3.4 Photolyses of Salts

3.3.4.1 Photolyses of Salts Formed with Ethyl 9,10-Dihydro-9,10-ethenoanthracene-11-carboxylate-12-carboxylic Acid (36)

Photolysis of Salts 85 to 89

Salts **85** to **89** were photolyzed through a Pyrex filter in solution and in the solid state. After photolysis the solvent was removed under vacuum and the residue dissolved in diethyl ether. The resulting solution was washed thoroughly with 15% aqueous HCl, dried over $MgSO_4$, treated with ethereal diazomethane to produce the corresponding methyl esters and analyzed by GC (DB-17) to determine product ratios and the extent of conversion. The results are listed in Table 3-10.

Table 3-10   Photoproduct Mixture Composition of Salts **85** to **89** as a Function of the

Photolysis Medium

Salt of acid **36** with:	Medium	Concentration (M)	Photoproduct ratio **32a:33a**[a]
Sodium (**85**)	Crystals		100:0
	H_2O	0.0063	100:0
Calcium (**86**)	Crystals		100:0
	Acetone	0.020	100:0
	Benzene	0.020	100:0
	Methanol	0.022	100:0
Diethylamine (**87**)	Crystals		100:0
	Acetone	0.013	75:25
	Benzene	0.011	100:0
	Methanol	0.013	100:0
Pyrrolidine (**88**)	Crystals		100:0
	Acetone	0.011	68:32
	Benzene	0.0093	100:0
	Methanol	0.0098	100:0
Piperidine (**89**)	Crystals		100:0
	Acetone	0.0076	70:30
	Benzene	0.013	100:0
	Methanol	0.010	100:0

[a] As determined by GC after correction for unreacted starting material. The estimated error in the GC analyses is ±5%.

189

Photolyses of S-(-)-Proline Salt 90a

S-(-)-Proline salt **90a** (116 mg, 0.267 mmol) was irradiated for 12 h at room temperature as a powder sandwiched between two Pyrex microscopic slides. The reaction mixture was dissolved in diethyl ether and extracted three times with 15% aqueous HCl and twice with saturated aqueous NaCl solution. The organic layer was dried over MgSO$_4$ and treated with excess diazomethane to produce the corresponding methyl esters. The solvent was removed under vacuum and the residue subjected to silica gel column chromatography eluted with 15% ethyl acetate in petroleum ether. This afforded the known photoproducts **32a** and **33a** (7.2 mg, 0.0216 mmol, 8%) as a mixture. The regioisomeric and enantiomeric compositions were determined by 400 MHz ^{1}H-NMR. For enantiomeric excess determination, use was made of the chiral shift reagent (+)-Eu(hfc)$_3$ (Aldrich). The signals monitored were the methyl singlets at $\delta = 3.9$ ppm and $\delta = 3.7$ ppm for compounds **32a** and **33a** respectively. The NMR revealed that compound **32a** was formed in 83% yield and 42% enantiomeric excess, whereas compound **33a** was formed in 17% yield with no observed enantiomeric excess. In addition, the sign of rotation of the predominant enantiomer was measured by polarimeter and found to be positive.

The solid state photolyses of S-(-)-proline salt **90a** were repeated as described above but at varying temperatures. The conversion was kept below 20% to minimize melting and each experiment was repeated at least once. The results are listed in Table 3-11.

Table 3-11   Solid State Photoproduct Mixture Composition for S-(-)-Proline Salt 90a

as a Function of Temperature

Temperature	Photoproduct 32a		Photoproduct 33a	
	Yield[a] (%)	ee[b]	Yield[a] (%)	ee[b]
20°C	83	(+)-42	17	nil
0°C	90	(+)-55	10	nil
-25°C	90	(+)-66	10	nil
-40°C	94	(+)-76	4	nil

[a] As determined by NMR after correction for unreacted starting material; [b] The estimated accuracy in these values is ±5%; the sign of rotation of the predominant enantiomer is shown in parentheses.

S-(-)-Proline salt 90a (69.8 mg, 0.160 mmol) was dissolved in ethanol (250 mL) and nitrogen was bubbled through the solution for 25 min. The resulting solution was irradiated for 4 h. The photoproducts were isolated following the same procedure used for isolating the photoproducts in the solid state photolysis of S-(-)-proline salt 90a. This yielded a mixture containing photoproducts 32a and 33a (15.4 mg, 0.047 mmol, 30%) in the ratio 47:53 respectively with no enantiomeric excess as determined by ^{1}H-NMR.

Photolysis of Salts 90b to 98

Salts 90b, 90c, 92, 93, 94, 95, 96, 97 and 98 were irradiated in the solid state at -40°C. The regioisomeric and enantiomeric composition of the photoproducts for each

photolysis was studied in the same way as for the solid state photolysis of S-(-)-proline salt 90a. The results of these experiments are summarized in Table 3-12.

Table 3-12   Solid State Photoproduct Mixture Composition for Photolyses of Salts 90b, 90c and 92 to 98

Optically Active Amine	Photoproduct 32a		Photoproduct 33a	
	Yield[a] (%)	ee[b]	Yield[a] (%)	ee[b]
R-(+)-Proline (90b)	96	(-)-80	4	nil
(±)-Proline (90c)[c]	84	nil	16	nil
S-(-)-Proline methyl ester (92)	93	(+)-58	7	nil
S-(+)-2-Prolinol (93)	100	(-)-37	-	-
S-(-)-Prolineamide (94)	100	(-)-24	-	-
S-(+)-2-(Methoxymethyl)-pyrrolidine (95)	100	(-)-16	-	-
S-(-)-Proline tert-butyl ester (96)	100	>(+)-95	-	-
(S,S)-(+)-Pseudoephedrine (97)	87	(-)-87	13	73
(-)-Strychnine (98)	65	(+)-14	35	nil

[a] As determined by ^{1}H-NMR; [b]The estimated accuracy in these values is ± 5%; the sign of rotation of the predominant enantiomer is shown in parentheses. [c]Photolyses carried out at -20°C.

Salts 90b, 90c, 92, 96 and 98 were irradiated in solution. The regioisomeric and enantiomeric composition of the photoproducts was studied in the same way as for the photolysis of S-(-)-proline salt 90a in acetone. The results of these experiments are summarized in Table 3-13.

Table 3-13   Solution Photoproduct Mixture Composition for Salts **90a, 90b, 90c, 92**

and **98**

Optically Active Amine	Solvent	Photoproduct 32a		Photoproduct 33a	
		Yield[a] (%)	ee	Yield[a] (%)	ee
R-(+)-Proline (90b)	Ethanol	50	nil	50	nil
R,S-(±)-Proline (90c)	Ethanol	50	nil	50	nil
S-(-)-Proline methyl ester (92)	Benzene	95	nil	5	nil
S-(-)-Proline tert-butyl ester (96)	Acetone	50	nil	50	nil
(-)-Strychnine (98)	Ethanol	60	nil	40	nil

[a] As determined by ^{1}H-NMR after correction for the starting material. The estimated accuracy in these values is ±5%.

3.3.4.2   Photolyses of Salts Formed with 12-Methyl-9,10-dihydro-9,10-ethenoanthracene-11-carboxylic Acid (37)

Photolyses of (S,S)-(+)-Pseudoephedrine Salt 105a

(S,S)-(+)-Pseudoephedrine salt **105a** (328 mg, 0.767 mmol) was irradiated through a Pyrex filter at -40°C for 3 days. The reaction mixture was dissolved in diethyl ether and extracted three times with 15% aqueous HCl and twice with saturated aqueous NaCl solution. The organic fraction was dried over MgSO$_4$ and excess diazomethane was

added to produce the corresponding methyl esters. The solvent was removed under vacuum and the residue chromatographed on silica gel eluted with 10% ethyl acetate in petroleum ether. The resulting oil was recrystallized from ethanol to yield photoproduct 52 (52.1 mg, 0.189 mmol, 25% yield). The enantiomeric composition of the photoproduct was determined by 400 MHz ^{1}H-NMR using the chiral shift reagent Eu(hfc)$_3$. The signal monitored was the methyl singlet at δ = 1.90 ppm which showed that compound 52 was formed in greater than 95% enantiomeric excess. The optical rotation was measured and found to be positive ([α]$_D$= (+)-59 (Chloroform, C=5.2)).

A mixture of (S,S)-(+)-pseudoephedrine (19.1 mg, 0.116 mmol) and acid 37 (27.0 mg, 0.102 mmol) was dissolved in acetone (20 mL) and irradiated through a Pyrex filter for 3 h. The photoproduct was isolated following the same procedure as used for the isolation of the photoproduct in the solid state photolyses of (S,S)-(+)-pseudoephedrine salt 105a. This yielded photoproduct 52 (25.8 mg, 0.0935 mmol, 92%) which was formed without any enantiomeric excess as determined by polarimetry.

Photolysis of Salts 103, 104 and 105b

Salts 103, 104 and 105b were irradiated in the solid state at -40°C. The enantiomeric composition of the photoproduct was studied in the same way as for solid state photolysis of (S,S)-(+)-pseudoephedrine salt 105a. The photolyses were stopped before 40% conversion. The results are summarized in Table 3-14.

Table 3-14   Solid State Photoproduct Mixture Composition for Salts **103, 104** and

105b

Optically Active Amine	Photoproduct 32a ee[a]
S-(+)-2-Prolinol (**103**)	(+)-38
S-(-)-Proline *tert*-butyl ester (**104**)	(+)-26
(R,R)-(-)-Pseudoephedrine (**105b**)	≥(-)-95

[a]The estimated accuracy in these values is ± 10%; the sign of the rotation of predominant enantiomer is

shown in parentheses.

The enantiomeric composition of the photoproduct of the solution photolyses of

salts **103, 104** and **105b** was studied in the same way as for the solution photolysis of

(S,S)-(+)-pseudoephedrine salt **105a**. The results of these experiments are summarized in

Table 3-15.

Table 3-15   Solution Photoproduct Mixture Composition for Salts **103, 104** and **105b**

Optically Active Amine	Solution	Photoproduct 52 ee[a]
S-(+)-2-Prolinol (**103**)	Acetone	nil
S-(-)-Proline *tert*-butyl ester (**104**)	Acetone	nil
(R,R)-(-)-Pseudoephedrine (**105b**)	Acetone	nil

[a] The estimated accuracy in these values is ±5%.

3.3.4.3 Photolyses of Salts Formed with 9,10-Dihydro-9,10-ethenoanthracene-11-carboxylic Acid (40)

Photolyses of Piperidine Salt 134

A solution of piperidine salt **134** (77.5 mg, 0.232 mmol) in acetone (250 mL) was purged with nitrogen for 30 min and irradiated through a Pyrex filter for 4 h. The solvent was removed under vacuum and the residue dissolved in diethyl ether and washed three times with 15% aqueous HCl and two times with saturated aqueous NaCl solution. The organic fraction was dried over $MgSO_4$ and treated with excess diazomethane to produce the corresponding methyl ester. GC (DB-17) indicated formation of photoproduct **135** with little remaining starting material. The solvent was removed under vacuum and the residue chromatographed on silica gel eluted with 10% ethyl acetate in hexane. The resulting oil was crystallized from ethanol to yield compound **135** (47.5 mg, 0.181 mmol, 78% yield).

Product **135** was characterized as methyl 4b,8b,8c,8d-tetrahydro-dibenzo-[a,f]cyclopropa[c,d]pentalene-8c-carboxylate. The spectra are identical to those reported by Ciganek.[58]

MP: 165-168°C (lit.[58] 169.5-170.5°C).

IR (KBr) v_{max}: 1715 (C=O), 1252 (C-O) cm^{-1}.

MS m/e (relative intensity): 262 (M+, 31), 219 (6), 203 (100).

Exact mass calculated for $C_{18}H_{14}O_2$: 262.0994. Found: 262.0998.

^{1}H-NMR (400 MHz, CDCl$_3$) δ 7.3-7.0 (m, 8H, aromatic H), 4.98 (s, 1H, benzylic H),

3.78 (s, 2H, cyclopropyl H), 3.72 (s, 3H, CO$_2$CH$_3$) ppm.

^{13}C-NMR (50 MHz, CDCl$_3$) δ 172.39 (C=O), 150.18, 135.47 (aromatic c), 127.00,

126.64, 124.76, 121.32 (aromatic C-H), 62.08 (cyclopropyl C), 53.95, 51.98 (benzylic C-

H and CO$_2$CH$_3$), 47.04 (cyclopropyl C-H) ppm.

Crystals of piperidine salt **134** (16.7 mg, 0.0501 mmol) were irradiated through a

Pyrex filter for 12 h. The crystals turned yellow and cloudy upon irradiation. Afterwards

they were dissolved in diethyl ether and the resulting solution was washed thoroughly

with 15% aqueous HCl solution, dried over MgSO$_4$ and excess diazomethane was added.

GC (DB-17) analyses indicated 62% conversion to photoproduct **135**.

Crystals of piperidine salt **134** were irradiated with γ-rays from a ^{60}Co source

(Gammacell 220 by AECL, 200Ci) for a month. The crystals looked undamaged but

slightly yellow. Individual crystals were dissolved in diethyl ether, acidified, treated with

excess diazomethane and analyzed by GC(DB-17) to reveal formation of photoproduct

135 with conversion varying from 10 to 25%.

3.3.4.4 Photolyses of Salts Formed with Dimethyl 9-Amino-9,10-dihydro-9,10-ethenoanthracene-11,12-dicarboxylate (39)

Photolyses of Hydrochloride Salt 112

Hydrochloride salt **112** (145 mg, 0.391 mmol) was dissolved in acetonitrile (300 mL) and the resulting solution was purged with nitrogen for 0.5 h and irradiated for 4h. GC (DB-17) indicated formation of photoproduct **60** with little remaining starting material. The solvent was removed under vacuum. The residue was dissolved in ethyl acetate and extracted with three portions of 10% aqueous sodium hydroxide solution followed by two portions of aqueous saturated sodium chloride solution. The organic layer was dried over MgSO$_4$ and concentrated under vacuum. The residue was subjected to a silica gel column eluted with 10% ethanol in petroleum ether to yield photoproduct **60** (77.9 mg, 0.233 mmol, 60%).

Crystals of hydrochloride salt **112** (20 mg, 0.0539 mmol) were irradiated through a Pyrex filter for 10 h. The irradiated crystals were dissolved in ethyl acetate, washed thoroughly with 10% aqueous sodium hydroxide solution, dried over MgSO$_4$ and analyzed by GC (DB-17) which indicated 10% conversion to form photoproduct **60**.

Photolyses of R-(-)-10-Camphorsulfonic Acid Salt 116a

R-(-)-10-Camphorsulfonic acid salt **116a** (233 mg, 0.398 mmol) was crushed between Pyrex plates and irradiated at -40°C for 24 h. The photolyzed solid was dissolved in ethyl acetate and the resulting solution extracted with three portions of 10%

aqueous sodium hydroxide solution followed by two portions of aqueous saturated sodium chloride solution. The organic layer was dried over $MgSO_4$ and concentrated under vacuum. The photoproduct was purified on silica gel eluted with 10% ethanol in petroleum ether to yield photoproduct **60** (18.0 mg, 0.0537 mmol, 14%). Compound **60** was analyzed for enantiomeric excess by 400 MHz ^{1}H-NMR using (+)-Eu(hfc)$_3$ as the chiral shift reagent. The signal monitored was the methyl ester singlet at $\delta = 3.83$ ppm which revealed that compound **60** was formed in 68% enantiomeric excess. In addition, the sign of the rotation of the predominant enantiomer was measured by polarimeter and found to be positive.

A mixture of amine **39** (191 mg, 0.570 mmol) and R-(-)-10-camphorsulfonic acid (136 mg, 0.587 mmol) was dissolved in acetone (300 mL). This solution was purged with nitrogen for 0.5 h and irradiated for 1.5 h. GC (DB-17) showed 90% conversion to compound **60**. The photoproduct was purified following the same procedure as for the photoproduct in the solid state photolysis of R-(-)-10-camphorsulfonic acid salt **116a**. Compound **60** (163 mg, 0.487 mmol, 86%) was formed with no enantiomeric excess as determined by ^{1}H-NMR.

Photolyses of Salts 116b and 117

Salts **116b** and **117** were irradiated in the solid state at -40°C and in acetone solutions at room temperature. The solid state photolyses were stopped before 60% conversion. The regioisomeric and enantiomeric ratios of the photoproducts for each photolysis were studied in the same manner, as for the photolyses of R-(-)-10-camphorsulfonic acid salt **116a**. Isolation of the photoproducts revealed that regioisomer **60** was the sole compound formed, except in the case of the solid state irradiation of salt

117 where a small amount of photoproduct **61** was detectable (ca. 15%). The results are listed in Table 3-16.

Table 3-16   Enantiomeric Excess in Photoproduct **60** as a Function of Photolysis Medium and Sulfonic Acid Structure

Optically Active Sulfonic Acid	Solid State ee (%)[a]	Solution Phase ee (%)[a]
R-(-)-10-Camphorsulfonic acid (**116a**)	(-)-68	nil
S-(+)-10-Camphorsulfonic acid (**116b**)	(+)-64	nil
(-)-3-Bromocamphor-8-sulfonate (**117**)	(-)-30[b]	nil

[a] The estimated accuracy in these values is ± 5%; the sign of rotation of the predominant enantiomer is shown in parentheses. [b] Only in the case of salt **117** was a small amount of photoproduct **61** detectable (ca 15%).

3.3.4.5 Photolyses of Salts Formed with Dimethyl 9-Carboxy-9,10-dihydro-9,10-ethenoanthracene-11,12-dicarboxylate (38)

Photolyses of (R,S)-(-)-Ephedrine Salt 108

(R,S)-(-)-Ephedrine salt **108** (70.7 mg, 0.131 mmol) was crushed between Pyrex plates and irradiated at -40°C for 3 days. The photolyzed crystals were dissolved in diethyl ether, extracted three times with 15% aqueous HCl and twice with saturated aqueous NaCl. The organic fraction was dried over MgSO$_4$ and excess diazomethane was

added. The solvent was removed under vacuum and the residue chromatographed on a silica gel column eluted with 15% ethyl acetate in petroleum ether. This yielded a mixture of the achiral compound **68** and the chiral compound **67** in the ratio 9:1, respectively (8.1 mg, 0.207 mmol, 16%).

A solution of acid **38** (51.3 mg, 0.3125 mmol) and (R,S)-(-)-ephedrine (20.7 mg, 0.125 mmol) in acetone (20 mL) was irradiated through a Pyrex filter for 2 hours. The photoproducts were isolated following the same procedure as used for the isolation of the photoproduct in the solid state photolysis of (R,S)-(-)-ephedrine salt **108**. This yielded a mixture of photoproducts **67** and **68** (26.7 mg, 0.0681 mmol, 55%) in the ratio 81:19 as determined by GC (DB-1). No optical activity was observed when the photoproduct mixture was subjected to polarimetry.

Photolysis of (S,S)-(+)-Pseudoephedrine Salt 109

A mixture of acid **38** (27.0 mg, 0.102 mmol) and (S,S)-(+)-pseudoephedrine (17.3 mg, 0.105 mmol) in acetone (20 mL) was irradiated for 2 h through a Pyrex filter. The regioisomeric and enantiomeric composition of the photoproducts was studied in the same way as for the photolysis of the (R,S)-(-)-ephedrine salt **108** in acetone. These studies showed that photoproducts **67** and **68** (25.8 mg, 0.0683 mmol, 67%) were formed in the ratio 9:1 and exhibited no optical activity.

Photolysis of Salts 108 and 109 in the Solid State, Followed by Diazoethane Workup

Crystals of salts **108** and **109** were irradiated at -40°C. The photolyses were stopped before 25% conversion. The reactions were worked up as before, but

diazoethane was substituted for diazomethane. This afforded the known photoproducts 69 and 70 as a mixture. The regioisomeric and enantiomeric composition of these mixtures was determined by 400 MHz ^{1}H-NMR. For the enantiomeric excess determination, use was made of the chiral shift reagent (+)-Eu(hfc)$_3$. The signals monitored were the methyl singlets at δ 3.4 and 3.5 for compounds 69 and 70 respectively. In addition, the sign of rotation of the predominant enantiomer was measured by polarimetry. The results of these experiments are summarized in Table 3-17.

Table 3-17   Solid State Photoproduct Mixture Composition for Salts 108 and 109, after Diazoethane Workup

Optically Active Amine	Photoproduct 69		Photoproduct 70	
	Yield (%)	ee[a]	Yield (%)	ee[a]
(R,S)-(-)-Ephedrine (108)	10	24	90	≥-(-)-95
(S,S)-(+)-Pseudoephedrine (109)	80	16	20	18

[a] The estimated accuracy in these values is ± 5%; the sign of rotation of the predominant enantiomer is shown in parentheses.

3.3.5 Absolute Configuration of Some Photoproducts

3.3.5.1 Absolute Configuration of 4b,8b,8c,8d-tetrahydrodibenzo[a,f]cyclopropa[c,d]pentalene-8b,8c-dicarboxylic acid, 8c-methyl 8b-ethyl ester (32a)

(S)-(-)-Proline *tert*-butyl ester salt 96 (189 mg, 0.287 mmol) was photolyzed at -40°C for 5 days. The photoproduct was isolated following the same method as for the solid state photolysis of S-(-)-proline salt 90a. This yielded the colorless oil of photoproduct 32a (16.6 mg, 0.0497 mmol, 17%). The optical rotation was measured by polarimetry and the specific rotation was calculated assuming quantitative optical yield; $[\alpha]_D$ = (+)-27° (chloroform, C= 0.02).

The absolute configuration of photoproduct 32a was obtained by transforming it into the di-isopropyl ester derivative 35, which has a known absolute configuration.[43] This was done in the following manner: a mixture of photoproduct 32a (16.6 mg, 0.0497 mmol) from the photolysis described above, anhydrous isopropanol (25 mL) and H_2SO_4 (0.5 mL) was refluxed for 3 weeks. GC (DB-17) showed formation of compound 35 with little remaining starting material. The solvent was removed under vacuum and the residue dissolved in diethyl ether, washed with saturated aqueous NaCl solution and dried over $MgSO_4$. After filtration, the solvent was removed under vacuum and the resulting oil chromatographed on silica gel eluted with 20% ethyl acetate in petroleum ether to give, as a colorless oil, compound 35 (11.2 mg, 0.0298 mmol, 60%). The optical rotation was measured and the specific rotation was calculated assuming quantitative optical yield, $[\alpha]_D$= (+)-26° (chloroform, C=0.01). Garcia-Garibay et al.[43] showed that

the (+)-enantiomer of compound **35** has the absolute configuration (R,R,R,R) and therefore it can be concluded that compound **32a** has the same absolute configuration.[43]

Compound **35** was characterized as diisopropyl 4b,8b,8c,8d-(R,R,R,R)-tetrahydrodibenzo[a,f]cyclopropa[c,d]pentalene-8b,8c-dicarboxylate. All the spectra were identical to those reported by Garcia Garibay.[57]

IR (CDCl$_3$) v$_{max}$: 1723 (C=O), 1249 (C-O) cm^{-1}.

MS m/e (relative intensity): 376 (M$^+$, 15), 316 (13), 289 (28), 275 (16), 247 (100), 202 (71).

Exact mass calculated for C$_{24}$H$_{24}$O$_4$: 376.1675. Found: 376.1674.

^{1}H-NMR (400 MHz, CDCl$_3$) δ 7.4-7.0 (m, 8H, aromatic H), 5.22 (m, 1H, CO$_2$CH(CH$_3$)$_2$), 5.05 (m, 1H, CO$_2$CH(CH$_3$)$_2$), 5.00 (s, 1H, benzylic H), 4.45 (s, 1H, cyclopropyl H), 1.5-1.2 (m, 12H, CO$_2$CH(CH$_3$)$_2$) ppm.

3.3.5.2 Absolute Configuration of Methyl 8b-Methyl-4b,8b,8c,8d-tetrahydro-dibenzo[a,f]cyclopropa[c,d]pentalene-8c-carboxylate (52)

Crystals of (S,S)-(+)-pseudoephedrine salt **105a** were photolyzed at -40°C for 4 days. The photoproduct was isolated following the same procedure as described before, yielding crystals of photoproduct **52** (95.1 mg, 0.350 mmol, 35%). The optical rotation of compound **52**, was measured by polarimetry and the specific rotation was calculated to be [α]$_D$ =(+)-59° (chloroform, C= 0.095) by assuming quantitative optical yield.

A resolved chiral handle was attached to product **52** allowing the determination of absolute configuration by X-ray structure analysis. This was done in the following way; photoproduct **52** (64.2 mg, 0.34 mmol) from the photolysis described above was hydrolyzed by dissolving in methanol (15 mL) with the addition of K$_2$CO$_3$ (40.7 mg,

204

0.295 mmol). The resulting solution was refluxed for 14 h. Afterwards the solvent was removed under vacuum and the residue dissolved in saturated aqueous $NaHCO_3$ and washed with ethyl acetate to remove unreacted starting material. The aqueous fraction was made acidic with conc. HCl and extracted with ethyl acetate. The organic layer was washed with saturated aqueous NaCl, dried over $MgSO_4$ and the solvent removed under vacuum. The resulting oil was recrystallized from ethanol to yield crystals of compound 115 (49.8 mg, 0.191 mmol, 82%). The optical rotation was measured and the specific rotation calculated assuming quantitative optical yield, $[\alpha]_D$= (+)-73° (chloroform, C = 0.050).

Compound 115 was characterized as 8b-Methyl-4b,8b,8c,8d-tetrahydro-dibenzo[a,f]cyclopropa[c,d]pentalene-8c-carboxylic acid.

MP: 223-224°C.

IR (KBr) v_{max}: 3400-2400 (O-H, C-H), 1678 (C=O), 1257 (C-O) cm^{-1}.

MS m/e (relative intensity): 262 (M$^+$, 4), 216 (100), 189 (12).

Exact mass calculated for $C_{18}H_{14}O_2$: 262.0994. Found: 262.0995.

^{1}H-NMR (400 MHz, CDCl$_3$) δ 7.3-7.0 (m, 8H, aromatic H), 4.98 (s, 1H, benzylic H), 3.64 (s, 1H, cyclopropyl H), 1.94 (s, 3H, cyclopropyl CH$_3$) ppm, no O-H signal detectable.

^{13}C-NMR (50 MHz, CDCl$_3$) δ 177.5 (C=O), 149.9, 149.0, 138.7, 138.4 (aromatic C), 127.3, 126.9, 126.7, 126.5, 124.6, 123.9, 121.2, 121.2 (aromatic C-H), 66.1, 54.7 (cyclopropyl C), 54.5, 52.4 (cyclopropyl C-H and benzylic C-H), 16.5 (cyclopropyl CH$_3$) ppm.

Anal. calculated for $C_{18}H_{14}O_2$: C, 82.42; H, 5.38. Found: C, 82.53; H, 5.29.

A resolved chiral handle was introduced into compound 115 in the following way: a solution of compound 115 (33.3 mg, 0.127 mmol) and oxalyl chloride (1 mL) in

anhydrous chloroform (6 mL) was refluxed for 30 min. The solvent and excess oxalyl chloride were removed under vacuum to yield a yellow oil assumed to be the corresponding acid chloride. The acid chloride was dissolved in anhydrous chloroform (10 mL), S-(-)-α-methylbenzylamine (1 mL, 0.94 g, 7.8 mmol) was added and the resulting solution was refluxed for 30 min. The reaction mixture was washed three times with saturated aqueous NaHCO₃ solution and twice with saturated aqueous NaCl solution. The solvent was removed under vacuum and the residue chromatographed on silica gel eluted with 30% ethyl acetate in petroleum ether. This yielded a colorless oil which was crystallized from ethanol to give compound **106** (42.0 mg, 0.110 mmol, 92%). The optical rotation was measured with a polarimeter and the specific rotation calculated assuming quantitative optical yield, $[\alpha]_D$ = (+)-81° (chloroform, C = 0.016). The absolute configuration of compound **106** was obtained by an X-ray crystal structure analysis.[69]

Compound **106** was characterized as N-(S-1-phenylethyl) 8b-Methyl-4b,8b,8c,8d-(S,R,S,S)-tetrahydrodibenzo[a,f]cyclopropa[c,d]pentalene-8c-carboxylic amide.

MP: 174-175°C.

IR (KBr) v_{max}: 3600-3200 (N-H and C-H), 1634 (C=O), 1538 (N-H) cm⁻¹.

MS m/e (relative intensity): 365 (M+, 1), 217 (100), 202 (47), 105 (26).

Exact mass calculated for $C_{26}H_{23}NO$: 365.1781. Found: 365.1786.

¹H-NMR (400 MHz, CDCl₃) δ 7.4-7.0 (m, 13H, aromatic H), 5.82 (m, 1H, NH), 5.20 (m, 1H, HNC**H**), 4.68 (s, 1H benzylic H), 3.55 (s, 1H, cyclopropyl H), 1.80 (s, 3H, cyclopropyl CH₃), 1.52 (m, 3H, HNCHC**H₃**) ppm.

¹³C-NMR (100 MHz, CDCl₃) 168.2 (C=O), 149.5, 148.5, 143.0, 139.5, 137.1 (aromatic C), 128.7, 128.7, 127.4, 127.0, 126.9, 126.6, 126.5, 126.3, 126.2, 126.1, 124.9, 124.1, 121.1, 120.9 (aromatic C-H), 68.32 (cyclopropyl C), 55.71 (benzylic C-H), 52.24

(cyclopropyl C-H), 49.2, 49.1 (cyclopropyl C-H and HN$\underline{CH}$), 21.62, 15.99 (cyclopropyl CH$_3$ and HNCH$\underline{CH_3}$) ppm.

3.3.5.3 Absolute Configurations of Dimethyl 8d-Amino-4b,8b,8c,8d-tetrahydro-dibenzo[a,f]cyclopropa[c,d]pentalene-8b,8c-dicarboxylate (60)

In order to obtain the absolute configuration of photoproduct 60, a resolved chiral handle was introduced into a racemic mixture of compound 60. The two diastereomers that formed were separated and an X-ray structure analysis of one of the diastereomers was used to determine its absolute configuration. This was performed in the following way; R-(-)-α-methoxyphenylacetic acid (104 mg, 0.627 mmol) and oxalyl chloride (5 mL) were dissolved in anhydrous chloroform (30 mL) and refluxed for 30 min. The solvent and excess oxalyl chloride were removed under vacuum to yield a yellow oil which was assumed to be the corresponding acid chloride. The acid chloride was dissolved in anhydrous chloroform (50 mL) and compound 60 (205 mg, 0.611 mmol) was added. The resulting solution was refluxed for 12h. GC (DB-1) indicated formation of compounds 120 and 121 in the ratio 1:1 with little remaining starting material. The solvent was washed thoroughly with saturated aqueous NaHCO$_3$ solution, dried over MgSO$_4$ and removed under vacuum to yield a mixture of compounds 120 and 121 (227 mg, 0.470 mmol, 77%). Diastereomers 120 and 121 were separated on a preparative HPLC column eluted with 30% ethyl acetate in n-hexane. All attempts to crystallize compound 121 from various solvents failed, while diastereomers 120 was recrystallized from an acetone-n-hexane solution to give prism-like crystals. X-ray analysis of compound 120 showed that it crystallizes with one equivalent of acetone and that is has the (R,R,S,S,R) configuration.[69]

Compound **120** was characterized as dimethyl N-(R-(α)-methoxyphenyl acetic acid)-4b-amino-4b,8b,8c,8d-(R,S,S,R)-tetrahydrodibenzo[a,f]cyclopropa[c,d]pentalene-8b,8c-dicarboxylate.

$[\alpha]_D$ = (+)-17° (chloroform, C = 0.005, assuming quantitative optical yield).)

MP: 100-103°C.

IR (KBr) ν_{max}: 3406 (N-H), 1724, 1700 (C=O), 1504 (N-H), 1294, 1248, 1223 (C-O) cm^{-1}.

MS m/e (relative intensity): 483 (M+, 4), 424 (9), 392 (10), 302 (9), 260 (9), 217 (8), 121 (100).

Exact mass calculated for $C_{29}H_{25}NO_6$: 483.1683. Found 483.1684.

^{1}H-NMR (400 MHz, CDCl$_3$) δ 7.8-7.1 (m, 14H, aromatic H and N-H), 4.78 (s, 1H, CH$_3$OCH), 4.42 (s, 1H, cyclopropyl H), 3.82 (s, 3H, CO$_2$CH$_3$), 3.55 (s, 3H, CO$_2$CH$_3$), 3.19 (s, 3H, OCH$_3$) ppm.

^{13}C-NMR (75 MHz, CDCl$_3$) δ 170.8, 168.4, 166.0 (C=O), 149.3, 148.2, 136.6, 131.8, 130.7 (aromatic C), 128.2, 128.1, 127.9, 127.8, 127.7, 127.2, 127.1, 125.9, 119.0, 118.6 (aromatic C-H), 83.7 (COCH$_3$), 74.8, 71.2 (benzylic C and cyclopropyl C), 57.6 (CHOCH$_3$), 53.7 (cyclopropyl C), 52.5, 51.8 (CO$_2$CH$_3$), 49.02 (cyclopropyl C-H) ppm.

Compound **121** was characterized as dimethyl N-(R-(α)-methoxyphenyl acetic acid)-4b-amino-4b,8b,8c,8d-(S,R,R,S)-tetrahydrodibenzo[a,f]cyclopropa[c,d]pentalene-8b,8c-dicarboxylate.

$[\alpha]_D$= (+)-53° (chloroform, c =0.023, assuming quantitative optical yield).

IR (CHCl$_3$) ν_{max}: 3375 (N-H), 1738, 1731, 1698 (C=O), 1289, 1221 (C-O) cm^{-1}.

MS m/e (relative intensity): 483 (M+, 2), 424 (3), 392 (4), 260 (14), 217 (13), 149 (24), 121 (100).

Exact mass calculated for $C_{29}H_{25}NO_6$: 483.1683. Found 483.1688.

¹H-NMR (400 MHz, CDCl₃) δ 7.7-6.7 (m, 14H, aromatic H and N-H), 4.70 (s, 1H, CH₃OCH), 4.44(s, 1H, cyclopropyl H), 3.82 (s, 3H, CO₂CH₃), 3.50 (s, 6H, CO₂CH₃ and CH₃OCH) ppm.

¹³C-NMR (100 MHz, CDCl₃) δ 171.1, 168.3, 166.5 (C=O), 149.2, 148.1, 136.8, 131.6, 130.7 (aromatic C), 128.4, 128.3, 128.2, 127.8, 127.7, 127.6, 126.8, 126.6, 125.7, 118.8, 118.4 (aromatic C-H), 83.9 (CH₃OCH), 74.7, 70.7 (benzylic C and cyclopropyl C), 58.3 (CH₃OCH), 54.2, 52.6 (CO₂CH₃), 48.7 (cyclopropyl C-H) ppm.

The absolute configurations of the photoproduct **60** and the starting material, R-(-)-10-camphorsulfonic acid salt **116a** were correlated as follows: crystals of R-(-)-10-camphorsulfonic acid salt **116a** (136.1 mg, 0.253 mmol) were photolyzed at -40°C for 2 days. The photoproduct was isolated following the same procedure as described before, yielding crystals of photoproduct **60** (38.9 mg, 0.116 mmol, 50%), which were formed in 70% enantiomeric excess as determined by 400 MHz ¹H-NMR using chiral shift reagent, (+)-Eu(hfc)₃. The optical rotation was measured by polarimeter and the specific rotation calculated as $[\alpha]_D$= (-)-27° (chloroform, C = 0.039).

A portion of photoproduct **60** (11.8 mg, 0.0352 mmol) from the photolysis described above was dissolved in anhydrous chloroform (10 mL) and R-(-)-α-methoxyphenyl acetic acid chloride (0.275 mmol) was added. This solution was refluxed for 30 min, washed thoroughly with water and dried over MgSO₄. The solvent was removed under vacuum to yield a mixture of compounds **120** and **121**. GC (DB-1) analysis showed formation of compounds **120** and **121** in the ratio 86:14, respectively. The product ratio was further supported by a ¹H-NMR study. It may therefore be concluded that (-)-enantiomer of **60** which is the major photoproduct from solid state irradiations of R-(-)-10-camphorsulfonic acid salt **116a**, has the absolute configuration (4bS, 8bR, 8cR, 8dS).

REFERENCES

1 a Morrison, J.D.; Mosher, H.S.; in *Asymmetric Organic Reactions*, American Chemical Society, Washington, D.C., **1976**

b *Asymmetric Synthesis*, Morrison, J.D.; Ed., Academic Press Inc., New York, **1983**, Vol. 1-5.

c Kagan, H.B.; Fiaud, J.C.; *Top. Stereochem.*, **1978**, *10*, 175.

2 Addadi, L.; Lahav, M.; *Pure & Appl. Chem.*, **1979**, *51*, 1269.

3 a Green, B.S.; Lahav, M.; *J. Mol. Evol.*, **1975**, *6*, 99.

b Addadi, L.; Lahav, M.; in *Origins of Optical Activity in Nature*, Walker, D.C., Ed., New York, **1979**, Chapter 14.

c Bonner, W.A.; *Top. Stereochem.*, **1988**, *18*, 1.

d McBride, J.M.; Carter, R.L.; *Angew. Chem. Int. Ed. Engl.*, **1991**, *30*, 293.

4 a Rau, H.; *Chem. Rev.*, **1983**, *83*, 535.

b Inoue, Y.; *Chem. Rev.*, **1992**, *92*, 741.

c Inoue, Y.; Yamasaki, N.; Yokoyama, T.; Tai, A.; *J. Org. Chem.*, **1992**, *57*, 1332.

5 a Green, B.S.; Lahav, M.; Rabinovich, D.; *Acc. Chem. Res.*, **1979**, *12*, 191.

b Ramamurthy, V.; *Tetrahedron*, **1986**, *42*, 5753.

c Scheffer, J.R.; Garcia-Garibay, M.A.; in *Studies in Surfaces Science and Catalysis*, Anpo, M.; Matsuura. T.; Eds.; Elsevier, Amsterdam, **1989**, Vol. 47, 501.

d Hollingsworth, M.D.; McBride, J.M.; in *Advances in Photochemistry*, Volman, D.; Hammond, G.; Gollnick, K.; Eds., Interscience, New York, **1990**, Vol. *15*, 279.

e Vadia, M.; Popovitz-Biro, R.; Leiserowitz, L.; Lahav, M.; in *Photochemistry in Organized and Constrained Media*, Ramamurthy, V., Ed.; **1991**, Chapter 6.

6 a Dunitz, J.D.; *X-ray Analysis and the Structure of Organic Molecules*, Cornell University Press, Ithaca, New York, **1979**, p 312.

b   Buckert, U.; Allinger, N.L.; *Molecular Mechanics*, Am. Chem. Soc. Monograph, Washington, D.C., **1982**, p 177.

7 a   Riiber, C.N.; *Chem. Ber.*, **1902**, *35*, 2411.
   b   Ciamician, G.; Silber, P.; *Chem. Ber.*, **1902**, *35*, 4128.

8 The following is a list of some of the review articles on the subject of chemical studies in organic crystals in recent years.
   a   Gavezzotti, A.; Simonetta, M.; *Chem. Rev.*, **1982**, *82*, 1.
   b   Hasegawa, M.; *Chem. Rev.*, **1983**, *83*, 507.
   c   McBride, J.M.; *Acc. Chem. Res.*, **1983**, *16*, 304.
   d   Trotter, J.; *Acta Crystallogr., Sect B*, **1983**, *B39*, 373.
   e   Green, B.S.; Arad-Yellin, R.; Cohen, M.D.; *Top. Stereochem.*, **1986**, *16*, 131.
   f   Ramamurthy, V.; Venkatesan, K.; *Chem. Rev.*, **1987**, *87*, 433.
   g   *Organic Solid State Chemistry*, Desiraju, G.R., Ed.; Elsevier, Amsterdam, **1987**.
   h   *Organic Chemistry in Anisotropy Media*, Scheffer, J.R.; Turro, N.J.; Ramamurthy, V.; Eds., Tetrahedron Symposia-in-Print, Number 29, *Tetrahedron*, **1987**.
   i   Cohen, M.D.; *Tetrahedron*, **1987**, *43*, 1211.
   j   Scheffer, J.R.; Garcia-Garibay, M.; Nalamasu, O.; in *Organic Photochemistry*, Padwa, A.; Ed., Marcel Dekker, New York, **1987**, Vol. 2, Part 2, Chapter 20.
   k   *Photochemistry on Solid Surfaces*, Anpo, M.; Matsuura, T.; Eds., Elsevier, Amsterdam, **1989**.
   l   *Photochemistry in Organized and Constrained Media*, Ramamurthy, V., Ed.; VCH, New York, **1991**.
   m   Chen, J.; Scheffer, J.R.; Trotter, J.; *Tetrahedron*, **1992**, *48*, 3251.

9   Kohlshutter, H.W.; *Z. Anorg. Allg. Chem.*, **1918**, *105*, 121.

10 a   Cohen, M.D.; Schmidt, G.M.J.; Sonntag, F.I.; *J. Chem. Soc.*, **1964**, 2000.
    b   Schmidt, G.M.J.; *J. Chem. Soc.*, **1964**, 2014.

11 a   Cohen, M.D.; Schmidt, G.M.J.; *J. Chem. Soc.*, **1964**, 1996.
    b   Schmidt, G.M.J.; *Pure Appl. Chem.*, **1971**, *27*, 647.

12 a   Cohen, M.D.; *Angew. Chem., Int. Ed. Engl.*, **1975**, *14*, 386.
    b   Cohen, M.D.; *Mol. Cryst. Liq. Cryst.*, **1979**, *50*, 1.

13   Ramamurthy, V.; Weiss, R.G.; Hammond, G.S. in *Advantages in Photochemistry*, Hammond, G.S.; Neckers, D.C.; Volman, D.; Eds., Interscience, New York, in press.

14   Wegner, G.; *Pure Appl. Chem.*, **1977**, *49*, 443.

15 a Jones, W.; Nakanishi, H.; Theocharis, C.R.; Thomas, J.M.; *J. Chem. Soc., Chem., Commun.*, **1980**, 610.
     b Nakanishi, H.; Jones, W.; Thomas, J.M.; Hursthouse, M.B.; Motevalli, M.; *J. Chem. Soc., Chem. Commun.*, **1980**, 611.
     c Nakanishi, H.; Jones, W.; Thomas, J.M.; Hursthouse, M.B.; Motevalli, M.; *J. Phys. Chem.*, **1981**, *85*, 3636.

16 a Ariel, S.; Askari, S.; Scheffer, J.R.; Trotter, J.; Walsh, L.; *J. Am. Chem. Soc.*, **1984**, *106*, 5726.
     b Ariel, S.; Askari, S.; Evans, S.V.; Hwang, C.; Jay, J.; Scheffer, J.R.; Trotter, J.; Walsh, L.; *Tetrahedron*, **1987**, *43*, 1253.
     c Scheffer J.R.; Trotter, J. in *The Chemistry of Quinonoid Compounds*, Patai, S.; Rappoport, Z.; Eds.; John Wiley & Sons, **1988**, Vol. 2, Chapter 20.

17 a Appel, W.K.; Jiang, Z.Q.; Scheffer, J.R.; Walsh, L.; *J. Am. Chem. Soc.*, **1983**, *105*, 5354.
     b Scheffer, J.R.; Trotter, J.; Guðmundsdóttir, A.D.; in *Handbook of Organic Photochemistry and Photobiology*, Horspool, W.M.; Ed., CRC Press, in press.

18   Guðmundsdóttir, A.D.; Scheffer, J.R.; *Tetrahedron Lett.*, **1989**, *30*, 423.

19   Gavezzotti, A.; *J. Am. Chem. Soc.*, **1983**, *105*, 5220.

20   Gavezzotti, A.; *Tetrahedron*, **1987**, *43*, 1241.

21   Wang, W.N.; Jones, W.; *Tetrahedron*, **1987**, *43*, 1273.

22   Yap, M.P.; Ph.D. Thesis, University of British Columbia, 1992.

23   Jacques, J.; Collet, A.; Wilen, S.H.; *Enantiomers, Racemates and Resolutions*, Wiley Interscience, New York, **1983**.

24 a   Buerger, M.J.; *Elementary Crystallography*, Wiley, New York, **1963**, 199.
    b   Hahn, T.; Klapper H.;, in *International Tables for Crystallography*, Hahn, T.; Ed., Reidel, Dordrecht, Holland, **1983**, Vol. A, Chapter 10.

25   For discussion of Pasteur's work on sodium ammonium tartrate, see Fieser, M.; in *Advanced Organic Chemistry*, Reinhold, New York, **1961**, p 69.

26 a   Pincock, R.E.; Wilson, K.R.; *J. Am. Chem. Soc.*, **1971**, *93*, 1291.
    b   Pincock, R.E.; Perkins, R.R.; Ma, A.S.; Wilson, K.R.; *Science*, **1971**, *174*, 1018.

27   Desiraju, G.R.; *Crystal Engineering: The Design of Organic Solids*, Elsevier, New York, **1989.**

28   Green, B.S.; Lahav, M.; Schmidt, G.M.J.; *Mol. Cryst. Liq. Cryst.*, **1975**, *29*, 187.

29   Elgavi, A.; Green, B.S.; Schmidt, G.M.J.; *J. Am. Chem. Soc.*, **1973**, *95*, 2058.

30   Rabinovich, D.; Shakked, Z.; *Acta Crystallogr., Sect. B*, **1975**, *B31*, 819.

31   Warrshel, A.; Shakked, Z.; *J. Am. Chem. Soc.*, **1975**, *97*, 5679.

32   Hasegawa, M.; in *Organic Solid State Chemistry*, Desiraju, G.R.; Ed., Elsevier, New York, **1987**, p 153.

33 a   Addadi, L.; Lahav, M.; *J. Am. Chem. Soc.*, **1978**, *100*, 2838.
    b   Addadi, L.; Lahav, M.; *J. Am. Chem. Soc.*, **1979**, *101*, 2152.
    c   Addadi, L.; van Mil, J.; Lahav, M.; *J. Am. Chem. Soc.*, **1982**, *104*, 3422.

34 a   Hasegawa, M.; Kunita, A.; Chung C.; Hayashi, K.; Sato, S.; *Chem. Lett*, 1989, 641.
    b   Hasegawa, M.; Chung, C.M.; Muro, N.; Maekawa, Y.; *J. Am. Chem. Soc.*, 1990, *112*, 5676.

35 a   Evans, S.V.; Garcia-Garibay, M.; Omkaram, N.; Scheffer, J.R.; Trotter, J.; Wireko, F.; *J. Am. Chem. Soc.*, **1986**, *108*, 5648.

b   Evans, S.V.; Trotter, J.; *Acta Crystallogr., Sect. B*, **1989**, *B45*, 500.

36 a   Toda, F.; Yagi, M.; Soda, S.; *J. Chem. Soc., Chem. Commun.*, **1987**, 1413.

b   Sekine, A.; Hori, K.; Ohashi, Y.; Yagi, M.; Toda, F.; *J. Am. Chem. Soc.*, **1989**, *111*, 697.

37 a   Feng, X.W.; McBride, J.M.; *J. Am. Chem. Soc.*, **1990**, *112*, 6152.

b   McBride, J.M.; Bertman, S.B.; Cioffi, D.Z.; Segmuller, B.E.; Weber, B.A.; *Mol. Cryst. Liq. Cryst. Inc. Nonlin. Opt.*, **1988**, *161*, 1.

38 a   Holland, H.L.; Richardson, M.F.; *Mol. Cryst. Liq. Cryst.*, **1980**, *58*, 311.

b   Chenchaiah, P.C.; Holland, H.L.; Richardson, M.F.; *J. Chem. Soc., Chem. Commun.*, **1982**, 436.

39 a   Hixon, S.S.; Mariano, P.S.; Zimmerman, H.E.; *Chem. Rev.*, **1973**, *73*, 531

b   Zimmerman, H.E.; in *Rearrangements in Ground and Excited States*, de Mayo, P.; Ed., Wiley Interscience, New York, **1980**, Vol. 3. Chapter. 16.

40 a   Zimmerman, H.E.; Grunewald, G.L; *J. Am. Chem. Soc.*; **1966**, *88*, 183.

b   Zimmerman, H.E.; Binkley, R.W.; Givens, R.S.; Sherwin, M.A.; *J. Am. Chem. Soc.*, **1967**, *89*, 3932.

41   De Lucchi, O.; Adam, W.; in *Comprehensive Organic Synthesis*, Trost, B.M.; Fleming, I.; Paquette, L.A.; Eds, Pergamon Press, Oxford, **1991**, Vol. 5.

42 a   Scheffer, J.R.; Trotter, J.; Garcia-Garibay, M.; Wireko, F.C.; *Mol. Cryst. Liq. Cryst. Inc. Nonlin. Opt.*, **1988**, *156*, 63.

b   Garcia-Garibay, M.; Scheffer, J.R.; Trotter, J.; Wireko, F.C.; *Acta Crystallogr., Sect. B*, **1990**, *B46*, 79.

c   Trotter, J.; Wireko, F.C.; *Acta Crystallogr., Sect. C*, **1991**, *C47*, 793.

43 a   Garcia-Garibay, M.; Scheffer, J.R.; Trotter, J.; Wireko, F.; *J. Am. Chem. Soc.*; **1989**, *111*, 4985.

b   Garcia-Garibay, M.; Scheffer, J.R.; Trotter, J.; Wireko, F.; *Acta Crystallogr., Sect. B,* **1990,** *B46,* 431.

44   Bijvoet, J.M.; Peerdeman, A.F.; Van Bommel, J.A.; *Nature,* **1951,** *168,* 271.

45 a   Chan, R.S.; Ingold, C.; Prelog, V.; *J. Chem. Soc., London,* **1951,** 612.
     b   Chan, R.S.; Ingold, C.; Prelog, V.; *Experientia,* **1956,** *12,* 81.
     c   Chan, R.S.; Ingold, C.; Prelog, V.; *Angew. Chem., Int. Ed. Engl.,* **1966,** *5,* 385.

46   Diels, O.; Alder, K.; *Justus Liebigs Ann. Chem.,* **1931,** *486,* 191.

47 a   Morgan, G.T.; Harrison, H.A.; *J. Soc. Chem. Ind.; London, Trans. Commun.,* **1930,** *49,* 143.
     b   Bartlett, P.D.; Cohen, S.G.; *J. Am. Chem. Soc.,* **1940,** *62,* 1183.

48   Bartlett, P.D.; Greene, F.D.; *J. Am. Chem. Soc.,* **1954,** *76,* 1088.

49   Adam-Briers, M.; Fierens, P.J.C.; Maritims, R.H.; *Helv. Chim. Acta,* **1955,** *38,* 2009.

50   Vaughan, W.R.; Milton, K.M.; *J. Am. Chem. Soc.,* **1952,** *74,* 5623.

51   Chen, J.; Ph.D. Thesis, University of British Columbia, **1991.**

52   Lindgren, B.O. Nilsson, T.; *Acta Chem. Scand.,* **1973,** *27,* 888.

53   Zimmerman, H.E.; in *Organic Photochemistry,* Ed. Padwa, A.; Marcel Dekker, New York, **1991,** Vol. 10, 1.

54 a   Garcia-Garibay, M.; Scheffer, J.R.; Watson, D.G.; *J. Chem. Soc.,* **1989,** 600.
     b   Garcia-Garibay, M.; Scheffer, J.R.; Watson, D.G.; *J. Org. Chem.,* **1992,** 26, 241.

55 a   Cristol, S.J.; Parungo, F.P.; Plorde, D.E.; Schwarzenbach, K.; *J. Am. Chem. Soc.,* **1965,** *87,* 2879.
     b   Cristol, S.J.; Parungo, F.P.; Plorde, D.E.; *J. Am. Chem. Soc.,* **1965,** 87, 2870.
     c   Cristol, S.J.; Bopp, R.J.; Johnson, A.E.; *J. Org. Chem.,* **1969,** *11,* 3574.

56   Silverstein, R.B.; Bassler, G.C.; Morill, T.C.; *Spectrometric Identification of Organic Compounds*; John Wiley & Sons, **1981**, Chapter 3.

57   Garcia-Garibay, M.; Ph.D. Thesis, University of British Columbia, **1988**.

58   Ciganek, E.: *J. Am. Chem. Soc.*, **1966**, 88, 2882.

59   Rattray, G.; Yang, J.; Guðmundsdóttir, A. D, Scheffer, J.R.; *Tetrahedron Lett.*, **1993**, *34*, 45.

60   Bordwell, F.; Lynch, T.Y.; *J. Am. Chem. Soc.*, **1989**, *111*, 7558.

61   Ceppi, E.; Eckhardt, W.; Grob, C.A.; *Tetrahedron Lett.*, **1973**, *37*, 3627.

62   Cristol, S.J.; Kaufman, R.L.; Opitz, S.M.; Szalecki, W.; Bindel, T.H.; *J. Am. Chem. Soc.*, **1983**, *105*, 3226.

63   Paddick, R.G.; Richards, K.E.; Wright, G.J.; *Aust. J. Chem.*, **1976**, *29*, 1005.

64   Richards, K.E.; Tillman, R.W.; Wright, G.J.; *Aust. J. Chem.*, **1975**, *28*, 1289.

65   Iwamura, M.; Tukada, H.; Iwamura, H.; *Tetrahedron Lett.*, **1980**, *21*, 4865.

66 a   Gunther, H.; *Tetrahedron Lett.*, **1970**, *52*, 5173.
    b   Hoffman, R.; *Tetrahedron Lett.*, **1970**, *52*, 2907.
    c   Hoffman, R.; Stohrer, W-D.; *J. Am. Chem. Soc.*, **1971**, *93*, 6941.
    d   Gunther, H.; Wehner, R.; *J. Am. Chem. Soc.*, **1975**, *97*, 923.

67   X-ray crystal structures done by Guðmundsdóttir, A.D.; Chemistry Department, University of British Columbia.

68   Demuth, M.; Amrein, W.; Bender, C.O; Braslavsky, S.E.; Burger, U.; George, M.V.; Lemmer, D.; Schaffner, K.; *Tetrahedron*, **1981**, *37*, 3245.

216

69   X-ray crystal structures done by Rettig, S.J.; Chemistry Department, University of British Columbia.

70   Paquette, L.A.; Bay, E.; *J. Am. Chem. Soc.*, **1984**, *106*, 6693.

71   Pokkuluri, P.R.; Ph.D. Thesis, University of British Columbia, **1990**.

72   Zimmerman, H.E.; Givens, R.S.; Pagni, R.M.; *J. Am. Chem. Soc.*, **1968**, *90*, 6090.

73   Zimmerman, H.E, Bender, C.O.; *J. Am. Chem. Soc.*, **1970**, *92*, 4366.

74   Pokkuluri, P.R.; Scheffer, J.R.; Trotter, J.; *J. Am. Chem. Soc.*; **1990**, *112*, 3676.

75   Asokan, C.V.; Kumar, S.A.; Das, S.; Rath, N.P.; George, M.V.; *J. Org. Chem.*; **1991**, *56*, 5890.

76   Zimmerman, H.E.; Zuraw, M.J.; *J. Am. Chem. Soc.*, **1989**, *111*, 7974.

77   Pokkuluri, P.R.; Scheffer, J.R.; Trotter, J.; *Tetrahedron Lett.*; **1989**, *30*, 1061.

78   Kumar, C.V.; Murty, B.A.R.C.; Lahiri, S.; Chakachery, E.; Scaiano, J.C.; George, M.V.; *J. Org. Chem.*; **1984**, *49*, 4923.

79   X-ray crystal structure done by Kaftory, M.; Chemistry Department, University of British Columbia.

80   Guðmundsdóttir, A.D.; Scheffer, J.R.; *Tetrahedron Lett.*, **1990**, *31*, 6807.

81   Morrison, R.T.; Boyd R.N.; *Organic Chemistry*, 4th ed, Allyn and Bacon, **1983**.

82   Scheffer, J.R.; Fu, T.; Trotter, J.; Unpublished results.

83   Parker, D.; *Chem. Rev.*; **1991**, *91*, 1441.

84   Crans, D.C.; Whitesides, G.M.; *J. Am. Chem. Soc.*; **1985**, *107*, 7019.

85   Meresse, A.; Courseille, C.; Lerory, F.; Chanh, N.B.; *Acta Crystallogr., Sect. B,* **1979**, *B35*, 2087.

86   Chen, J.X.; Garcia-Garibay, M.A.; Scheffer, J.R.; *Tetrahedron Lett.*, **1989**, *30*, 6125.

87   Nakanishi, F.; Nakanishi, H.; Tasai, T.; Suzuki, Y.; Hasegawa, M.; *Chemistry Lett.*, **1974**, 525.

88   Guðmundsdóttir, A.D.; Scheffer, J.R.; *Photochemistry and Photobiology*; **1991**, *4*, 535.

89   X-ray crystal structure done by Li, W. and Trotter, J., Chemistry Department, University of British Colombia.

90   a   Barrett, G.C.; in *Techniques of Chemistry*, Bentley, K.W; Kirby, G.W.; Eds.; **1963**, Vol. 4 , Chapter 8.
     b   Purdie, N.; Swallows, K.A.; *Analytical Chemistry*, **1989**, *61*, 77A.

91   Lewis, T.J.; Rettig, S.J.; Scheffer, J.R.; Trotter, J.; Wireko, F.; *J. Am. Chem. Soc.*, **1991**, *112*, 3679.

92   Jones, R.; Scheffer, J.R.; Trotter, J.; Yang, J.; *Tetrahedron Lett.*, **1992**, *33*, 5484.

93   Durr, H.; *Angew. Chem., Int. Ed. Engl.*, **1989**, *28*, 413.

94   Exelby, R.; Grinter, R.; *Chem. Rev.*; **1965**, *65*, 247.

95   The UV-visible spectra and the ESR spectra were obtained by Ramamurthy, V.; Central Research and Development, the Dupont Company, Delaware.

96   Thompson, C.; in *Electron Spin Resonance: A Specialist Periodical Report*, The Chemical Society, London, **1973**, Vol. 1, Chapter 1.

97   Pokkuluri, P.R.; M.Sc. Thesis, University of British Columbia, 1987.

98   a   Rehm, D.; Weller, A.; *Isr. J. Chem.*; **1970**, *8*, 259.
     b   Mariano, P.S.; Stavinoha, J.L.; *Synthetic Organic Photochemistry*, Horspool, W.M., Ed.; Plenum Press, **1984**, Chapter 3.
     c   Mattes, S.L.; Farid, S.; in *Organic Photochemistry*, Padwa. A., Ed.; Marcel Dekker, New York, **1983**, Vol. 6, Chapter 4.
     d   Eberson, L.; Rees, C.W.; *Electron Transfer Reactions in Organic Chemistry*, Springer Verlag, Berlin, **1987**.

99   Sakaguchi, H.; Nagamura, T.; Matsuo, T.; *J. Chem. Soc., Chem. Comm.*, **1992**, 209.

100   Effio, A.; Griller, D.; Ingold, K.U.; Scaiano, J.C., Sheng, S.J, *J. Am. Chem. Soc.*, **1980**, *102*, 6063.

101   Cox, S.D.; Dirk, C.W.; Moraes, F.; Wellman, D.E.; Wudl, F.; Solits, M.; Strouse, C.; *J. Am. Chem. Soc.*, **1984**, *106*, 7131.

102   Scheffer J.R.; Watson, D.; unpublished results.

103   a   Diaz de Delgado, G.C.; Wheeler, K.A.; Snider, B.B.; Foxman, B.M.; *Angew. Chem. Int. Ed. Engl.*, **1991**, *30*, 420.
     b   Restaino, A.J.; Mesrobian, R.B.; Morawetz, H.; Ballantine, D.S.; Dienes, G.J.; Metz, D.J.; *J. Am. Chem. Soc.;* **1956**, *78*, 2939.
     c   Katchalsky, A.; Blauer, G.; *Trans. Faraday. Soc.*, **1951**, *47*, 1360.
     d   Morawetz, H.; J. *Polym. Sci. (C)*, **1966**, 79.

104   *Radiations Chemistry, Principles and Applications*, J.E. Willard in Farhataziz, Roger, M.A.J., Eds.; VCH, Weinheim, **1987**, 395.

105   Perrin, D.D.; Armarego, W.L.F.; Perrin, D.R.; *Purification of Laboratory Chemicals*, 2nd ed., Pergamon Press, Oxford, **1980**.

106   Figeys, H.P.; Dralants, A.; *Tetrahedron*, **1972**, *28*, 3031.

107   Mead, J.F.; Rapport, M.M.; Senear, A.E.; Maynard, J.T; Koepfli, J.B.; *J. Biol. Chem.*, **1946**, *163*, 465.

108 a   Murov, S.H.; *Handbook of Photochemistry*, Marcel Dekker, Inc., New York, **1973**.
     b   Horspool, W.M.; *Synthetic Organic Photochemistry*, Horspool, W. Ed.; Plenum Press, **1984**, Chapter 9.

109   Hemetzberger, H.; Holstein, W; Werres, F.; *Tetrahedron*, **1983**, *39*, 1151.